The cantilever rolling gate

A rolling gate for a maritime navigation lock
without mechanical parts under water

J.W. Borghans

TU Delft Delft University of Technology

ingenieursbureau Boorsma

The cantilever rolling gate

A rolling gate for a maritime navigation lock without mechanical parts under water

by

J.W. Borghans

to obtain the degree of Master of Science
at the Delft University of Technology,
to be defended publicly on 14 December, 2021 at 2:00 PM.

Student number: 4009231

Thesis committee:	Prof. Dr. Ir. S.N. Jonkman,	TU Delft
	Ir. W.F. Molenaar,	Rijkswaterstaat & TU Delft
	Dr. Ir. H.R. Schipper,	TU Delft
	Ir. A.J. Breimer,	Ingenieursbureau Boorsma
	G.A. Bouwman	Rijkswaterstaat

Coverphoto: https://beeldbank.rws.nl, Rijkswaterstaat

TU Delft Delft University of Technology

ingenieursbureau Boorsma

Preface

This master thesis report shows a technical elaboration of a new gate concept to improve and maybe one day replace the conventional rolling gates in maritime navigation locks. The thesis research is the last piece of work to finish my civil engineering master degree at the TU Delft.

Initially, work on this thesis started in December 2015. Unfortunately it was suddenly disrupted in spring 2016 due to personal health problems. After years of struggling with my health, I was finally able to continue my work part-time in fall 2020. Taking this into account, I am very happy that this research is finished and my studies at TU Delft can finally be concluded. During this long process, I have had help from many people whom I would like to thank here:

Firsly, I would like to thank the graduation committee members Bas Jonkman, Wilfred Molenaar, Roel Schipper, Anne Jan Breimer and Gerard Bouwman for their reviews and feedback over the years. I am especially gratefull that both Wilfred Molenaar and Anne Jan Breimer wanted to keep on supervising me closely, even after the long break of multiple years. Gerard Bouwman, thank you (and Rijkswaterstaat) for cooperating and sharing your knowledge and information on wheels, rails and rolling gates.

Special thanks to Anne Jan Breimer and Ingenieursbureau Boorsma for the initial idea which led to this research. I want to thank Ingenieursbureau Boorsma for their friendly welcome at their office in Drachten in the first months of the thesis work.

I also need to thank Sjaak Michielsen and Johan den Toom of Rijkswaterstaat for providing me with information and answering my questions about the Westsluis in Terneuzen. This info helped a lot for the elaboration of my case study.

Penultimately, I want to thank all my friends and family for their support during this long process. Special thanks to Cornel, Karel, Teije, Sander, Jan & Merijn for reviewing parts of my work. Koen, thank you for the good company and all the coffee breaks in the library the last year, especially during the covid lockdowns.

Lastly I would like to thank my parents for their unconditional support. Without them I would not have been able to finish this thesis and my studies.

J.W. Borghans
Delft, December 2021

Summary

The idea of a new innovative rolling gate which has all the wheels and rails at the top of the gate was initially coined by *Ingenieursbureau Boorsma* during a preliminary design study for the new maritime navigation lock at Terneuzen. Unfortunately, the concept was not further detailed, as their client only permitted proven technologies. However, this initial idea and the possible benefits gave reason to delve further into the subject and subsequently led to this thesis research.

The rolling gate is a type of gate which is most commonly applied for large maritime navigation locks that are over 40 metres wide. All current rolling gates have a wheel-rail bearing system which is partly located under water (Wheelbarrow type) or fully under water (Wagon type). While these gate types have been applied and proven themselves multiple times, some troublesome aspects still exist. The main disadvantage is that sensitive mechanical parts, like rails and wheels, are located at up to 25 meters water depth. Sensitive mechanical parts positioned under water are hard to access, making any inspection, maintenance or revision costly and time consuming. Unexpected failure of these elements therefore generally leads to long down-time of the locks and expensive repair works.

The objective of this research is to design and evaluate a new type of rolling gate for the Western lock (*Westsluis*) in Terneuzen, for which all sensitive and heavily loaded mechanical parts are both easily accessible and located above water. Having all mechanical parts above water not only makes them easier to inspect and maintain, but it also makes them less prone to fouling or obstruction by debris. In this way, the risk of premature gate failure due to failure of wheels/rails is expected to be lower, increasing the overall availability during the lifetime of the lock.

In this thesis six variants are designed and evaluated using a qualitative Multi Criteria Analysis (MCA) and the Cantilever rolling gate is evaluated most feasible. The Cantilever rolling gate concept is a system in which all the rolling supports are located on an extension to the side of the gate, see Figure 1. The gate is balanced by a counterweight and in a way 'hangs' in the gate chamber. The carriages are connected to the gate by hinges, which ensure the perpendicular horizontal movement of the gate in closed position to seal the lock against rubber profiles on the sill, gate chamber and recess.

The Cantilever rolling gate is preferred over the other variants because:

- It consists of one single structure.
- The forces are transmitted through the gate itself, without the need for an extra external structure.
- It does not increase the gate opening and closing time.
- It requires relatively few additional mechanical components.

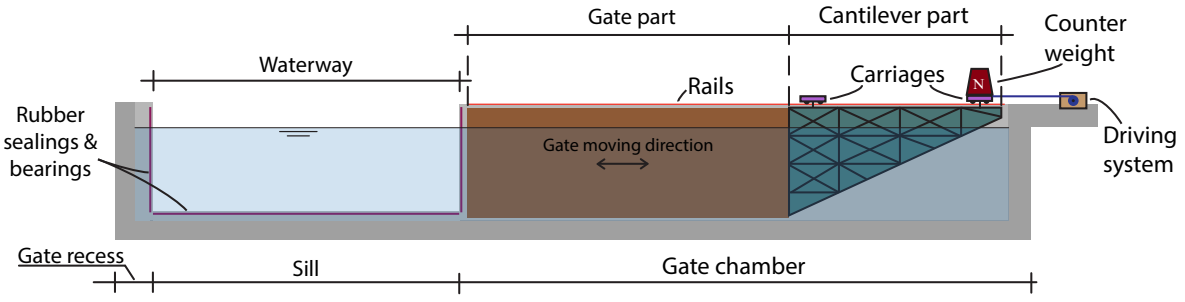

Figure 1: A cross-section of the conceptual design of a Cantilever rolling gate, indicating the most important components.

Subsequently the Cantilever rolling gate is further elaborated at the case study location, the Western lock in Terneuzen, by means of structural calculations. The focus of the design calculations is on the load balance of the gate and supports in the longitudinal direction. To minimise the required extension of the gate chamber, the added cantilever length is kept as short as possible. To find the most optimal cantilever length, limits are defined regarding the minimum required force acting downwards on the carriages to maintain equilibrium and the maximum design capacities of the wheels and rails with respect to strength and fatigue.

Two sub-variants are elaborated to initiate the required counter force for the cantilever mechanism, namely a counterweight and an anchored top rail. The counterweight sub-variant is favoured because the balance of forces is achieved in the gate structure itself, it is a simpler design and it requires less highly loaded sensitive materials like rails. Also, as opposed to the anchored top rail sub-variant, the wheels do not require any tight tolerance restrictions and the carriages are not trapped between two rails and therefore can be freely replaced.

Based on the performed calculations, the most optimal Cantilever rolling gate design for the Western lock in Terneuzen has the following properties:

- An added cantilever part with a length of 16.6 meters.
- A cantilever truss structure constructed of Circular Hollow Sections (69 t).
- A counterweight directly below the back carriage (1083 t).
- An 8-wheel front carriage (9 m long).
- A 4-wheel back carriage (6 m long).
- An increased buoyancy chamber volume in the gate part by 116 m^3 (total is 1140.7 m^3).

Figure 2 shows a 3D view of the final conceptual design. The added cantilever structure of 16.6 m extends the gate part of 44.6 m by 37%. The designed cantilever rolling gate fits at the location of the case study, but the lock chamber and rails should be lengthened by 16.6 m to fit the extended gate.

The possible applicability of the Cantilever rolling gate concept at other locations depends on the available space, as there must be enough room for the extended gate chamber. The scalability of the concept to larger lock widths (e.g. 50 to 70 m) is uncertain, as for larger gate lengths the gate weight and arm both increase and therefore the required counteracting moment increases quadratic. This increase in moment force requires the cantilever length to be considerably larger, which could make it a less suitable solution.

Based on this research it is expected that the concept of a Cantilever rolling gate is technically possible. However, it is not yet certain whether the Cantilever rolling gate will also be feasible in practice. Some additional development is still required before the design can be considered fully technically feasible. For example, it is important that the horizontal force transmission and guidance is further evaluated. It is also recommended to calculate the actual availability and determine whether the difference in availability between the Cantilever rolling gate and the conventional rolling gate outweighs the cost.

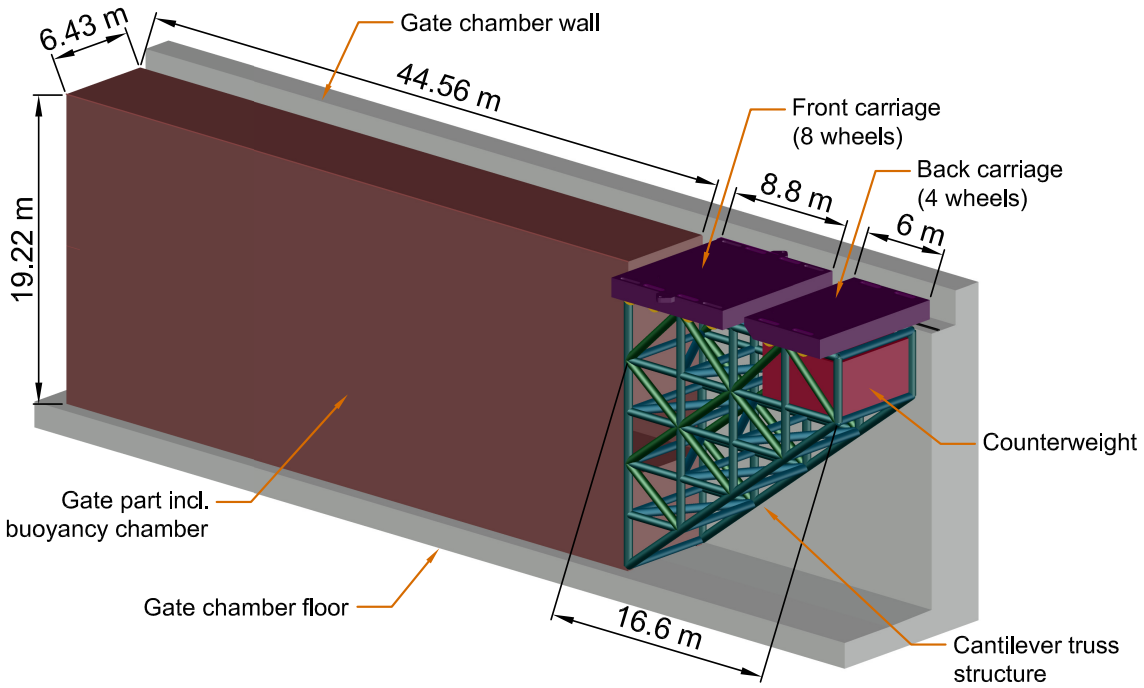

Figure 2: A 3D view of the final cantilever rolling gate design for the case study location of the Western lock (Westsluis) in Terneuzen. To highlight the gate structure and its components, the front wall and back of the gate chamber are not shown.

Contents

1 Introduction

This chapter gives an introduction to the thesis. The background on the thesis problem can be found in Section 1.1. In Section 1.2, the goal and the scope of this thesis are stated, leading up to the main research question. Section 1.3 elaborates on the research sub-questions and the corresponding methodology on how this research is performed. Lastly, section 1.4 shows the structure of the report and the internal relations of the chapters and appendices.

1.1. Background and problem

Over the last few years, a lot of new large maritime navigation locks have been or are being constructed. For instance in the Netherlands (IJmuiden and Terneuzen locks), Belgium (Van Cauwelaert and Kieldrecht locks), Germany (Kaiserlock Bremershaven and 5th lock in Brunsbüttel), Italy (Malamoco lock) and Panama (new Panama canal locks). The commonalities for all these locks are the increased lock and gate dimensions to facilitate the next generation of large ocean going vessels. Another similarity is the application of a rolling gate, which is the predominant type of gate for navigation locks with a width of more than 40 metres [22].

The rolling gate is a type of gate which is often applied for large maritime navigation locks due to:

- their effective way of opening and closing large distances;
- their double retaining function;
- their capacity against a collision.

Besides the relatively newer hydro-feet sliding gates[1] (e.g. Oranjesluis Amsterdam and Malamocco lock Venice), all rolling gates have a wheel-rail bearing system which is partly positioned under water (Wheelbarrow type) or fully under water (Wagon type). While these gate types have been applied multiple times and have proven themselves, some troublesome aspects still exist.

The main disadvantage of these conventional gates is that sensitive mechanical parts, like wheels and rails, are located below water at up to 25 meters water depth. Due to their position under water they are hard to access, making any inspection, maintenance or revision costly and time consuming. In most cases these kind of activities lead to unavailability of the lock system, resulting in high costs for the idle ocean going vessels.

Another disadvantage with submerged mechanical parts is that they need to be resistant against salt water, silt, sediments and any surface organism growth (like shells). Specific coatings can mitigate some of the negative effects of these harsh conditions, such as corrosion. However, the conditions at hand impose uncertainty to the loading conditions of the gate. Especially fouling and sediment accumulation may significantly increase the working loads on wheels and rails.

From 2013 until 2015, engineering firm *Ingenieursbureau Boorsma* was commissioned by the Dutch and Belgian government to formulate a preliminary design for the new maritime navigation lock at Terneuzen in Zeeland. During this engineering process, *Ingenieursbureau Boorsma* coined the idea of a new innovative rolling gate design [15], which had all the wheels and rails at the top side of the gate

[1] The hydro-feet sliding gate uses two hydrostatic slide bearings which create a pressurized water filter to carry its vertical loads and provide movability in horizontal direction. See Section 2.3.3

and would hang as a cantilever system. Unfortunately, the concept was not further detailed, as their client only permitted proven technologies. However, the potential benefits of this idea triggered further research and resulted in this thesis.

1.2. Objective and scope

The initial concept of *Ingenieursbureau Boorsma* sparked the idea to look further into the possibilities of a rolling gate without any mechanical moving parts under water. The objective is to design and evaluate a new type of rolling gate for the Western lock (*Westsluis*) in Terneuzen, for which all sensitive and heavily loaded mechanical parts are both easily accessible and located above water. Thereby taking into account all the advantages and eliminating or mitigating some of the disadvantages of a conventional rolling gate. This goal has been rewritten into the main research question as follows:

> *What is the most optimal conceptual design for a horizontal translation gate in the Western lock in Terneuzen, for which all heavily loaded mechanical supporting elements are both easily accessible and located above water?*

The most optimal conceptual design is evaluated at the case study of the Western lock (*Westsluis*) in Terneuzen, using the current configuration and operational conditions of this lock.

This thesis will focus on the technical design verification of a new type of rolling gate. Economic feasibility and other non-technical factors are left out of consideration for this study.

1.3. Research questions & methodology

The previously defined objective and main research question can be divided into multiple sub-questions. The research questions will each be answered by means of a systematic approach and working method which will be explained for each of the questions.

To arrive at a good design, the current situation with regard to rolling gates must first be examined. This has led to the following sub-question:

- **What is the state-of-the-art and what are the known problems and shortcomings for rolling gates in maritime navigation locks?**

  This question aims to create an overview of maritime navigation locks and rolling gates. It is answered by zooming in from the larger overview of a lock towards the specific rolling gate parts. The second part of the question is answered by evaluating the functions, advantages and disadvantages of conventional rolling gates. It is specifically touched upon by showing the different aspects of availability of a navigation lock and subsequently giving an overview of examples of past wheel-rail connection failures of rolling gates. This question is answered in Chapters 2 and 3.

The results of the previous sub-question are used to elaborate possible variants for the horizontal translation gate by answering the following question:

- **Which conceptual gate variants for a horizontal translation gate can be designed having all mechanical supporting elements above water, and which one is the most feasible?**

  This question is answered by devising all kinds of possible rolling gate variants, which meet the condition that they do not have any heavily loaded mechanical parts under water. To generate ideas for new variants a morphological chart is used. All of the variants are evaluated by performing a qualitative Multi Criteria Analysis (MCA), where the criteria are based on the points of difference between a conventional gate and the new designs. The conventional Wheelbarrow and Wagon rolling gate are also taken into account in the MCA for comparison purposes. This qualitative MCA is then used to determine the design which will be further elaborated. The answer to this question can be found in Chapter 4.

Following the MCA, the Cantilever rolling gate is ranked best and then further developed within the case study location of the Western lock in Terneuzen. The configuration, operation and local environment of the Western lock are used as a starting point for the design (see Chapter 5). A case study is used because it allows the design to quickly become more tangible. This is beneficial for the research, as it can be shown whether the design is technically feasible or not. This information can then be used in future design studies for lock gates at other locations. To determine the exact design of the Cantilever rolling gate, the subsequent questions need to be answered:

- **What would be the most optimal dimensions of the cantilever gate extension which still complies to all the design safety standards for the case study location of the Western lock in Terneuzen?**

  In this question, most optimal means the minimum use of material (steel and concrete), which is achieved by an as small as possible cantilever construction. A static model of the gate is used to determine the requirements to create an equilibrium under all circumstances and to calculate the differences in loading on the supports/carriages. The cantilever length is set as a variable in the calculations. All of the requirements regarding equilibrium, strength and fatigue are used as inputs. The design capacities of the wheel/rail connections are set as a limit to determine the minimum required cantilever length for the different sub-variants and all of the design checks. From all of these minima the maximum value determines the required and most optimal cantilever length. The calculations and answer to this question can be found in Chapters 6 and 7.

- **What is the best way to initiate the longitudinal balance of the Cantilever rolling gate in case the gate is applied at the case study location of the Western lock in Terneuzen?**

  This question is answered by calculating and evaluating possible sub-variants regarding the balance of the cantilever gate in vertical and longitudinal direction (along the longest axis of the gate). It combines the results of the previous sub-question and the pros and cons of the sub-variants to decide on the most optimal design. The question is answered in Chapters 6 and 7.

In this thesis, the calculations regarding the cantilever rolling gate are limited to the balance in longitudinal direction in the vertical plane. The guidance in horizontal perpendicular direction is assumed to be somewhat identical to the current situation of the case study location and is not further examined in this study.

1.4. Report structure

The structure of the report and internal connections of the chapters are shown in Figure 1.1. Chapter 1 gives an introduction to the topic and the defined problem. Chapter 2 provides an overview of the lay-out of a rolling gate in a maritime navigation lock and Chapter 3 analyses the pros and cons and known problems of conventional rolling gates.

This provides a solid base for the general design part which can be found in Chapter 4, in which new gate concepts are elaborated and ranked qualitatively. A single gate type is chosen as most optimal and is subsequently further optimised for the case study location in Terneuzen. Chapter 5 provides the basis on which this design is made. In Chapter 6 then shows the calculations regarding the balance and the wheel/rail loads of the cantilever rolling gate. After which the final design is presented in Chapter 7.

All of the performed work is then evaluated and discussed in Chapter 8. Finally, Chapter 9 gives the conclusions and recommendations of the thesis research.

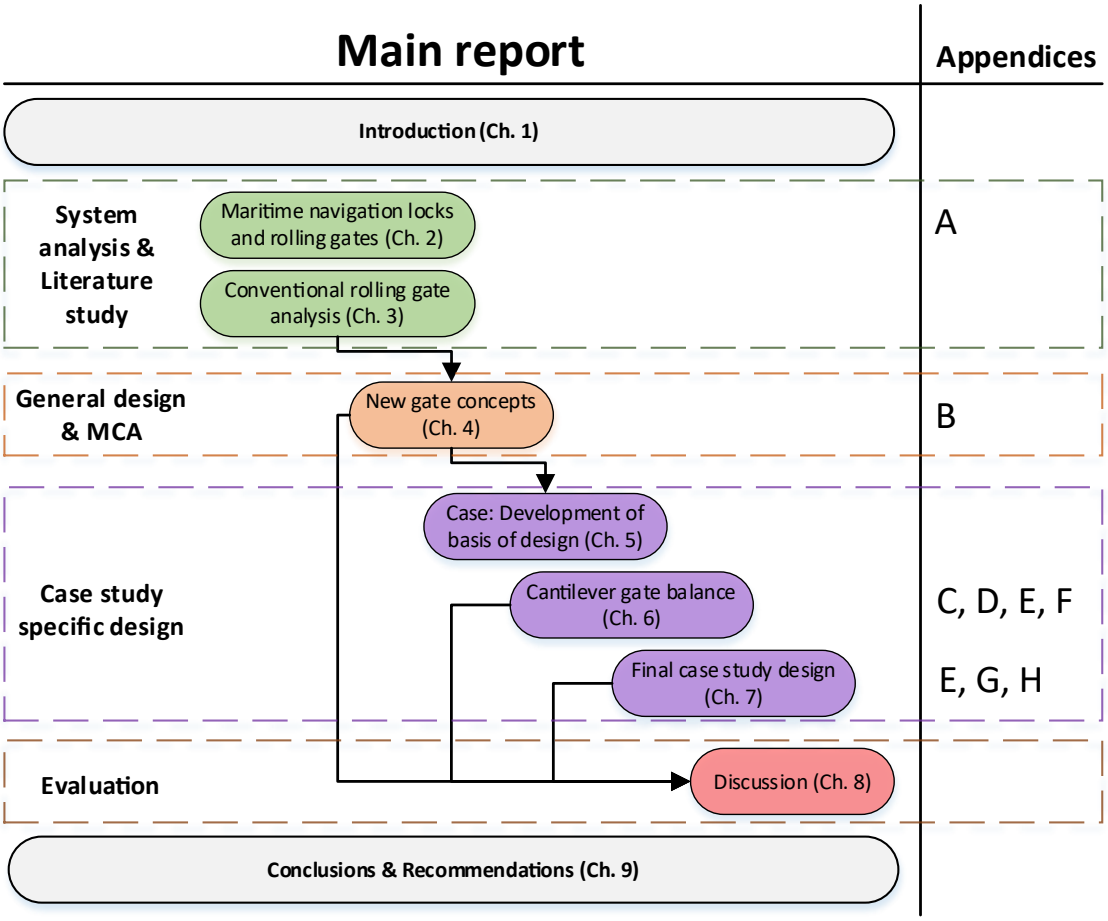

Figure 1.1: Report structure. Indicating the different parts and the linked chapters and appendices.

2

Maritime navigation locks and rolling gates

This chapter provides an overview of information regarding maritime navigation locks and rolling gates. It gradually zooms in from the type of locks towards the different details of a rolling gate. Section 2.1 describes the different type of locks and possible gates. Section 2.2 shows the lay-out and parts of a maritime navigation lock with a rolling gate. After which Section 2.3 goes into dept about the different type of rolling gates that exist nowadays. Lastly, Section 2.4 specifies all the different parts of a rolling gate.

2.1. Type of locks

According to the dictionary, a sluice (in hydraulic engineering) is defined as 'an artificial channel for conducting, often fitted with a gate at the upper end for regulating the flow'. Multiple type of lock structures fall within this wider definition of a sluice[37], as they are all used for water retention and the passage of water and/or ships:

- Dewatering gate
- Stop lock
- Guard lock
- Navigation lock

The dewatering gate and the stop lock are both used to discharge water from a basin or canal to another water body. The guard lock (or storm surge barrier) is used to retain water in case of extreme water level situations. Under normal situations this gate type is open and the water level is equal and vessels can pass. The navigation lock enables ship passage between two bodies of water with different water levels.

2.1.1. Navigation locks

In general, a navigation lock is constructed in a waterway whenever it seems necessary to retain water for safety reasons and/or if the water level (quality) has to be maintained, but simultaneously ship navigation has to be provided. A lock makes it possible to navigate a vessel between two water bodies with differing water levels. Locks are designed to retain the water and allow the horizontal and vertical transportation of ships. This transportation can be obtained in two different ways [36]: Adjusting the water level in a closed chamber which can be closed by gates (a navigation lock), or by transporting both vessel and water together in a closed chamber (ship-lift, inclined plane, pente d'eau, rotating wheel). The latter are more often applied if vessels need to be lifted over a relatively large water level difference (more than 25 meter). The Netherlands is located in a flat floodplain of multiple rivers, and therefore the required lift of locks has a maximum of 6 meter. Hence the navigation lock is the predominant type of lock applied there as it is most suitable for these lift heights.

Location

Navigation locks can (in general) be split up into two types; inland navigation locks and maritime navigation locks. This distinction is mainly related to the location of the lock with respect to the hydraulic conditions, but also to the determinant ship type and size which has to be able to pass the lock. The

name describes the difference, as inland navigation locks are mainly located in inland waterways such as rivers and canals, while maritime navigation locks are located at the border of the sea to the river or canal.

In Europe, inland navigation locks are designed in accordance with the Conférence Européenne Des Ministres de Transports (CEMT) classes. In order to ensure the passage of the largest CEMT class (VII), a lock has to be at least 270 meter long and 34,2 meter wide [57]. Inland navigation locks are mostly used to pass weirs or other water level dividing structures.

Maritime navigation locks are often applied as a port infrastructure. They are constructed to protect the ports against high water levels, to eliminate tidal influences and/or to maintain a relatively constant water level in the port basin. The water level difference over the lock is in the order of meters and can be defined as relatively small. In contrast to inland navigation vessels, no clear classification exists for normative maritime vessels and the related lock dimensions. This is due to the variety in ships and ship sizes which have to pass a maritime navigation lock. It is mostly designed to transfer the (future) largest possible ship such as a tanker or container vessel.

Lock gates

Besides a differentiation in ship type and size, traditional navigation locks can be distinguished by their gate type. A lock gate is a movable structure which provides an almost watertight sealing during the locking process and can be opened to ensure the passage of ships. In maritime navigation lock design, the predominant type of gates are rolling gates and mitre gates. For inland navigation locks all different type of gates are applied. The type of gate is dependent on the specific project due to differing boundary conditions and requirements. The following lock gates can be distinguished:

- Mitre gate
- Rolling gate (horizontal translation)
- Vertical lift gate
- Sector gate
- Submersible gate
- Segment gate
- Flap gate
- Single leaf gate

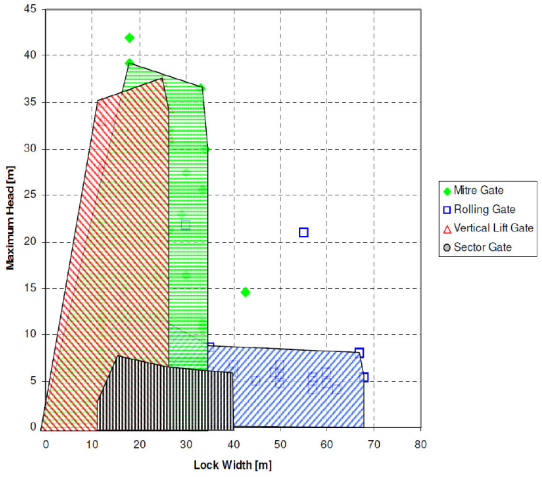

Figure 2.1: Application area per lock gate type [22]

In 2012, J.W. Doeksen performed a study on lock data of large (minimum of 12 m chamber width) locks all around the world [22]. In this study, 220 locks where analysed and compared by lock dimensions, gate type and year of construction. Four type of gates were found to be applied most: Mitre, Rolling, Vertical Lift and Sector gates. As a result of this study, Doeksen presented the application area for these four type of gates, using the maximum head and lock width as input. Figure 2.1 clearly shows the field of application of the rolling gate, which is indicated in blue. For navigation locks with a width of more than 40 meters, the rolling gate is predominant.

2.2. Typical large maritime navigation lock

Figure 2.2 shows a top overview of a general maritime navigation lock with rolling gates. The figure shows a single rolling gate on each side. In reality the number of gates may differ per lock, as some may have double gates on each side for extra redundancy.

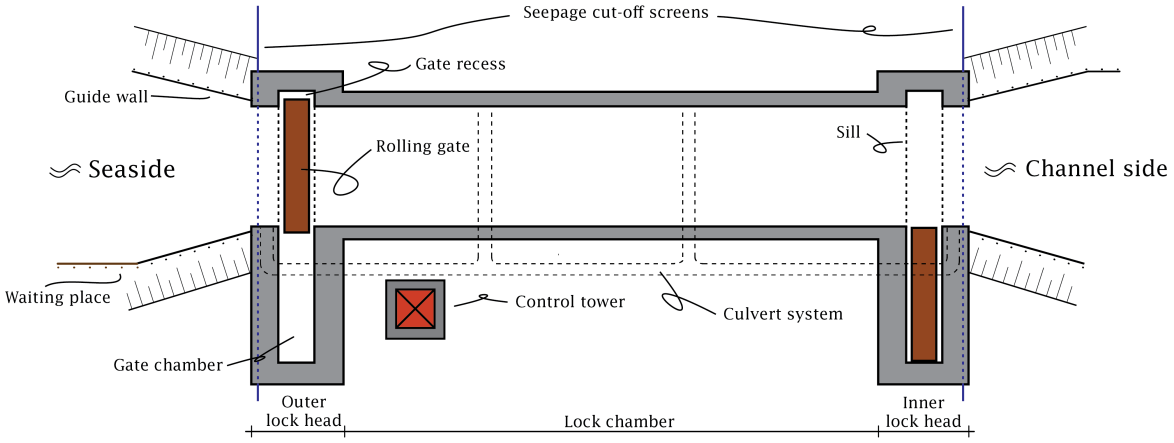

Figure 2.2: Top overview of a maritime navigation lock with rolling gates

Most large maritime navigation locks have a separate culvert system which is used to level the water inside the lock. In some unique cases water levelling is done through the gate, but for larger maritime navigation locks the waterjet and flow velocities are too high for the vessels inside the lock and therefore a culvert system is often preferred. The culvert system is sometimes also used to flush water from the channel to the sea.

The lock structure consists of a lock chamber and an inner and outer lock head constructed of reinforced concrete. In earlier years the lock chamber would be constructed as a monolithic structure for which the walls and the floor were rigidly connected. These type of constructions could be set dry for maintenance. Nowadays, mainly due to increased size and cost considerations, the lock chamber floor and walls are designed as a non-monolithic structure and the walls and floor are not rigidly connected. These type of constructions are never dewatered and maintenance is done in the wet. The walls are separate retaining walls and the floor has to have its own load balance by applying tension foundation poles.

The lock head consists of a gate chamber, a sill and rolling trench and a gate recess. The lock head ensures a solid foundation for the gate and the operating mechanisms and often incorporates filling and emptying culverts and valves. The structure has to resist loads resulting from water level differences. The gate chamber houses the gate if it is in open position. In closed position the gate locks into the recess on the opposite site and bears its loads to the sill and the walls of the chamber and recess.

The driving mechanism of the gate is (often) located in a building at the end of the gate chamber. The control tower houses the operators and provides an overview of the whole lock. The operators control the opening and closing of the gate, opening and closing of the valves in the culvert system, the traffic lights and guidance of the vessels.

Both sides of the lock have waiting places for vessels on the right (starboard) side of the sea entrance or channel. Guiding walls guide the ships in the lock and prevent any ships from colliding with the lock heads. Seepage cut-off screens prevent piping and water flow under the lock.

In Figure 2.2 the road traffic connection is ensured by the rolling gates. However, in some cases the road traffic function is provided by a separate bridge connection in the lock complex

2.3. Type of rolling gates

The most commonly applied gate in large maritime navigation locks is the rolling gate, which makes a horizontal translation with respect to the lock. Maritime navigation locks with rolling gates are primarily located in relatively flat delta's in Europe (see appendix A), with the exception of the new Panama channel locks.

The rolling gate is a large rectangular box which is typically supported by carriages which roll over a rail track. Its function is to open or close the upstream or downstream ends of a lock [76]. In open position, the gate is stored in a gate chamber on the side of the lock. In closed position the gate locks into a recess on the other side and bears and seals against this recess, the gate chamber and a sill on the bottom. Three different type of rolling/sliding gates can be distinguished:

- Wagon rolling gate
- Wheelbarrow rolling gate
- Hydrofeet sliding gate

2.3.1. Wagon rolling gate

The wagon rolling gate rests on two roller carriages, both located at the bottom of the gate as can be seen in Figure 2.3. The roller carriages provide vertical bearing and movement of the gate. The roller carriages roll over rail tracks which are located in a trench at the bottom of the lock. Each carriage typically contains four wheels each. The carriages are both loaded equally by making good use of balance tubes and buoyancy chambers. A certain overweight is present on the carriages during opening and closing of the gate to provide stability. The advantages and disadvantages of rolling gates are further elaborated in Chapter 3, Sections 3.4 and 3.5.

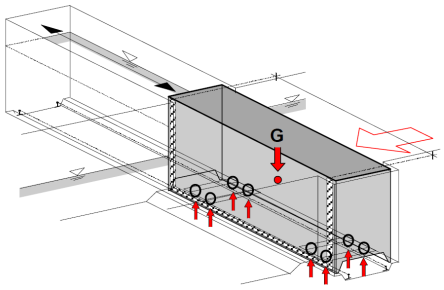

Figure 2.3: Wagon rolling gate [17]

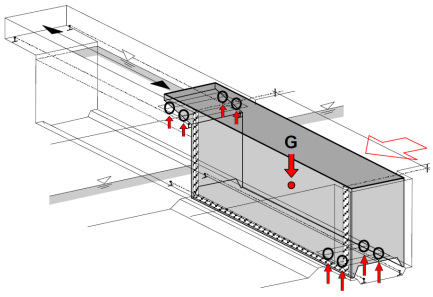

Figure 2.4: Wheelbarrow rolling gate [17]

2.3.2. Wheelbarrow rolling gate

The wheelbarrow rolling gate also rests on two roller carriages. But in contrast to the wagon type of rolling gate, the wheelbarrow rolling gate has one carriage located at downside end of the gate and one at the top of the gate. As can be seen in Figure 2.4, this system kind of looks like a wheelbarrow, hence its name. The wheelbarrow rolling gate is relatively stable with respect to the wagon and sliding gates as it is supported on the top on one side. The resultant of the horizontal hydraulic loads and the centre of gravity of the gate structure are both located close to the diagonal connecting the two carriages. The overturning stability is therefore much better, which is the reason that most of the largest gates in the world are of the wheelbarrow type [76]. Due to less parts and a shorter rail length under water, less maintenance is required in total for the wheelbarrow gate. However, the lower rail track and carriage require more frequent maintenance due to the heavier loading conditions.

2.3.3. Hydro-feet sliding gate

As can be seen in Figure 2.5, the hydro-feet sliding gate uses two hydrostatic slide bearings to carry its vertical loads and provide movability in horizontal direction. Figure 2.6 shows the working principle of a hydrostatic slide bearing. The bearing consists of a rubber hinge connected to a steel foot with 4 'triangle' openings. Each part is connected to a water pump with tubes through the shaft and can be controlled by a pressure restrictor, which divides the pressure evenly over the slide bearing. Due to the created pressurized water filter, the gate is lifted by a few millimetres. The Ultra-High Molecular PolyEthylene (UHMPE) track and the water filter have a very low friction, making it possible for the heavy gate to move. In theory, the hydro-feet sliding gate requires less maintenance compared to conventional rolling gates due to the reduced mechanical friction. Such a system does not wear as fast as a rail track or roller carriage. However, it has only been applied a few times in the world and still needs to prove its durability over a longer period of time.

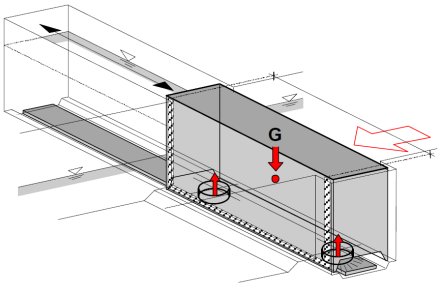

Figure 2.5: Hydro-feet sliding gate [17]

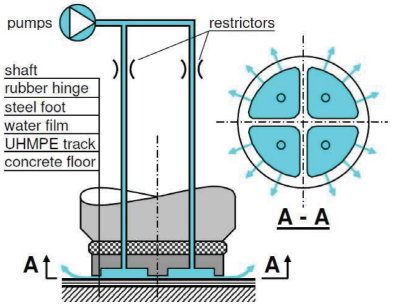

Figure 2.6: Working principle hydrostatic slide bearing [17]

2.4. Parts of a rolling gate

The rolling gate consists of different components which have different functions. The following components can be considered:

- The main structure
- The watertight sealing
- The vertical load bearing
- The horizontal load guidance
- The buoyancy chambers
- The driving mechanism

2.4.1. Main structure

The function of the main structure is to lead the loads to the bearings and to seal off. Almost all rolling gates are constructed of steel. However, in recent years some relatively smaller hydraulic gates have been constructed with Fibre-Reinforced Polymers (FRP), but it has not yet been applied for rolling gates. The main steel structure exists of two walls of multiple horizontal and vertical girders with vertical plating, which are horizontally (and sometimes diagonally) connected by beams. The steel plating functions as a watertight sealing. Stiffeners are often placed in between the girders. A rolling gates death weight is often more than 1000 tonnes and therefore requires buoyancy/ballast tanks to reduce the loading. Figure 2.7 shows some examples of cross-sections of large rolling gates.

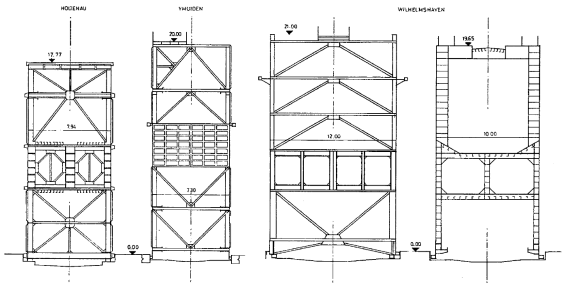

Figure 2.7: Various types of rolling gate cross-sections [51]

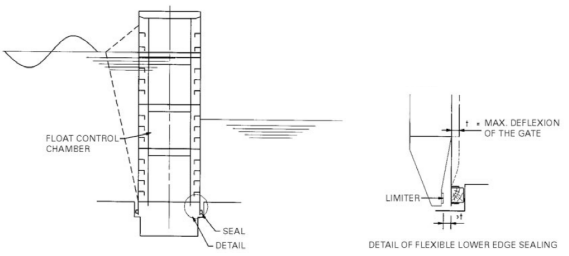

Figure 2.8: Working principle elastic plate [72]

2.4.2. Watertight sealing

At both sides at the bottom of the gate structure, elastic plates connected to hard timber provide a watertight sealing. During opening and closing of the gate, the elastic plate preferably does not touch the sill of the lock. Due to a horizontal load on the closed gate, the gate moves in lateral direction, pushing the elastic plate against the sill. The hard timber (azobé) provides a watertight sealing, while the elastic plate is able to deform elastically in order to adjust to the bending line of the gate in horizontal direction. As the gate is mainly supported by the wall of the gate chamber and the gate recess, plate bending in one direction occurs. Giving the largest sag in the middle of the gate. Behind the elastic plate, a backup structure is placed in case the gate deforms to its limit, ensuring the proper sealing of the gate during an extreme event. The working of the elastic plate is shown in Figure 2.8. On the left and right side of the gate (in the gate recess and the gate chamber), hard timber (azobé) and/or synthetic (UHMPE) strips function as a sealing.

2.4.3. Vertical load bearings

In principal, the roller carriages and the rails function as vertical load bearings. The vertical loads go from the main gate structure to the carriage, to the wheels, onto the rail tracks to the foundation. The gate structure has to be able to displace in lateral direction, to make use of the horizontal load bearings and to seal of the water. Therefore, a vertical load bearing which is able to move in lateral direction is required in between gate and carriage. In general, two type of connections are applied; lateral movement rollers and elastometric bearings.

For the lateral movement rollers, an inclined foot plate is connected to the gate which rests on a roller on the carriage. Under a certain horizontal load, the foot plate can move sideways over the roller until most of the horizontal loads are taken by the horizontal bearings. The two lateral rollers give a high lateral stiffness, but do not provide any load equalization. The connection is statically simple, but gives unfavourable acting horizontal loads on the wheels [17]. Figure 2.9 shows the roller carriage of the Kaiserlock, in which lateral movement rollers are applied.

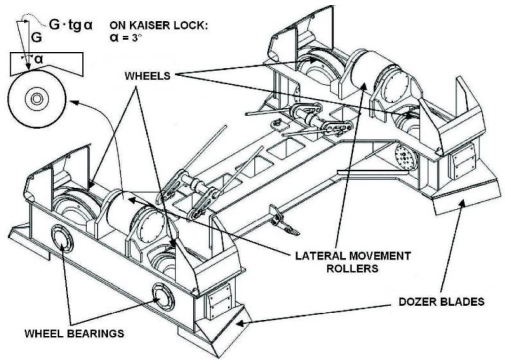

Figure 2.9: Roller carriage of the Kaiserlock [17]

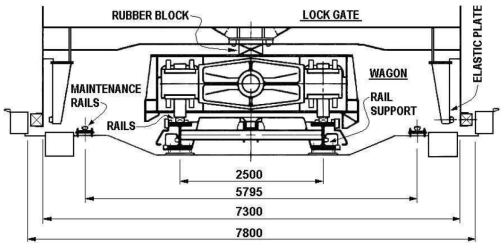

Figure 2.10: Roller carriage of the Northlock at IJmuiden [17]

In a simplified way, elastometric bearings are rubber blocks placed in between the gate and the roller carriage. Often applied in bridge design, these type of bearings where just recently introduced in rolling gates. The elastometric bearing provides lateral displacement of the gate. The rubber block is able to absorb small shocks and equalize the loads between the wheels and rails. Due to the equalization of loads, the rails can be placed much closer to each other. This bearing system has been applied in the roller carriage of the Northlock in IJmuiden, as shown in Figure 2.10.

2.4.4. Horizontal load guidance

The horizontal load guidance of the gate can be provided in a passive or active manner. The following loading phases can be distinguished: loading during opening of the gate, closing of the gate and when the gate is in closed position. In closed position, the gate has to bear really large horizontal forces due to the large water level difference between sea and channel. In this situation a gate always guides horizontal loads in a passive way to the sides on both recesses. These side bearings are often constructed of hard timber (azobé) beams and synthetic UHMPE strips and also function as a watertight sealing.

Except for the moment just after opening, no water level difference is present during opening or closing of the gate and the gate is only loaded by horizontal forces due to water density differences or waves created by wind or passing vessels.

During the first part of opening of the gate a water level difference of 10 to 30 cm is still acting as a load on the gate. The gate already starts opening under this water level difference to shorten the total lockage time. Waiting for these water levels to equalize by themselves would take a very long time due to the decreasing water pressure which slows down the water flow through the culverts.

In some cases all of these horizontal loads during opening or closing are taken in a passive way by slide bearings on the bottom of the gate. This gives high friction forces and therefore often requires a strong driving mechanism. To reduce these friction forces often an active guiding system is present, which actively pushes the gate in its central position. These push-off devices can be located at the bottom inside the carriage (see Figure 2.11) and/or at the top of the recess and gate chamber.

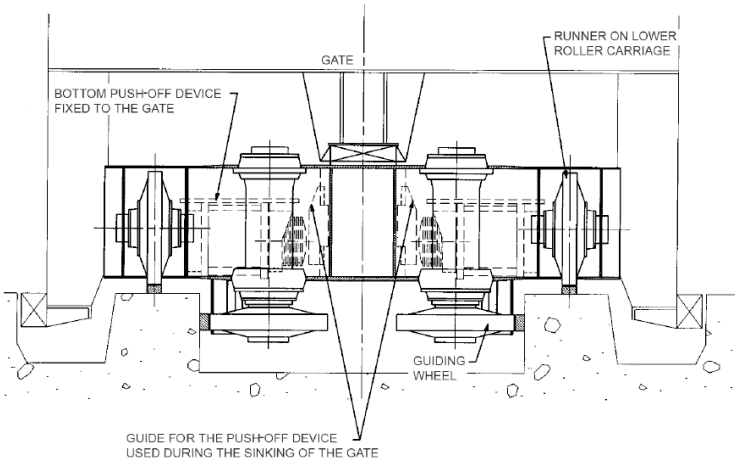

Figure 2.11: Roller carriage with push-off device of the Westsluis at Terneuzen [72]

2.4.5. Buoyancy chambers

The buoyancy chambers in the gate provide extra buoyancy to release the vertical load bearings from the otherwise way to heavy loads. To provide buoyancy under all circumstances but also provide the most optimal stability, these chambers are often located just under the lowest possible water level. The buoyancy chambers consist of different type of compartments that are connected to pressure pumps which control the amount of air or water inside. These can then be used to stabilize the gate under different circumstances. As for most of the large rolling gates, the buoyancy chambers also provide floating stability to transport the gate from its construction site to the lock location. The self-floating requirement can also be necessary if the gate chamber does not function as a maintenance dock and the gate thus has to be transported to a separate one. In the latter case a spare gate is necessary as a replacement or the lock has to be constructed with double doors to ensure availability of the lock complex.

2.4.6. Driving mechanism

The driving mechanism of a rolling gate is often provided by a mechanical drive system like a cable winch. The cable can be connected to the gate in various ways. In general, a top roller carriage is provided with cable wheels on it. Two cables leave the winch and are connected to a counter weight via variable cable wheels. The motor can go forward and backwards to open or close the gate. The cables can also be directly connected to the gate via a load equalizing beam. In this case the cables roll over guidance wheels on top of the concrete structure and are tensioned by a hydraulic wire rope tensioner. A disadvantage of this wire rope and winch drum drive system is the wire ropes which tend to lose tension over time and therefore the tensioners frequently need to be adjusted [76].

3

Conventional rolling gates analysis

The previous chapter gradually zoomed in from a general maritime lock overview towards the individual parts of a rolling gate. Next, these conventional rolling gates are analysed to find the pros and cons and distinguish the current problems of rolling gates.

Firstly, the functions and failure definitions of a lock and the different design approaches with respect to navigation locks will be summarized in Section 3.1. Secondly, the non-availability aspects of rolling gates in large maritime navigation locks are elaborated in Section 3.2. Section 3.2 then zooms in upon examples of unplanned non-availability of conventional rolling gates due to failure of the wheel-rail connection. Lastly, the advantages and disadvantages of conventional rolling gates are respectively described in Section 3.4 and Section 3.5.

3.1. Lock system aspects

While being one of the most important objects in a lock, a rolling gate is still part of a larger system. In order to explain the functionality of the gate, the total system of the lock has to be analysed first. Things like lock functions, availability or reliability aspects have to be taken into account for the total system, before something meaningful about the rolling gate can be said.

3.1.1. Lock functions and failure definitions

For a maritime navigation lock, the following six functions and their related failure definitions are specified [25]:

1. *Ship passage*:
   A principal function of the lock system is the ability to provide passage of vessels between the adjacent water bodies. Failure of this functions occurs if a vessel is not able to pass the lock within a given norm time after arriving at the lock.
2. *Maintain water separation:*
   The lock has to be able to maintain a water level difference between the two adjacent water sections. Failure of this function occurs if there is an open connection between the upstream and downstream waterbodies, which is larger than a certain percentage of the cross-sectional area of the lock chamber.
3. *High water retention*:
   A maritime navigation lock is often part of a (primary) water defence and therefore has to be able to withstand a specific high water level[1]. This function fails if there is (1) a certain excess amount of water overtopping or (2) if a certain excess amount of water is coming through the lock system or (3) if the lock has a constructive failure. The 'Leidraad Kunstwerken' (Guideline Water Retaining Structures) defines the following failure criteria (TAW, 2013):
   - Retaining height:
     With respect to retaining height failure the chance of a certain normative volume of water flowing over a closed hydraulic structure is required to be lower than the normative exceedance probability (norm). This requirement gives a minimum retaining height for the structure.

[1] Related to the probability of exceedance norm of the dike ring as stated in the Dutch 'Waterwet' (Water Act).

- Reliability of closing mechanisms:
  For closing mechanisms the yearly chance of the exceedance of a maximum inflow volume through one of the opened mechanisms should be smaller than 0.1 times the normative exceedance probability. This requirement dictates the maximum failure probability of the closing mechanism.
- Strength and stability:
  Regarding strength and stability the yearly probability of structural failure under a normative extreme water level should be lower than 0.01 times the normative probability of exceedance. Due to the extreme consequences of a structural failure, this norm is even higher than the previously two mentioned requirements. To fulfil this requirement, the extreme loading situations to the various components should be taken into account.

4. *Water discharge (quantitative water management):*
   The lock has to be able to control the water discharge through the lock system. Dependent on the local conditions, the lock needs to minimise the water loss or do the opposite and flush a certain amount of water. For example at the new Panama locks, fresh water loss from the upper lake should be minimized and therefore water saving basins are applied to save water during the locking process. Contrary, at the Terneuzen lock complex and the IJmuiden lock complex, excess fresh water from the channel is flushed through respectively the navigation locks itself (Terneuzen) and a separate flushing sluice (IJmuiden). The water discharge function fails if the discharge opening deviates more than a specific percentage from the desired discharge opening for a given continuous period of time.
5. *Fresh/salt water separation (qualitative water management):*
   A maritime navigation lock often has to prevent salt water from penetrating the fresh water body to a certain degree to protect the hinterland, which needs the fresh water for drinking or irrigation purposes. Solutions to prevent this during opening of the gate are an air bubble screen at the outer head of the lock or salt water basins at the inner head of the lock, which flushes the heavier salt water during the right conditions. The fresh/salt water separation function fails if the actual capacity to prevent salt penetration deviates with a certain percentage from the required capacity for a given period of time.
6. *Road traffic passage:*
   In most cases the lock system also provides passage to road traffic, either over one of the closed gates or over a separate movable bridge. Sometimes this function is seen as a separate additional or sub-function, as road passage is not seen as one of the primary functions of a lock. This function fails if road traffic is not able to pass within a certain normative time period.

3.1.2. Wider design approach based on asset management

For several years now, a broader design approach is being applied for the construction of large hydraulic structures, focussing on the total life cycle of the structure and taking into account Reliability, Availability, Maintenance and Safety (RAMS) aspects. Life cycle analysis is mostly done by calculating the Life Cycle Cost (LCC), which is a method to determine the most cost-effective option among comparable alternatives for purchasing, operating, maintaining and disposing any project or processes. RAMS is a tool used in the risk-based operations and maintenance of objects and systems ([76] & Appendix A). Both of these terms will be elaborated more thoroughly for the case of a rolling gate in a maritime navigation lock.

Life Cycle Costs (LCC)

The calculation of the life cycle cost of a navigation lock incorporates an economic analysis of all the costs related to the design, construction, operation and demolition. This can be applied to the whole lock or to separate parts; for instance the gate. Life cycle costing provides insight into the cost contributors of a project. The main objective is to provide input for decision making regarding the evaluation and comparison of alternatives and/or the assessment of viability of a lock project [38]. The life cycle of a hydraulic engineering project can be split up into four phases [77]:

- Planning and design
- Production and construction
- Operation (and maintenance)
- Removal/demolition

The Life Cycle Costs only takes into account the direct costs related to the lock project. A Whole-Life Costs analysis can be used to also incorporate indirect costs and benefits related to the environmental and social surroundings. It is however difficult to express these indirect costs in monetary terms and directly compare them with the direct costs of a project.

Reliability
Reliability can be quantified by the probability that no operational interruptions occur during a certain time period. Reliability is closely connected to availability. Reliability is related to the probability of a component or system surviving a certain time period, while availability refers to the execution of the function at a certain time.

A high reliability of components is demanded as failure of one of the main functions has large consequences. If reliability of one component cannot be assured, but a higher reliability is required, the component or system should be executed in a redundant way. Examples of extra redundancy are spare parts which can be placed within a short time interval or double gates in order to ensure function of a lock during planned or non-planned maintenance of one of the gates.

Availability
Availability is defined as the probability that the required function can be performed at any given time under specific conditions [60]. In practice this corresponds to a percentage or fraction of time that the required function can be performed. The availability requirements are often expressed as a non-availability, related to the failure of a function. Non-availability of a function can be split up into non-availability which respectively has a plannable cause and a non-plannable cause. Examples per type are [25]:

- *Non-availability due to planned causes:*
  - Inspections and testing
  - Planned maintenance/revision
  - Incompatibility of functions
- *Non-availability due to non-planned causes:*
  - External natural causes
  - Software failure
  - Human mistakes
  - Calamities/incidents
  - Technical failure of structural parts

Besides the plannability the non-availability can also be ordered in system related and system unrelated non-availability. System unrelated non-availability is caused by external influences like natural causes or ship collision.

The impact of the non-plannable non-availability causes is dependent on the probability of occurrence and the required recovery time. Non-availability due to planned causes and non-availability due to non-planned causes are sometimes related to or dependent on each other. For instance, an increase of planned non-availability like maintenance or inspections, can lead to less non-planned non-availability like technical failures.

For most marine navigation lock systems, the required availability of the ship passage function is most important. Downtime of the lock creates no revenue as commercial navigation pays for use of the lock. Besides the lost revenues for the lock owner, downtime of the lock also is very costly for the owner of the passing vessels, as these large ocean-going vessels have high operational costs and thus idle time is very costly.

The ship passage availability requirement is often decisive for the design choices made (for instance related to choices regarding double gates or replacement and maintenance tactics). For the function ship passage in a maritime navigation lock the required availability percentage is often more than 95%. For instance the requirement for ship passage availability at the new lock in IJmuiden is 98% of the time [2]. For the new Panama locks the lane availability time is even higher with 99.6% [76].

Maintainability
Maintainability is the probability that a maintenance activity is possible within the specified time, in order to continue to perform the required functions. Maintainability is therefore directly linked to the criterion of availability. To determine maintainability, the accessibility and interchangeability of parts which are sensitive to wear, like the driving mechanism and the rolling gate are of main interest. Parts that are (continuously) under water are generally more difficult to maintain due to their inaccessible location.

Maintainability is directly related to the maintenance costs and initial investment costs. Often a design with a good maintainability will have higher initial investment costs but lower maintenance costs (and vice versa). A Life Cycle Cost (LCC) analysis can be helpful to give insight into this.

3.2. Non-availability of rolling gates

This part will focus on non-availability of the functions of the lock due to anything related to the rolling gate. As described before, non-availability can be split up into planned and non-planned non-availability of a certain function. First the planned non-availability will be analysed.

3.2.1. Inspection (Planned)

Inspection of the gate and its mechanical components usually takes place multiple times a year, dependent on the specific part. As most of the gate parts are located under water (up to 70% according to PIANC WG173 [76]), a specialized diving team is necessary to perform some of these inspections. The gate structure and its carriages can be inspected inside the gate chamber. The roller carriage which is located under water can be rigged up for inspection (or maintenance). Non-availability will occur if it is just a single gate configuration. In case of double gates the second gate can take over.

While a roller carriage can be rigged up and be inspected on land, a rail track is founded solidly in the sill and thus always requires inspection under water. The rails are inspected for cracks and other irregularities. An inspection of the rails by divers leads to a short unavailability of the locking function as no vessels may pas during it. Often these type of inspections are combined with other inspection or maintenance works in and around the lock, to reduce the total impact. As underwater inspection is relatively costly and labour intensive, it only takes place once in a while. For the rest of the time, the exact state of these parts is unfortunately relatively unknown. The inspection regime of a lock differs per location, depending on the specific experience of the executive body or administrator of the lock. As an example, the rail tracks in the Westsluis of Terneuzen are inspected previous to a planned maintenance in order to decide what steps to take.

Other inspections like testing the emergency drive unit, inspection of the driving unit (gearbox, tensioners, cables etc.) and guiding systems above the water line can all be done without interfering with the locking function.

3.2.2. Maintenance (planned)

The total lay-out and setup of the lock has a big influence on the non-availability due to maintenance on one of the gates. For instance, if a gate chamber can also functions as a drydock, the gate can be maintained in its chamber and does not have to move to a separate drydock. This will reduce the downtime in case of maintenance. A drydock is created by inserting a maintenance gate or stop logs at the end of the gate chamber and pumping out the water. Maintenance inside the chamber drydock does not impose any unavailability of the lock function if the lock system is constructed redundant with multiple gates (two on both sides). If only a single gate is used it needs to be switched with the spare gate, leading to short unavailability of the locking function. The carriage of the gates should be brought onto land to maintain any parts like the wheels, bearings and steel structure. Often one or two spare carriages are used to switch in case one of the active carriages requires maintenance.

Just like inspection, maintenance of the rails is really difficult and has to be performed by divers. Small maintenance like tightening the bolts which connect the rail to the concrete is often combined with inspection. Larger maintenance activities like complete revision of the rail system are a lot more complicated. Revision of the rails can either be done by applying a pressurized diving bell caisson (cofferdam) to create a pressurized working space, or completely under water with divers. For locks with multiple gates the caisson is designed in such a way that a vessel is still able to pass, but only when no one is working inside. This ensures continuation of the locking function, but with a stricter regime. In case of a single gate the use of a diving bell leads to long periods of non-availability. Replacing the rails with divers always blocks the lock system. Revision of the rails is roughly planned every 30 years, but can last two to three months. Other rough approximations of replacement intervals are:

- Rail replacement: 25 to 30 years
- Gate conservation: 15 to 30 years
- Carriage maintenance/replacement: 7 to 15 years
- Guidance and driving parts replacement: ~15 years
- Overhaul of hydraulic installations: ~25 years
- Overhaul of electrical and mechanical installations: ~40 years

3.2.3. Incompatibility of functions

Non-availability due to incompatibility of functions occurs when one of the functions of the lock blocks another function. These incompatibilities can have a planned or non-planned cause. For instance, a planned incompatibility occurs in case water is discharged through the lock and ship passage is thus not possible due to the high waterflow. Also, due to the tides, certain windows can only be used to discharge water as the water level on the channel side is higher than the seaside water level. Non-planned incompatibilities occur if it cannot be foreseen in advance. E.g. in case of a storm the lock has to perform its high water retention function, the gate has to be kept closed and thus ship passage cannot be performed anymore.

3.2.4. External natural causes

Non-availability of the lock function can occur due to external natural causes. For most locks, there is a certain threshold for which the lock cannot be used anymore by (certain) vessels. For instance, above a particular high wind speed large vessels may not enter the lock as they become uncontrollable. Or in case of fog and thus bad visibility the ships cannot be guided and the lock passage is also not possible. Another external natural cause is lightning strikes. Most locks will be equipped with a lightning conductor, but there is still a possibility of a lightning strike which ultimately can cause fire or power failure.

3.2.5. Software failure

Nowadays most larger locks and gates are equipped with a lot of computers and machines to operate the gate from the (external) control tower. These computers require software and hardware to control all the lock parts. As with all computers, bugs or crashes can occur which can lead to the gate not being able to be operated.

3.2.6. Human mistakes

A large lock makes use of computers to control it, but still has to be operated and maintained by humans. All humans make mistakes and these mistakes can lead to non-availability of the lock functions. Mistakes are minimized by applying solid protocols and rules, but of course they can still happen.

3.2.7. Calamities/incidents

Calamities or incidents can occur in and around the lock and cause obstruction of certain functionalities. External power failure is one example of a calamity. Most lock gates are equipped with an emergency generator and backup drive to take over when necessary. The gate can then still be opened and closed (however at a much slower pace) and thus the lock can still function.

One of the most important possible incidents for a maritime navigation lock and its gate is a ship collision. In case of the rolling gate the gate is susceptible to collision in closed position. The gate is designed such that it can take the blow of a normative vessel and still provide the water separation function. However, ship collision can lead to down times of the lock as the gate may not be able to move again and/or the gate has to be replaced by a spare gate.

3.2.8. Technical failure of structural parts

The structural parts in a maritime navigation lock mainly consist of reinforced concrete and all types of steel. As with all structures, technical failure can occur with a certain probability. All structural parts are designed with a certain maximum probability of failure subject to (local) norms and standards. Dependent on the part of the gate (or lock) failing, non-availability of certain functions may occur. Especially mechanically moving are parts are susceptible to wear and tear and therefore form a relatively high risk in a rolling gate. The connection between wheels and rails is susceptible to (early) failure, which will be further elaborated in the next section.

3.3. Wheel/rail technical failure analysis

Experience learns that the rail to wheel connection is a delicate one, which is prone to failure due to different reasons. Many examples are known in which the rails or wheels have been rolled out way before their design technical lifetime. The early failure of a rail or wheel system and its replacement has a large impact due to the unplanned unavailability of the lock. This section looks into the wheel/rail failure cases and tries to answer the question why these rails and/or wheels failed prior to their original design life. Whereas each lock system and gate structure is designed differently and has different boundary (loading) conditions, each case is handled separately.

3.3.1. Northern lock IJmuiden (old rail system)

The old rail system of the Northern lock (Noordersluis) in IJmuiden had to be replaced multiple times due to rolling out. Reason for rolling out of the rails was the uneven distribution of forces on the wheels. The steel gate structure rested on the carriage by two wedges on rollers. This wedge to roller connection made it possible for the gate to move sideways under a head difference by pushing the gate up and sideways on the inclined plane. When the head difference decayed, the gate automatically slid back in its middle position by its own weight. However, due to this connection type, a horizontal load on the gate (due to residual head differences or waves) caused a moment inside the gate structure. This moment created an uneven force distribution over the wheels, increasing the load on one side of the carriage and decreasing the load on the other. This extra force effect was not taken into account during the design of the gate in the 1920's, and thus caused rolling out of the wheels and rails.

As other equipment was outdated as well, it was decided to completely renovate the mechanical system of the Noordersluis in 1980, also installing a new type of rail and roller carriage system. The gate is connected to the carriage by an UHMWPE rubber block which only transvers vertical loads onto the carriages. The horizontal loads are taken by the new guidance system.

3.3.2. Westlock Terneuzen

Within ten years after the Westlock (Westsluis) in Terneuzen was opened in 1968, the wheels of the carriage already had to be replaced due to broken spokes in the wheels. 20 years later, around 2000, it was found that the wheels had been rolled out and thus action had to be taken again. The wheels were annealed and welded and put back on the rails, only to find out that the wheels had been rolled out again several years later. Therefore TNO was commissioned by Rijkswaterstaat to research the cause and advise them on further improvements [64].

The research concluded that the combination of the geometry and materials were such that the contact stresses became too high and led to plastic deformations of the wheels and rails. It was advised to change the geometry of the wheels and to apply a stronger type of steel. The wheels had a curvature perpendicular to the rolling direction of the wheels, which created the contact between the rails and the wheels to be a point. In line with the Hertzian contact theorem[2], this point contact led to high local stresses. Therefore it was advised to apply no curvature perpendicular to the rolling direction in order to create a line load between the wheel and rail. It was also advised to create rounded wheel edges in order to prevent peak stresses at the side. Between 2007 and 2009 the old wheels have been replaced by new surface hardened ones with a yielding strength of 550 MPa [33].

3.3.3. Roompotlock Eastern Scheldt Barrier

After a first inspection of the Roompotlock (Roompotsluis), just four years after its completion in 1984, it was noticed that the wheels and rail track had been rolled out. An extensive technical research performed by the department of waterways and public works (*Bouwdienst Rijkswaterstaat*) [62] could not relate the damage to causes like overloading or uneven wheel loads. Rolling out of the wheels of the Roompotlock was mainly caused by shear forces acting on the wheels. The shear forces were transferred to the wheels whenever the guiding system had made no contact yet.

Some years later it was found that certain other rolling gates in the Netherlands (the Krammerlock in the Philipsdam and the Middlelock in Terneuzen) had the same kind of problems (rolled out rails or wheels). Therefore, in 1994, the *Bouwdienst Rijkswaterstaat* (department of waterways and public works) started a research called 'Onderzoek Wielbelast' [70] to find an explanation for the wheels and rails being rolled out. The scope of this research was widened by adding locks which had not had any problems yet; the Westsluis in Terneuzen and the lock in Hansweert.

[2] Theory coined by Heinrich Hertz in 1882. A theory derived from the elastic theory equations under half-space approximation, which relates properties of elliptical contacts to the stress developed in those bodies.[24]

This research confirmed the results from the previous research carried out in 1988 after the failure of the Roompotlock; Rolling out of the wheels was caused by structurally repeated shear loads acting on the wheels. Rolling out only occurred at rolling gates which were structurally loaded (every opening/closing) in a transverse direction. Structural transverse loads can be caused by:

- Residual decay just before opening
- Density differences over the gate just before opening
- Horizontal eccentric forces due to a one sided driving mechanism

A structural transverse load occurs every time at the same point in the opening or closing cycle, causing a shear stress peak and according deformations on a specific point of the rail. Due to its re-occurring location, this kind of load is more harmful than a wind- or waveload occurring at a random moment in the opening or closing cycle. Especially the one sided driving mechanism increases the risk of rolling out, due to opposing loads created by the reversal of the driving force at exactly the same moment of the opening and closing cycle and thus the exact same spot of the rail every time.

Part of the 'Onderzoek Wielbelast' focused on the development of a new calculation method to predict any failures due to rolling out. The 'Eindverslag Onderzoek Wielbelast' [70] carried out by S.P. van Vlaenderen, combined the normal and shear stresses into a reference stress to evaluate the stress level in the wheel. The ratio between the normal stress and the shear stress was input to define the maximum allowable stress level.

3.3.4. Kallolock Antwerp

The Kallolock provides acces to the Western Waasland harbour of the port of Antwerp. The Kallolock was (until the Kieldrecht lock was opened in 2016) the only connection to the left bank of the port of Antwerp since its opening in 1979. While the expected lifetime of the rails of the lock was 50 years, the rails already had to be replaced in 2006, after just 25 years. The rails and wheels were completely rolled out. T. Ory analysed the cause of the rolling out in his master thesis [50]. According to Ory, rolling out of the wheels and rails was caused by an underestimation of the loads during the design of the gate. The normal forces acting on the carriage were much higher due to the accumulation of silt on top of the buoyancy chambers. Also, residual decay, waves and density differences during opening of the gate caused horizontal shear forces and unevenly distributed vertical normal forces acting on the wheels. This was not taken into account in the design of the wheel to rail connection.

3.3.5. Kaiserlock Bremen

In autumn 2014, the Kaiserlock was closed just 4 years after it was put into operation. A routine inspection found out the rails of the outer gate had been rolled out and settlements and consequential cracks had occurred in the sills of the outer and inner lock heads [35]. The exact cause of this early failure is still unknown to the public. Due to the settled and cracked sill, the rails had to be completely re-aligned in a freshly poured concrete foundation. Due to the complex repair works the reparation took more than a year and costed more than 14 million Euro [30]. In June 2019 the lock was closed again for 3 months to once again renew the rails for a stronger version [28] [8].

3.3.6. Conclusion

The most sensitive and delicate parts of a rolling gate are its rail - wheel connections which are often located under the waterline. The mentioned examples show that rails and/or wheels failed often well before their intended design life due to various reasons. As these failures came unexpected, they led to long down-time of the locks, in-dept investigations and expensive repair works. Table 3.1 shows an overview of the known wheel-rail failure cases of rolling gates.

Table 3.1: An overview of wheel-rail failure cases of rolling gates

Lock	Year of construction	Failure mode
Northern lock IJmuiden	1929	Rails rolled out
Western lock Terneuzen	1968	Broken wheel spokes (1978) and rolled out wheels (2000)
Roompotlock	1982	Both wheels and rail track rolled out (1986)
Kallolock Antwerp	1979	Rails rolled out (2006)
Kaiserlock Bremen	2011	Settlements and cracks in the sill and rolled out rails (2014)

For most cases, rolling out of wheels and/or rails mainly occurred due to reoccurring horizontal shear forces which were unaccounted for in the design. All gates are loaded in a horizontal direction by for instance a residual decay (just before opening), density differences or wave loads. However, it depends on the total gate and lock design how and if these horizontal forces are transmitted to the wheels and rails. The examples show that horizontal shear forces on the wheels and rails should be prevented at all costs. The design of the connection between gate and carriage and the gate horizontal guiding system are of utter importance to this. The case at the Kallolock showed that a one sided driving mechanism should be avoided as it creates an unfavourable eccentric horizontal force.

Another important factor is the specific geometry and the chosen materials for the wheels and the rails. The geometry and the chosen materials of the rails and wheels define the specific contact area and subsequently the maximum occurring stresses. Based on the Hertz theory and the analysis done in TNO's report on the Westsluis[64], the design of the wheels and rails should ideally form a line contact and have rounded edges to reduce peak stresses at the edges of the wheel and rail.[3]

An additional problem was the in-variance in extra weight due to shell growth and accumulation of silt in the gate. Nowadays the accumulation of silt is often prevented by applying an air pressure system on top of the buoyancy chambers, which blows the silt off the gate. However, shell growth and suppletion of debris is still a problem and should be accounted for in the design of a gate.

3.4. Advantages of conventional rolling gates

It is for good reason rolling gates are currently the dominant gate type for maritime navigation locks. The horizontal translating gate has a lot of advantages. One of the main advantages is the large possible width (and height) of the gate, which provides really wide locks that can allow the largest of ocean going vessels. The current longest gate is located in IJmuiden and has a length of 72 metres in combination with a height of 23 and a width of 10,5 metres.

These large widths are primarily possible due to the large structure of the gate and the bending loading profile in closed position. However, due to the lateral horizontal movement of the gate, the profile moving through the water and thus the hydraulic resistance is relatively small compared to the size and weight. A rolling gate can therefore be operated by a relatively small driving force.

In addition, the opening and closing times of these rolling gates are relatively low compared to other gate types and taking into account the large lock width which has to be traversed. An average rolling gate for a lock width of more than 40 metres takes only 3 till 5 minutes to close. The driving mechanism is relatively simple (often a cable winch) and has a low risk of failure due its low number of components and easy way of maintenance. The driving machinery is always located on one side of the lock chamber.

Another big advantage of a rolling gate is its possible two-sided loading. The rolling gate can seal off and take loads in both directions and is therefore ideal in tidal regions for which the water level differences over time. Due to the gate retracting in a horizontal way, there is no height limitation to the passing vessels. Structures on the lock itself even have to be placed a certain distance away from the side of the lock chamber to provide a large enough free profile for the protruding parts on top of a vessel. Another advantage of the gate retracting in lateral direction is its safe storage in open position. Therefore the gate only has a risk of collision in closed position.

Some of the positive features of a rolling gate depend on the specifics of the lock or choices made in the design phase. A possible feature is the ability to use the gate chamber as a dry dock. The rolling gate can then be maintained inside the chamber and does not have to be moved elsewhere. Depending on the total lock design this can reduce maintenance time and non-availability of the lock passage function. Another extra possible feature of the rolling gate is its use as a roadway bridge. In case traffic needs to be able to cross, the rolling gate can function as a bridge which eliminates the need for a separate bridge. This requires good traffic guidance as gates and thus the roadway can be open one at a time. For some locks, levelling the water in the lock can be done through the gate instead of through a separate expensive and complex culvert system. However, for larger gates and head differences this option is often not viable due to the large hawser forces on vessels created by the flushing jets.

The conventional rolling gate is a proven system which has been applied for many years. Therefore, expertise on this gate is widely available and organizations and operators of these lock/gate types know how to maintain and operate these type of gates.

[3] The advantages and disadvantages of a line vs. point contact are further discussed in Section 8.2.

A summary of the advantages of a rolling gate:

- Large possible width
- 2-sided loading
- Low opening/closing times
- Low hydraulic resistance of the gate during opening/closing
- Simple driving mechanism (low risk of failure, low number of components)
- Clear space above the door (no limitation for large vessels)
- Safe to collision in gate chamber
- Gate chamber can function as a dry dock
- Can be used as a roadway bridge
- Flushing through the gate if possible
- Well proven system, expertise widely available

3.5. Disadvantages of conventional rolling gates

While a rolling gate has many advantages and is the predominant type of gate for large maritime navigation locks, this gate types also has some disadvantages and recurring problems. Some of these disadvantages have already been described in the section about non-availability of rolling gates and will be summarized here.

One of the most important disadvantages of a conventional rolling gate are the hard-to-reach mechanical components (rails, roller carriages, push-off devices etc.) which are located deeply under water. Therefore inspection and maintenance has either to be performed under water (e.g. a diver team or diving bell caisson) or by bringing the components above the waterline. Which is both cost and time consuming and can lead to down-time of the lock. Due to the components being under water and difficult to inspect the exact state is unknown for most of the time.

Due to the maritime navigation lock being located in a saline environment, the (steel) materials need to be protected against corrosion. This requires a specialized coating system or cathodic protection which is very costly and also requires extra maintenance. Due to the gate's location at sea, shell growth occurs on the surfaces and material and sand supplements sinks into the sill and other parts in the gate. These add extra gate weight to the gate and thus higher unknown variable loads.

The wheel/rail failure analysis showed that wheel and rails are delicate parts which have a risk of early unexpected failures like rolled out or broken wheels and rails. The exact probability of occurrence is unknown, but the consequences are disastrous as (especially for the rail) it will lead to long non-availability of the lock complex.

In closed position the gate is vulnerable to ship collision. In case of such a collision the gate may not be able to be retracted into its chamber. In an even worse scenario, the gate is damaged such that it creates an open connection between the upper and lower waterbodies and the water separation and high water retention functions have both failed.

Due to the perpendicular movement of the gate with respect to the lock direction, the lock requires a lot of space on the side of the lock for the gate chamber structure. This can be up to 2,5 times the width of the lock itself. Due to the high loads and the heavy gate structure the rolling gate requires an extensive concrete foundation for the recess, chamber and sill and rail track. Also, a rolling gate is really heavy due to its size and massive steel structure. It's placement on location is often a challenge and the gate requires many buoyancy chambers and accompanying air pressure systems to provide lift for placement and during normal operation.

A summary of the disadvantages of a rolling gate:

- Delicate parts located under water are hard to reach. Exact state is relatively unknown.
- Inspection and maintenance is costly in time and money. Can lead to down-time of the lock.
- Shell growth and material supplements on the gate
- Salt environment requires protection which gives high cost/maintenance
- Risk of rolling out of rails and/or wheels which has major consequences
- Vulnerable to ship collision when in closed position
- Large lock width due to perpendicular movement of gate
- Requires extensive concrete foundation

4

New gate concepts

This chapter presents new gate design concept variants. Firstly, the design goal, the points of parity and difference with respect to a conventional gate and the process of coming up with new ideas and concepts are elaborated in Section 4.1. Section 4.2 then elaborates the criteria to evaluate all of the new concepts with. The explanation of the new gate concept variants and their ranking with respect to each criterion are then touched upon in Sections 4.3 till 4.8. Lastly, Section 4.9 provides an overview with the ranking of all the criteria and concepts, and draws intermediate conclusions.

4.1. Design goal and points of parity and difference

As was concluded in the Chapter 3 Section 3.3, the wheels and rails of conventional rolling gates located under water are a risk to the availability of the lock complex. These sensitive and high loaded parts are located under water and are therefore hard to reach, which makes inspection, maintenance and/or replacement difficult and costly.

The design goal is to design a horizontal translating gate for which all sensitive and heavily loaded mechanical parts are both easily accessible and located above the water.

The hypothesis is that this will lead to less down-time and non-availability of the lock, as the lock is not blocked while doing an inspection or replacement of these parts. In order for this to work, the lock would require double gates on each side of the lock, to use the 2nd gate in case the 1st gate is under maintenance. Otherwise, replacement still imposes non-availability of the total lock complex. Also, as the mechanical parts are now all easily accessible, inspection is easier and can be done more regularly. Signs of technical failure can be noted earlier and mitigating actions can be taken before failure occurs. Failure of the wheels and rails does not lead to non-availability of the total locking function, as all repair works can be performed without interfering the waterway.

At the moment, the wheelbarrow (~65%, see appendix A) and wagon (~30%) rolling gate are the dominant gate types applied in maritime navigation locks with a width of more than 40 meters. Therefore both the conventional wheelbarrow and wagon rolling gate types will function as a base case to evaluate and compare new design variants to.

4.1.1. Changes with respect to conventional rolling gates

The last two sections of Chapter 3 described the advantages and disadvantages of currently applied conventional rolling gates. It is useful to know to what extent the new designs may solve some of these shortcomings. A distinction is made between shortcomings which are completely removed, which are mitigated and which are insoluble by the new design variants. The probable outcome is noted in brackets for each of the shortcomings below. The disadvantages that may be worsened or mitigated are highlighted in bold.

- Delicate parts located under water are hard to reach. Exact state is relatively unknown. **(removed)**
- Inspection and maintenance is costly in time and money. Can lead to down-time of the lock. **(mitigated)**
- Shell growth and material supplements on the gate (insoluble)
- Salt environment requires protection which gives high cost/maintenance (insoluble)

- Risk of rolling out of rails and/or wheels which has major consequences **(insoluble/mitigated)**
- Vulnerable to ship collision when in closed position **(insoluble/worsened)**
- Large lock width due to perpendicular movement of gate **(insoluble/worsened)**
- Requires extensive concrete foundation **(insoluble/worsened)**

With respect to the advantages of the conventional rolling gate, the following changes may occur in the new design. The advantages that may be altered are highlighted in bold.

- Large possible width (unaltered)
- 2 sided loading (unaltered)
- Low opening/closing times **(unaltered/worsened)**
- Low hydraulic resistance of the gate during opening/closing (unaltered)
- Simple driving mechanism **(unaltered/worsened)**
- clear space above the door (unaltered)
- Safe to collision in gate chamber (unaltered)
- Gate chamber can function as a dry dock (unaltered)
- Can be used as a roadway bridge **(unaltered/worsened)**
- Flushing through the gate if possible (unaltered)
- Well proven system, expertise widely available (not applicable)

4.1.2. Points of parity and difference

The starting point for the design is the conventional rolling gate. The conventional rolling gate (with at least one carriage located under water) has many advantages that should be kept in the new design and thus should not be changed. Those are defined as the points of parity. These are the things which should remain the same for the conventional gate and all new design variants.

Points of parity:

- Free space above the gate (no limitation in height for large vessels)
- The transverse movement of the gate (with respect to the lock direction)
- 2 sided loading of the gate
- Low hydraulic resistance of the gate during opening/closing
- Safety to collision in gate chamber
- Gate chamber can function as a dry dock
- Flushing through the gate if possible

The points of parity are offset by the points of difference: the things which will differ between the conventional gate and the new designs. Most of these points are used to determin the criteria on which the gates are scored relative to each other and the conventional gates.

Points of difference:

- The way the vertical loads are transferred to the foundation
- The way horizontal loads (especially during opening and closing) are transferred. Thus the guidance system
- The accessibility and maintainability of mechanical components
- The amount of mechanical components
- The constructability of the gate system and its proof of concept
- The required lock space
- The size and material used for the gate and its additional components
- Impact of a collision if gate is in closed position
- Opening/closing time
- Possibility (or not) to use as a road bridge?
- The driving mechanism

4.1.3. Idea generation

The new variants are designed to comply to the mentioned design goal. Multiple design tools are used to come op with new designs. The most import one being the morphological chart. Such a chart is used to define possible solutions for different parts or aspects. These separate solutions can then be combined to find new designs. Appendix B shows two of the initial morphological charts that have been used. Another method to find and check new concepts was by building some of the designs in 3D from K'nex to see if it could work. Section B.2 of Appendix B shows some of the constructed K'nex models.

4.2. Criteria

This part describes all the criteria used to evaluate and rank the new gate variant designs. Most of the ranking criteria are based upon the points of difference mentioned in the previous paragraph. The following criteria are used:

Spread and balance of vertical forces
This criterion ranks the complexity and way of the transfer of vertical forces for each of the variants. Due to the no underwater mechanical equipment design principle, the transfer of vertical forces through the gate changes completely. For each of the variants this transfer and spread of forces and the complexity of the required vertical load balance is different. A more complex system for which extra load balancing action is required is considered to be negative.

Spread and balance of horizontal forces
This issues the way horizontal forces are transferred to the foundation and how these forces are spread out. The design of the gate has an impact in how these forces can be transferred. If forces can be easily transferred and the gate is more stable (compared to other variants) it is considered positive.

Accessibility of mechanical components
One of the aims of the new variants is the increased accessibility of mechanically moving components. This criterion ranks to what extend the gate parts can be reached for inspection, maintenance or revision. Parts which are located above the waterline and in an easily reachable place are logically scored higher than parts which are located deeply under water.

Amount of mechanical components
Besides the accessibility, the number of mechanical components is also of importance. Extra components (easily accessible or not) will always lead to extra inspection and maintenance costs. An increase of movable parts often leads to a higher probability of failure for the total system.

Proof of concept
The proof of concept refers to the complexity of the design and the constructability of the variant. The criterion takes into account if the techniques used in the design have already been applied in a certain way or if it is totally new. A new design which never has been build before has a lower rank as knowledge is not yet present and therefore design and construction will probably take longer or will be more costly. Also, the complexity and size of the design will define part of the constructability of the gate.

Total use of lock space
Due to the size of the gate and added extra components the required space of the lock may be large. This criterion ranks the space usage of each of the variants. Increased space usage is regarded as negative. Especially a wider lock (perpendicular to the lock direction) is unwanted as a maritime navigation lock often has to fit in immovable existing surroundings. Also, both a wider and longer lock will naturally lead to higher construction costs.

Material usage
The material usage depends on the size of the structure(s). Most components will probably be constructed of steel. An increase in material usage has its downside with respect to costs and sustainability. Therefore a larger amount of material is negatively ranked.

Impact of a ship collision
All gates in navigation locks have a certain probability of a collision with passing ships and vessels. However, the risk of such a collision is also defined by its consequences (risk = probability * consequences). This criterion looks at the consequences of such an collision. The impact of a collision on the gate structure is of importance. Can the gate still be retracted after a collision? And is the operating system still functional after a collision? Those are questions which will define the score with respect to this criterion.

Gate opening and closing time
This criterion ranks the opening and closing time of the gate. Due to added components or structures in the new variants opening and closing times may increase. This impacts the total lock passage times for vessels. A longer passage time is considered as negative as laying still costs money for the vessels.

4.2.1. Criteria ranking system

Each conceptual variant is evaluated with respect to the criteria in a qualitative way. The review of each criterion is done with words and a judgement in pluses and minuses. The ranking is a five points scale and varies from -- til ++ and is done relative to all the conceptual variants and the base cases. Due to this ranking method no distinction is made in the importance of the individual criteria compared to the rest. It is merely used as a first analysis to distinguish the significant differences between the possible solutions and the conventional gates and to give a quick qualitative overview of the ranking of the concepts.

4.2.2. Important aspects which are not taken into account

The fore mentioned criteria are useful to indicate the differences between the possible variants. However, some other important aspects have deliberately not been taken into account for various reasons. These reason are given below:

Cost

Costs are an important aspect for the selection process of a gate type. However, costs aspects are not yet taken into account at this stage, as the conceptual design of the variants has not been worked out well enough yet and thus nothing meaningful can be said about it. Off course cost should come into play into a later stage.

Road connection possible

The road connection function over the gate is an optional function. It can be beneficial in some situations as no separate bridge structure has to be constructed. A road connection is possible for all the proposed variants and therefore is not compared as a criterion. However, it should be noted that the integration of such a road connection is easier for certain variant types. This can play a role in the further design of one of the variants.

Driving system

The type of driving system and the location of the driving system do have an impact on the loading and the lay-out of the gate and gate chamber structure. However, the driving system does not directly influence the choice of the proposed concepts. Therefore it is not taken into account during the evaluation.

4.3. Rotating bascule beam rolling gate

The bascule beam rolling gate concept is a combination of the already existing bascule beam and a rolling gate (see Figure 4.1). A beam with a counterweight (bascule) is located on both sides of the gate. The bascule beam is wider than the gate itself, as it has to be connected to the fixed rotating point in the bascule chambers which are located on both sides of the gate chamber. Rolling tracks are located on the bascule beam which, in closed position, connect to the rolling tracks in the gate chamber. This makes it possible for the gate to move in open and closed position.

The gate hangs on multiple carriages which are connected to the gate by a hinges that can move in perpendicular lateral direction to the opening and closing direction of the gate. A conventional gate would have two carriages, but this gate type can apply even more carriages to spread out the loads. In closed position and during opening and closing of the gate the vertical load (of mainly the gate its weight) is transferred to the foundation via the bascule beam. This beam therefore has to be able to both carry its own weight and the (reduced) weight of the gate.

Due to the hinges the gate can move sideways and therefore the gate can seal watertight in closed position. The gate fully hangs on the carriages and therefore has a natural tendency to centre itself which is advantageous with respect to the horizontal load balance. Just before opening and during opening and closing, the push-off devices which are located at the top of the gate push against the bascule beam to transfer the horizontal loads acting on the gate and put the gate in a central position. The top of the gate is actively guided against the bascule beam and the bottom of the gate is passively guided against the sill by means of UHMWPE and/or timber profiles.

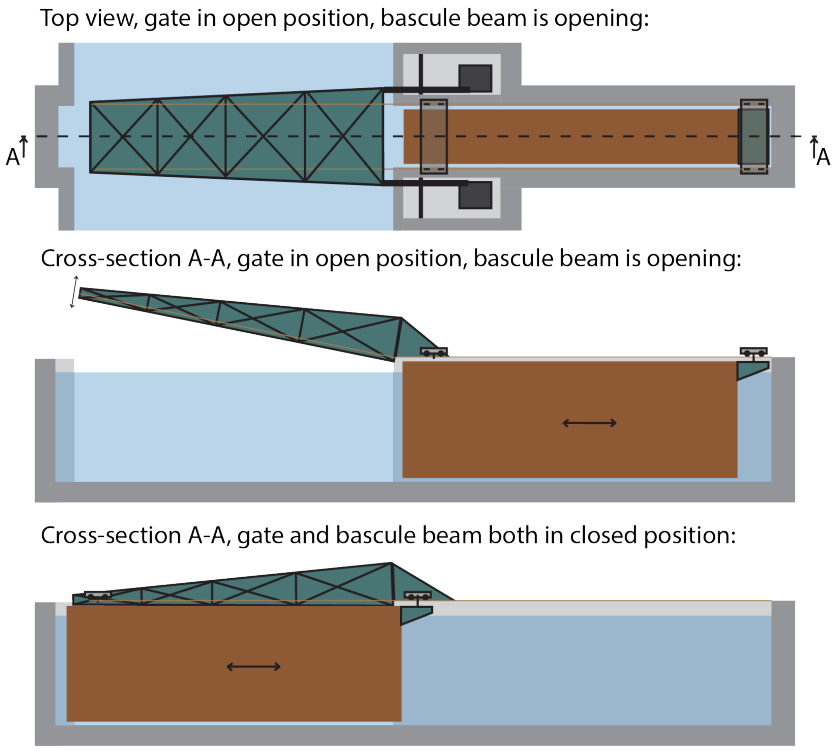

Figure 4.1: Working principle of a rotating bascule beam rolling gate

Advantages:

+ All mechanically moving systems are located above the waterline and relatively easy accessible
+ The gate fully hangs on the beam and is therefore stable during opening and closing as it centres automatically
+ Horizontal guidance is favourable as horizontal loads can both be transferred by the bascule beam and the sill
+ The bascule beam can also be applied as a fully functioning traffic bridge which both transports traffic over the lock and carries the gate. This makes it unnecessary to build a separate bridge structure.

Disadvantages:

– Complex mechanical connection due to two moving bodies and connection of rails. Connection between solid rail (on recess) and moving rail (on bascule beam) is critical and a risk. It creates a nudge and therefore an expected increase of local fatigue due to wheels rolling over it
– More space required for a large cellar on both sides of the gate to house the bascule contra-weight. Thus an increased width per gate
– The operating time of the gate increases as the beam first has to close before closing the gate
– Collision may lead to gate being stuck in lock due to bascule beam damage
– Two driving mechanisms, one for the gate and one for the bascule beam
– More complex concrete structure necessary for the placement of the bascule beam on both sides of the gate chamber

4.3.1. Review of criteria

Spread and balance of vertical forces (++)

The transfer of vertical forces is relatively easy due to the placement of the bascule beam. The vertical balance of the bascule beam is obtained by the lever arm and the contra-weight. This beam is constructed such that it can carry the residual weight of the gate and its own weight.

Spread and balance of horizontal forces (++)

The bascule beam can also be used to transfer horizontal forces from the top of the gate to the foundation. This is really favourable as the gate is supported at the top during the whole opening and closing process. Push-off devices push the gate in the middle position. The bottom of the gate is guided by

UHMWPE and timber beams against the sill. During opening and closing the gate is thus supported both on the top and bottom which is really favourable. Also, due to the gate fully hanging, centring the gate is relatively easy.

Accessibility of mechanical components (+)
All mechanical components are located above the water and accessible. The rotating point and the bascule and bascule driving system can be reached inside the bascule chambers which are located just besides the gate chamber. The only downside is the upwards location of the rails if the bascule is in open position. The rails on the beam can therefore only be inspected and maintained while the beam is closed.

Amount of mechanical components (-)
The number of mechanical components increases significantly. The moving mechanism of the bascule beam is completely added to the amount of mechanical components. As the gate completely hangs, the amount of roller carriages can also be increased (which will lower the loads and thus the necessary strength of these wheels and carriages.)

Proof of concept (-)
Both the rolling gate and the bascule beam (bridge) have been applied before and are constructable. However, these techniques have never been combined before. This imposes a risk to the constructability of the total system. Both these systems have to be constructed really close to each other to be combined. This can form an issue for the concrete foundation of the bascule system. Also, the connection between the rails on the gate chamber and the bascule beam is a risk.

Total use of lock space (-)
The bascule chambers on each side of the gate increase the necessary width per gate. Thus the total length of the lock increases.

Material usage (--)
The bascule beam requires a lot of extra material. Also, the foundation of the bascule requires an extra concrete foundation and bascule chamber which is material costly.

Impact of a ship collision (-)
The impact of a ship collision can be relatively large as the beam may also be a risk to being hit. The consequence may be that the beams (and/or the gate) cannot be retracted anymore.

Gate opening and closing time (--)
The gate opening and closing time increases as the beam first has to be opened or closed before the gate can be moved. For a conventional gate the opening time is 3-5 minutes. This time will likely be doubled by the addition of the moving time of the bascule beam. However, the total lock passage time (including vessel moving, mooring, filling & emptying etc.) is for a conventional large maritime navigation lock on average more than 45 minutes[37]. Thus the total passage time is increased by 5 till 12% due to the added opening/closing time of the beam.

4.4. Rolling cantilever beam rolling gate

The rolling cantilever beam rolling gate is a gate system in which the gate is supported during opening and closing by a movable rolling beam. The rolling cantilever beam rolls out first, creating a rail track over the chamber, making it able for the gate to close. The rolling cantilever beam is longer than the gate itself, as it requires a cantilever arm with a counterweight to balance the vertical loads during opening and closing. The operating time of the gate increases as the beam first has to close before the gate closes.

The gate hangs on two carriages which are connected to the gate by a hinges that can move in perpendicular lateral direction to the opening and closing direction of the gate. The front carriage rolls over the rails which are located on the cantilever beam, while the back carriage rolls over rails that are located on the recess. The back carriage is attached to an extension arm in a similar manner as the top carriage at a conventional wheelbarrow gate. A free profile is required at the bottom of the cantilever beam for the movement of both carriages. The front carriage is wider compared to the back carriage, as the rails attached to cantilever and the cantilever beam itself have to be able to move around the back carriage (see the cross-section in Figure 4.2).

In closed position and during opening and closing of the gate the vertical load (of mainly the gate its weight) is transferred to the foundation via the bascule beam. This beam therefore has to be able to

both carry its own weight and the (reduced) weight of the gate. Both the rolling gate and the cantilever beam have a separate driving system. During opening and closing of the cantilever beam the gate has to be locked in the recess to ensure it does not start moving as well.

Due to the hinges the gate can move sideways and therefore the gate can seal watertight in closed position. The gate fully hangs on the carriages and therefore has a natural tendency to centre itself which is advantageous with respect to the horizontal load balance. Just before opening and during opening and closing, the push-off devices which are located at the top of the gate push against the bascule beam to transfer the horizontal loads acting on the gate and put the gate in a central position. The top of the gate is actively guided against the bascule beam and the bottom of the gate is passively guided against the sill by means of UHMWPE and/or timber profiles.

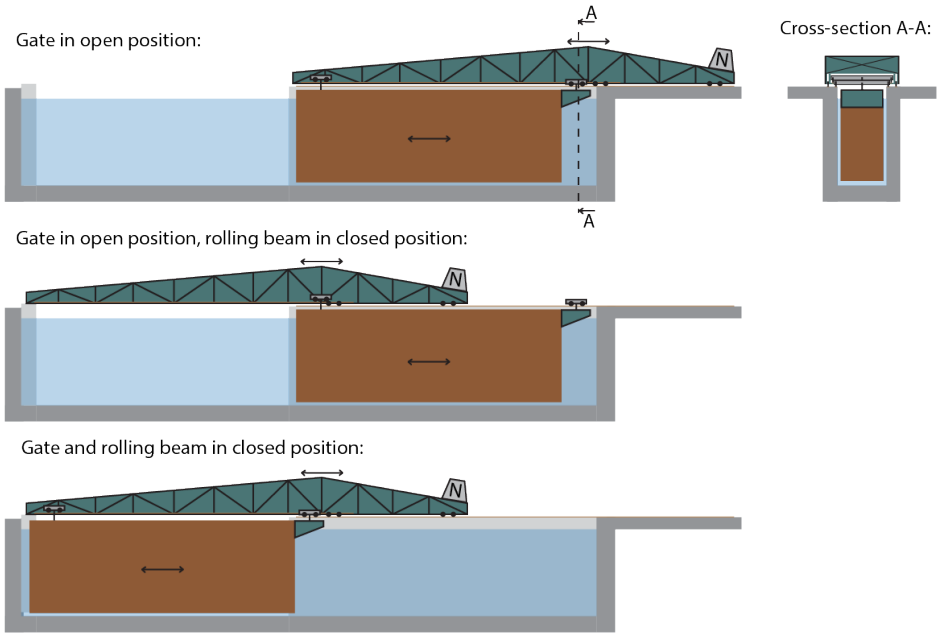

Figure 4.2: Working principle of a rolling beam rolling gate

Advantages:

+ All mechanically moving systems are located above the waterline and relatively easy accessible
+ The gate fully hangs on the beam and is therefore stable during opening and closing as it centres automatically
+ Horizontal guidance is favourable as horizontal loads can both be transferred by the bascule beam and the sill
+ The bascule beam can also be applied as a fully functioning traffic bridge which both transports traffic over the lock and carries the gate. This makes it unnecessary to build a separate bridge structure

Disadvantages:

– The operating time of the gate increases as the beam first has to close before closing the gate
– Collision may lead to gate being stuck in the lock due to damage to the rolling beam
– Two driving mechanisms, one for the gate and one for the rolling cantilever beam
– The cantilever beam increases the required width and length per gate
– The rolling beam requires an extended foundation
– The cantilever beam adds extra mechanically moving and sensitive parts required to move the beam. Total rail length is longer and amount of wheels is more compared to conventional gates

4.4.1. Review of criteria

Spread and balance of vertical forces (++)

The transfer of vertical forces is relatively easy due to the placement of the roller beams. However, the beams itself require a good vertical balance system with a cantilever arm and contraweight. Due to the gate fully hanging on the beams the balance and loading on the carriages is favourable.

Spread and balance of horizontal forces (++)
The rolling beams can also be used to transfer horizontal forces from the top of the gate to the foundation. This is really favourable as the gate is supported at the top during the whole opening and closing process. Push-off devices push the gate in the middle position. The bottom of the gate is guided by UHMWPE and timber beams against the sill. During opening and closing the gate is thus supported both on the top and bottom which is really favourable. Also, due to the gate fully hanging, centring the gate is relatively easy.

Accessibility of mechanical components (++)
The mechanical components are all located above water and easily reachable when both gate and rolling beam are in open position. Inspection and maintenance can therefore easily be performed. The only downside may be the large beam structure which can be an obstacle to reach certain places like for instance the front carriage.

Amount of mechanical components (-)
The amount of mechanical moving components increases significantly. Besides the rolling carriages which are also applied in the conventional gates, extra wheels, rails and driving mechanisms are required to move the rolling beam.

Proof of concept (-)
Both the rolling gate and the rolling beam (bridge) have been applied before and are constructable. However, these techniques have never been combine before. This imposes a risk to the constructability of the total system. The combination makes the connection and the total system more complex.

Total use of lock space (-)
The rolling cantilever beam is wider than the gate recess itself and therefore the width required for each gate increases. Also, the rolling beam requires an extended cantilever arm with a contra-weight. This also increases the necessary total lock complex width as this cantilever part is longer than the gate itself.

Material usage (--)
The rolling beam requires a lot of extra material compared to a conventional rolling gate. The gate chamber foundation needs to be adjusted to carry the beam (and the gate) and the rolling beam itself also is a large heavy structure.

Impact of a ship collision (-)
The impact of a ship collision can be relatively large as the beam also risks being hit. The consequence may be that the beam (and/or the gate) cannot be retracted anymore.

Gate opening and closing time (--) The gate opening and closing time increases as the beam first has to be opened or closed before the gate can be moved. For a conventional gate the opening time is 3-5 minutes. This time will likely be doubled by the addition of the moving time of the bascule beam. However, the total lock passage time (including, vessel moving, mooring, filling & emptying etc.) in a conventional large maritime navigation lock is on average more than 45 minutes (source: HS Locks dictaat) thus the total passage time is increased by 5 till 12% due to the added opening/closing time of the beam.

4.5. Cable stayed rolling gate

The Cable-stayed rolling gate (as seen in Figure 4.3) is a wheelbarrow type of rolling gate in which the lower carriage has been replaced by a system of cables and a tower. The cables provide vertical support to the gate by a connection over the top of a tower to a winch. This winch has to tension the cables in order to carry the vertical loads. During closing and opening the winch has to operate very precisely to provide stability to the gate. The height of the tower probably has to be relatively high in order to decrease the required tension forces in the cables, as the vertical force component of the gate has to be carried partly by these cables.

The tower is located at the end of the recess but such that the required free-profile for vessels is assured. In this design the tower houses 8 rollers over which the cables roll. The 2 cables attached to the end of the gate are located most outward to ensure stability. Each of the subsequent cable locations is located more inwards. All of the cables roll over a winch at the end of the recess. Each winch can be tensioned to the required tension strength. The horizontal driving mechanism opens and closes the gate by means of the roller carriage. During opening and closing the winches and the tension forces in the cables have to be monitored really careful and adjusted accordingly.

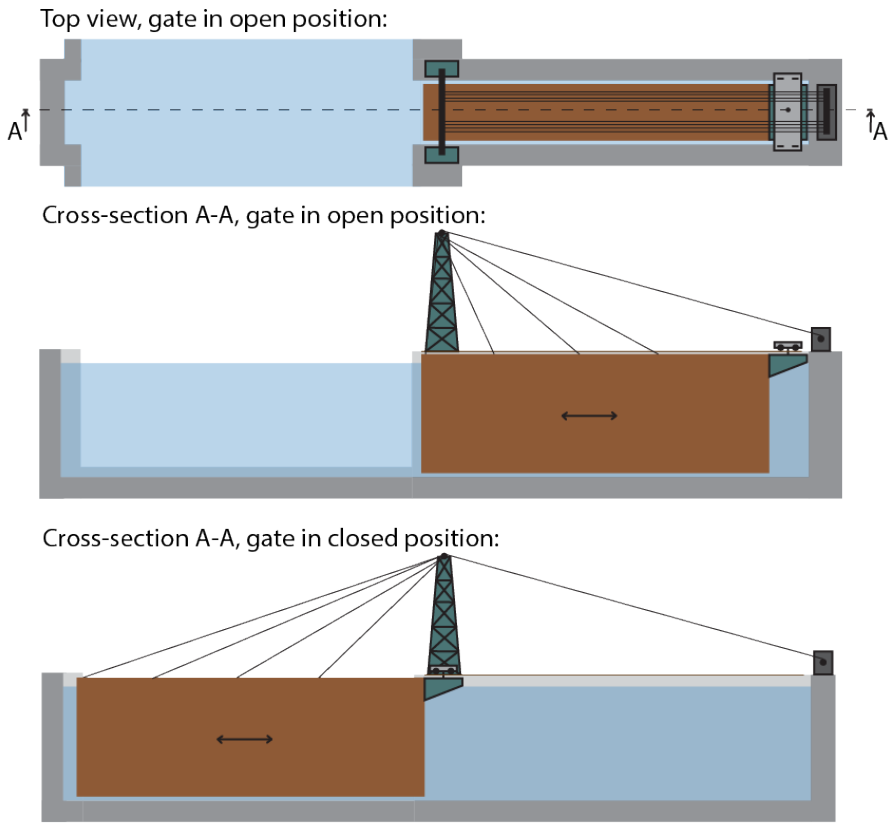

Figure 4.3: Working principle of a cable-stayed rolling gate

Advantages:

+ All mechanically moving systems are located above the waterline
+ Only one roller carriage
+ Same operating time as current gates

Disadvantages:

– Complex operating system due to cables being adjusted exactly to the correct length and tension
– Requires strong and adaptable winches for each of the cables
– Could be unable to close after collision due to snapped or damaged cables/winches
– A high tower is necessary
– Horizontal balance is worsened compared to conventional gates

4.5.1. Review of criteria

Spread and balance of vertical forces (--)
The transfer and balance of vertical forces is really complex due to the cables each having a different angle and the required difference in tension on all of the cables. A complex monitoring system which is coupled to the power of the winches may be able to balance this. But it has never been applied and will probably be really complex or even non-executable.

Spread and balance of horizontal forces (-)
The transfer of horizontal forces can only be provided by the push-off devices at the top of the gate recess and chamber and by the UHMWPE or timber beams sliding against the sill.

Accessibility of mechanical components (++)
All mechanical components are located above the water. The mechanical components such as the winches at the end of the gate are easily accesible. The rollers at the top of the tower over which the cables roll are accessible by the stairs in the tower.

Amount of mechanical components (-)
The amount of mechanical components is relatively large due all the cables, winches and cable rollers. Also, still one roller carriage is applied, although above the waterline.

Proof of concept (--)
The cable-stayed rolling gate is a completely new system type which has never been used in such a fashion. The vertical bearing requires a complex system of cables and winches which has never been constructed in such a combination. The tower and cable system may be able to be constructed but the execution and monitoring can be problematic.

Total use of lock space (+/-)
The total use of lock space almost stays the same as the gate size doesn't change. The width required per gate may increase somewhat due to the added width of the tower and its foundation.

Material usage (-)
Some extra material is necessary for the tower and all the cables.

Impact of a ship collision (+/-)
The impact of a ship collision is comparable to the conventional gates. The risk of failing buoyancy chambers is still there. The cables may be an extra liability as they can fail due to the collision and as a result the gates vertical load transfer fails and the gate cannot be retracted anymore.

Gate opening and closing time (+/-) The gate opening and closing time is comparable to the conventional gate types.

4.6. Cantilever rolling gate side extension

The cantilever rolling gate side extension is a rolling gate which is constructed as a cantilever system for which all rolling supports are located on an extension to the side of the effective gate. In a way, the gate 'hangs' in the gate recess, see Figure 4.4. The vertical balance of the cantilever is ensured by contra-weight located at the outer carriage and by extra uplifting buoyancy chambers inside the effective gate. Due to the cantilever arm, the total gate length and thus the gate chamber length is increased. The carriages are connected to the gate by hinges which ensure the perpendicular horizontal movement of the gate in closed position. These roller carriages roll over rail tracks located on the extended gate recess.

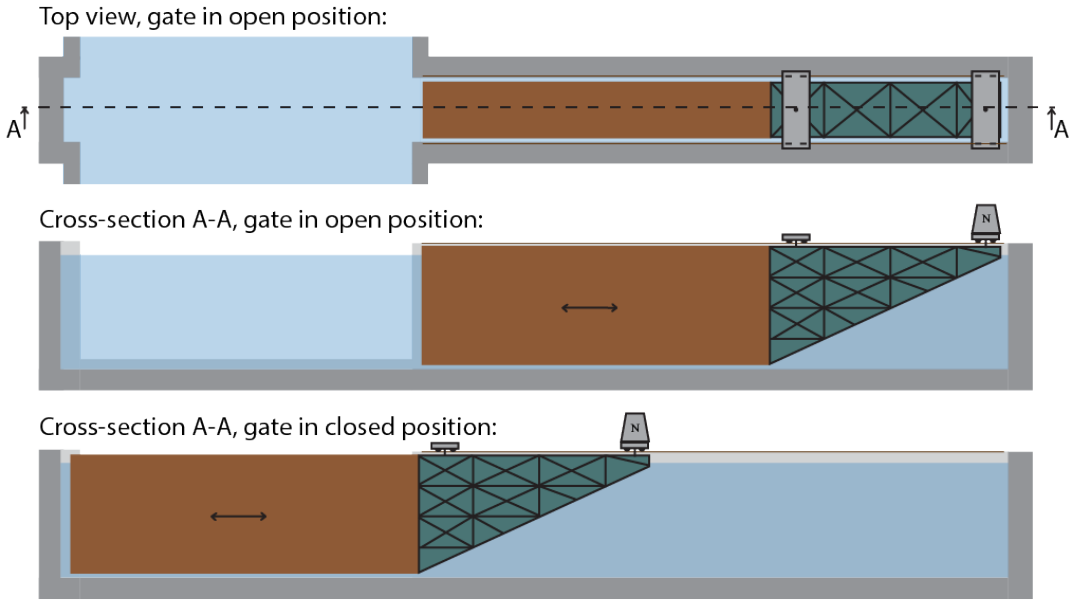

Figure 4.4: Working principle of a cantilever (side extension) rolling gate

The effective height of the gate is used to transfer all the vertical internal forces and moments to the two rolling supports. In order to acquire vertical balance in the gate the contra-weight and added upward buoyancy forces should counter the downward forces of the gate. The aim is to have a downward force on both carriages under all loading conditions. Otherwise the cantilever will fail and the gate will float up or gets stuck.

The cantilever arm is also beneficial for the transfer of horizontal forces. Push-off devices are applied on top side of both ends of the cantilever arm. Due to the cantilever arm this results in a 'clamped' support in horizontal direction at the recess side of the gate, instead of a rotating support for conventional gates.

This is advantageous for the transfer of horizontal forces acting on the gate during opening and closing. Besides these active push-off devices the gate slides against the sill with an UHMWPE and/or timber profile.

Advantages:

+ All mechanically moving systems are located above the waterline
+ Effective height of the gate is used to lead forces to the roller carriages
+ Makes use of carriages in the same way as current gates
+ Same operating times as current gates
+ Due to the clamped support in horizontal direction the gate may be more resistant against a collision

Disadvantages:

– A large extra cantilever structure is needed to transfer the forces
– The length of the gate recess and the required foundation becomes much larger. Thus the width of the total lock complex is much wider
– Requires a lot of extra concrete for the extended gate chamber
– Balancing system for the cantilever system is complex. Delicate system required to ensure balance and limit the vertical forces on both carriages

4.6.1. Review of criteria

Spread and balance of vertical forces (+/-)
The balance and transfer of vertical forces is much more complex compared to the conventional gates. Balancing is delicate as the loads on the rolling carriages have to be limited to a certain degree. Therefore the use of counterweights and extra buoyancy is necessary to impose a downward force on the carriages at all time. The loading inside the gate is also completely different due to the cantilever mechanism, which has to be incorporated in the design of the gate. However, the already existing gate height and the added side extension is relatively favourable for the transfer of vertical forces and moments as the height of the gate itself is used.

Spread and balance of horizontal forces (+)
The cantilever extension creates an opportunity with respect to the transfer of horizontal forces. Due to the extension the gate can kind of be clamped in position which is favourable for the load transfer during opening and closing of the gate. Push-off devices are located at the top of the gate chamber and recess on both sides. Those will push the gate in a more central position. A push-off device is also present on the far end of the gate extension. This devices clamps the gate. The bottom of the gate will 'slide' against the sill with an UHMWPE or timber beam.

Accessibility of mechanical components (++)
All roller carriages and respective mechanical components are located above the waterline and easily accessible from ground level.

Amount of mechanical components (+)
The amount of mechanical components is equivalent to the conventional gate(s). The only difference being them located above water and in a different position.

Proof of concept (-)
Rolling cantilever systems (like a rolling bridge) have been constructed in the past, but never as a gate structure and in this size. The rolling carriage work in the same way as the upper carriage in a conventional wheelbarrow gate. However, the loads inside the gate are completely different compared to conventional gates due to the cantilever mechanism. The balancing and loading on the roller carriages is new and therefore adds extra risk to the constructability and design of this variant. Also, the cantilever extension has to be placed separately as the total gate including the extension cannot be floated in. This adds extra complexity to the construction and revision of the gate.

Total use of lock space (--)
The side extension which creates the cantilever increases the width of the lock chambers considerably. For conventional gates the total width needed for the gate chamber and recess is often more than 2,5 times the actual width of the lock chamber. A rough estimate for this cantilever variant is 4 times the actual lock width.

Material usage (--)
The added side extension logically increases the material usage. The concrete foundation for the gate chamber has to be larger and the extra extension also uses more steel. The extension is estimated to be 1/2 the length of the actual gate. Due to the triangular form the extra needed steel is therefore assumed to be 1/4 of the actual gate.

Impact of a ship collision (+)
Due to the clamped extension the total gate may have an even beter resistance against a collision than the conventional gate(s). However, collision imposes still a big risk regarding the failure of the buoancy chambers and the possible failure to retract the gate back in open position.

Gate opening and closing time (+/-)
The gate opening and closing time is comparable to the conventional gate types.

4.7. Cantilever rolling gate top extension

The cantilever rolling gate side extension is a rolling gate which is constructed as a cantilever system for which all rolling supports are located on an extension to the side but above the effective gate, see Figure 4.5. In a way, the gate 'hangs' in the gate recess. It is as if a bridge is added on top of the gate structure to transfer all the forces to the carriages. Due to the cantilever arm being on top of the gate, the gate recess does not have to be extended. However, the added structure on top needs to carry all the vertical internal forces and moments to the supports by its own. It cannot make use of the effective height of the gate. Also, the connection of the extended gate structure to the carriages could be complex due to the construction being above the carriages/rails. Instead of the side extension where the gate 'hangs', the top extension 'leans' on the carriages.

The vertical balance of the cantilever is ensured by contra-weight located at the outer carriage and by extra uplifting buoyancy chambers inside the effective gate. Due to the cantilever arm, required foundation and width of the total lock is increased. The carriages are connected to the cantilever arm by UHMWPE compression supports which ensure the perpendicular horizontal movement of the gate in closed position. The roller carriages roll over rail tracks located on the extended gate recess.

The cantilever system works in the same way as for the cantilever rolling gate side extension mentioned in the previous section. The only difference being that the vertical forces are now transferred via the top extension instead of the side extension. This transfer through the top is less beneficial as it is not in line with the effective gate structure.

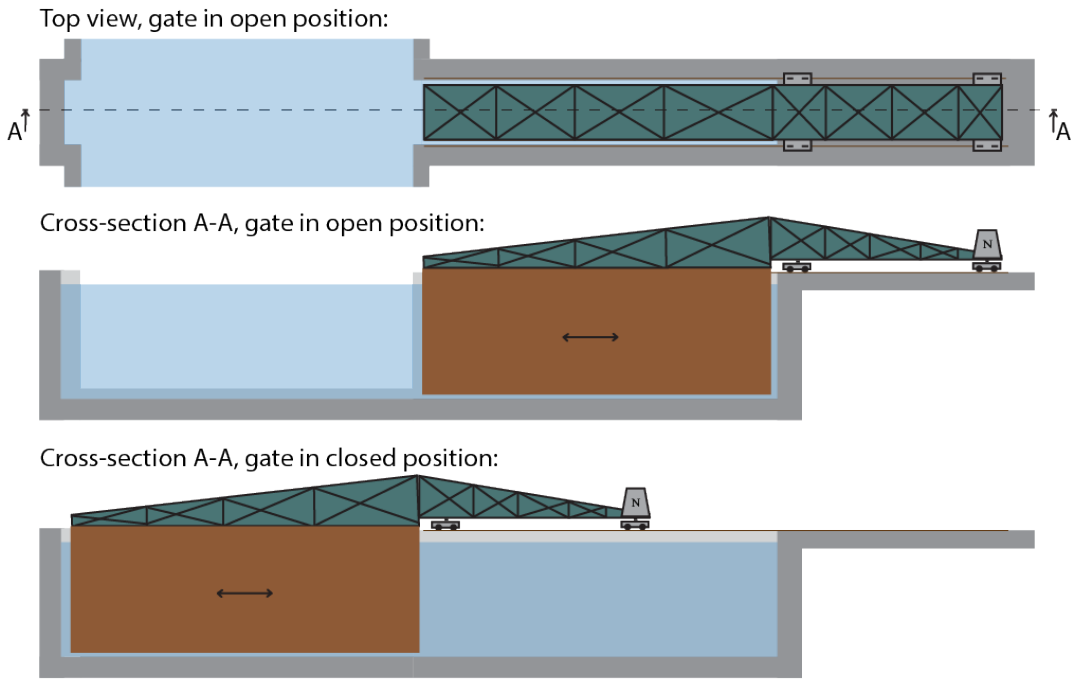

Figure 4.5: Working principle of a cantilever (top extension) rolling gate

Advantages:

+ All mechanically moving systems are located above the waterline
+ Makes use of carriages in the same way as current gates
+ Same operating times as current gates
+ Due to the clamped support in horizontal direction the gate may be more resistant against a collision

Disadvantages:

– Effective height of the gate is not used to transfer vertical forces to the supports
– A large extra cantilever structure is needed to transfer the forces
– The length required foundation becomes much larger. Thus the width of the total lock complex is much wider
– Balancing system for the cantilever system is complex. Delicate system required to ensure balance and limit the vertical forces on both carriages
– Connection from top structure to carriages is more complex compared to a hinge system.

4.7.1. Review of criteria

Spread and balance of vertical forces (+/-)
The balance of and transfer of vertical forces is much more complex compared to the conventional gates. Balancing is delicate as the loads on the rolling carriages have to be limited to a certain degree. Therefore the use of counterweights and extra buoancy is necessary to impose a downward force on the carriages at all time. The vertical forces acted upon the gate have to be completely transferred by the top extension to the roller carriages. For this variant the height of the gate cannot be used to transfer these vertical forces and moments (if compared to the side extension).

Spread and balance of horizontal forces (+/-)
The cantilever extension creates an opportunity with respect to the transfer of horizontal forces. Due to the extension the gate can kind of be clamped in position which is favourable for the load transfer during opening and closing of the gate. The bottom of the gate will 'slide' against the sill with an UHMWPE or timber beam. Push-off devices are located on the two ends of the cantilever arm and push the gate against the recess. Due to these two locations of push off devices the effective gate gets kind of clamped. One issue is the transfer of these horizontal forces from the top extension to the gate. Due to the extension being located at the top of the gate the horizontal forces cannot be transferred gradually to the top of the gate. This will give high peak loads at the corner between the effective gate and the cantilever beam.

Accessibility of mechanical components (+)
All roller carriages and respective mechanical components are located above the waterline and easily accessible from ground level. However, the rolling carriage are located below the cantilever structure and are therefore hard to replace as the cantilever structure blocks the removal path. This makes it more complex compared to the side extension.

Amount of mechanical components (+)
The amount of mechanical components is equivalent to the conventional gate(s). The only difference being them located above water and in a different position.

Proof of concept (-)
Rolling cantilever systems (like a rolling bridge) have been constructed in the past, but never as a gate structure and in this size. The rolling carriages support work in the same way as a lower carriage in a conventional gate. However, the loads inside the gate are completely different compared to conventional gates due to the cantilever mechanism. The balancing and loading on the roller carriages is new and therefore adds extra risk to the constructability and design of this variant. Also, the placement of the top extension probably has to be connected separately on site. This adds extra complexity to the construction and revision of the gate.

Total use of lock space (--)
For the top extension the chamber does not have to be increase. However, the foundation to transfer all the loads has to be longer. And the necessary width for the lock complex is significantly longer due to the added length of the cantilever extension. For conventional gates the total width needed for the gate chamber and recess is often more than 2,5 times the actual width of the lock chamber. A rough estimate for this cantilever variant is 4 times the actual lock width.

Material usage (--)
The added top extension logically increases the material usage. The concrete foundation for the cantilever extension has to be larger and the extra extension also uses more steel. As the top cantilever structure has to carry all the vertical forces and moments this structure is expected to be relatively large and therefore requires quite some extra (steel) material.

Impact of a ship collision (+)
Due to the clamped extension the total gate may have a better resistance against a collision than the conventional gate(s). However, collision imposes still a big risk regarding the failure of the buoyancy chambers and the possible failure to retract the gate back in open position.

Gate opening and closing time (+/-)
The gate opening and closing time is comparable to the conventional gate types.

4.8. Self-propelled floating gate

The concept of the self-propelled floating gate has been brought up by ANAST, part of the University of Liege. They based the idea on the already existing concept of a floating gate opened by tugs, which is already used for closing dry docks, canals and weirs. However, in this case the floating gate is not driven by the tugs but by a propeller system inside the gate (just like a boat). Most of the information regarding this concept which is presented here, is derived from a project review published by PIANC on InCom – WG29 [52]. This report mentions that the concept has already been considered on a project level, but has not yet been implemented.

The gate is designed as a large floating caisson with more room for buoyancy tanks (see Figure 4.6. If the gate needs to be moved, the weight of the gate is reduced by pumping out water from these tanks and therefore the gate starts floating. Inside the gate is a large tube with propellers which create a water flow and moves the gate in position. ANAST indicates a required power of 300 kW for a gate which is 70 x 23 x 7 meter. After the gate is moved into position the buoyancy tanks are filled again and the gate lays on the concrete floor.

This design completely avoids the mechanical frictions forces in vertical direction (no wheels and rails) and doesn't require a separate driving system as the driving system is integrated in the gate. However, the ANAST report mentions a critical issue concerning the stability of the gate. The floating gate is prone to roll and heave motions due to wave actions during opening and closing. This can lead to high loads on the horizontal guidance system as the gate may collide with the top and bottom guides. The gate can therefore not be used under high lateral waves which decreases the actual availability of this gate type.

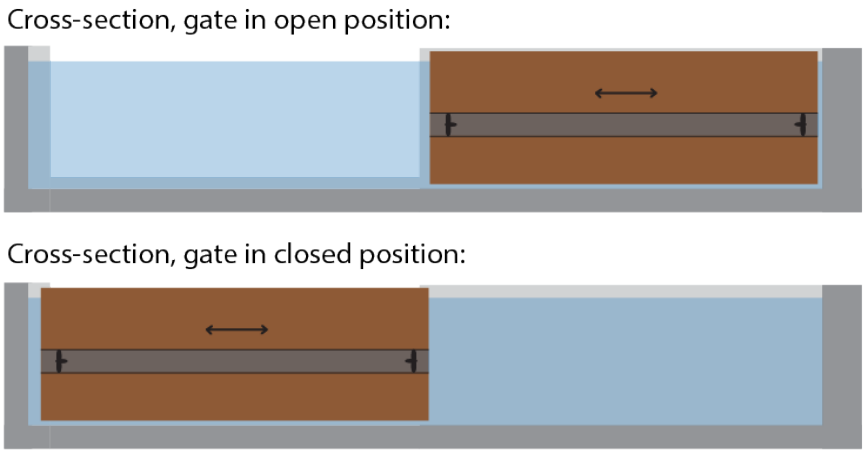

Figure 4.6: Working principle of a self-propelled floating gate

Advantages:

+ No heavy loaded rolling mechanism underwater
+ No carriages and rails required

Disadvantages:

- Buoyancy chambers have to be filled and emptied every gate procedure. Adds extra complexity and may lead to longer opening/closing times
- Has stability issues (Cannot be opened under high lateral waves)
- Moving mechanism and balancing system adds new type of maintenance
- Moving mechanism and balancing system are harder to access as they are inside the gate
- Gate has to be wider than normal to create enough floating stability

4.8.1. Review of criteria

Spread and balance of vertical forces (+)
This gate variant is floated in its position and therefore does not have to transfer any forces to the foundation. This is off course favourable for the spread of forces and the required foundation. The balance inside the gate is more of an issue as it requires stability in all directions. This is ensured by the placement of buoyancy tanks and an air pressure buoyancy levelling system.

Spread and balance of horizontal forces (--)
The design of the self-propelled floating gate has known issues regarding the horizontal floating stability. Studies show that the gate cannot be opened under high lateral waves. The gate can only be guided by guidance systems on the recess and gate chamber. This is a big downside of this concept.

Accessibility of mechanical components (--)
The accessibility of the components is not really good due to them all being located inside the gate or even under water. Off course the thrusters are loaded in a different way than the conventional roller carriages which are located under water. But still these parts are located under water and therefore harder to reach. Also the buoyancy levelling system is completely integrated in the gate and therefore can only be reached by entering the gate itself.

Amount of mechanical components (+)
The amount of mechanical components is reduced by the elimination of the rolling carriages and the winch driving system. The buoyancy levelling system and the thrusters/propellors add some new mechanical components but it's probably less compared to the conventional gate.

Proof of concept (-)
The concept has been applied for gates which don't have to be opened that often, but never for the case of a large navigation lock which needs to operational all year round. This imposes different requirements to the design and the concept has not yet been proven for this case.

Total use of lock space (+)
The lock space is reduced compared to conventional gates as there is no need for carriages and a driving mechanism at the end of the gate. The total required width of the lock is therefore a tiny bit smaller. Each gate is a bit wider to assure floating stability, but this is compensated compared to a conventional gate by the removal of the gate carriages and therefore does not change the total length of the lock.

Material usage (+/-)
The elimination of the roller carriages reduces the required material for the movement of the gate. However, the gate has to be wider for floating stability reasons and therefore requires more material for the steel gate itself.

Impact of a ship collision (-)
The buoyancy of the gate is even more important to the ability of the gate to be opened and closed. Therefore a collision (which may result in buoyancy leakage) can have a big impact. This is a risk for this gate type.

Gate opening and closing time (-) The filling and emptying of the uplifting buoyancy chambers needs to be done very precise and probably therefore requires some time. Also, the movement of the gate by the thrusters also needs to be done cautious and slowly as the speeding up and slowing down needs to be completely done by the thrusters/propellors. The opening and closing time will therefore be somewhat longer than a conventional gate.

4.9. Overview and conclusion

The previous sections described the conceptual variants which are possible within the design goal. Subsequently, each of these variants has been evaluated in writing and by a qualitative score for nine different criteria. Table 1 shows a summary of the rankings in plusses and minuses for each of the criteria and variants.

	Bascule beam rolling gate	*Rolling cantilever beam rolling gate*	*Cable-stayed rolling gate*	*Cantilever rolling gate (side extension)*	*Cantilever rolling gate (top extension)*	*Self-propelled floating gate*	*Conventional wheelbarrow rolling gate*	*Conventional wagon rolling gate*
Spread and balance of vertical forces	++	++	--	+/-	+/-	+	+	+/-
Spread and balance of horizontal forces	++	++	-	+	+/-	--	-	-
Accessibility of mechanical components	+	++	++	++	+	--	-	--
Amount of mechanical components	-	-	-	+	+	+	+	+
Proof of concept	-	-	--	-	-	-	+	+
Total use of lock space	-	-	+/-	--	--	+	+	+
Material usage	--	--	-	--	--	+/-	+/-	+/-
Impact of a ship collision	-	-	+/-	+	+	-	+/-	+/-
Gate opening and closing time	--	--	+/-	+/-	+/-	-	+/-	+/-

Table 4.1: Overview of criteria scores and concept variants

Important notice: This Multi-Criteria Analysis (MCA) does not contain any numerical values and does not distinguish how import one criteria is to another. Therefore, no total summary of scores is given. The analysis and the summarizing table can therefore only be used to give a short overview of qualitative scores and as a guidance to a first evaluation.

4.9.1. Evaluation of conceptual variants

In this section, each of the variants is shortly evaluated and compared with the conventional rolling gate types and the other concepts.

Rotating bascule beam rolling gate

Compared to the *conventional rolling gates*, the *Rotating bascule beam rolling gate* improves significantly with respect to the balance of horizontal and vertical forces and the accessibility of mechanical components. The addition of the beam requires more material and mechanical components, but the opening and closing of the gate is way easier. Opening and closing of the beam increases the total lock passage time per gate cycle as the beam first has to be brought into position before the gate can be moved. On the long term this added time may be compensated by the increased availability of the lock. The main issue compared to the *Rolling cantilever beam rolling gate*, is the connection of the bascule beam rails to the rails on the gate chamber. This connection will never be smooth. The little gap between the rails creates local increased stress points when the wheels of the carriages roll over it, which is really unfavourable for fatigue loading of the rails and the wheels.

Rolling cantilever beam rolling gate

The *Rolling cantilever beam rolling gate* functions the same as the *Rotating bascule beam rolling gate*, except that the beam is rolled instead of rotated in place. The rolling beam has improved wheel-rail loading compared to the rotating beam as both carriages roll over separate rails and do not have to cross any little gaps. The front carriage rolls over its own rails on the beam and the back carriage rolls over its own rails on the gate chamber. The *Rolling cantilever beam rolling gate* also favours horizontal

and vertical loading and is especially favourable with respect to the accessibility of the components. The rolling beam stays on ground level and therefore is easily reachable. The main downsides of this variant are; the extension of the rolling beam and thus the little increase of total lock width, and the use of extra material and mechanical components. The opening and closing time of the gate is also increased, but this is probably compensated by the increased total availability of the lock.

Cable-stayed rolling gate
The *Cable-stayed rolling gate* is the least viable solution of the proposed concept variants. It scores worse or the same on every criteria compared to the *conventional rolling gates*, except for the accessibility of the components. This solutions is completely new and relatively complex, especially regarding the vertical balance of forces and the corresponding support system of cables and winches.

Cantilever rolling gate (side extension)
The *Cantilever rolling gate with a side extension* scores almost similar to the variant with a top extension. Compared to *conventional rolling gates* it has improved balancing of horizontal forces and impact of a ship collision and better accessibility of components. The side extension is favourable (compared to the top extension) as it makes use of the height of the gate to transfer vertical forces and has an easier transfer of horizontal forces and the clamped cantilever. The carriages are easy to reach and replace. The main downsides of the cantilever rolling gate are the increased required lock space and the major increase of material use.

Cantilever rolling gate (top extension)
The *Cantilever rolling gate with a top extension* has some criteria for which it scores better than the *conventional rolling gates* (balance of horizontal forces, accessibility of components & impact of a ship collision). The top extension scores a bit worse compared to the side extension version, as it does not make use of the already existing gate height for its transfer of vertical forces and has a more complex support system onto the carriage which complicates the accessibility of these mechanical components. The main downsides of the cantilever rolling gate are the increased required lock space and the major increase of material use.

Self-propelled floating gate
The *Self-propelled floating gate* totally removes the rolling supporting system by making the whole gate like a floating boat. The complete removal of the rolling supports is beneficial, but it comes with many downsides regarding the horizontal and vertical balance of forces and stability issues. It does not score better on any of the evaluated criteria compared to the conventional rolling gates. Also, the propelling system in the gate and the buoyancy balancing system add extra mechanical components which are located under water, albeit under lower loading conditions then for the conventional gates.

4.9.2. General conclusion

Based on all the qualitative assessments and elaboration of conceptual variants, the *Rolling cantilever beam rolling gate* and the *Cantilever rolling gate side extension* stand out. Both options are shown in Figure 4.7.

Compared to conventional rolling gates, the *Rolling cantilever beam rolling gate* is favourable regarding the spread and balance of horizontal and vertical forces due to the beam structure which is moved in place before movement of the gate. The *Cantilever rolling gate side extension*, on the other hand, is favourable due to the single structure and the cantilever arm which creates a clamped support in horizontal direction. A downside is that both these variants require an added structure which is material costly and increases the required space for the lock. They also both require some sort of counterweight and/or load balancing for the cantilever to work. Due to the single structure and the same amount of carriages of the *Cantilever rolling gate side extension*, the opening and closing time and the amount of mechanical components does not change compared to the conventional rolling gates. In contrast to the *Rolling cantilever beam rolling gate*, which increases the opening and closing time and adds extra mechanical components due to the addition of the separate rolling beam.

Between the two variants the *Cantilever rolling gate side extension* stands out as it is constructed of one structure and does not increase the gate opening and closing time. Compared to the *Rolling cantilever beam rolling gate* it requires less mechanical components and can probably be designed such that the balance of horizontal and vertical forces is still more beneficial than the conventional rolling gates.

Therefore the *Cantilever rolling gate* with a *side extension* is chosen as the most suitable option. In order to further test this design variant, it is incorporated into the case study location of the Westsluis in Terneuzen. The next design step is to incorporate the gate in this location and see if it can fulfill to all of the requirements and still be feasible.

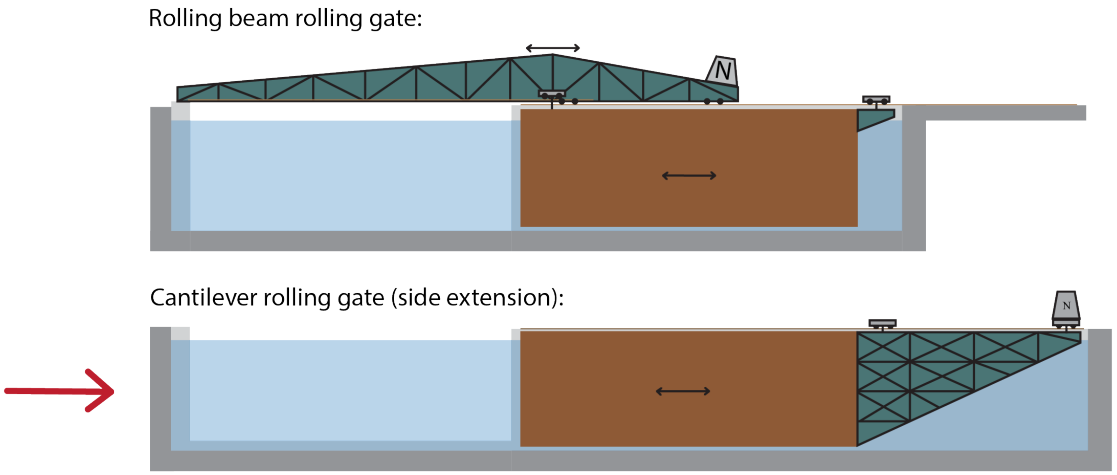

Figure 4.7: The two favourable conceptual variants according to the MCA, with the chosen option (Cantilever rolling gate) indicated by the red arrow.

5

Case: Development of basis of design for the cantilever rolling gate

This chapter provides an outline for the case study and the general assumptions plus starting points which are used to validate the design of a cantilever rolling gate concerning its technical feasibility. The case study gives a limited framework in which the design for the new type of rolling gate can be made and can be compared with current proven and commonly used type of gates. The Western lock (Westsluis) in Terneuzen is used as a case study (see Section 5.1). The current dimensions, configuration and environment of the lock and gate of the Western lock are used to design the new gate. The relevant boundary conditions for the case study location are given in Section 5.2. Section 5.3 elaborates on the general assumptions and Section 5.4 shows the general starting points.

5.1. Case Study: Western lock Terneuzen

In recent years, the construction of two new large maritime navigation locks have started in the Netherlands. The first one is located in IJmuiden and the second one in Terneuzen. Both locks make use of conventional rolling gates like the wheelbarrow and the wagon rolling gate. *Ingenieursbureau Boorsma*, who initiated the idea of the cantilever rolling gate, aided the executive agency of the Ministry of Infrastructure (called Rijkswaterstaat) with parts of the preliminary design of the new lock in Terneuzen. Due to Ingenieursbureau Boorsma's knowledge and information on this specific location, the locks in Terneuzen are an ideal start for a case study on the concept of the cantilever rolling gate.

The city of Terneuzen is located in the south western part of the Netherlands in the province of Zeeland. The lock complex is located on soil of the municipality of Terneuzen, west of the city. For the city of Terneuzen the lock complex is an important road connection to the Western Scheldt (Westerschelde) Tunnel. This tunnel connects the people of Terneuzen to the rest of Zeeland and the Netherlands.

The first lock at Terneuzen was constructed at the time of the initial construction of the Ghent-Terneuzen channel in 1827 [53]. The channel connects the Ghent industrial channel zone to the Western Scheldt, which is directly connected to the sea. The lock complex at the entrance of the channel eliminates the tide and keeps a constant water level in the channel. The channel is of a major importance to the economy of Ghent as it connects the 3^{rd} largest harbor of Belgium (after Antwerp and Zeebrugge) to the sea.

Nowadays the lock complex has three separately operating navigation locks; the Eastern lock (Oostsluis), the Middle lock (Middensluis) and the Western lock (Westsluis) and a new larger lock is under construction (see Figure 5.1 for the locations). The Middle lock is the oldest and is mainly used to flush water. The Eastern lock and the Western lock were both constructed in 1968. The Eastern lock is mainly used by inland navigation vessels, as the western lock is designed for maritime vessels. The lock and normative maximum allowed ship dimensions for the locks are shown in Table 5.1.

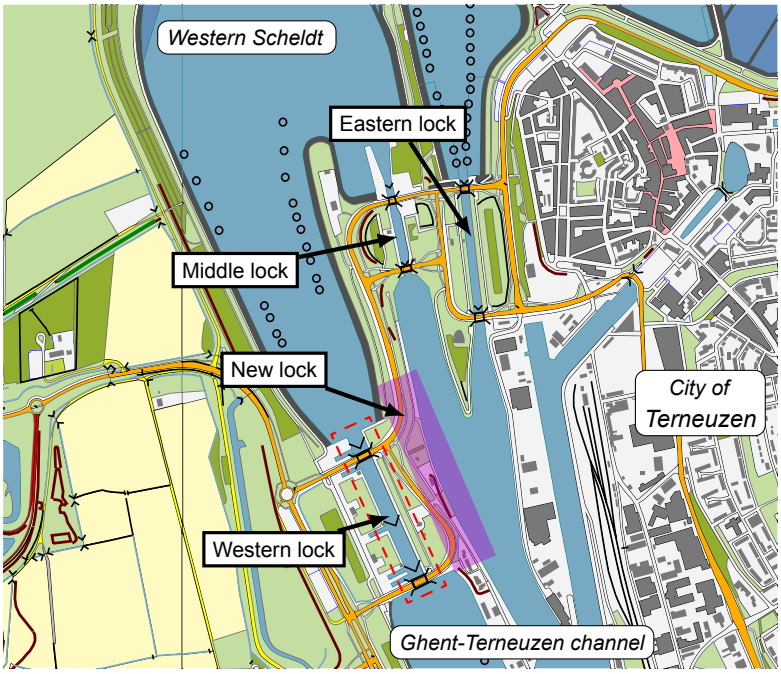

Figure 5.1: Map of Terneuzen lock complex. The Western lock (Westsluis) is indicated by a dashed red line and the new Terneuzen lock is indicated by the purple plane. (Background map TOP10Vector provided by TU Delft)

Figure 5.2: Map of the Netherlands and the location of Terneuzen

Table 5.1: Lock and normative maximum allowed ship dimensions for the Terneuzen lock complex [80]

	Lock dimensions			Normative ship dimensions		
	Length [m]	Width [m]	Sill level [+m $N.A.P.$]	Length [m]	Width [m]	Maximum draft [m]
Western lock	290	40	-12.98	265	34 (37)	12.5 [a]
Eastern lock	270	24		200	23	4.3
Middle lock	140	18		140	17.4	6.5

[a] Entering from Ghent-Terneuzen channel

At the start of this research, the tender of the new navigation lock in Terneuzen still had to be started and therefore little was known about the exact procedure and final design of the new lock. In contrast to the new lock, there is a lot of information available of the current Western lock (Westsluis) in Terneuzen, as it has been in operation for more than 50 years. In addition, the current Western lock is smaller compared to the new lock, which makes it more suitable for a case study. Both of these arguments led to the decision to use the Western lock in Terneuzen as a Case study. It is of a decent but not too large size and the information on this lock is readily available.

5.1.1. Western lock Dimensions

The total length of the Western lock is 440 meter, while the useful lock length inside the gates is 290 meter. The lock has five gates: two gates on both the Western Scheldt and the channel sides and one gate in the middle. The lock chamber can be divided by this middle gate in two parts of 170 meters and 112 meters. Two bascule bridges provide passage for road traffic. One bascule bridge is located in between the two gates at the seaside and the other is located on the channel side of the channelside gates.

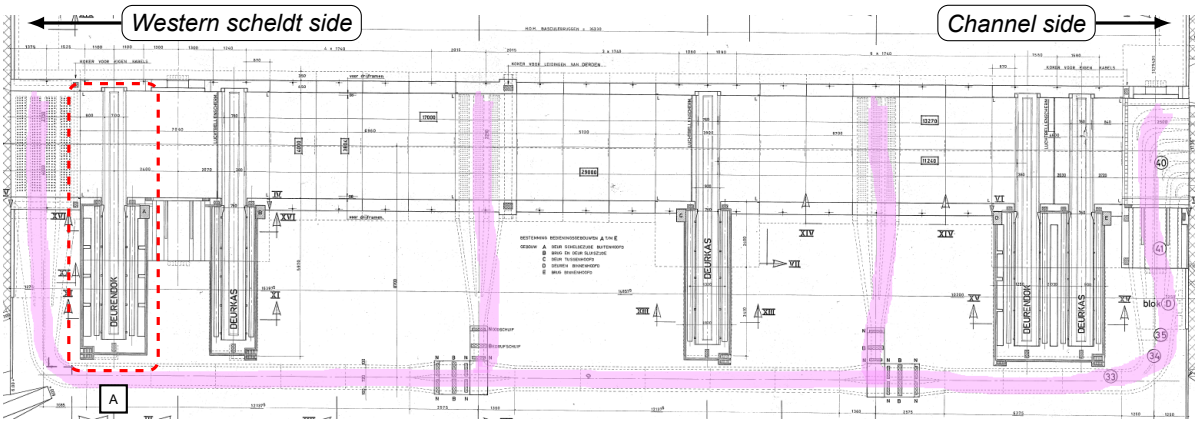

Figure 5.3: Overview of Western lock lay-out - (A) indicates the governing gate location and the lay-out of the culvert system is marked pink (Source of background map: [67])

The width of the lock is 40 m. Each side of the lock has floating fenders of 1 meter wide, reducing the operating width to 38 m. The maximum ship width is 37 m under certain conditions. If a ship has a width in between 34 and 37 m, the maximum length of the ship is 230 m. For vessels entering the Ghent-Terneuzen channel the maximum draft is 12,5 m, while for vessels leaving the channel the draft is limited to 12.3 m. The minimum keel clearance is 1 m. Next to these size restrictions, vessels with a draft exceeding 9.1 m are only allowed to enter the lock between specific tide intervals and vessels longer than 180 m have to be guided by tugboats [74].

Levelling of the water inside the lock is done by a single-sided bypass culvert system located on the Western side of the lock. The openings to the culverts are located in the lock floor and run through the western side of the lock to the outside of the gates. As the lock can be divided into two parts, both parts have an in/outlet for the culvert system as can be seen in Figure 5.3. The opening on the channel side is relatively big as it also functions as the flushing inlet.

The Western lock has been constructed in the dry and has a shallow foundation. The lock heads, lock chamber and culvert system are all made out of gravel concrete [80]. The lock is build up from several sections which are connected by watertight sealing compounds. The walls go up to a height of +6.00 meter N.A.P. and are clamped onto the bottom floor. The underside of the concrete floor is located at -19.00 meter N.A.P., while the top of this floor is at -12.82 meter N.A.P. (which is the bottom of the lock). The gate chambers, in which the gates open and close, have a depth of -14.00 meter N.A.P. [7]. The lock can't be set dry for maintenance, as they are not designed to withstand such forces. The gate recess of each gate can be set dry in order to perform maintenance to the gates.

5.1.2. Gate specifics

The Western lock has five rolling gates installed, which can retain water in both directions. As stated before, there are two gates for both outer sides of the lock and one gate in the middle. According to the original design documents from 1967 [13] & [14], each gate is 44.56 m long, 19.22 m high and 6.43 m wide. The rolling gates are of the 'wagon' type and vertical loads on the gate are transferred through two lower carriages. However, each gate also has one upper carriage to guide the gate in and out of the gate chambers. This upper carriage provides horizontal load guidance and is (in combination with the lower carriages) used to push the gate in a central position in horizontal transverse direction.

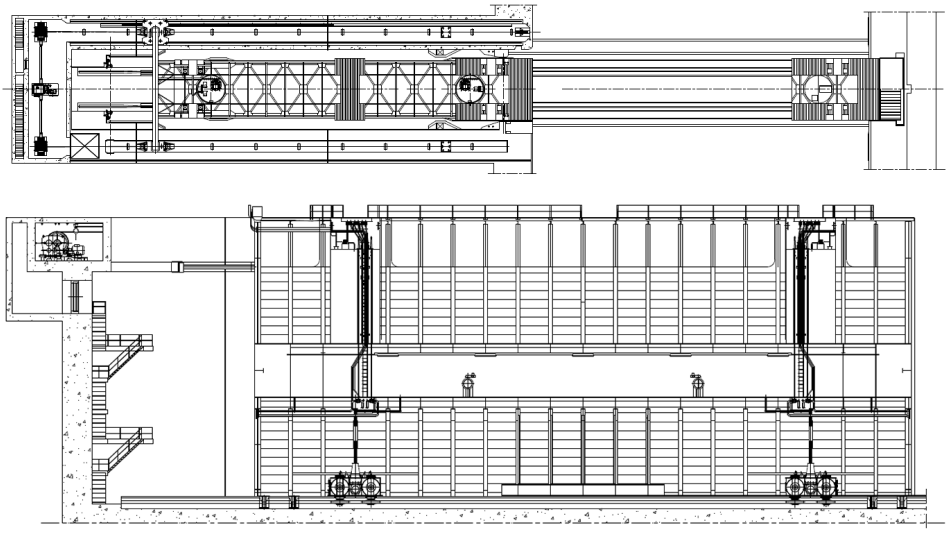

Figure 5.4: Top and side view of the gate inside the gate chamber of the Western lock Terneuzen [21]

According to the structural recalculations from 2009 [3], the gate is mostly made out of steel type LQMC 52 or S355 which has a yielding strength ($f_{y,rep}$) of 355 MPa. The original design documents [13] define the total weight of the steel gate structure including the fixed ballast to be 946000 kg. The buoyancy chambers are 3.614 m high, 44.22 m long and 6.412 m wide and thus have a total maximum volume of $44.22m \cdot 6.412\ m \cdot 3.614\ m = 1024.7\ m^3$. Certain parts of this volume (on both sides of the gate) are separated tanks particularly for ballasting and trimming of the gate during operation (see Figure 5.5). The fixed ballast has a volume of 39.73 m^3 and ads a weight of 200 tonnes. Due to problems with the wheels and rails around 2006, a volume of 75 m3 polystyrene foam has been added to each gate [64]. [1]

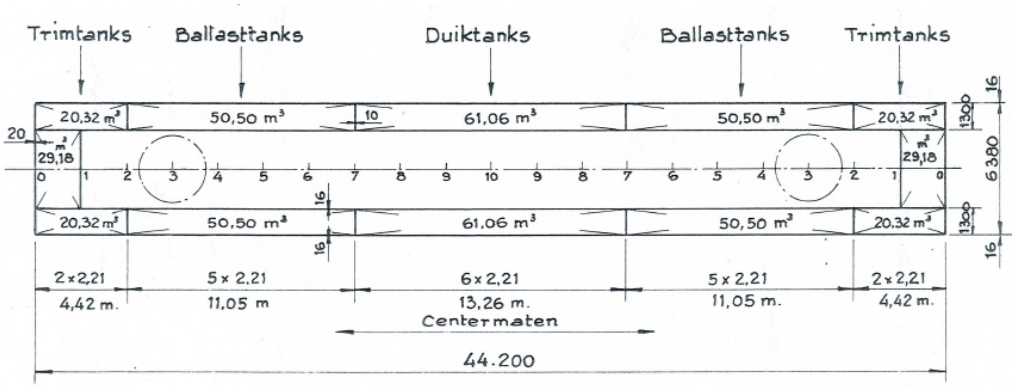

Figure 5.5: Horizontal cross-section of the buoyancy chambers in the gate of the Western lock [14]

There are a total of 12 lower carriages, of which 10 are operational and two are located in the maintenance area of the lock as a backup. The gate structure transfers its vertical loads to the carriages via rubber bearings. Each of the lower carriages has 4 wheels with a diameter of 1200 mm and a wheel width of 150 mm. According to technical drawings and documents of the lock from the *Department of Waterways and Public Works (Rijkswaterstaat)*, the old wheels were made of GSt 52 [20] but had been rolled out. TNO did an analysis on the rolling out behaviour and advised the *Rijkswaterstaat* to replace the wheels and rails. Therefore the wheels of the lower carriages have been replaced between 2007 and 2009 [33] by new wheels, made of surface hardened forging steel 42CrM05-04 [19]. These wheels have a yielding strength (fy) of 550 MPa and a Brinell Hardness (HB) of 400 MPa.

The upper carriage only provides horizontal guidance and therefore does not take any vertical load. The two lower carriages and the upper carriage (see Figure 5.8) each have four guiding wheels to transfer horizontal loads during opening and closing. While the carrying wheels have been adjusted over time due to design flaws and rolling out, the guiding wheels still have the same original design.

[1] This foam is not taken into account in the calculations.

The wheels are spoked ones with trapezoidal holes in them. The dimensions of the guiding wheels are the same as the carrying wheels.

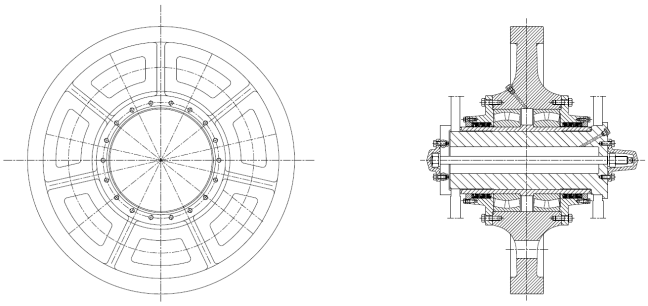

Figure 5.6: Side view (left) and Cross-section (right) of the carrying wheels of the Western lock Terneuzen [19]

Problems with rolling out also occurred at the rails of the Western lock. The previously mentioned report by TNO concluded the rails should also be replaced for new harder ones. According to Sjaak Michielsen from Rijkswaterstaat [34], the rails of gates A, C & D have been replaced around the same time as the wheels in 2007. Rails of gate B and E have recently been replaced in 2017. All of the rails were replaced by a team of divers, which led to a downtime of 5 times 8 hours per gate. The rails and mounting bolts are inspected and maintained once every year. This check leads to a 6 hour downtime per gate per year. Each gate is set dry once per 8 years to clean and check for inspection .

The rails are blockrails clamped on the concrete and made out of 110 CrV. The rails have a tension strength (ft) of 1080 MPa, a Brinell Hardnes (HB) of 320 MPa and are 150 mm wide at the top [33].

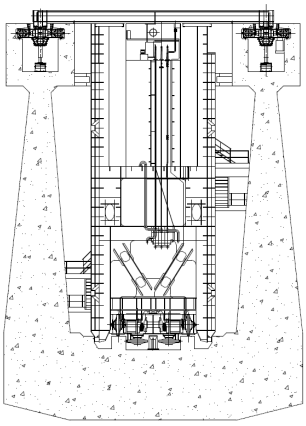

Figure 5.7: Cross-section of the gate including upper and lower carriage [21]

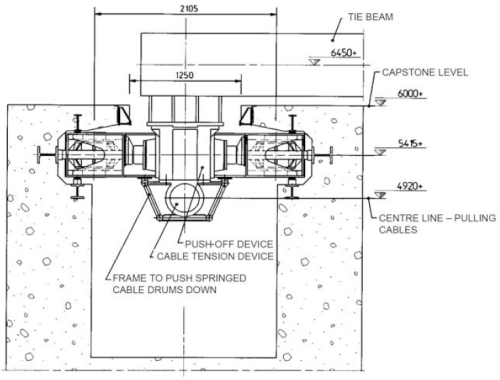

Figure 5.8: Horizontal top rolling gate guide with push-off device [72]

In each of the carriage a horizontal pressure system is located to function as a centering device. This centering device pushes the gate in its central position just before opening. Each gate has eight hydraulic cylinders. Four for the two lower carriages and four for the upper carriage. These cylinders are pressurized by three hydraulic power units located inside the gate. Thus one for each carriage [4].

Driving System

The information regarding the driving system and the gate operating data are extracted from a risk assessment report on the Western lock by *IV-Infra* [6]. The driving system of each gate consists of a winch (cable drum and pulleys) which move the upper carriage via cables and a steel outrigger. A cable tensioning device, consisting of a spiral ring, is present in the upper carriage to ensure a minimum tension in the cables and a predictable cable run.

According to the *IV-Infra* report [6] the movement speed of the gate is 0.277 m/s, while the crawl speed of the gate is 0.055 m/s. This crawl speed is applied just before the gate will arrive at its opened or closed position. A drawing of *Rijkswaterstaat* [21] shows that the gate has to travel a distance of 41.375 m in order to open and close. Opening or closing of the gate can be started after the gate has been pushed in its central position. The full gate operating data are shown in Table 5.2

Table 5.2: Gate operating data of the Western lock Terneuzen [6] & [21]

Parameter	$Abbreviation$	$Value$	$Unit$
Gate movement speed	v_{move}	0.277	m/s
Gate crawl speed	v_{crawl}	0.055	m/s
Gate end/start speed	v_{end}	0	m/s
Total movement distance	m_{move}	41.375	m
Accelerating time	t_{acc}	33	s
Decelerating time to crawlspeed	$t_{deccrawl}$	11	s
Decelerating time to final speed	t_{decend}	2	s
Crawl distance	s_{crawl}	0.825	m

5.2. Relevant boundary conditions

This section describes the relevant boundary conditions in and around the Western lock in Terneuzen. These boundary conditions will be used in the further design of the cantilever rolling gate.

5.2.1. Seaside water levels

The Terneuzen lock system is on one side located to the Western Scheldt and is thus exposed to a semidiurnal tide. The average, spring and neap tide, high and low water levels are shown in Table 5.3. The mean water level of the average tide is +0.20 m $N.A.P.$ [55].

Table 5.3: Average tide waterlevels for Terneuzen [56]

Type	High water level [+m $N.A.P.$]	Low water level [+m $N.A.P.$]	Tidal difference [m]
Average tide	2.29	-1.90	4.19
Spring tide	2.68	-2.13	4.81
Neap tide	1.79	-1.56	3.35

The highest water level recorded at Terneuzen was on 1 februari 1953: +4.96 m $N.A.P.$, while the lowest recorded water level was on 31 januari 1956: -3.40m $N.A.P.$ [55]. The Western lock is a primary water defence of the Netherlands. It is part of dike ring 32 (Dutch Flanders) and has to be able to independently retain water. The norm frequency for the dike ring is 1/4000 per year. Which translates into a design water level of +5,80 m $N.A.P.$, as calculated by the hydraulic conditions 2006 [69].

The locking process is halted if the water level on the Western Scheldt exceeds +3,50 m $N.A.P.$, which on average occurs 2 times a year [12] .

5.2.2. Channel water levels

In 1960, the Netherlands and Belgium signed a treaty with respect to any associated matters related to the channel between Ghent and Terneuzen [78]. In article 33 of this treaty it was agreed that the level of the channel should be +2.13 m $N.A.P.$, with a maximum deviation of 0.25 m. Therefore, the maximum water level in the channel is +2.38 m $N.A.P.$. and the minimum water level is +1.88 m $N.A.P.$

5.2.3. Water properties

The Western Scheldt is directly connected to the North sea and is thus salt water. The Terneuzen lock is part of the 'physical' barrier between the salt water in the Western Scheldt and the fresh water in the channel. The current locks all have measures to reduce the inflow of salt water in the channel as the channel provides irrigation water to nearby agriculture. The maximum density of the salt water is $1025\,kg/m^3$, whereas the minimum density of the fresh water is $1000\,kg/m^3$.

5.2.4. Windwaves

In a report for the RINK 2011 [5], IV-Infra analysed and calculated the significant wave parameters for the Western Scheldt in case of high water retention and under normal locking conditions. The parameters for the Western Scheldt side are shown in Table 5.4:

Table 5.4: Wind wave parameters Western Scheldt side [5]

Design circumstance	Significant wave height (Hs) [m]	Significant wave period (Tp) [s]
Maximum lockage level (+3.50 m $N.A.P.$)	0.39	4.21
High water retention (+5.80 m $N.A.P.$	0.69	3.27

The waves on the channel side have also been determined in the same report by IV-Infra. The input parameters used are an average channel bottom level of -16.70 m $N.A.P.$, a water level of +2.38 m $N.A.P.$ and wind speeds on 10 meter above the water of 16.70 m/s for normal lockage and 18.90 m/s for high water retention. This gives the wave parameters shown in Table 5.5:

Table 5.5: Windwave parameters channel side [5]

Design circumstance	Significant wave height (Hs) [m]	Significant wave period (Tp) [s]
Maximum lockage level (+2.13 m $N.A.P.$)	0.34	2.16
High water retention (+2.38 m $N.A.P.$)	0.39	2.30

5.2.5. Ship waves

The Western lock in Terneuzen is mainly used by large ocean going vessels. While these ships are relatively large and have a big draught, the entering speed into the lock is relatively low (circa 2 knots or 1 m/s [31]). Therefore these vessels do not generate significant waves while entering the lock.

However, passage of vessels going full speed on the Western Scheldt can cause significant ship waves. In 2015, Svasek was issued by Ingenieursbureau Boorsma to perform measurements on waves at the Western lock and Middle lock due to passing vessels on the Western Scheldt [1]. They performed measurement for a period of 3 hours for the Western lock and for two weeks at the Middle lock. The maximum water difference at the Western lock during the combined measurement was due to the passing vessel called Millau Bridge (366 m long, 51 m wide, 12.5 m draught and 7.2 m/s speed). This passing caused a minimum of -0.20 m and maximum of +0.13 m water difference. Svasek used the numerical flow model FINEL2D to verify and implement these measurements to calculate a significant wave by the passing of the largest vessel. The MSC London (399 m long, 54 m wide, 10.3 m draught and 8.8 m/s speed) caused the biggest water difference at the middle lock during the two week measurements. This wave data was then interpolated using the FINEL2D model to give a significant wave difference of -0.48 m and +0.25 m at the Western lock. This water difference was measured to be twice the water difference at the middle lock. This is probably caused by the specific geometrical layout of the harbor in front of the lock system. It should be noted that these values may change due to the construction of the new sealock.

5.2.6. Transport operations

One of the functions of the Western lock is to transfer large ocean-going vessels from the Western Scheldt to the Ghent-Terneuzen channel. The most recent available ship passage data on the Western lock was found in a report [26] from 2010. It used data from the IVS90 database of Rijkswaterstaat to analyse the amount of ocean-going vessels from 1999 till 2007. The distribution of inland and maritime vessels over the different locks is shown in Table 5.6

In 2005 a total of 12,854 ships passed the Western lock. From 1999 till 2007 the average number of ocean-going vessels passaging the Western lock was circa 9,500 per year. It is not known in which way the construction of the new sealock at Terneuzen will alter the amount of vessels passing the Western lock. For now, it is assumed that the lock passages of the Western lock are mainly determined by the ocean-going vessels and will stay constant and have 9,500 passages per year.

Table 5.6: Vessel traffic intensities per lock in 2005 [26]

	Western lock		**Middle lock**		**Eastern lock**		**Total**	
Vessel type	Nr.	Percentage	Nr.	Percentage	Nr.	Percentage	Nr.	Percentage
Inland	5,262	41%	12,355	84%	33,207	96%	50,825	82 %
Ocean-going	7,592	59%	2,371	16%	1,451	4%	11,414	18 %
Total	12,854		14,726		34,658		62,239	100 %

5.3. General Assumptions

The general most important assumption is that the current Western lock in Terneuzen is used as starting point for the design of the cantilever gate. The new gate is designed as if the current gate and lock chamber of the Western lock were to be expanded by adding the cantilever system. This simplifies the initial design process as much of the parameters are already defined and thus the focus can be on the feasibility of the new cantilever gate. Of course in reality, if the cantilever gate were ever to be constructed, the gate structure has to be designed for the new lock dimensions for the concept and the location. For now, the current structure of the gate part is assumed to be able to transfer all the loads in the new design.

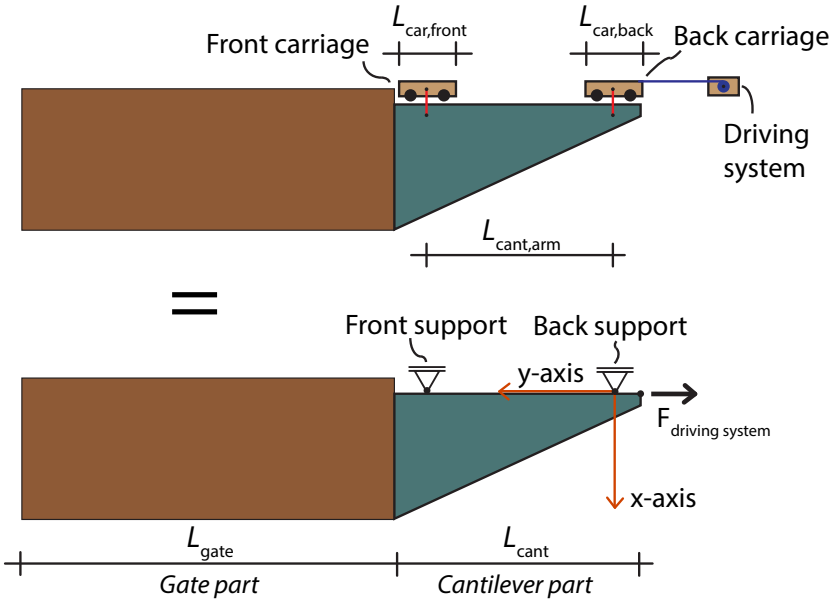

Figure 5.9: Schematisation of the cantilever rolling gate. The bottom of the figure shows the cantilever gate with the modelled supports and the location of the x,y-axis

The 'gate part' is defined as the part of the cantilever gate that closes off the lock. The 'cantilever part' is the added construction that functions as an arm. Two carriages on both ends of the cantilever part are present to transfer the reaction loads towards the foundation. For the design of the cantilever gate and the load transfer, the gate and cantilever are both modelled as rigid bodies which are rigidly connected. For most calculations the three dimensional gate is simplified as a 2D structure in which the roller carriages are interpreted as roller supports which only take vertical loads. To create a statically determined system the driving system is assumed to be a constant force. Figure 5.9 shows the schematisation.

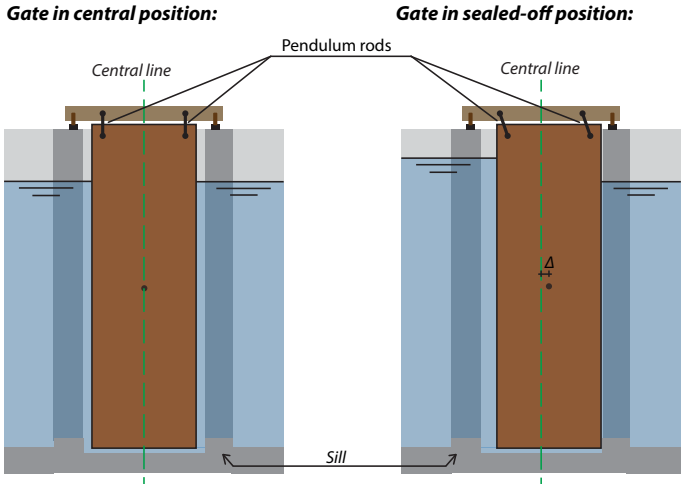

Figure 5.10: The way the gate seals off under a water level difference in closed position. The gate and cantilever part are connected to the carriages by two pendulum rods each, which enables the gate to move sideways.

sealing of the lock
The connection between the cantilever and the carriages is hinged by pendulum rods. Figure 5.10 shows this connection and how it enables the gate to move sideways to seal of the lock chamber under a water level difference (if the gate is in closed position).

Due to the pendulum connection the gate part can seal off against the sill on the bottom, and the gate chamber and gate recess on both sides (shown in Figure 5.11). The seals on the gate are assumed to be constructed of timber that connect to Ultra-high-molecular-weight polyethylene (UHMWPE) rubber profiles mounted on the concrete surface.

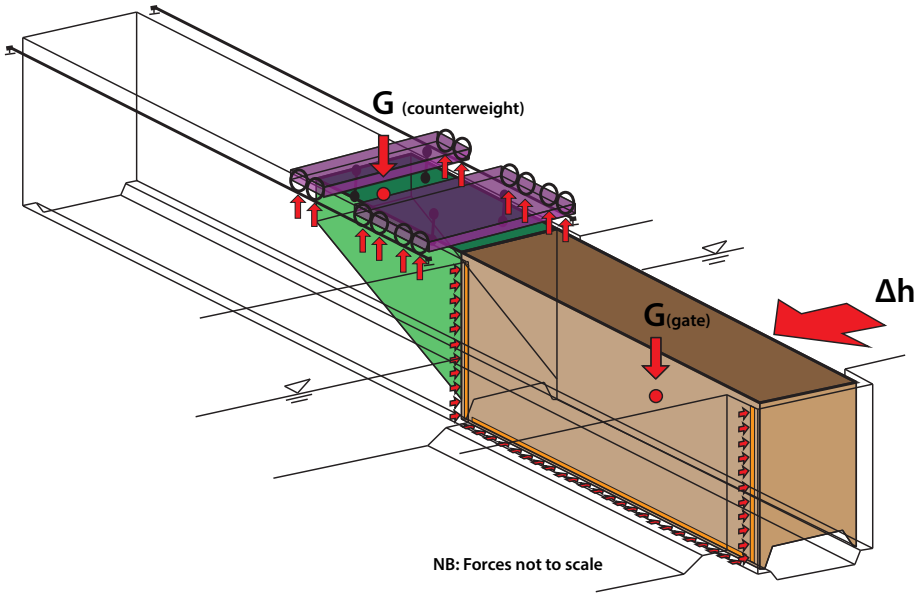

Figure 5.11: A 3D-schematisation of the load transfer of the cantilever gate under a water level difference in closed position. The horizontal waterload is transferred to the gate chamber, recess and sill via UHMWPE and timber profiles. The vertical forces of the weight of the cantilever gate and the counterweight are transferred to the rail-foundation via the carriage wheels.[2](Adaptation of [17])

Guidance
The current Western lock uses an active guidance system to center and guide the gate during opening and closing. Likewise, it is assumed that an active guidance system is applied for the initial design of the cantilever rolling gate. As there are no rolling carriages under the cantilever gate, the active guidance rollers are assumed to be placed directly on the gate itself. These lower guidance rollers push against the sill. For the top part of the gate, the active guidance rollers are located on the gate chamber and thus push against the gate. These active guidance rollers retract once the gate is in closed position so the gate is pushed and sealed against the recess, chamber and sill. Figure 5.12 shows the locations of the active guidance rollers.

The double gates of the current Western lock are also present in the new design. In this situation, the gate chambers also can function as a dry dock. This temporary dry dock can be used to perform maintenance to the gates on site. This is important, as the extra length of the cantilever extension makes it impossible to move the complete cantilever gate structure out of the gate chambers due to the gate being longer than the lock width. The cantilever structure cannot be detached and thus it is important that maintenance can be performed on site. The double gates ensure the continuation of the ship locking process in case one of the gates is out of service.

The design calculations are based on the limit states [44] and are achieved by the partial factor method. The relevant design values are obtained by using the characteristic loads in combination with partial safety factors. These values of the safety factors are elaborated at the calculations in Chapter 6

[2]In this figure the gate is assumed to be constructed with a counterweight that balances out the cantilever and therefore only downward forces act from the wheels on the rails.

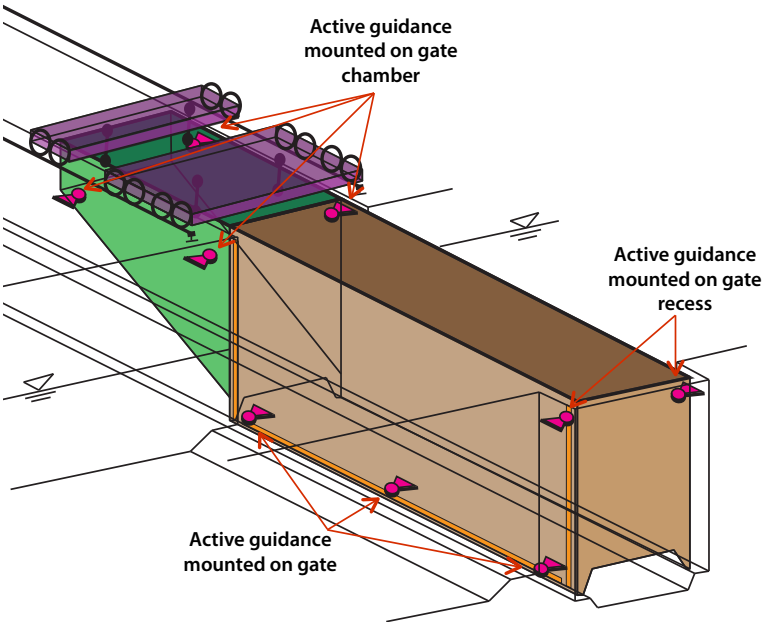

Figure 5.12: The schematic locations of the active guidance rollers for the cantilever rolling gate. These are used to guide the gate during opening and closing of the gate and to prevent any horizontal forces on the wheels of the carriages. (Adaptation of [17])

Carriages

The current Western lock utilizes relatively short carriages with four wheels on which the gate structure is supported. The carriages of the cantilever rolling gate will be different, as the cantilever structure will 'hang' on the carriages. The carriages have to stretch over the full width of the gate. Carriages with four and eight wheels are both used in sub-variants of the cantilever rolling gate.

The width of the carriage (spanning the gate width) is assumed to be 9 m. For a carriage with four wheels, the length of the carriage (in longitudinal direction of the gate) is assumed to be 6 m, while for a carriage with eight wheels this length is assumed to be 9 m.

As the weight of the carriages of the Western lock is unknown, the weight of the carriages of the Krammersluis is used as a starting point [16]. Therefore the weight of a carriage with a length of 6 m and four wheels is 12 tonnes. The weight of a carriage with eight wheels is taken proportional to the length (6 m vs. 9 m). Which leads to a weight of 18 tonnes for the 8 wheel carriage.

To prevent uplift of a carriage, a minimum downward safety force of 200 kN is required in accordance with examples from the PIANC report *InCom-wg173; Movable bridges and rolling gates* [76].

Wheels and rails

The wheels and rails are assumed to be constructed identical to the current ones applied at the Western lock (see Section 5.1.2). An overview of the wheel and rail dimensions and materials are given in respectively Table 5.7 and Table 5.8.

Table 5.7: Wheel specifications [19] & [33]

Name	$Abbreviation$	$Value$	$Unit$
Wheel diameter	D_w	1200	mm
Wheel width	b_w	150	mm
Wheel crown radius	$r_{crown,w}$	∞	mm
Wheel corner radius	$r_{corner,w}$	5	Mm
Wheel material name		$42CrMo5-04$	
Wheel yield strength	$f_{y,w}$	550	MPa
Wheel ultimate tension strength	$f_{u,w}$	800	MPa
Wheel unit conform hardness (Brinell)		400	HB

Table 5.8: Rail specifications [18] & [33]

Name	$Abbreviation$	$Value$	$Unit$
Rail width	b_r	150	mm
Rail crown radius	$r_{crown,r}$	∞	mm
Rail corner radius	$r_{corner,r}$	0	Mm
Rail material name		$110CrV$	
Rail yield strength	$f_{y,r}$	1080	MPa
Rail ultimate tension strength	$f_{u,r}$	1080	MPa
Rail unit conform hardness (Brinell)		320	HB

Gate lifetime and cycles
It is assumed that consequence class of the gate is level 3 and has a lifetime of 50 years. The average number of gate cycles per year is 9500, see Section 5.2.6. Which gives a total of 475000 gate cycles for the lifetime of the gate. The assumptions is made that the wheels of the gate carriages are replaced every 25 years, thus once in the lifetime of the gate. Every cycle the gate displaces 88 meters. (44 m when closing and 44 m during opening).

Silt and accretion
Silt will settle on the buoyancy chambers and clams and other things will start growing on the gate over time. As a reference, the assumptions made by *Rijkswaterstaat* and *Ingenieursbureau Boorsma* for the preliminary design of the new gate for the New lock in Terneuzen are also applied in this case [63].

For silt accumulation they assumed a maximum of 0.15 m silt with a specific weight of 13 kN/m^3 (with a minimum of 5% of the deadweight of the gate) on top of the buoyancy chambers. This can only be assumed in case mixers (agitation screws) are applied on top of the buoyancy chambers. In this case situation, the same presumption is made.

It is also assumed that 500 clams with a weight of 20 grams each can grow on every square meter. Deducting the buoyancy of the shells, this leads to a weight of $0.10\ kN/m^2$.

5.4. General starting points

For now, only the design of the cantilever gate structure and its load transfer to the foundation is considered. Thus the design of the gate chamber and recess and other aspects of the total lock are not further elaborated. However, the additional material for the construction of the extended gate chamber (due to the cantilever extension of the gate) is taken into account in the design. To minimise the use of gate chamber material, *one of the design goals is to make the cantilever extension as short as possible*. Naturally, this minimal length should still take into account the maximum possible loading on the components of the cantilever gate, especially the wheels and rails.

As was concluded in Section 3.3, the wheel - rail interface in a rolling gate is relatively sensitive to corrosion and unequal loading and thus susceptible to failure. This could lead to problems when the interface is below the waterline as there is more contamination possible than above the waterline and it is also harder to reach. The cantilever rolling gate significantly lowers contamination vulnerability and solves the inaccessibility by applying all the wheels and rails above the waterline. Nevertheless, the precise loading of the wheel and rails is also extremely important for this new design. To ensure a safe load transfer, the balance in longitudinal direction of the gate should be carefully considered. *Therefore the main focus for the design of the cantilever gate lies on the loading balance in longitudinal direction of the gate.*

In line with ROK 1.4 [58], the cantilever gate (being a hydraulic structure) is considered as a bridge in the design verification. The structural safety level for the concrete lock structure is set to have reliability class RC 3 (& Consequence class CC3), at a reference period of 100 years. The gate itself is designed with a reference period of 50 years.

Gate part dimensions
The gate part is assumed to be exactly the same as the current gate of the Western lock, see Table 5.9.

Table 5.9: Gate part dimensions [13] & [14]

Specification	$Abbreviation$	$Value$	$Unit$
Length of gate part	L_g	44.56	m
Width of gate part	B_g	6.43	m
Height of gate part	H_g	19.22	m
Weight of gate part	W_g	946	t
Top of gate (from N.A.P.)	$h_{g,top}$	6	m
Bottom of gate (from N.A.P.)	$W_{g,bot}$	-13.22	m

Cantilever part dimensions
The cantilever part has the same width as the gate part (6.43 m). The length of the cantilever part is set variable as it is one of the optimisation parameters of the cantilever design. A sub-goal of the design is to minimise the length of the cantilever part to reduce the required material and length of the gate chamber and the structure itself.

Initially, the cantilever length is set to be 24 m to calculate a reference dimension and weight (see Appendix D). In the subsequent calculations the weight and volume of the variable cantilever length are based on this reference situation by interpolating linearly.

Buoyancy chambers
In the current gate of the Western lock, the top of the buoyancy chambers is located at -2,6 m $N.A.P.$. As the lowest water level is at -3,4 m $N.A.P.$, a large part of these chambers is not utilised in case of extreme low water. For the current gate this has later been solved by adding additional foam to increase the buoyancy force. To ease the calculation and to ensure the upward buoyancy force under all conditions, the buoyancy chambers for the new cantilever gate are assumed to be located below this lowest water level. The size and chamber partitioning (see Figure 5.5) is assumed to be the same as the current gate and consists of 20 regular chambers, 4 trimming chambers, 4 ballasting chambers and 2 diving chambers. It is assumed that for regular operation all of the trimming, ballasting and diving chambers are always filled with water. The relevant details of the buoyancy chambers are shown in Table 5.10.

Table 5.10: buoyancy chamber Details [14]

Specification	$Abbreviation$	$Value$	$Unit$
Top (from N.A.P.)	$h_{b,top}$	-3.4	m
Bottom (from N.A.P.)	$h_{b,bot}$	-7.014	m
Height	H_b	3.614	m
Width	W_b	6.412	m
Length	L_b	44.22	m
Total volume	V_b	1024.7	m^3
Volume of steel, ballast and wood under chamber	$V_{s,below}$	76.9	m^3
Volume of steel above chamber till $+3.5$ m $N.A.P.$	$V_{s,above}$	39.1	m^3
Volume of trim, diving and ballast tanks	V_{tanks}	405.4	m^3

6

Cantilever gate balance

This chapter analyses and elaborates on the load balancing of the cantilever gate. The goal of this analysis is to determine the most optimal length of the cantilever structure, taking into account all the loading conditions and safety limitations of relevance to the cantilever gate. It distinguishes two sub-variants regarding the balancing of the gate and four possible options for the carriage configuration.

Firstly, the load model and the relevant loads are listed in Section 6.1 and all of the loading situations and combinations are presented in Section 6.2. Then Section 6.3 elaborates on the influence of the cantilever length and the gate buoyancy on the equilibrium of the gate. It also presents possible solutions to balance the gate in the form of two sub-variants (counterweight vs. upper rail). Section 6.4 defines the design capacities of the wheel-rail interface, which are used as a limiting input parameter in the subsequent calculations. Section 6.5 shows the results of the calculations regarding the loading of the front carriage (identical for both sub-variants). And sections 6.6 and 6.7 show the results of back carriage calculations for respectively the counterweight sub-variant and the upper rail sub-variant. Section 6.8 considers other ways of spreading the loads on the wheel-rail interface. The penultimate Section 6.9 shows a comparison of the minimum cantilever length of all the possible options and variants. And finally the conclusions of this chapter are given in Section 6.10.

6.1. Loads and load model

This section describes the load model and the loads taken into account for the design of the cantilever gate. Based on this model the minimum length of the cantilever is determined.

6.1.1. Load model

The 3D cantilever gate is simplified as a 2D rigid body, in which the roller carriages are assumed to be roller supports, see Figure 5.9. In reality the roller carriages are connected to the frame of the cantilever gate by pendulum rods which only can transfer forces radially to the rod, and therefore this assumptions can be made. In the assumed model the location of the roller-supports is somewhat inwards of the total length of the cantilever part due to the size of the carriages and the rods being located in the middle of those carriages . The effective cantilever arm ($L_{cant,arm}$) can be calculated by taking the cantilever length (L_{cant}) and subtracting half the length of each of the roller carriages:

$$L_{cant,arm} = L_{cant} - \frac{L_{car,front}}{2} - \frac{L_{car,back}}{2}$$

Figure 6.1 shows the load model, where all of the loads of importance to the balance of the cantilever gate are included. The model makes a distinction between the gate and the cantilever part and the corresponding dead weight and buoyancy loads. The loads of importance to the balance of the cantilever gate are:

- Dead weight (permanent)
- Upward buoyancy (permanent)
- Weight of silt and accretion (permanent)
- Resultant of resistance forces during opening/closing (variable)
- Leakage of 15% of the buoyancy chambers (accidental)

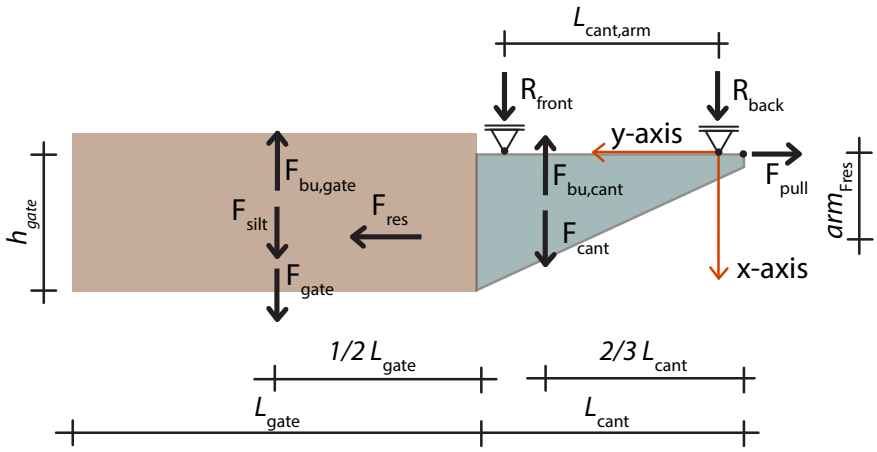

Figure 6.1: Load model of the loads on the cantilever rolling gate. Indicating the location of the forces and the roller carriages modelled as roller supports.

The calculations within the load model are based on basic statics. In order to calculate the reaction force on the front carriage (R_{front}), the sum of moments around the pin support of the back carriage is determined. The pin support has infinite rotational capacity and therefore the sum of moments at this location is zero. All of the vertical and horizontal forces and their respective 'arms' to the back carriage are taken into account. The reaction force in the back carriage (R_{back}) is then determined by taking the sum of forces of the rigid body, which should be in equilibrium (because $\sum F = 0$). In this model an upward force is assumed to be negative, while a downward force is positive.

The values for each of the individual loads for the different loading situations (see Section 6.2.1) are shown in the following subsections.

6.1.2. Dead weight (Permanent)

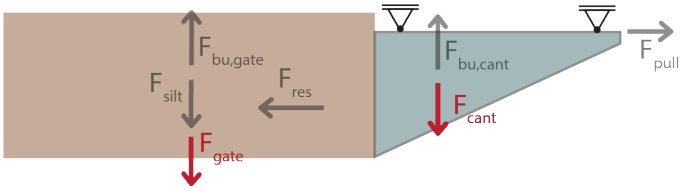

Figure 6.2: The dead weight forces highlighted red in the load model.

The **dead weight of gate part** (F_{gate}, see Figure 6.2) is equal to the weight of the current gate, which is 946 tonnes. This is equal to a gate dead weight force of $(9.81\ m/s^2 \cdot 946\ t =)\ 9280\ kN$. The resultant of this force acts downwards, at exactly the middle of the gate part.

The **dead weight of cantilever part** (F_{cant}) is dependent on the layout of the cantilever structure and the chosen cantilever length. The cantilever extension is assumed to be designed as a truss structure, as it does not have to seal off and retain water and the truss structure has an effective use of materials in combination with a relatively strong load-bearing capacity.

Appendix D shows the calculation and preliminary design of a triangular shaped open truss cantilever structure, consisting of Circular Hollow Sections (CHS). The dead weight of the structure is calculated to be 56.14 tonnes for the reference cantilever length of 24 m (see Section 5.4). In subsequent calculations, the dead weight of the cantilever part is taken directly proportional to this reference value and the corresponding cantilever length. Which can be translated in the following formula for the dead weight:

$$W_{cant} = \frac{56.14\ t}{24\ m} \cdot l_{cant}$$

In which W_{cant} is the dead weight of the cantilever part and l_{cant} is the length of the cantilever part. The force of this cantilever weight is calculated by:

$$F_{cant} = W_{cant} \cdot 9.81\ m/s^2$$

In the calculations in appendix D it is shown that the centre of gravity of the cantilever structure is almost equivalent to the centre of gravity of a triangle. Therefore, from here on, the centre of gravity for the cantilever structure is assumed to be located at 2/3 of the length of the cantilever (from the rightmost side). The force of the dead weight of the cantilever acts downwards at this location.

Both the dead weight of the gate and the cantilever part are constant for all loading situations. The dead weight of the cantilever part is dependent on the design variable: the cantilever length.

6.1.3. Upward buoyancy (Permanent)

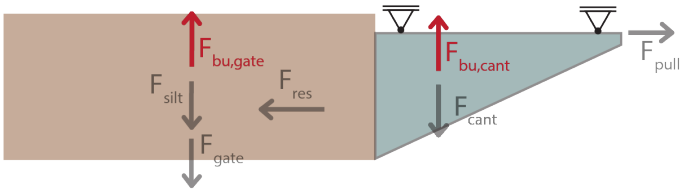

Figure 6.3: The upward buoyancy forces highlighted red in the load model.

The buoyancy volume force is dependant on the water level. Three water levels are of importance to the design of the cantilever gate:

- + 3.50 m N.A.P. - Highest lockage water level (*HW*)
- + 0.20 m N.A.P. - Median of high and low tide (*MW*)
- - 3.40 m N.A.P. - Lowest lockage water level (*LW*)

The highest (HW) and lowest lockage (LW) water level situations are of importance to the equilibrium and strength calculations, whereas the median water level (MW) is used in case of fatigue (see Section 6.2.1).

For the calculation of the buoyancy force, a water density of 1000 kg/m^3 is assumed.

The **upward buoyancy of the gate part** ($F_{bu,gate}$, see Figure6.3) is equal to the buoyancy volume of the current gate of the Western lock in Terneuzen. Table 6.1 shows the buoyancy volumes and upward forces for the three significant water levels. Upward forces are noted with minus sign.

Table 6.1: Buoyancy volume and upward force of the gate part for significant water levels

Water level	Buoyancy volume gate part m^3	Upward force gate part kN
HW	735.3	-7213
MW	716.6	-7030
LW	696.2	-6830

The **upward buoyancy of cantilever part** ($F_{bu,cant}$) is dependent on the volume of steel circular hollow sections under water and is calculated in appendix D and table D.14. Table 6.2 shows a summary of the buoyancy volume and the accompanying upward force for the three significant water levels for a cantilever length of 24 meter.

Table 6.2: Buoyancy volume and upward force of the cantilever part for significant water levels and a cantilever length of 24 meter

Water level	Buoyancy volume cantilever part m^3	Upward force cantilever part kN
HW	26.5	-260
MW	19.7	-193
LW	10.7	-105

It is assumed that, just as for the cantilever dead weight, the buoyancy volume of the cantilever part is taken linearly proportionate to the cantilever length with respect to the base values shown in table 6.2. Which can be translated in the following formula for the buoyancy volume:

$$V_{b,cant} = \frac{V_{b,cant,24m}}{24} \cdot l_{cant} \quad tonnes$$

In which:

$V_{b,cant}$ is the buoyancy volume of the cantilever part,
$V_{b,cant,24m}$ is the specific buoyancy volume of the cantilever part with a length of 24 m and
l_{cant} is the length of the cantilever part.

6.1.4. Silt and fouling (Permanent)

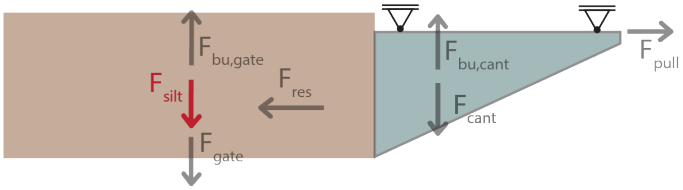

Figure 6.4: The silt and fouling weight force highlighted red in the load model.

Section 3.3 concluded that possible presence of accumulation of silt, shell growth and debris can lead to a significant additional weight to the gate. The presence or absence of silt plays a significant role in the balance calculations of the cantilever gate. The additional weight is variable over time and therefore difficult to predict exactly.

Just after completion and at the start of operation of the gate, no silt has had time to settle and shells haven't grown yet. Somewhere in the lifetime of the gate the maximum possible silt and aggregation will be present.

Taking into account the assumptions made in Section 5.3 (max of $0.15\ m$ silt with a specific weight of $13\ kN/m^3$, the maximum weight of silt on top of the buoyancy chambers is calculated by:

$$0.15\ m \cdot 13\ kN/m^3 \cdot 44.56\ m \cdot 6.43\ m = 559\ kN$$

The surface area of the gate is estimated by:

Gate plating (x4): $44.56 \cdot 19.22 \cdot 4 = 3425\ m^2$
Buoyancy chamber plating (x2): $44.56 \cdot 6.43 \cdot 2 = 484\ m^2$
Assumed other steel surface area: $1500\ m^2$

Which gives a total of approximately 5500 m^2 steel area. Taking into account the assumption of $0.10 kN/m^2$ for the weight of the clams, the total weight of shell accretion is then:

$$5500\ m^2 \cdot 0.1\ kN/m^2 = 550\ kN$$

The total maximum silt and accretion weight is then: $559 + 550 = 1109\ kN$. Which is a weight of $110.9\ tonnes$. The resultant silt force (F_{silt}), see Figure 6.4) acts downwards at exactly the middle of the gate part.

Due to the circular cross-sections of the cantilever structure no silt is able to settle on the cantilever part. As a conservative assumption, the possible accretion of clams on the cantilever part is not taken into account in the calculation.

6.1.5. Resultant resistance force during opening/closing (Variable)

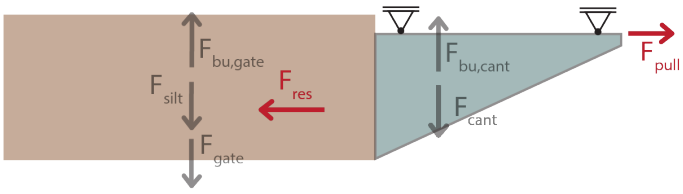

Figure 6.5: The pulling and resistance force highlighted red in the load model (direction is during opening of the gate).

In order to move the gate in open or closed position, the driving system has to be able to exert a force which is bigger than the resultant resistance force (F_{res}, see Figure 6.5) of the gate. This resultant resistance force can consist of:

- Mass inertia of the gate
- Mass inertia of the driving mechanism
- Hydrodynamic resistance due to the suction effect
- Hydrodynamic resistance due to waterflow allong the gate
- Rolling resistance of the wheels
- Friction force due to a residual water-head
- Friction force due to a water density difference
- Friction force due to a translation wave
- Friction force due to wind waves
- Friction force due to an extreme ship wave

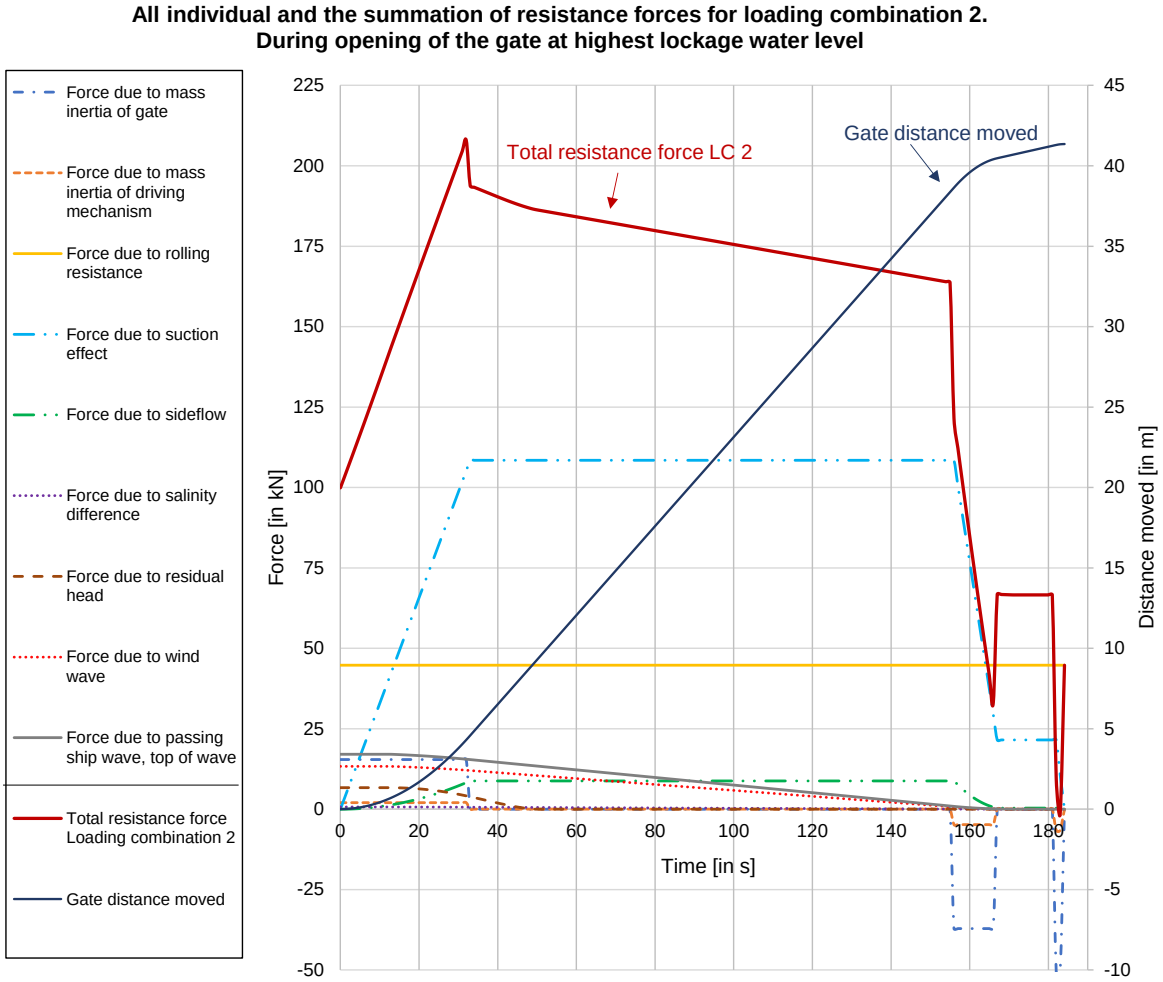

Figure 6.6: Individual and summation of resistance forces of the significant loading combination during opening of the gate at highest lockage water level (see appendix C for complete calculation). The left y-axis shows the force in kN, whereas the right y-axis shows the distance moved in m. The distance moved by the gate is displayed by the blue line.

The thruster forces of vessels entering or leaving the lock are not taken into account as they mainly cause a load when the gate is in closed position. The magnitude of the forces differs over the opening/closing sequence of the gate, mainly depending on the portion of the gate protruding the lock and the speed and acceleration of the gate at a specific moment in time.

The values for each of these forces during opening and closing of the gate and the possible loading combinations are elaborated in appendix C. An example of the individual and the summation of one of the loading combinations during opening of the gate at the highest lockage waterlevel is shown in Figure 6.6. This graph shows the difference in magnitude between the individual resistance forces over the opening sequence of the gate. The opening sequence is based on the gate operating data shown in Table 5.2 and displayed as respectively the gate speed and protruded gate part over time in Figures C.1 and C.2.

Table 6.3 shows the conclusion of the calculations from appendix C. It shows the maximum resistance/pulling force exerted on the gate during the highest and lowest lockage water levels during opening and closing of the gate.

Table 6.3: Overview of the maximum resistance forces during movement of the gate for different situations

	Opening (O)	Closing (C)
Highest lockage water level (HW)	$208\ kN$	$191\ kN$
Lowest lockage water level (LW)	$166\ kN$	$149\ kN$

The resultant of the resistance forces and the pulling force of the driving mechanism form a couple that exerts a moment-force on the cantilever gate, as shown in Figure 6.7. This figure shows that the opening of the gate creates a clockwise moment, whereas closing of the gate creates a anti-clockwise moment. The moment is calculated by multiplying the maximum resultant of the resistance force by the orthogonal distance (or 'arm') between the pulling force and the resultant of the resistance forces.

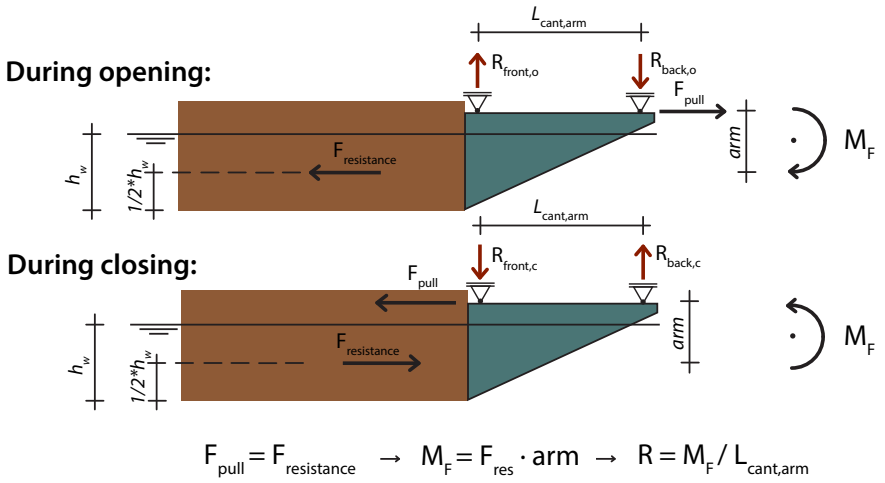

Figure 6.7: Assumptions regarding the direction and location of the forces which are of importance to the calculation of the moment-force created by the gate movement during opening and closing.

For ease of calculation, it is assumed that the point of application of the resultant of the resistance forces is located at half the water height (1/2 h_w), as the suction effect is the main contributor to the resistance forces. It should be noted that this is an overestimation. In reality this point of application is probably somewhat higher and closer to the pulling force.

The pulling force of the driving mechanism acts at the level of the contact between wheels and rails (as this is also the location where the moment force needs to be transferred to). It is assumed that the wheel/rail contact (and therefore the pulling force) is located at +4 m N.A.P., 2 meter lower than the top of the gate. Table 6.4 shows the length of the arm between pulling and resultant resistance force and the corresponding moment force. A clockwise moment force is set to be negative, and an anti-clockwise moment force is positive.

For the Median Water situation in case of fatigue, the average value of the resultant resistance force for high and low water is taken and the moment arm is determined by the Median Water level ($+0.20\ m\ N.A.P.$)

Table 6.4: Overview of the resistance forces and acting moment forces due to the resistance/pulling force moment couple (clockwise moment is negative)

Loading situation	Resultant resistance force kN	Waterheight relative to bottom (h_w) m	$1/2\ h_w$ m	Moment-arm m	Moment-force kNm
HW & O	-208	16.72	8.36	8.86	-1843
LW & O	-166	9.82	4.91	12.31	-2044
HW & C	191	16.72	8.36	8.86	1692
LW & C	149	9.82	4.91	12.31	1834

6.1.6. Leakage of buoyancy chambers (accidental)

For the balance of the gate the volume of air or water inside the buoyancy chambers is relatively important. Any leakage or sudden change can be detrimental. This load takes into account the accidental occasion in which the gate is in closed position and is hit by a vessel and some of the buoyancy chambers start leaking and the gate still has to be opened. The buoyancy chambers are divided in multiple compartments and thus the volume will not suddenly fill up completely. The main part of the buoyancy chamber consists of 20 parts. It is assumed that a maximum of three of those chambers, or 15% of the available buoyancy volume get filled due to a ship collision.

Other incidental loads (e.g. collision or ice loads) are not taken into account as they are mainly of influence to the horizontal perpendicular loading of a completely closed gate which is not taken into account in these calculations.

6.2. Loading situations and combinations

The balance of the gate should be guaranteed under all loading situations & combinations relevant in the longitudinal direction of the gate. This section elaborates these situations and combinations.

6.2.1. Loading situations

The longitudinal balance of the gate depends, among other things, on the gate's buoyancy volume. The maximum and minimum buoyancy of the gate is determined by the maximum and minimum water levels at which the gate is still operational. At higher or lower water levels than these limits, the gate will remain in closed position and the lock will no longer allow vessels to pass. In this case, only the high water retention function is active and the ship passage function is no longer performed (see Section 3.1). While retaining high water, the cantilever gate still has to be in balance. However, the significant loading situation for the balance occurs during opening or closing of the gate as the movement of the gate adds considerable extra resistance forces (see Section 6.1.5). Therefore, the maximum and minimum water levels at which the ship passage function is still provided (and the gate is opened and closed) are the governing situations for the balance of the gate.

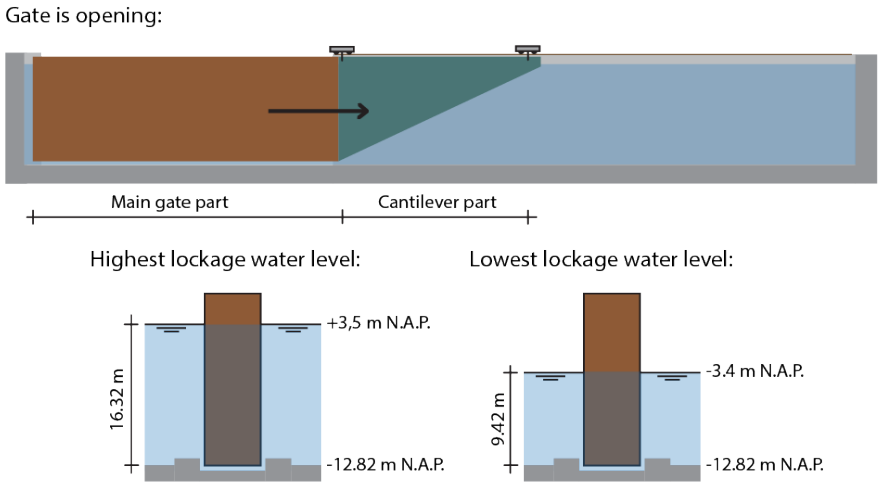

Figure 6.8: Indication of the opening direction of the gate (top) and the highest and lowest waterlevel at which the gate still opens and closes (bottom).

The two extreme water levels for which the gate still is operational are:

1. Maximum lockage waterlevel at +3.5 m N.A.P. (Maximum water level for which the gate can still be opened)

2. Minimum lockage waterlevel at -3.4 m N.A.P. (Lowest measured water level in history)

Figure 6.8 shows both of these water levels and the corresponding water height from the bottom of the gate structure. Opening of the gate is defined as the situation in which the gate is retracting inside the gate chamber.

The load situation during the gate movement (opening and closing) is normative due to the additional forces arising during motion. In order to simplify the force calculations of the cantilever construction, all forces from the movement (resistance etc.) are combined into one representative force. As shown in Section 6.1.5, the size and direction of the resultant resistance force and the associated moment-force is dependant on the direction of travel of the gate and the water level. Therefore the loading of the gate is different for the following four situations:

- High Water (HW) & Opening (O)
- High Water (HW) & Closing (C)
- Low Water (LW) & Opening (O)
- Low Water (LW) & Closing (C)

6.2.2. Loading combinations

A loading combination is a collection of different loads, load cases and/or loading situations, which may occur simultaneously. It is important that all possible load combinations are verified to be sure that the structure is safe. All listed loads, load situations and load combinations are related to the loading in longitudinal direction of the gate. The calculations are based on the limit state method and application of partial safety factors for each of the characteristic loads.

Most of the calculations in this case study are related to the Ultimate Limit State (ULS), as the research looks into the ultimate and optimal design of the cantilever rolling gate. In the determination of the load factors, a Consequence Class 3 (CC3) is taken into account. Eurocode EN1990 [44] states that the following ultimate limit states shall be checked:

- Loss of static equilibrium of the structure or any part of it (EQU);
- Internal failure or excessive deformation of the structure or structural members (STR);
- Failure caused by fatigue or other time-dependent effects (FAT)

Therefore, a distinction is made with regard to loads, load combinations and the corresponding safety factors between situations involving equilibrium (EQU), strength (STR) and fatigue (FAT). With respect to the gate design the strength and fatigue checks are mainly of importance to the design of the wheel-rail interface, while the equilibrium of use to the correct balancing of the gate. In accordance with [72], the dead weight, buoyancy force and the weight of silt and accretion are all regarded as permanent loads.

Silt or no silt

Due to the variability of the weight of silt and accretion over time, silt is taken into account in the possible loading combinations. A distinction is made between the gate at start of operations (where no silt or accretion is present yet) and the maximum loading situation during the gates lifetime (where the maximum possible silt and accretion weights on the gate).

(Un)favourable loads

For the equilibrium (EQU) and Strength (STR) checks, a distinction is made for the loading combinations between the combination of an favourable dead weight and an unfavourable buoyancy force and vice versa. This distinction is of importance due to the balancing and load transfer nature of the cantilever rolling gate. The significant normative load of the different combinations depends on the considered situation. For instance, with respect to the balancing of the loads on the supports/carriages, a situation in which the dead weight is favourable and the buoyancy is unfavourable can lead to the significant load for which the front carriage doesn't get uplift (in case of equlibrium check) or the back carriage has to resist the highest load (in case of a strength check).

Simplified loading combination tables
For simplicity's sake, only the load combinations with a difference between (un)favourable dead weight and buoyancy and silt or no silt (and the incidental load situation where 15 % leakage occurs) are shown in tables. The magnitude and direction of the shown loads are still dependent on the considered water level and the direction of movement of the gate. Thus the amount of possible load combination is larger than shown in the tables. All of these combination still need to be multiplied by the four loading situations mentioned in Section 6.2.1 (HW/LW · O/C), as for each combination the water level and the force direction of the resistance force is different.

The incidental loading combination only distinguishes between high water and low water as this situation only occurs if the gate has to be pulled back into the gate chamber from a closed position. The load combination tables in the subsequent subsection show five combinations, but in reality the total number of combinations for EQU and STR is 18.

6.2.3. Equilibrium (EQU)
The equilibrium loading combinations are related to the balance and equilibrium of the cantilever gate. These combinations have to be used in case of any equilibrium checks. Table 6.5 shows the load combinations and their partial safety factors to be used with the calculations regarding equilibrium of the gate, in accordance with the Richtlijn Ontwerp Kunstwerken (ROK 1.4)[58] and Eurocode NEN-EN 1990/NB [44] & [45].

Table 6.5: Load combinations and their partial safety factors in case of equilibrium check [45]

LOAD COMBINATION:	**EQU 1** DW unfavourable Bu favourable No silt	**EQU 2** DW favourable Bu unfavourable No silt	**EQU 3** DW unfavourable Bu favourable Max silt	**EQU 4** DW favourable Bu unfavourable Max silt	**EQU 5** Leakage of Bu Max silt
Permanent loads					
Dead weight (DW) of gate	1.05	0.95	1.05	0.95	1
Upward buoyancy (Bu) of gate	0.95	1.05	0.95	1.05	1
Silt and shell accretion weight	0	0	1.05	0.95	1
Variable loads					
Combination of resistance forces during opening or closing	1.5	1.5	1.5	1.5	1
Accidental loads					
Leakage of 15% of buoyancy chambers	0	0	0	0	1

Each of these loading combinations has to be multiplied by the four different loading situations due to High/Low water and Opening/Closing. Except for the incidental combination, which only takes into account a difference in High and Low water as it can only occur during opening of the gate.

The shown partial safety factors only apply in case of any ULS checks related to the equilibrium of the cantilever rolling gate. Therefore these values are used to assess the (internal) balancing of the gate structure.

6.2.4. Strength (STR)
Table 6.6 shows the load combinations and their partial safety factors to be used with the calculations regarding strength of the gate, in accordance with the Richtlijn Ontwerp Kunstwerken (ROK 1.4)[58] and Eurocode NEN-EN 1990/NB [44] & [45]. The partial safety factors are determined considering Consequence Class 3 (CC3) and taking into account unfavourable loads.

Each of these loading combinations is combined with each of the four different loading situations due to High/Low water en Opening/Closing. Except for the incidental combination, which only takes into account a difference in High and Low water as it can only occur during opening of the gate.

The strength (STR) partial safety factors and load combinations are used in case parts of the cantilever gate have to be checked for ULS strength. These strength loading combination are mainly used for the calculation of the wheel-rail interface loads and the determination of the loads on the frame of the cantilever structure.

Table 6.6: Load combinations and their partial safety factors in case of strength check [45]

LOAD COMBINATION:	STR 1 DW unfavourable Bu favourable No silt	STR 2 DW favourable Bu unfavourable No silt	STR 3 DW unfavourable Bu favourable Max silt	STR 4 DW favourable Bu unfavourable Max silt	STR 5 Leakage of Bu Max silt
Permanent loads					
Dead weight of gate	1.25	0.9	1.25	0.9	1
Upward buoyancy of gate	0.9	1.25	0.9	1.25	1
Silt and shell accretion weight	0	0	1.25	0.9	1
Variable loads					
Combination of resistance forces during opening or closing	1.5	1.5	1.5	1.5	1
Accidental loads					
Leakage of 15% of buoyancy chambers	0	0	0	0	1

6.2.5. Fatigue (FAT)

The fatigue loading situation/combination is somewhat different to the equilibrium and strength checks. It considers the average loading situation recurring everyday, instead of the extreme loading situation. Therefore for fatigue calculations with respect to the balance and forces in longitudinal direction of the gate, the Mean Water level (MW) of $+0.20\ m\ N.A.P.$ is considered (which is the mean of the high and low daily tide). In this case study fatigue is mainly related to the wheel-rail interface. The daily operation of the gate creates stress alterations in the wheels and the rails which can lead to fatigue failure.

Table 6.7 shows the load combinations and their partial safety factors to be used with the calculations regarding fatigue of the gate, in accordance with NEN 6786 [40] and EN 13001-1 [41].

Table 6.7: Load combinations and their partial safety factors in case of fatigue check [40] & [41]

LOAD COMBINATION:	FAT 1 Fatigue load combination, silt present
Permanent loads	1
Dead weight of gate	1
Upward buoyancy of gate	1
Silt and shell accretion weight	1
Variable loads	
Combination of resistance forces during opening or closing	1
~~**Accidental loads**~~	
~~Leakage of 15% of buoyancy chambers~~	0

As can be seen in the table, in case of fatigue loading, all partial safety factors are 1 and an average daily re-occurring loading situation is assumed. Therefore the mean water level (MW) is used in this situation as it is an average of all the different possible water levels. The accidental loads are neglected in case of fatigue as they are extraordinary, while fatigue loading is all about re-occurring loads. This sole loading combination still has to differ in the direction of the loading due to the resistance forces during opening/closing of the gate. For fatigue thus only 2 loading combinations are of importance.

6.3. Gate equilibrium

This section investigates and elaborates ways of reaching equilibrium in the gate and on its supports.

6.3.1. Influence of the cantilever length

The length of the cantilever part has a major influence on the reaction forces on the supports/roller carriage. Figures 6.9a and 6.9b show the reaction forces on the front and back carriage at highest and lowest lockage water level for respectively opening and closing of the gate. In this calculation both carriages are assumed to be pin supported and not able to move in vertical direction. The graphs show the forces in case of an 8-wheel front carriage and a 4-wheel back carriage. The full calculations of the characteristic reaction forces can be found in the first part of appendix F.

A negative force means that the support reaction force is acting upwards. The front support has a force acting downwards, while the back support has a force acting upwards. The graphs show the influence of the length of the cantilever structure on the size of the support forces. Logically, an increased cantilever length increases the distance between the supports and therefore the gate is balanced more evenly

and the reaction forces become smaller. As can be seen in both graphs, the reaction forces increase significantly if the cantilever length becomes shorter than approximately 13 m. This is an indication that a relatively short cantilever length is not possible as the forces become too large.

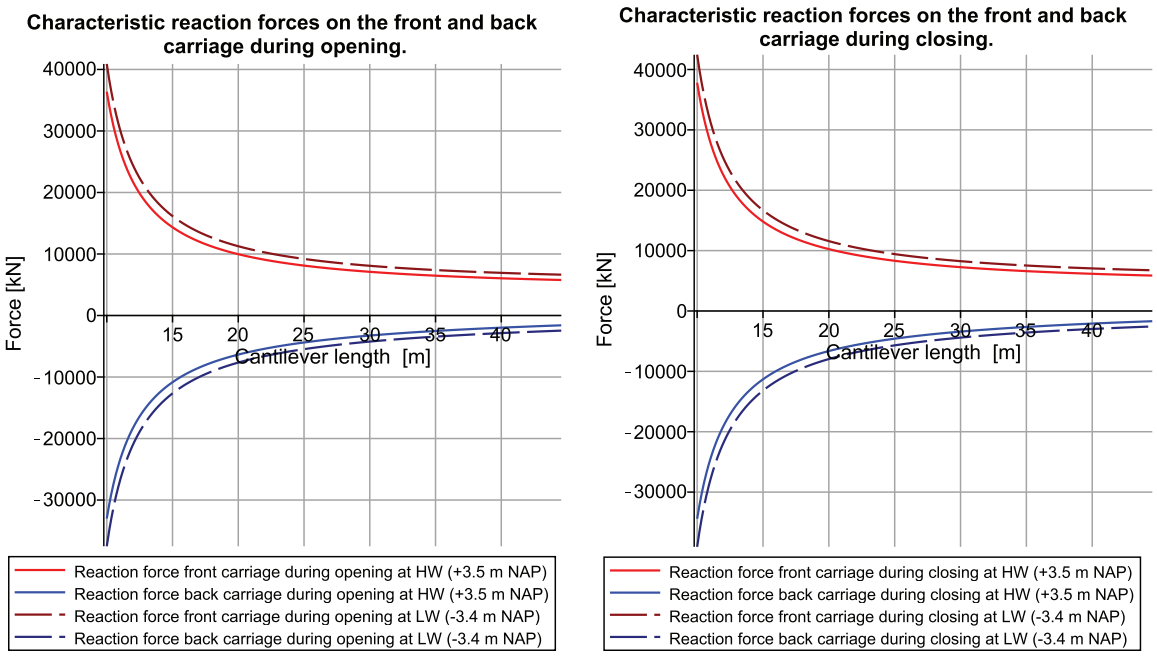

(a) Opening (b) Closing

Figure 6.9: The characteristic reaction forces on the front and back carriage during opening (left) and closing (right) at the highest and lowest lockage water level, plotted against the cantilever length. A negative force means that it is pointed upwards

6.3.2. Extra buoyancy volume

The least intrusive way to try to balance out the cantilever gate is by adding extra buoyancy volume to the gate part. In this way extra uplift is created countering the downward force and decreasing the overturning moment. However, there is one issue and it is related to the possible uplift of the gate under certain conditions. The cantilever gate should be in balance (and have a certain safety) under all circumstances and loading conditions. As this issue relates to the balancing of the gate, the loading combination of Equilibrium (EQU) mentioned in Section 6.2.3 should all be checked.

The maximum additional buoyancy volume is found by looking for the limit to which the front carriage does not float up under the most extreme loading situation. The governing and defining loading situation is a combination of the highest lockage water level (HW), the maximum resistance force during opening of the gate (O), no silt present yet and the dead weight and buoyancy volume respectively taken as favourable and unfavourable. This loading situation creates the smallest force on the front carriage and should be at least 200 kN downwards to safely prevent the possibility of uplift of the carriage.

Figure 6.10 shows the maximum possible extra buoyancy volume plotted against a variable cantilever length. The graph shows that, dependent on the cantilever length, the maximum extra buoyancy volume is somewhere in between 111 and 123 m^3.

Without any extra buoyancy the maximum buoyancy volume of the gate part is 1024.7 m^3. This volume can be increased by a maximum of circa 11% to decrease the downward momentum of the cantilever gate and still ensure no lift for the governing equilibrium loading situation.

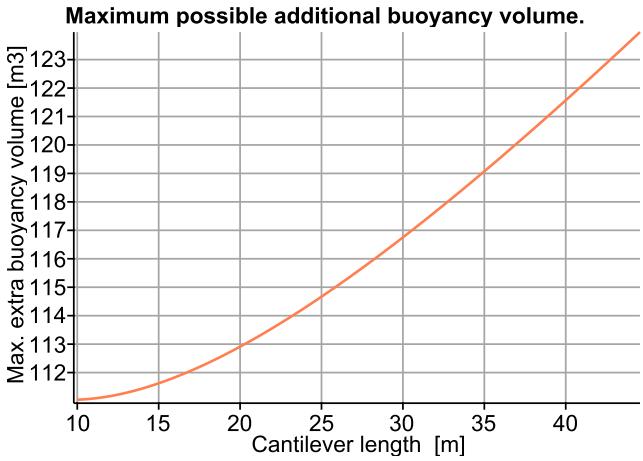

Figure 6.10: The maximum possible additional buoyancy volume which still ensures that the front carriage does not float up under the governing loading situation (ULS EQU, HW, Opening, no silt, buoyancy unfavourable, dead weight favourable), plotted against the cantilever length.

6.3.3. Sub-variants

Section 6.3.2 showed that the amount of additional buoyancy volume is limited due to restrictions to the uplift of the front carriage. Without any additions, the balance of the cantilever gate cannot be brought in equilibrium as there would be an upward force on the back carriage for certain loading situations. Two sub-variants that can solve this problem are:

- A counterweight located right below the back carriage.
- An upper rail on top of the trajectory of the back carriage.

Both sub-variants are respectively shown in Figures 6.11 and 6.12.

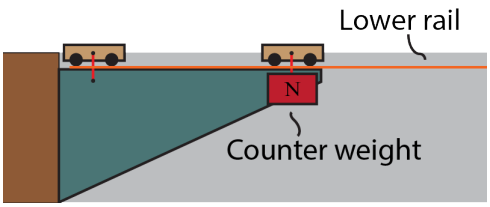

Figure 6.11: The counter weight sub-variant

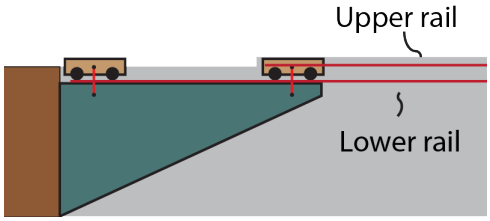

Figure 6.12: The upper rail sub-variant

Within each of the two sub-variants, a distinction is made with respect to the amount of wheels on the front carriage. A 'normal' situation is considered in which the front carriage has four wheels, and on the other hand a 'strengthened' option is elaborated in which the front carriage is extended and the amount of wheels is doubled to eight wheels. In both situation the back carriage consists of four wheels.

Initially, the dimensions of the wheels and rails will not be changed and only the amount of wheels and the size of the carriage differs. For all of the carriages (both with four and eight wheels) the wheel-rail interface is identical to the current one of the Western lock in Terneuzen. Thus all wheels have a wheel diameter (D_w) of 1200 mm and the wheel/rail width (b_w or b_r) is 150 mm.

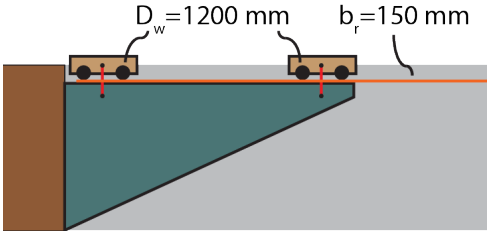

Figure 6.13: The 4-wheel front carriage option (with the wheel-rail interface identical to the current Western lock)

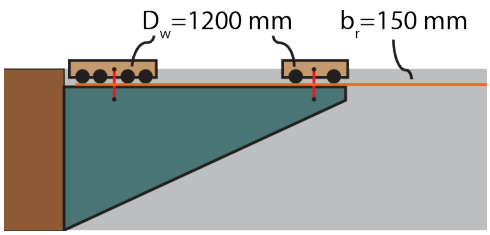

Figure 6.14: The 8-wheel front carriage option (with the wheel-rail interface identical to the current Western lock)

The main change caused by the larger front carriage is the shortening of the cantilever arm (in case of a similar cantilever length). A disadvantage of this shortening is the increased loads due to the shorter cantilever arm. However, the extra wheels strengthen the front carriage, which allows it to carry higher loads.

The two sub-variants only differ in load transfer with respect to the back carriage. Therefore the front carriage design is independent on the sub-variant choice and can thus be evaluated separately.

8-wheel carriage examples

While a 4-wheel carriage is the predominant type for rolling gates, an 8-wheel carriage has been applied in two cases. Both of these 8-wheel carriages are located in locks in IJmuiden (Northern lock and the new lock). The Northern lock has two lower carriages which both have eight wheels on each carriage (see Figure 6.15). The carriage consists of one large steel structure.

At its completion, the new lock in IJmuiden will be the largest lock in the world. Its gates are of the wheelbarrow type and the lower carriage will have eight wheels, as shown in Figure 6.16. This figure shows that the 8-wheel carriage is split into two parts (with each four wheels) that are connected to each other by a load equalizer. This ensures that the central point load from the gate is evenly spread over all of the eight wheels.

Figure 6.15: A picture of the bottom of the 8-wheel lower roller carriage of the Northern lock in IJmuiden [49]

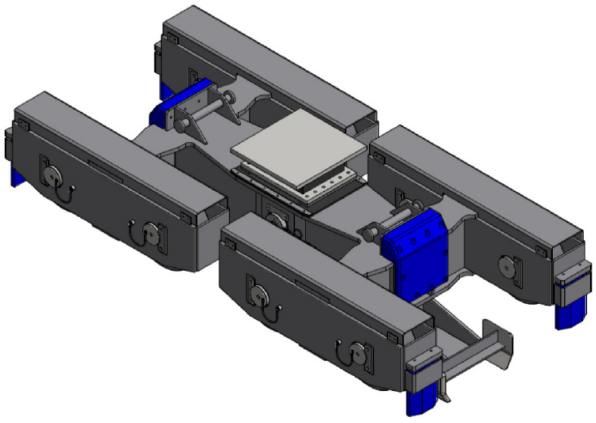

Figure 6.16: An isometric view of the 8-wheel lower carriage of the new lock in IJmuiden. The picture clearly shows the load equalizer which spreads the loads evenly over the eight wheels [32]

Both of these examples are lower carriages and therefore loaded by the gate via rubber bearings. The structures are relatively small as the rail track and carriage have to fit in the recess of the sill. In comparison to these type of carriages, the upper carriage of the cantilever gate has to be much wider and will also be loaded in a different way, as the gate 'hangs' instead of standing on top of the carriage. Despite this, these examples show that an 8-wheel carriage is a proven technology and can therefore be applied in this case study.

6.4. Wheel/rail capacities

The rail - wheel connection is one of the most sensitive and delicate parts of a rolling gate, as was concluded in Section 3.3.6. The wheels and rails have certain capacities to which they can be loaded before failure occurs. In this case study it is assumed that the wheels and rails are identical to the current ones of the Western lock in Terneuzen. Therefore, in this situation, the limits of the wheels and rails can be calculated and be used as an input to design the cantilever structure (especially the length of the cantilever arm).

The aim is to define the maximum allowable resistance design force on the wheels and rails of the carriage of the cantilever rolling gate for both the strength and the fatigue loading situation. Three different safety norms were found to specify loading capacities for wheel/rail contacts, that is NEN 6786 (VOBB) [40], DIN19704:1998 [48] and EN13001 [41]. The calculations in these norms are all based on the general Hertz theory [24]. The loading capacity of the wheel is in all calculation methods dependant on the material strength (squared), the diameter of the wheel and the width of the wheel-rail contact area. The extent to which other factors are included depends on the sophistication of the calculation method.

Hertz distinguishes between a point and a line contact [24]. As was concluded in Section 3.3.6, the geometry of the wheel and rail should ideally be such that it creates a line contact to reduce the peak stresses at the edges of the wheel and rail. Thankfully, the assumed wheel and rail of the Western lock in Terneuzen are both completely flat in perpendicular direction to the rail (thus both crown radii are infinite). Due to this geometry the contact surface always forms a line.

A full analysis and evaluation of these calculation methods and the exact calculation of the static and fatigue limit design resistance forces for both a front carriage with four and eight wheels can be found in appendix E.

The result of the calculations is given in tables 6.8 and 6.9, which show both the static and fatigue limit design force per calculation method for respectively a four and an eight wheel carriage.

Table 6.8: Limit design force per wheel for 3 calculation method in case of a four wheel carriage

	NEN 6786 VOBB	EN13001	DIN19704	HERTZ THEORY
Static limit design force (in kN)	6049	7794	8917	1872
Fatigue limit design force (in kN)	1368	1969	2092	-

Table 6.9: Limit design force per wheel for 3 calculation methods in case of an eight wheel carriage

	NEN 6786 VOBB	EN13001	DIN19704	HERTZ THEORY
Static limit design force (in kN)	6049	7794	8917	1872
Fatigue limit design force (in kN)	1188	1599	2092	-

From the tables it can be concluded that the fatigue limit design force gives a stricter requirement to the loading of the wheel/rail.

From the three main calculation methods, the EN13001 calculation method is the most comprehensive and the NEN 6786 calculation is the most simplistic (see table E.1). NEN 6786 has the strictest safety standard, which is probably caused by the simpler calculation method. In further calculations the limit design forces of the NEN 6786 are used in order to be safe and fulfill to all of the safety standards.

6.5. Front carriage

Conform the load model presented in Section 6.1.1, the load on the front carriage (F_{front}) is calculated by taking the sum of moments around the back carriage (modelled as a pin-support thus the sum of moments in this point is zero). The formula to calculate this load, taking into account the general partial safety factors, is given by:

$$F_{front} = \Big[\left(F_g \cdot \gamma_d - (F_b + F_{b,extra}) \cdot \gamma_b + F_{silt} \cdot \gamma_s\right) \cdot L_{Arm,gate} + \left(F_{cant} \cdot \gamma_d - F_{bu,cant} \cdot \gamma_b\right) \cdot L_{Arm,cant} + F_{res} \cdot \gamma_{res} \cdot L_{Arm,res} \Big] \cdot \frac{1}{L_{cant,arm}}$$

In which:

F_g	is the downward force of the dead weight of the gate part
F_b	is the upward force of the existing buoyancy volume of the gate part
$F_{b,extra}$	is the upward force of the extra added buoyancy volume in the gate part
F_{silt}	is the downward force of the weight of the silt and aggregation
F_{cant}	is the downward force of the dead weight of the cantilever part
$F_{bu,cant}$	is the upward force of the buoyancy volume of the cantilever part
F_{res}	is the (horizontal) resultant of the resistance forces due to moving of the gate
$L_{Arm,gate}$	is perpendicular distance between the back carriage and the gate forces
$L_{Arm,cant}$	is perpendicular distance between the back carriage and the cantilever forces
$L_{Arm,res}$	is perpendicular distance between the back carriage and the resistance forces
$L_{cant,arm}$	is the distance between the two supports/carriages

This is the force acting from the cantilever gate structure onto the front carriage via the pendulum rods. The load per wheel ($F_{wheelmax,front}$) can then be calculated by adding the weight of the front carriage ($F_{car,front}$) and dividing this total by the amount of wheels of the carriage ($N_{r,wheels,front}$) :

$$F_{wheelmax,front} = \frac{F_{front} + F_{car,front}}{N_{r,wheels,front}}$$

In these formulas the cantilever length is set to be variable. The extra buoyancy volume is calculated in line with the calculation and graphs shown in Section 6.3.2.

6.5.1. Wheel strength verification front carriage

For the wheel strength verification of the front carriage, the loading combination of lowest lockage water-level (LW), closing of the gate (C), the present of silt & aggregation and the dead weight and buoyancy respectively taken unfavourable and favourable is governing. This situation creates the highest force on the front carriage due to the largest downward forces and the smallest upward forces and the anti-clockwise resistance moment-force during closing of the gate. The partial safety factors of the fourth column (STR 3) of table 6.6 must therefore be applied. The strength design force for this governing loading situation is plotted against a variable cantilever length in Figure 6.17a in case of a 4-wheel front carriage and in Figure 6.17b in case of an 8-wheel front carriage.

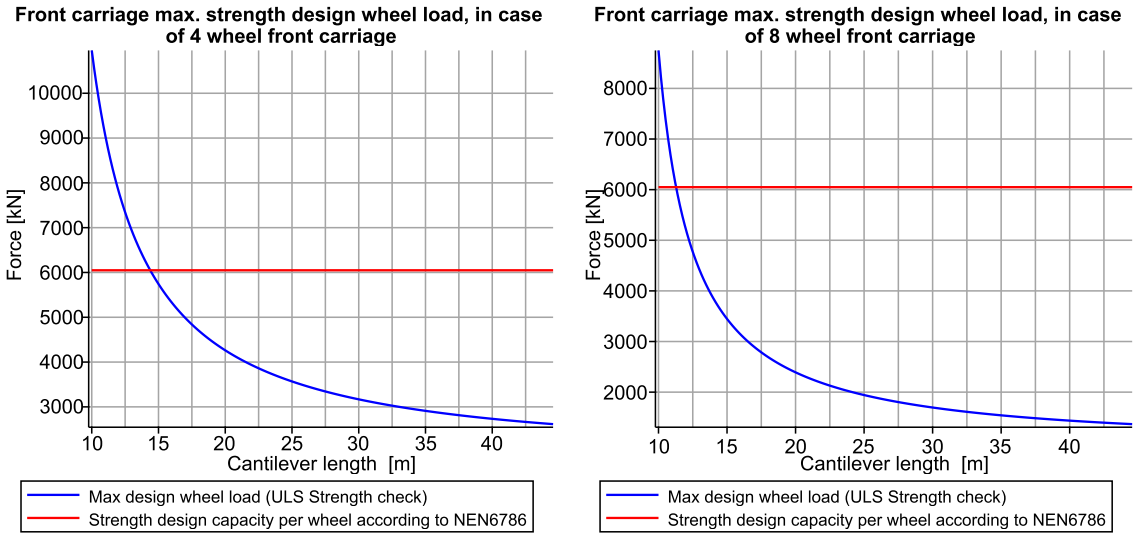

(a) *4-wheel* front carriage

(b) *8-wheel* front carriage

Figure 6.17: The governing maximum strength design wheel load of the front carriage, plotted against the cantilever length, in case of a *4-wheel* (left) and an *8-wheel* (right) front carriage with a wheel diameter of 1200 mm an wheel/rail width of 150 mm. The wheel strength design capacity (according to NEN6786) is indicated by the red line

Both graphs also show the wheel strength design capacity according to Dutch norm NEN 6786-1:2017 [40]. The elaborated calculation of the wheel strength design capacity of 6049 kN can be found in appendix E, Section E.3.

The point in the graphs at which the lines of the design load and the design capacity intersect, is the minimum cantilever length required to guarantee the safety of the wheel strength of the front carriage. In case of a 4-wheel front carriage, the cantilever length has to be at least 14.4 m. While for an 8-wheel front carriage, the length has to be at least 11.3 m to guarantee the fatigue safety of the wheels and rails of the front carriage.

6.5.2. Wheel fatigue verification front carriage

The wheel/rail combination is one of the most sensitive parts of the gate susceptible to fatigue.The fatigue wheel load is defined by the re-occurring load during the lifetime of the gate. The loading situation which occurs on average every load cycle is governing. For fatigue all of the partial safety factors are set to 1 and the internal loads are calculated in case of Mean Water (MW, average between high and low tide), during closing of the gate (highest force on front carriage) and with silt & accretion present. The fatigue design force for this governing loading situation is plotted against a variable cantilever length in Figure 6.18a in case of a 4-wheel front carriage and in Figure 6.18b in case of an 8-wheel front carriage.

The wheel/rail fatigue design capacities according to dutch norm NEN 6786-1:2017 [40] and European norm EN13001 [41] are also shown in the graphs. They indicate the maximum design capacity for each

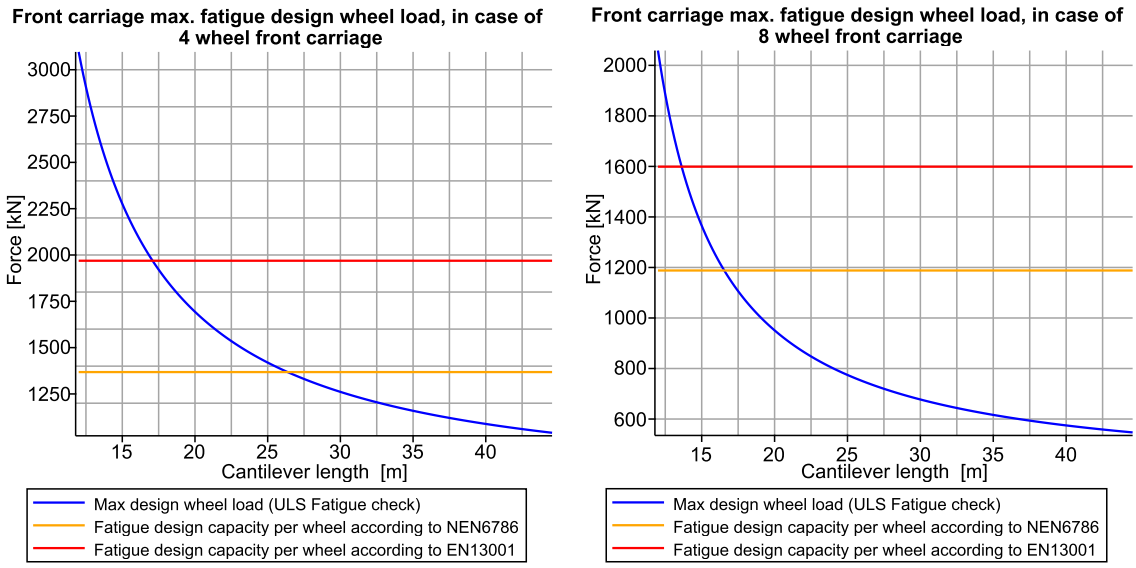

(a) *4-wheel* front carriage

(b) *8-wheel* front carriage

Figure 6.18: The governing maximum fatigue design wheel load of the front carriage, plotted against the cantilever length, in case of a *4-wheel* (left) and an *8-wheel* (right) front carriage with a wheel diameter of 1200 mm an wheel/rail width of 150 mm. The wheel fatigue design capacity is indicated by the yellow (NEN7686) and red (EN13001) lines

of the norms, as calculated in appendix E, Sections E.3 and E.5. In this case the design capacity of NEN6786 is lower than EN13001 and therefore taken as decisive.

The fatigue design capacity for a wheel/rail is dependant on the number of rollovers and therefore the amount of wheels on the front carriage is of influence to it. Thus the capacity differs between the 4-wheel front carriage and the 8-wheel front carriage. For the 4- and 8-wheel carriage (in case of NEN6786), the fatigue design capacities are respectively 1368 kN and 1188 kN.

The point in the graphs at which the lines of the design load and the NEN6786 design capacity intersect, is the minimum cantilever length required to guarantee the safety of the wheel/rail fatigue of the front carriage. In case of a 4-wheel front carriage, the cantilever length has to be at least 26.4 m. While in case of an 8-wheel front carriage the length has to be at least 16.6 m to guarantee the fatigue safety of the wheels and rails of the front carriage.

Compared to the strength capacity, the fatigue capacity is more stringent and therefore gives a larger minimum length of the cantilever.

6.6. Counterweight sub-variant

This sub-variant applies a counterweight in the cantilever structure right below the back carriage to bring balance to the cantilever rolling gate. The wheels of the carriages rest on a lower rail and therefore the forces coming from the gate and carriages always have to be downwards under all circumstances, otherwise the gate will rotate. This downward force is assured by adding the counterweight.

The weight cancels out the upward force created by the moment-force mainly due to the weight of the protruding gate part. The counterweight is integrated into the Circular Hollow Section structure of the cantilever part. For now it is assumed that the structure can carry this weight, but this has to be verified at a later moment. The counterweight has to be chosen such that it balances the gate (with a certain safety load) under all circumstances. In this sub-variant it is assumed that the maximum possible extra buoyancy volume as calculated in Section 6.3.2 is applied.

A downside of this option is the cost and placement of the required material for the counterweight. With respect to the other sub-variant (upper rail), the roller carriage can be freely changed and is not constrained. However, changing a roller carriage requires the gate and counterweight to be locked in place to keep a gate balance. How exactly this is to be carried out will have to be worked out at a later stage.

6.6.1. Required counterweight

In order to determine the minimum required counterweight, the governing loading situation has to be found. As it concerns the balance of the gate, table 6.5 regarding equilibrium applies. The loading combination which gives the smallest downward force (or biggest upward force) on the back carriage is defining. From all of the possible combinations stated in Section 6.2.3, the incidental combination for which 15% of the buoyancy chambers get filled due to collision and the gate still has to open (O) at the lowest lockage water level (LW) is the one which gives the lowest load on the back carriage. The size of the counterweight should be such that under this loading combination, still a downward safety force of 200 kN is applied on the back carriage.

As the counterweight is directly located below the back carriage, the calculation of the load on the front carriage does not change. Thus the calculation shown in Section 6.5 to calculate the load on the front carriage still applies, but this time the partial safety factors of the incidental loading combination have to be used and the 15% leakage has to be taken into account for the buoyancy volume. Now, the summation of vertical forces of the considered gate model, including the safety force (of 200 kN) and the counterweight force, should be zero. The only unknown is the counterweight force, which can be calculated by taking it to the other side of the equation. See appendix F for the full calculation.

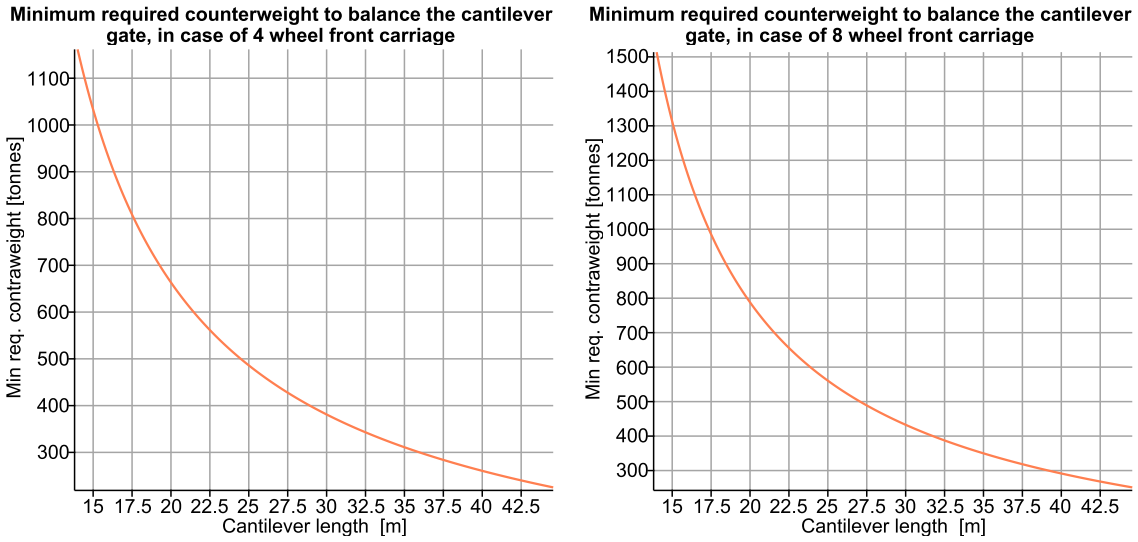

(a) *4-wheel* front carriage

(b) *8-wheel* front carriage

Figure 6.19: Minimum required counterweight to ensure a downward force on the back carriage under all loading situations (given that the extra buoyancy volume is also applied), plotted against the cantilever length. In case of a *4-wheel* (left) an *8-wheel* (right) front carriage.

Figures 6.19a and 6.19b show the minimum required counterweight (plotted against a variable cantilever length) for a cantilever gate with a front carriage with respectively four wheels and eight wheels. The size of the carriage is of importance due to the change in distance between the carriages/supports (in case of an equal cantilever length).

The minimum required counterweight quickly increases for shorter cantilever lengths as the distance between the two carriages becomes smaller. This calculated minimum size of the counterweight is assumed to be present in the gate structure in the subsequent calculations. Now that the counterweight has been determined, the wheels of the back carriage can be checked for safety.

6.6.2. Wheel strength verification back carriage

For the wheel strength verification of the back carriage in case of a counterweight, the loading combination of highest lockage waterlevel, opening of the gate, no silt & aggregation present and the dead weight and buoyancy respectively taken favourable and unfavourable is governing, as it gives the highest load of all the possible loading combinations. The partial safety factors of the third column (STR 2) of table 6.6 must therefore be applied. The strength design force is then calculated by adding the weight of the back carriage to this calculated force, and dividing it by the amount of wheels of the back carriage. The strength design force per wheel of the back carriage for this governing loading situation is plotted against a variable cantilever length in Figure 6.20a in case of a 4-wheel front carriage and in Figure 6.20b in case of an 8-wheel front carriage.

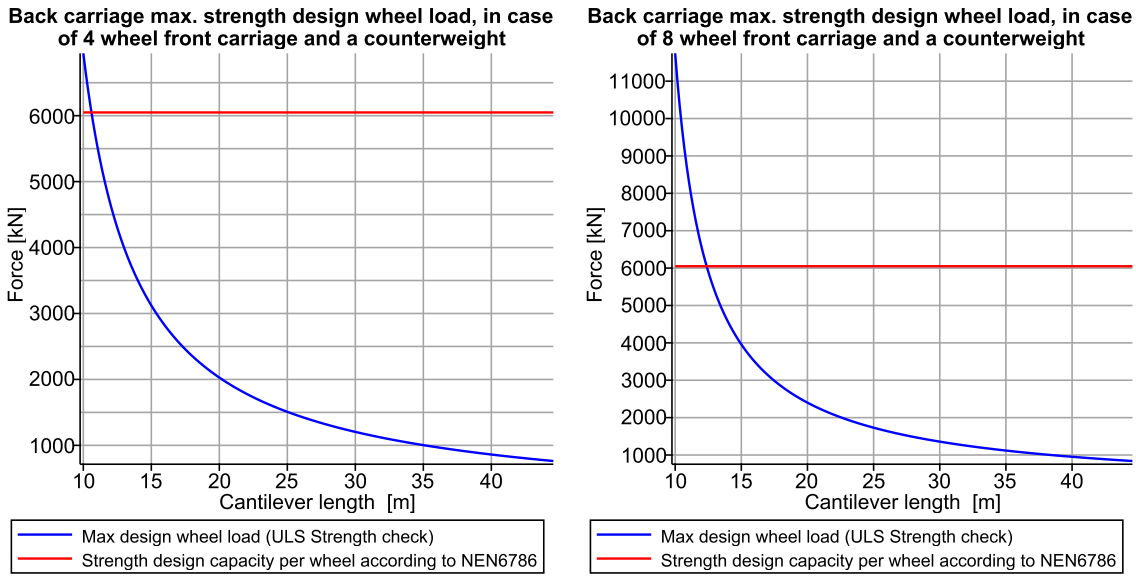

(a) *4-wheel* front carriage

(b) *8-wheel* front carriage

Figure 6.20: The governing maximum strength design wheel load of the back carriage, plotted against the cantilever length, in case of a *4-wheel* (left) and an *8-wheel* (right) front carriage and a *counterweight*. The wheels have a diameter of 1200 mm and a width of 150 mm. The wheel strength design capacity (according to NEN6786) is indicated by the red line

The point in the graphs at which the lines of the design load and the design capacity (6049 kN according to NEN6786, see appendix E) intersect, is the minimum cantilever length required to guarantee the safety of the wheel strength of the back carriage in case of a counterweight. In case of a 4-wheel front carriage, the cantilever length has to be at least 10.6 m. While in case of an 8-wheel front carriage the length has to be at least 12.4 m to guarantee the strength safety of the wheels and rails of the back carriage in case of a counterweight.

6.6.3. Wheel fatigue verification back carriage

For fatigue of the wheel/rail of the back carriage, all of the partial safety factors are set to 1 and the internal loads are calculated in case of Mean Water (MW), during opening of the gate (gives the highest downward force on back carriage) and with silt & accretion present. The fatigue design force for this governing loading situation is plotted against a variable cantilever length in Figure 6.21a in case of a 4-wheel front carriage and in Figure 6.21b in case of an 8-wheel front carriage.

The point in the graphs at which the lines of the design load and the design capacity (1368 kN according to NEN6786, see appendix E) intersect, is the minimum cantilever length required to guarantee the safety of the wheel/rail fatigue of the back carriage in case of a counterweight. In case of a 4-wheel front carriage, the cantilever length has to be at least 12.8 m. While for an 8-wheel front carriage the length has to be at least 14.7 m to guarantee the fatigue safety of the wheels and rails of the back carriage in case of a counterweight.

Just as for the calculations with respect to the front carriage, the minimum required cantilever length for the wheels of the back carriage is larger for the fatigue check compared to the strength check.

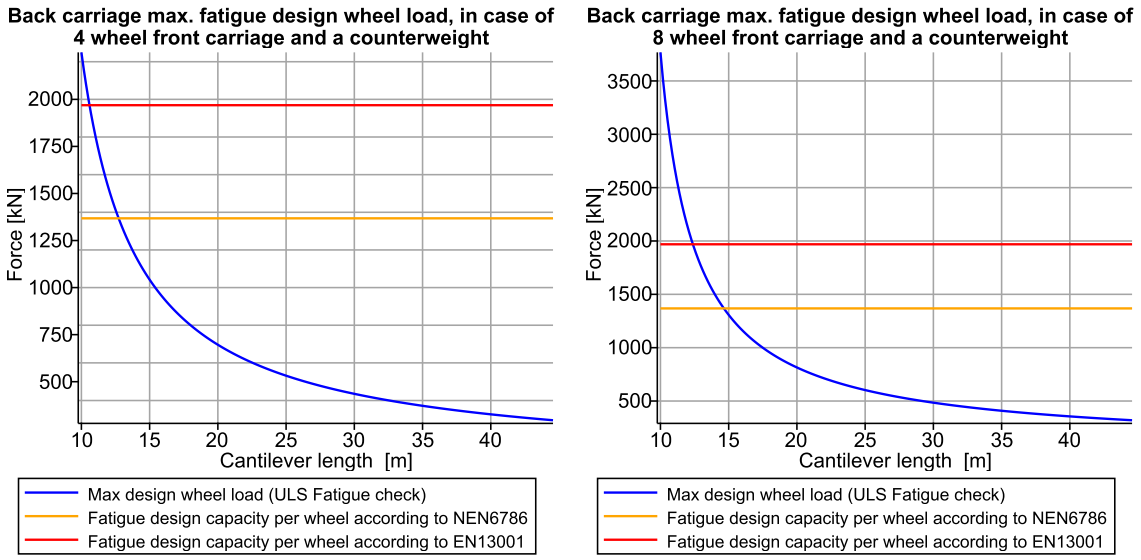

(a) *4-wheel* front carriage

(b) *8-wheel* front carriage

Figure 6.21: The governing maximum fatigue design wheel load of the back carriage, plotted against the cantilever length, in case of a *4-wheel* (left) and an *8-wheel* (right) front carriage and a *counterweight*. The wheels have a diameter of 1200 mm and a width of 150 mm. The wheel fatigue design capacity is indicated by the yellow (NEN7686) and red (EN13001) lines

6.7. Upper rail sub-variant

This sub-variant applies a static upper rail above the trajectory of the wheels of the back carriage, putting the wheels between a lower and upper rail. The upper rail is mounted on top of a concrete overhanging structure which is connected to the heavy concrete foundation of the gate chamber by cables and tension anchors. Any upward force coming from the cantilever gate is then transferred via the carriage towards the upper rail and taken by the structure. Any downward force is transferred via the lower rails toward the rail foundation.

A disadvantage of this option is that the roller carriage is more difficult to remove because it is wedged between the two rails. Secondly, the connection between the wheels and both wheels depends on tight tolerancing. The wheels cannot be clamped in between the rails as they need enough space to rotate. But at the same time the open space between the rail and the wheel can not become too large as then the gate moves considerably as the force direction on the back carriage changes. A third downside of the upper rail is the required strong foundation which increase material and construction costs.

For the verification of this option it is important that both the upper and lower rails and the wheels of the back carriage are able to take the maximum loads imposed by the gate. In this sub-variant it is assumed that the maximum possible extra buoyancy volume as calculated in Section 6.3.2 is applied.

6.7.1. Wheel strength verification back carriage

The wheel/rail connection of the back carriage has to be checked to see if it is within limits of the design capacity. For the wheel strength verification of the back carriage in case of an upper rail, the loading combination of lowest lockage waterlevel (LW), closing of the gate (C), silt & aggregation present and the dead weight and buoyancy respectively taken unfavourable and favourable is governing as it gives the highest (upward) load of all the possible loading combinations. The partial safety factors of the fourth column (STR 3) of table 6.6 must therefore be applied. This specific combination creates the largest upward force on the wheel/rail. The strength design force per wheel is then calculated by substituting the weight of the back carriage from this calculated force, and dividing it by the amount of wheels of the back carriage. The strength design force per wheel of the back carriage for this governing loading situation is plotted against a variable cantilever length in Figure 6.22a in case of a 4-wheel front carriage and in Figure 6.22b in case of an 8-wheel front carriage.

The point in the graphs at which the lines of the design load and the design capacity (6049 kN, see appendix E) intersect, is the minimum cantilever length required to guarantee the safety of the wheel/rail strength of the back carriage in case of an upper rail. In case of a 4-wheel front carriage, the cantilever length has to be at least 12.2 m. While in case of an 8-wheel front carriage the length has to be at least 14.1 m to guarantee the strength safety of the wheels and rails.

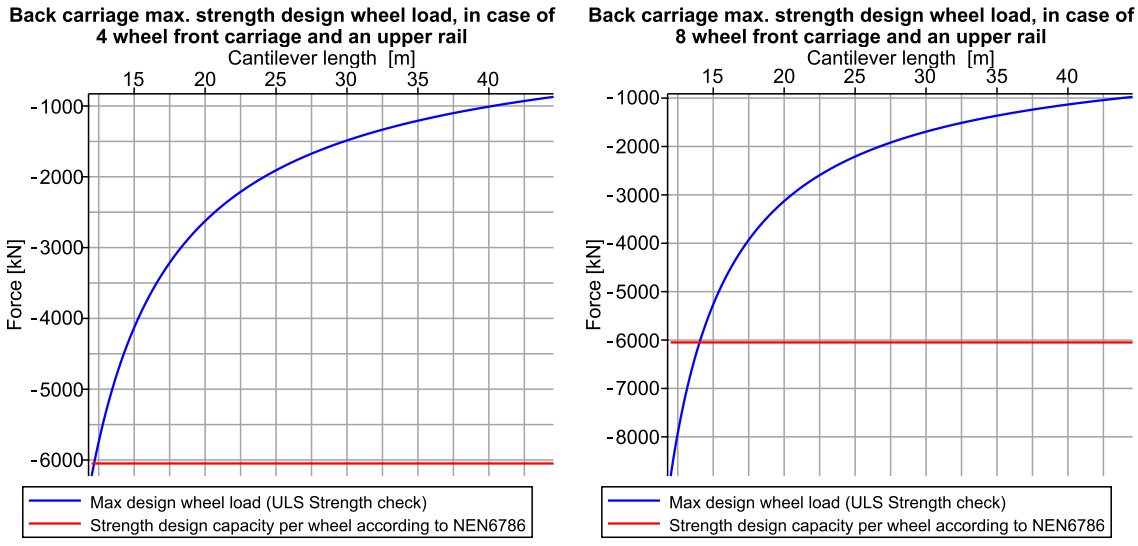

(a) *4-wheel* front carriage (b) *8-wheel* front carriage

Figure 6.22: The governing maximum strength design wheel load of the back carriage, plotted against the cantilever length, in case of a *4-wheel* (left) and an *8-wheel* (right) front carriage and an *upper rail*. The wheels have a diameter of 1200 mm and a width of 150 mm. The wheel strength design capacity (according to NEN6786) is indicated by the red line

These values are somewhat larger than the counterweight option, as the maximum force on the rail and wheel is not reduced by any balancing weight and therefore the reduction of the load has to come from a longer cantilever length.

6.7.2. Wheel fatigue verification back carriage

For fatigue of the wheel/rail of the back carriage in case of an upper rail, all of the partial safety factors are set to 1 and the internal loads are calculated in case of Mean Water (MW), during closing of the gate (gives the highest upward force on the back carriage) and with silt & accretion present. The fatigue design force for this governing loading situation is plotted against a variable cantilever length in Figure 6.23a in case of a 4-wheel front carriage and in Figure 6.23b in case of an 8-wheel front carriage.

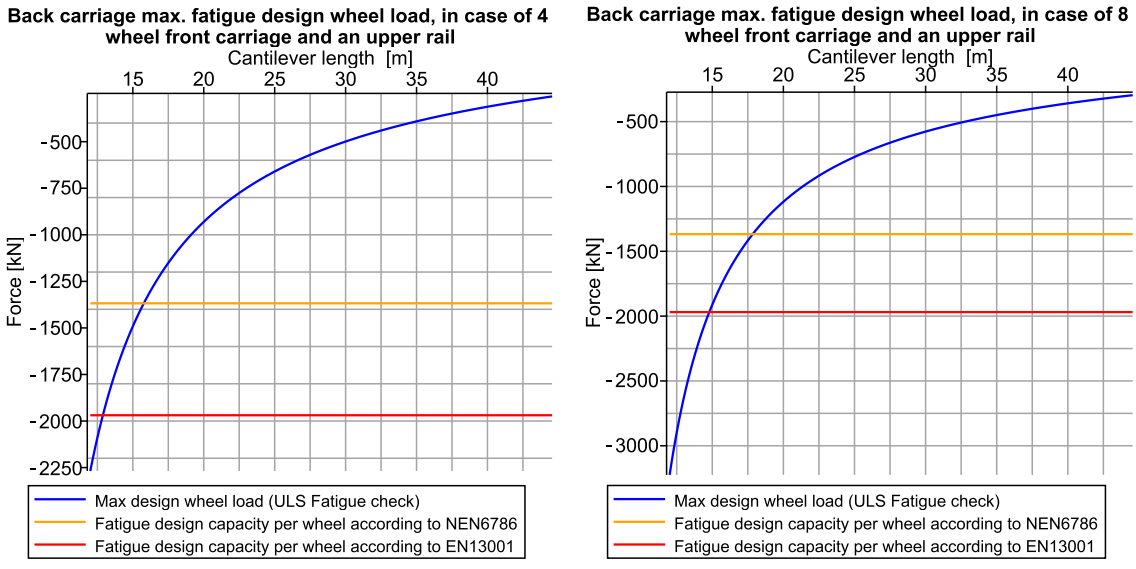

(a) *4-wheel* front carriage (b) *8-wheel* front carriage

Figure 6.23: The governing maximum fatigue design wheel load of the back carriage, plotted against the cantilever length, in case of a *4-wheel* (left) and an *8-wheel* (right) front carriage and an *upper rail*. The wheels have a diameter of 1200 mm and a width of 150 mm. The wheel fatigue design capacity is indicated by the yellow (NEN7686) and red (EN13001) lines

The point in the graphs at which the lines of the design load and the design capacity (1368 kN according to NEN6786, see appendix E) intersect, is the minimum cantilever length required to guarantee the

safety of the wheel/rail fatigue of the back carriage in case of an upper rail. In case of a 4-wheel front carriage, the cantilever length has to be at least 15.8 m. While for an 8-wheel front carriage the length has to be at least 17.9 m to guarantee the fatigue safety of the wheels and rails of the back carriage in case of an upper rail. In this case, the fatigue safety is also governing (with respect to the strength safety) for the minimum cantilever length.

6.8. Changing the wheel/rail dimensions

The previous analysis uses the current wheel and rail dimensions of the Western lock in Terneuzen and keeps them fixed. The option with an 8-wheel front carriage is looked into to spread out the high loads on the front of the cantilever gate, which is more advantageous for the minimum required cantilever length. An option to increase the capacity of the carriage is by increasing the wheel and/or rail dimensions. This section looks at the possibilities of increasing the dimensions of the wheels and/or rails of a 4-wheel roller carriage to allow for a shorter cantilever length.

6.8.1. Increased wheel diameter

The wheels of the current Western lock in Terneuzen have a diameter of 1200 mm. As far as is known, this is also the maximum size used for a rolling gate in a maritime navigation lock. However, bigger wheels are possible and certainly used in other applications (e.g. cable wheels).

Figure 6.24 shows the fatigue design limit plotted against an increasing wheel diameter. This plot was created by calculating the design limit in the same manner as the calculations shown in Appendix E, but with a wheel diameter that increases with steps of 100 mm. In this situation all of the other parameters presented in Section 5.3 are kept the same, thus the wheel and rail have a constant width of 150 mm.

For the NEN 6786 fatigue limit, the sudden increase from a diameter of 1600 mm to 1700 mm is caused by a change of the amount of rolling contacts of a wheel and the subsequent changed fatigue contact strength value deducted from Table E.2.

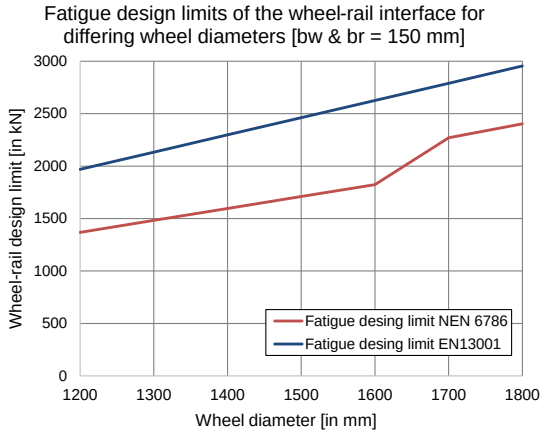

Figure 6.24: Fatigue design limits of the wheel-rail interface for differing wheel diameters [Wheel and rail width is 150 mm]

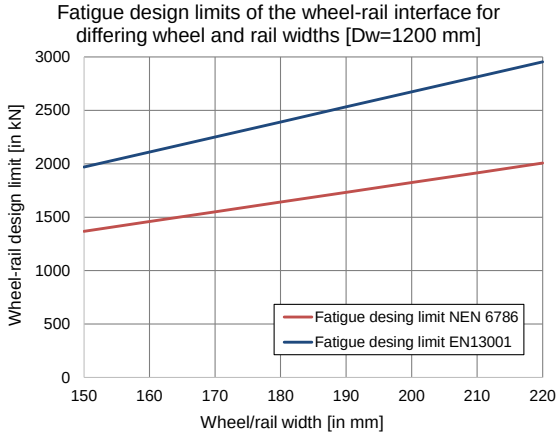

Figure 6.25: Fatigue design limits of the wheel-rail interface for differing wheel and rail widths [Wheel diameter is 1200 mm]

4-wheel carriage with a 1700 mm wheel diameter

Most of the large wheels used in rolling gates are custom designed and made for each specific lock. Technically a larger wheel size is definitely possible, albeit that it will push up the costs considerably. In this case the aim is to increase the wheel size to an extend that it can take higher loads and can accommodate a cantilever length in the same range as for an 8-wheel carriage with the current Western lock wheels. Which is the case for a wheel diameter of 1700 mm. In this assessment all of the wheel and rail parameters are kept the same as presented in Section 5.3, except for the wheel diameter. Due to the increased wheel size, the carriage size also has to be enlarged. Per wheel the diameter is increased by 500 mm and therefore each of the carriages is assumed to be extended by 1 m (from 6 m to 7 m). For interchangeability, both roller carriages are assumed to have the same size and wheel diameters. In case of an 1700 mm diameter and calculating in the same way as in Appendix E, the static and fatigue design limit (NEN 6786) of the wheel-rail interface are respectively 8570 kN and 2270 kN.

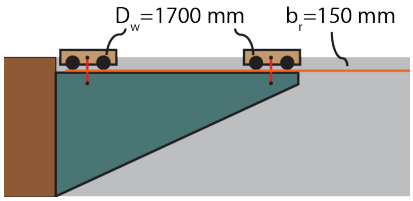

Figure 6.26: The option with an increased wheel diameter of 1700 mm (and a 4-wheel front carriage)

In the same way as presented in Appendix F and Sections 6.5 till 6.7, the minimum required cantilever length for both the front and back carriage and the 2 variants of an counterweight and upper rail are calculated. The calculation of the strength and fatigue safety of the front carriage is the same for both the upper rail and counterweight sub-variant, whereas the back carriage calculation differs between the two. For the front carriage the minimum required cantilever length to assure wheel/rail safety is respectively 12.5 m for the strength check and 16.3 m for the fatigue check. In case of a counterweight the back carriage wheel/rail safety requires a minimum length of 11.7 for the strength check and 11.1 for the fatigue check. Whereas for the upper rail the wheel/rail safety requires a minimum length of 13.3 m for the strength check and 13.1 m for the fatigue check. An overview of these results can be found in Table 6.13.

6.8.2. Increased wheel and rail width

Most of the wheels and rails of large maritime navigation locks have width of 150 mm due to standardization by steel manufacturers. Therefore it is not completely clear if the rail can simply be increased to any possible size as it would require a custom-made design. This would probably increase the costs of such a rail significantly. In order to get an idea of the influence of the rail width, the graph in Figure 6.25 shows different wheel/rail widths and the corresponding wheel/rail fatigue design capacities. Except for the wheel and rail width, all of the wheel and rail dimensions and materials presented in Section 5.3 are kept the same. The design limits are calculated in the same way as presented in Appendix E, but with an increasing wheel and rail width by steps of 10 mm. Logically, the fatigue design capacity shown in Figure 6.25 increases with an increasing wheel/rail width.

4-wheel carriage with a 220 mm wide wheel and rail

The only standardised rail size that is larger than the current rail of the Western lock has a width of 220 mm (profile MRS221, see [65]), which is considerably larger than the current rail. In order to use the full width of the rail, the wheel must also have this width. The rail profile is assumed to be manufactured of the same material as the current rail (110 CrV). The wheel diameter (1200 mm) and material (42CrMo5-04) are kept identical. In this combination of parameters the static and fatigue design limit (NEN 6786) of the wheel-rail interface are respectively 8872 kN and 2006 kN. In the same way as presented in Appendix F and Sections 6.5 till 6.7, the minimum required cantilever length for both the front and back carriage and the two variants of a counterweight and upper rail are calculated. In this situation it is assumed that both the front and back carriage have the increased wheel diameter.

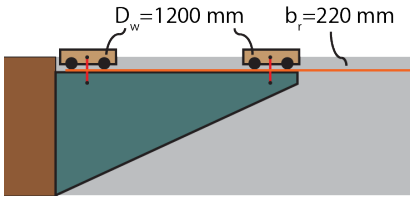

Figure 6.27: The option with an increased wheel/rail width of 220 mm (and a 4-wheel front carriage)

The calculation of the strength and fatigue safety of the front carriage is the same for both the upper rail and counterweight sub-variant, whereas the back carriage calculation differs between the two. For the front carriage the minimum required cantilever length to assure wheel/rail safety is respectively 11.1 m for the strength check and 16.8 m for the fatigue check. In case of a counterweight the back carriage wheel/rail safety requires a minimum length of 10.6 for the strength check and 10.5 for the fatigue check. Whereas for the upper rail the wheel/rail safety requires a minimum length of 12.2 m for the strength check and 12.8 m for the fatigue check. An overview of these results can be found in Table 6.14.

6.9. Comparison and minimum cantilever length

The minimum cantilever length has been determined for all of the checks relevant to the balance of the two sub-variants and the different wheel, rail and carriage lay-outs. In this section all of these lengths are gathered to find the normative design verification and the minimum required cantilever length for each of the two sub-variants and carriage options. Firstly, the options of a 4-wheel and 8-wheel front carriage are presented, where all of the wheels and rails have the same dimensions as the current Western lock in Terneuzen. Secondly, two options are shown where the sizes of the wheels and rails are altered.

6.9.1. 4-wheel front carriage (Wheel-rail interface conform Western lock Terneuzen)

Table 6.10 shows that in case of a 4-wheel front carriage which has an identical wheel-rail interface as the Western lock in Terneuzen, the fatigue safety of the front carriage is decisive for the minimum required length of the cantilever. For both sub-variants (counterweight vs. upper rail) the cantilever has to be at least 26.4 meter long to guarantee the fatigue safety. This length takes into account the maximum extra buoyancy volume and (in case of the counterweight) the minimum size of the counterweight as calculated in Sections 6.3.2 and 6.6. In case of a cantilever length of 26.4 meter and a 4-wheel front carriage, the maximum additional buoyancy volume is 114.6 m^3 and the counterweight has a minimum weight of 452 tonnes.

Table 6.10: The minimum required cantilever lengths to guarantee the safety of the wheel/rails of the carriages, in case of a *4-wheel* front carriage and wheel-rail interface conform the Western lock in Terneuzen ($D_w = 1200\ mm$ & $B_w = 150\ mm$)

Sub-variant	**Type of verification**	**Minimum required cantilever length** $[m]$
Both upper rail and counterweight	Wheel/rail strength safety of front carriage	14.4
	Wheel/rail fatigue safety of front carriage	**26.4**
Counterweight	Wheel/rail strength safety of back carriage	10.6
	Wheel/rail fatigue safety of back carriage	12.8
Upper rail	Wheel/rail strength safety of back carriage	12.2
	Wheel/rail fatigue safety of back carriage	15.8

6.9.2. 8-wheel front carriage (Wheel-rail interface conform Western lock Terneuzen)

Table 6.11 shows the minimum required cantilever lengths in case of a counterweight and an 8-wheel front carriage. In this situation, the wheel/rail fatigue safety of the front carriage is still defining, but the minimum length is considerably less than in case of a 4-wheel front carriage. The extra wheels spread out the loads more and therefore the front carriage can take a higher load. In case of a cantilever length of 16.6 meter and a 8-wheel front carriage, the maximum additional buoyancy volume is 112 m^3 and the counterweight has a minimum weight of 1083 tonnes. This counterweight is relatively large due to the much smaller cantilever length. It should carefully be considered if such a massive counterweight is possible. Otherwise the cantilever length should be taken larger in order to decrease the mass of the counterweight.

Table 6.11: The minimum required cantilever lengths to guarantee the safety of the wheel/rails of the carriages, in case of a *counterweight*, an *8-wheel* front carriage and wheel-rail interface conform the Western lock in Terneuzen ($D_w = 1200\ mm$ & $b_w = 150\ mm$)

Type of verification	**Minimum required cantilever length** $[m]$
Wheel/rail strength safety of front carriage	11.3
Wheel/rail fatigue safety of front carriage	**16.6**
Wheel/rail strength safety of back carriage	12.4
Wheel/rail fatigue safety of back carriage	14.7

Table 6.12 shows the minimum required cantilever length in case of an upper rail and an 8-wheel front carriage. Contrary to the other cases, in this situation the fatigue safety of the back carriage is decisive for the minimum required cantilever length. The minimum required cantilever length is 17.9 meter. With this length the maximum additional buoyancy volume is 112.3 m^3.

Table 6.12: The minimum required cantilever lengths to guarantee the safety of the wheel/rails of the carriages, in case of an *upper rail*, an *8-wheel* front carriage and wheel-rail interface conform the Western lock in Terneuzen ($D_w = 1200\ mm$ & $B_w = 150\ mm$)

Type of verification	**Minimum required cantilever length** $[m]$
Wheel/rail strength safety of front carriage	11.3
Wheel/rail fatigue safety of front carriage	16.6
Wheel/rail strength safety of back carriage	14.1
Wheel/rail fatigue safety of back carriage	**17.9**

6.9.3. 4-wheel front carriage (Increased wheel diameter)

Section 6.8.1 showed the wheel capacities in case the wheel diameters of the 4-wheel carriage were enlarged. This resulted in a design for which the wheel diameter was increased to 1700 mm instead of the regular 1200 mm. Due to te increased wheel sizes the carriage dimensions are also different. Table 6.13 shows the minimum required cantilever lengths for this situation. The fatigue safety of the front carriage is governing for both sub-variants (counterweight & upper rail) and requires a minimum length of at least 16.3 m. In case of this cantilever length and the increased wheel size of the 4-wheel carriages, the maximum additional buoyancy volume is 111.3 m^3 and the counterweight sub-variant requires a minimum weight of 1019 tonnes.

Table 6.13: The minimum required cantilever lengths to guarantee the safety of the wheel/rails of the carriages, in case of a *4-wheel* front carriage and a larger wheel diameter(D_w) of 1700 mm ($b_w = 150\ mm$)

Sub-variant	**Type of verification**	**Minimum required cantilever length** $[m]$
Both upper rail and counterweight	Wheel/rail strength safety of front carriage	12.5
	Wheel/rail fatigue safety of front carriage	**16.3**
Counterweight	Wheel/rail strength safety of back carriage	11.7
	Wheel/rail fatigue safety of back carriage	11.1
Upper rail	Wheel/rail strength safety of back carriage	13.3
	Wheel/rail fatigue safety of back carriage	13.1

6.9.4. 4-wheel front carriage (Increased wheel and rail width)

Section 6.8.2 showed the wheel capacities in case the wheel and rail width of the 4-wheel carriage were to be widened. Due to limitations with respect to standardization of rails, the rail (and wheel) width were decided to be widened from 150 mm to 220 mm. Table 6.14 shows the minimum required cantilever lengths for this situation. The fatigue safety of the front carriage is governing for both sub-variants (counterweight & upper rail) and requires a minimum length of at least 16.8 m. In case of this cantilever length and the increased wheel size of the 4-wheel carriages, the maximum additional buoyancy volume is 111.1 m^3 and the counterweight sub-variant requires a minimum weight of 903 tonnes.

Table 6.14: The minimum required cantilever lengths to guarantee the safety of the wheel/rails of the carriages, in case of a *4-wheel* front carriage and a larger rail b_r and wheel width b_w of 220 mm ($D_w = 1200\ mm$)

Sub-variant	**Type of verification**	**Minimum required cantilever length** $[m]$
Both upper rail and counterweight	Wheel/rail strength safety of front carriage	11.1
	Wheel/rail fatigue safety of front carriage	**16.8**
Counterweight	Wheel/rail strength safety of back carriage	10.6
	Wheel/rail fatigue safety of back carriage	10.5
Upper rail	Wheel/rail strength safety of back carriage	12.2
	Wheel/rail fatigue safety of back carriage	12.8

6.10. Conclusion

This chapter elaborated two ways of initiating the required counter force, and presented four different options for the carriage and wheel-rail lay-out. For each of these options the balance and the loads on the wheel-rail interface of each of the carriages were evaluated. Which resulted in a minimum required cantilever length to ensure safety with respect to equilibrium of the gate and fatigue and strength of the wheel-rail interface.

Counterweight vs. upper rail
The initiation of the counter force of the cantilever gate can be either done by a counterweight or via an upper rail. If both carriages have four wheels, the fatigue design load on the wheels of the front carriage is the limiting factor that defines the minimum required cantilever length. Therefore the counterweight or upper rail sub-variants do not differ with respect to the most optimal cantilever length, as only the loading on the back carriage differs between the two.

Limited extra buoyancy volume
To reduce the weight on both the front and the back carriage. Extra buoyancy volume can be placed in the gate part, reducing the downward force of the dead weight of the gate structure. However, the additional volume should not distort the equilibrium of the cantilever. The volume size is limited by the fact that a downward safety force of 200 kN must be present on the front carriage under all circumstances. If the buoyancy volume is too big, the gate may lift up.

Base case: the current carriage lay-out
In case of a 4-wheel front and back carriage with both a wheel-rail interface conform the current Western lock in Terneuzen ($D_w = 1200\ mm$ & $b_w = 150\ mm$), the length of the cantilever structure has to be at least 26.4 meter long for both sub-variants. The total gate length would then be $(44.56\ m + 26.4\ m =)\ 70.56\ m$. This is 60% longer than the conventional gate.

An 8-wheel front carriage
For a situation with a 4-wheel front carriage, the fatigue load of the front carriage wheels is the limiting factor for the length of the cantilever structure. One option to reduce the required cantilever length of 26.4 m is to increase the amount of wheels of the front carriage to eight. Therefore the loads are split over eight instead of four wheels. In case of an 8-wheel front carriage with a wheel-rail interface conform the current Western lock in Terneuzen ($D_w = 1200\,mm$ & $b_w = 150\,mm$), the minimum required cantilever length becomes 16.6 meter in case of the counterweight sub-variant. The counterweight required under the back carriage to balance out the gate has to weigh more than 1083 tonnes. Which is larger than the weight of the gate part itself. If an upper rail is applied instead of the counterweight, the fatigue load on the back carriage is the limiting factor for the cantilever length. A minimum cantilever length of 17.9 m is then required to carry the fatigue loads on the four wheels of the back carriage. Thus, both of the sub-variants with an 8-wheel front carriage require a much shorter cantilever length than the 26.4 m of the initial 4-wheel carriage.

Increasing the wheel and rail size
Another alternative to reduce the loads on the front carriage (and subsequently decrease the minimum required cantilever length) is to increase the sizes of the rail and/or wheels. This results in two options that both apply a 4-wheel front and back carriage but with increased dimensions. The first option is to increase the wheel size from 1200 mm to 1700 mm, which reduces the minimum required length to 16.3 m for both sub-variants. Whereas the second option is to increase the wheel and rail width from 150 mm to 220 mm, which reduces the minimum required length to 16.8 m (also for both sub-variants). Both these options require a considerably shorter cantilever length than the 4-wheel carriage with the regular wheel-rail interface.

Favourable option
Between the two sub-variants related to the counter force initiation, the counterweight variant is favoured because the balance of forces is achieved in the gate structure itself, it is a simpler design and it requires less highly loaded sensitive materials like rails. Also, as opposed to the anchored top rail sub-variant, the wheels do not require any tight tolerance restrictions and the carriages are not trapped between two rails and therefore can be freely replaced. Lastly, the counterweight sub-variant can also have a slightly shorter cantilever length.

Table 6.15 shows the optimal cantilever lengths for each of the considered front-carriage configurations in case they were applied with a counterweight. The base case with the 4-wheel front carriage with

regular wheels is not feasible because the required minimum cantilever length needs to be far too large. All of the other options show relatively similar optimal cantilever lengths, and therefore a favourite option cannot be chosen on this result alone. For now, the 8-wheel carriage seems most suitable. As opposed to the two options with increased wheel and/or rail dimensions, the 8-wheel carriage applies already proven wheel-rail sizes. In addition, the eight wheels spread the loads out more evenly which is advantageous for not only the load transfer in the wheel-rail interface, but also for the structure of the carriage and the foundation of the rail.

Table 6.15: The optimal cantilever lengths for the different front carriage configurations in case of the chosen counterweight sub-variant

Front-carriage configuration	**Optimal cantilever length** $[m]$
4-wheels with identical wheel-rail interface conform Western lock	26.4
8-wheels with identical wheel-rail interface conform Western lock	16.6
4-wheels with increased wheel and rail with from 150 mm to 220 mm	16.8
4-wheels with increased wheel diameter from 1200 mm to 1700 mm	16.3

7

Final case study design

This chapter presents the final design for the cantilever gate at the case study location. Section 7.1 performs some final calculations regarding the size of the counterweight and the dimensions of the trusses of the cantilever truss structure. Whereupon Section 7.2 shows a last verification of the equilibrium, strength and fatigue checks of the carriages and the gate and subsequently presents the final design with some 3D plots and overview figures.

7.1. Cantilever structure and counter weight

Section 6.10 concluded that a cantilever gate with an 8-wheel front carriage and an 4-wheel back carriage and a cantilever length of 16.6 m is the most optimal solution for now. For this configuration the minimum required counter weight is 1083 tonnes.

In case the counterweight would consist of concrete ($\rho_c = 2500\ kg/m^3$), it would require a volume of $433.2\ m^3$. This would require a concrete block size of circa 12x6x6 m. This is too large to be placed inside the gate right below the back carriage and is therefore impossible. If the counterweight is made of steel instead ($\rho_c = 7850\ kg/m^3$), it would require a volume of $(1083000\ kg/7850\ kg/m^3 =)\ 138\ m^3$. To fit this in the cantilever gate, the counterweight volume can have a maximum width of $6.4\ m$. In order to have the centre of mass right below the back carriage and at the same time stick within the limits of the cantilever length, the volume can have a maximum length equal to the length of the back carriage (which is $6\ m$). Taking into account both these limits, the counterweight volume should have a height of $(138\ m^3/6.4\ m/6\ m =)3.59\ m$. This is still a relatively large steel volume, but it is able to be placed inside the cantilever gate (as shown in Figure 7.4).

Due to the size and weight of the counter weight the design of the cantilever structure changes compared to the initial preliminary design. Initially the cantilever structure was designed as a full triangle. In the new design the top of the cantilever part has a rectangular truss Section with a height of 4 meters to make room for the counterweight. Below this rectangular Section, a triangular truss structure is located (see Figure 7.1).

The design process of the truss structure of the cantilever part is identical to the one presented in Appendix D, but with a different cantilever length. The horizontal length of the truss structure is the calculated cantilever length of 16.6 m. The cantilever structure is 16.8 m high and has a width of 6.43 m (identical to the gate part). The trusses are made of Circular Hollow Sections (CHS) of steel grade S355 ($f_y = 355\ N/mm^2$). According to Wardenier [73] a CHS has multiple advantages:

- It has a low drag coefficient as there are no sharp edges. Which is advantageous for opening/closing of the gate.
- A good protection regarding corrosion due to the rounded corners. Which is especially true for the joints. This increases the protection period of coatings.
- A high and effective torsional stiffness as the material is uniformly distributed along the polar axis
- The internal void can be used for buoyancy if required.[1]

[1] In this case the CHS are assumed to be hollow. Section 8.3 discusses the possibility of filling the internal volume with concrete

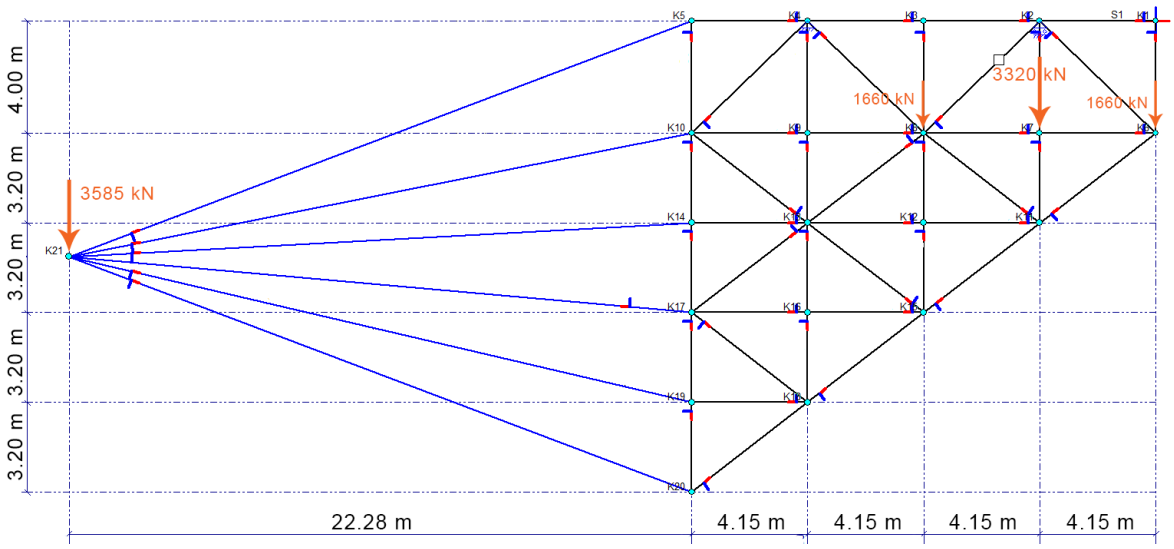

Figure 7.1: The MatrixFrame model of the side of the final cantilever structure design. The weight of the gate part structure and silt are applied on the structure by an equivalent point load at half the gate part length, which is transferred to the leftmost truss nodes by infinitely stiff bars.

The truss structure is modelled of bars with hinged joints in MatrixFrame to calculate the internal forces of each of the members. The analysis of the 3D cantilever truss structure is simplified by taking only one side and modelling it in 2D. The load of the gate part is modelled to act on a distance of 22.28 (half the gate part length) from the cantilever structure. The load of the counterweight is modelled as 3 separate point loads at the joints directly below the back carriage support.

Based on these internal forces the required sizes of the Circular Hollow Sections (CHS) of the truss structure are determined. The complete calculation can be found in Appendix G. A summary and overview of the chord and brace dimensions and verification of the 2D cantilever truss structure is shown in table 7.1.

Table 7.1: Overview of chord and brace dimensions, load capacities and unity checks for the 2D cantilever truss structure

Location	Load type	Member length	Outer diameter	Wall thickness	Cross-Sectional area	Thickness ratio	Capacity	Max. force	Unity check
		mm	mm	mm	mm^2	d_0/t_0	$(\chi\cdot)f_{y,0}\cdot A_0\ (kN)$	kN	
Diagonal chords	Compr.	5240	273	25	19478	11	6784	-6055	0.89
Top chords	Tens.	4150	273	25	19478	11	6915	4219	0.61
Horizontal braces	Compr.	4150	244.5	12.5	9111	20	3233	-2808	0.87
Vertical braces	Tens.	4000	273	20	15896	14	5643	5537	0.98
Diagonal braces diagonal part	Tens.	5240	273	20	15896	14	5643	4842	0.86
Diagonal braces top part	Tens.	5764	273	30	22902	9	8130	7362	0.98

Table G.12 in Appendix G calculates the total weight of the truss structure to be 69105 kg. This is considerably larger than assumed in earlier calculations. Mainly due to the fact that the cantilever structure is much shorter and requires heavier CHS elements to transfer the higher internal loads. Due to the larger truss structure weight and the bigger CHS member volume, the balance of the cantilever gate changes compared to the initial design. The extra buoyancy volume therefore has to be 116 m^3 (instead of 112 m^3) to guarantee the safety of the wheel-rail interface. This size of volume still ensures the minimum downwards safety force of 200 kN under all circumstances and therefore no uplift should occur for both of the carriages.

Due to the extra buoyancy volume the total buoyancy chamber volume is increased from $1024.7\ m^3$ to $1140.7\ m^3$. Taking into account the horizontal dimensions of the buoyancy chambers ($44.22\ m \cdot 6.412\ m$), the height of the new buoyancy volume becomes $4.01\ m$. The buoyancy chambers are therefore located from $-3.4\ m\ NAP$ till $-7.42\ m\ NAP$. Figure 7.2 shows a side view and a cross-Section which indicate the size and location of the buoyancy chambers in the gate.

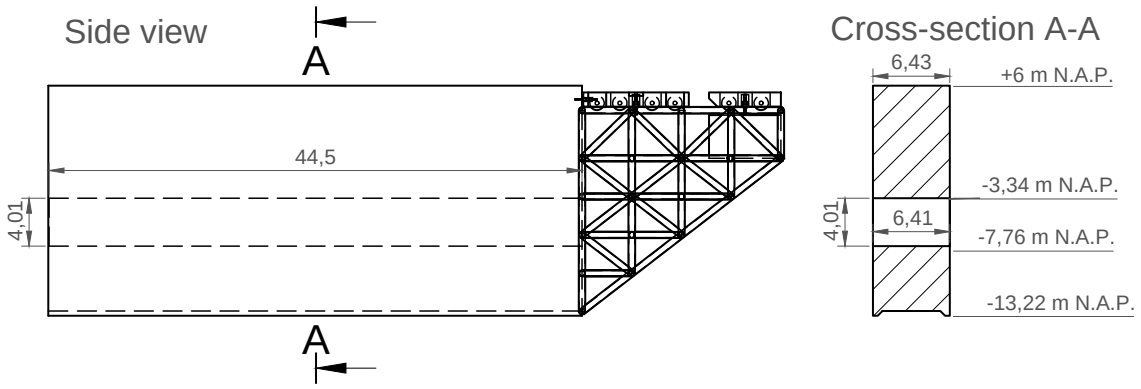

Figure 7.2: A cross Section of the gate which shows the dimensions and location of the buoyancy chamber. Dimensions are in meters.

7.2. Final design and verification

The final cantilever rolling gate design for the case study location of the Western lock in Terneuzen consists of (see Figure 7.3):

- Cantilever length of $16.6\ m$
- Cantilever structure constructed of Circular Hollow Sections with a weight of $69.15\ tonnes$
- Counterweight of 1083 tonnes right below the centre of the back carriage.
- Gate part buoyancy volume increased by $116\ m^3$ to $1140.7\ m^3$
- Front carriage with eight wheels and a length of $9\ m$
- Back carriage with four wheels and a length of $6\ m$
- Identical wheel/rail interface to Westlock Terneuzen ($D_w = 1200\ mm\ \&\ b_w = 150mm$)

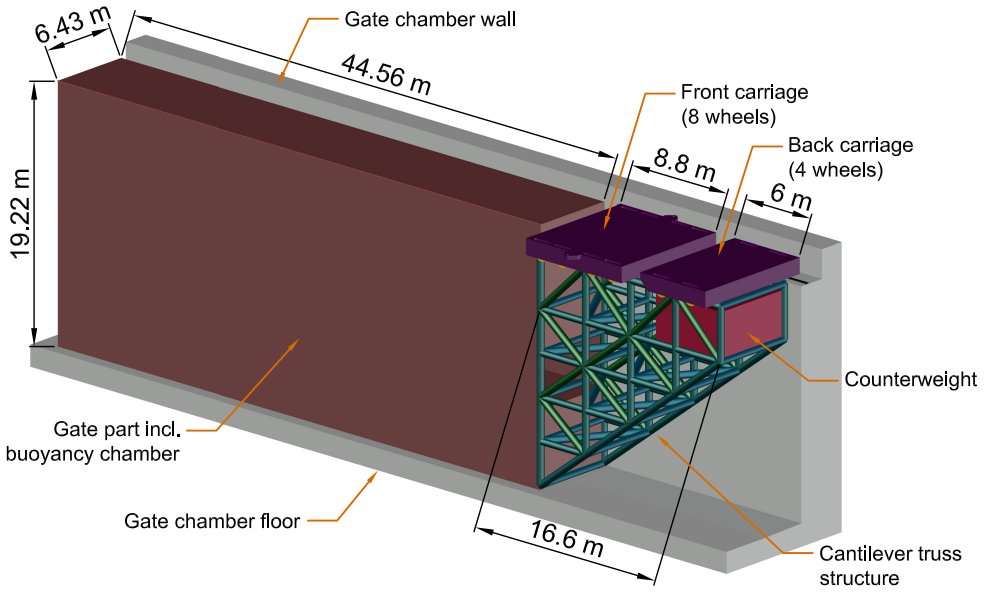

Figure 7.3: A 3D view of the final cantilever rolling gate design for the case study location of the Western lock (Westsluis) in Terneuzen

Figure 7.4 shows the three sideviews and a 3D view of the final design of the cantilever rolling gate, with the dimensions indicated in meters. The front carriage consists of eight wheels and has a load equalizer to distribute the loads evenly to the wheels. The rails and all of the wheels of both the front and back carriage have the same parameters as the current Western Lock in Terneuzen ($D_w = 1200\ mm\ \&\ b_w = 150mm$). Figure 7.5 shows a 3D view of the cantilever structure and the two carriages. The vertical forces are transferred from the cantilever structure to the carriages by vertical pendulum rods. Two horizontal pendulum rods on the front carriage transfer the horizontal forces by the driving system from the carriage to the gate. The cables of the driving system are connected to two protruding parts on the front carriage.

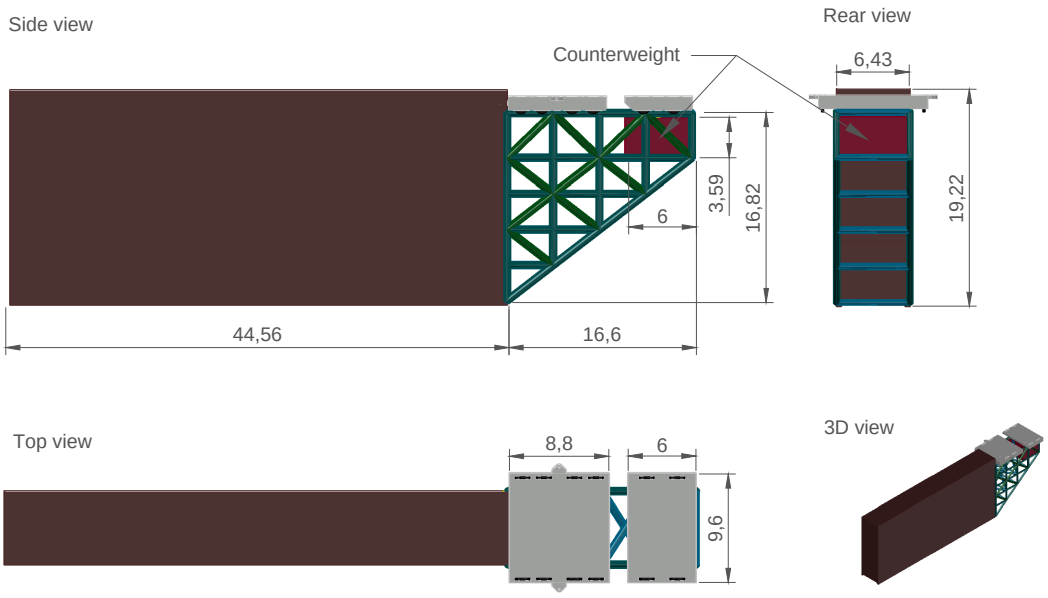

Figure 7.4: A top, side, rear and 3D view of the final cantilever gate design. The dimensions are indicated in meters.

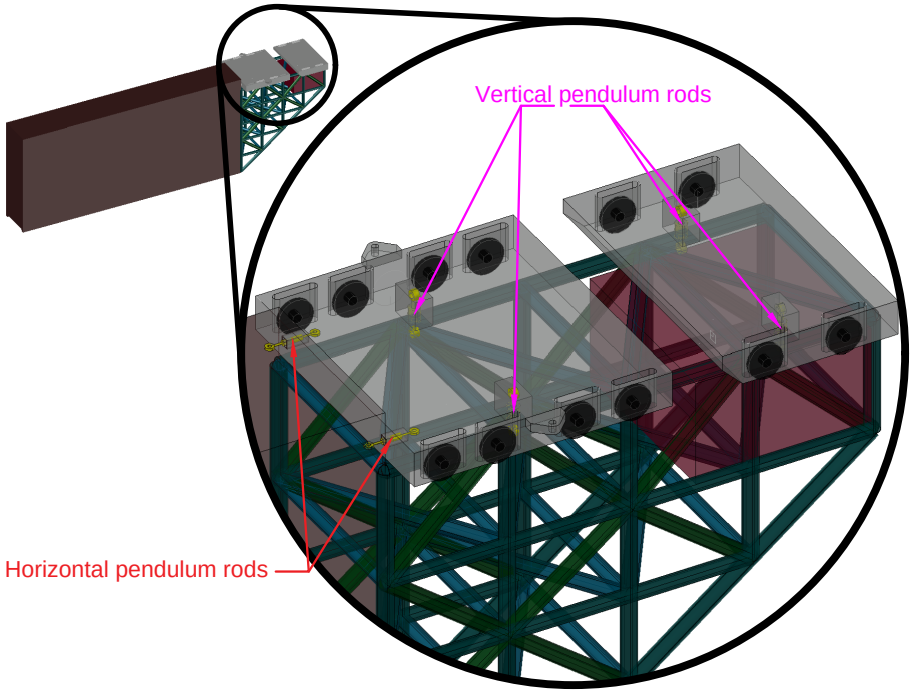

Figure 7.5: The cantilever structure and its two carriages. The vertical and horizontal pendulum rods which transfer the forces from the structure to the carriages are indicated.

Taking into acount all of these values, a final verification is performed regarding the equilibrium of the gate and the loads on the wheel-rail interface. This verification is in line with the load model and subsequent design checks explained in Chapter 6. An overview of the significant values and the corresponding requirements is shown in Table 7.2. The full (excel) calculations regarding equilibrium, strength and fatigue of this final design can be found in Appendix H.

Table 7.2: An overview of the design checks of the final case study design of the cantilever rolling gate with a cantilever length of 16.6 m. See Appendix H for the full calculation.

	Value	Requirement	Unit
Equilibrium checks (EQU)			
Minimum load front carriage	218	≥ 200 [a]	kN
Minimum load back carriage	335	≥ 200 [a]	kN
Strength check wheel loads (STR)			
Design strength load per wheel on front carriage (8 wheels)	3004	≤ 6049 [b]	kN
Design strength load per wheel on back carriage (4 wheels)	4047	≤ 6049 [b]	kN
Fatigue check wheel loads (FAT)			
Design fatigue load per wheel on front carriage (8 wheels)	1183	≤ 1188 [b]	kN
Design fatigue load per wheel on back carriage (4 wheels)	1134	≤ 1368 [b]	kN

[a] see Section 5.3, [b] see Section 6.4

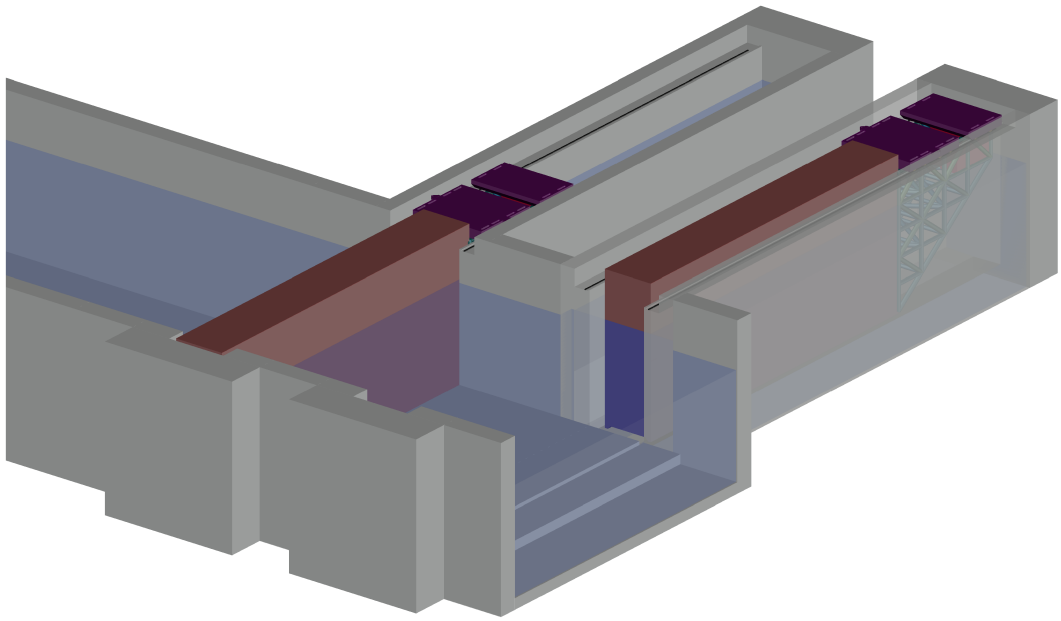

Figure 7.6: A 3D render of the double cantilever gate applied at the Western lock in Terneuzen. One gate being in closed position and one in open position. The chamber walls of the open gate are made transparent to show the gate in its chamber.

7.3. Comparison with the conventional gate

The original Western lock in Terneuzen has a conventional wagon type rolling gate with an additional top carriage for horizontal guidance. The lower carriages are all located under water and form a simply supported beam with the gate structure.

The biggest and most important change compared to the old gate is the location of the carriages above water. Therefore the connection between carriages and gate is completely different. The cantilever rolling gate fully 'hangs' instead of being simply supported on the carriages. The pendulum rod connection between the carriages (instead of rubber blocks for the current gate) allows horizontal perpendicular movement of the gate.

The specifications of the wheels and rails are identical to the ones used in the current gate. The lay-out and size of the carriages itself is completely different, as the cantilever rolling gate carriages have to

be wider than the gate to support on the gate chamber walls. Whereas the current carriages are really small to fit on the railroad track under water. Also, the front carriage has 8 instead of 4 wheels to allow larger loads.

The current cantilever design still has horizontal guidance located under water, albeit on the gate instead of on the lower carriage.

Extended gate implications

The additional cantilever structure and its counterweight require quite some extra steel and increase the total gate weight from 946 t to 2098 t. Due to the extended gate structure the cantilever gate is not able to move in and out of the gate chamber for maintenance, as is the case for the current gate. Therefore the cantilever gate has to be assembled, maintained and disbanded inside the gate chamber. Which implies that each gate chamber has to be spacious enough. Due to this limitation the cantilever rolling gate concept always has to be constructed with double gates on each side of the lock. For the case study this is already the case, but this may be different for other locations.

Due to the cantilevered instead of simply supported gate, the load transfer through the gate changes completely. The biggest moment force occurs right below the front carriage instead of in the middle of the gate part. The structure of the gate part still has to be checked for this new load distribution.

Increased gate and lock width

Due to the cantilever part of 16.6 m added to the original gate part of 44.56 m, the length of the gate increases by 37%. The lengthened gate requires the lock chamber to be longer in comparison to a lock with a conventional gate. To make space for the cantilever part, the gate chamber is assumed to be increased by the same length as the cantilever part (see Figure 7.7). Due to this lengthened gate chamber the total lock width also increases. The current Western lock in Terneuzen has a total width of 104.2 m. With an increase of 16.6 meter the total lock width increases by 16%. Due to the triangular shape and the more distant location of the current culvert system, the culverts don't have to be moved and can be incorporated into the structure of the extended gate chamber (see Figure 7.8).

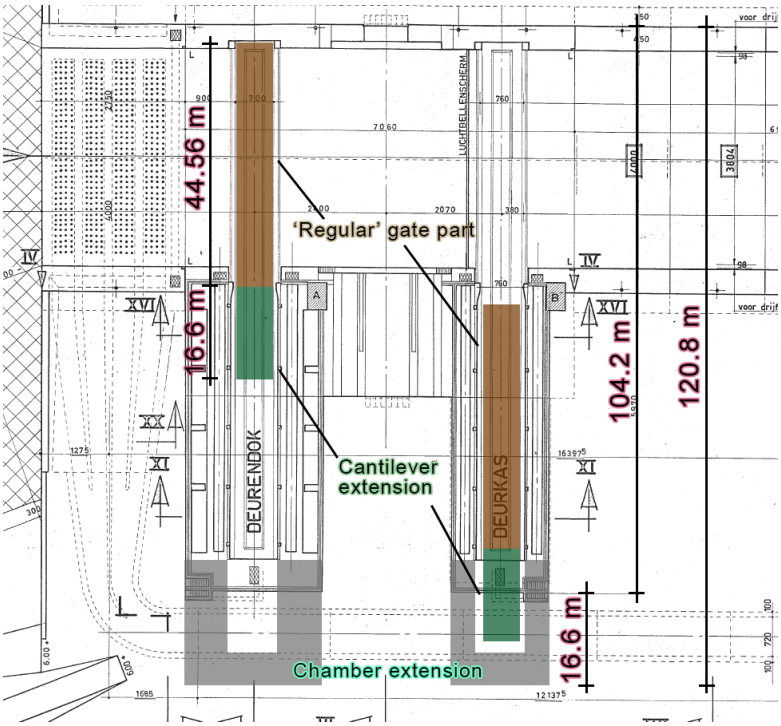

Figure 7.7: A top view of the required adjustments to the lock chamber to fit the cantilever rolling gate at the case study location of the Western lock in Terneuzen (Source of background map: [67])

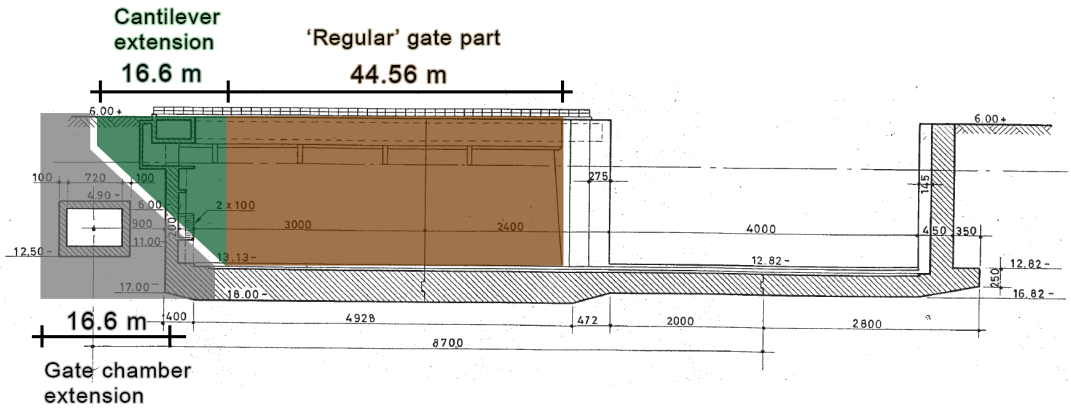

Figure 7.8: The necessary gate chamber extension projected on top of a cross-section of the current gate chamber of the Western lock in Terneuzen. The current culvert system can be incorporated in the new extended gate chamber structure. (Source of background cross-section: [67])

7.3.1. Overview

Table 7.3 shows an overview and comparison of the configuration and dimensions between the designed Cantilever rolling gate and the current conventional rolling gate at the case study location of the Western lock in Terneuzen.

Table 7.3: A comparison overview of the cantilever rolling gate and the current conventional rolling gate at the case study location of the Westsluis in Terneuzen

	Cantilever rolling gate	Current rolling gate
Total gate length	61.16 m	44.56 m
Total weight gate structure (incl. counterweight)	2098 tonnes	946 tonnes
Total buoyancy chamber volume in gate part	1141 m^3	1025 m^3
Total lock width	120.8 m	104.2 m
Lower carriages (under water)	0	2
Upper carriages (above water)	2	1
Number of wheels front carriage	8	4
Number of wheels back carriage	4	4

The advantages and disadvantages of the cantilever rolling gate compared to the current conventional wagon rolling gate at the Western lock in Terneuzen are stated below.

Advantages:

- Both carriages and rails located above water and therefore easy to maintain and replace
- Cantilever gate extension can be clamped by active horizontal guidance and therefore better take horizontal loads during opening/closing

Unchanged/equivalent:

- Gate operating time
- Double gates per side
- Active horizontal guidance below water

Disadvantages:

- Requires more lock space to house the extended gate
- Requires much more material for the cantilever structure, counterweight and extended gate chamber
- Gate cannot be moved out of the gate chamber for maintenance

8

Discussion

In this study a qualitative Multi Criteria Analaysis (MCA) was performed in which the Cantilever rolling gate scored highest. Thereafter, a conceptual design of this variant was engineered for the case study location. In this chapter, both the general concept of the Cantilever rolling gate, the final result of the case study design and the design method(s) are discussed.

8.1. Conceptual limitations

This section describes the things you have to consider and bear in mind when actually making the concept of a cantilever rolling gate.

Required space

The possible application of the cantilever rolling gate is limited by the available space at the location of the lock. The additional length of the cantilever part requires the lock to be wider compared to a lock with a conventional gate (e.g. a wagon or wheelbarrow rolling gate). This is not an issue for the case study location as enough space is available. For other locations the cantilever gate may not be a viable option due to lack of space. The cantilever concept is therefore only a suitable option if there is enough space to accommodate the lengthened gate.

The longer gate requires a longer gate chamber. This adds to the initial construction costs of the lock. The concrete structure of the current gate chamber of the Western Lock has a length of 59,7 m (from lock chamber till the end of the gate chamber). With the extra required length of 16.6 m for the cantilever part, this gate chamber foundation would then need to be 76,3 m. This is 28% longer. A rough assumption would be that the costs for the construction of the chamber would also increase by 28%.

For the case study the cantilever gate has been optimized to be as short as possible. If there is ample space available, it may be viable to apply a longer cantilever part to improve the gate balance and decrease the required counterweight and subsequent loads on the supports/wheels. However, the longer cantilever construction increases the required materials and maintenance, and therefore the costs.

Maintenance of the carriages

One of the benefits for bringing sensitive parts like wheels and rails to the surface, is to make them more accessible for inspection and maintenance. In conventional rolling gates a carriage is swapped once every few years by a spare one for maintenance purposes. The usual method of replacing a carriage is to temporarily remove the load on the carriage by floating of the gate, and subsequently hoist the carriage out. However, it is unclear whether this is also possible for the back carriage of the cantilever rolling gate. It should not be a problem for the front carriage as there is enough available buoyancy volume in the front part of the gate to make it float on that side. In the current design the back carriage cannot be floated up and be replaced in the conventional way due to the large counterweight located right below the back carriage.

Either the cantilever part has to be altered to provide more buoyancy volume or another solution should be found. For example, the gate could be lifted by a separate crane or could be jacked up on a temporary auxiliary construction or rebates inside the gate chamber.

It should be noted that due to the carriages location above the water, it is expected that they will need to be replaced less often as less wear and tear occurs because the wheels and rails are no longer submerged in salt water and mud.

Assembly and maintenance of the gate
Due to addition of the cantilever part, the cantilever rolling gate cannot be floated in and out of the gate chamber like a conventional rolling gate. Therefore, the gate and cantilever part have to be assembled inside the gate chamber. The exact assembly of these two parts still has some question marks. It is assumed that these two parts can be welded or bolted to each other on site, only to be dismantled at the end of the gate's lifetime.

As the gate cannot be floated out, maintenance to the gate structure has to be performed inside the gate chamber. Therefore each of the gate chambers with a cantilever rolling gate has to be wide enough to perform maintenance and has to be sealed off with bulkheads. This is a big limitation to the design as it reduces flexibility with regard to maintenance and the exchange of gates in the event of a collision. It also implies that a lock with cantilever rolling gates must have double redundant gates on each side to ensure the locking functionality during maintenance of one of the gates.

Larger lock widths
The elaborated design and its specifications are limited to the case study location of the Western lock in Terneuzen, which has a lock width of 40 m. It is questionable whether the cantilever concept can be applied at larger lock widths of 50 to 70 m width, as the weight and the arm of the gate part both increase and therefore the required counteracting moment increases quadratic.

An increased lock width will quadratically increase the moment force on the gate and cantilever construction and thus the required counterweight and/or cantilever length have to increase considerably as well. For the case study, the optimal cantilever length is governed by the fatigue load of the wheel-rail connection of the front carriage. In order to allow a wider lock and longer gate part the loading capacity of the front carriage should be increased or otherwise the required cantilever length would be much longer. A quick calculation were all design parameters are kept similar to the case study except for the lock width (60 m instead of 40 m) and gate part weight (1900 t instead of 946 t) results in a minimum required cantilever length of 45 m! The cantilever to gate part ratio is then 0.75, which is a lot more than 0.37 (16.6 m /44.56 m) for the case study situation.

The larger and heavier gate can only partly be compensated with additional buoyancy chamber volume. The maximum additional buoyancy volume is determined by the governing loading situation which gives the smallest downward force on the front carriage: this occurs when the gate is opening, it is high water, no silt is present yet and the dead weight and buoyancy volume are respectively taken as favourable and unfavourable. A larger gate increases the maximum resistance force during opening/closing of the gate and that is why in relative terms the additional buoyancy volume becomes smaller. Therefore, the ratio of dead weight to buoyancy volume in the gate part decreases for larger gates.

8.2. Methodological simplifications

This section describes things about the cantilever roller gate that could not be investigated or have been simplified.

Calculations limited to longitudinal direction
To validate the working principle of the cantilever rolling gate, only the forces in longitudinal direction of the gate are taken into account as they are most important to the working principle of a cantilever mechanism. A major limitation of this simplification is that the transverse loads are currently not included in the design verification of the structural components of the gate (except for the determination of the required resistance force at opening/closing). It is expected that these horizontal loads in itself will be smaller than the maximum vertical forces for which the cantilever part is currently designed. However, certain combinations of horizontal and vertical loads could lead to higher stresses in the cantilever truss structure. This is something that will have to be investigated in the future.

Horizontal guidance
In the calculations it is assumed that during opening and closing of the gate, the horizontal forces are transferred by an active guidance system located at both the top and bottom of the gate. For the current Western lock in Terneuzen, the guidance of the lower part of the gate is provided via guidance wheels on the carriage. As no carriages are present under the cantilever rolling gate, the lower active guidance

system is assumed to be mounted on the gate itself. However, this is something which has not been done before and is therefore a component in the current design that is a bit risky.

A possible limitation of the cantilever gate design is that due to horizontal loads and or changes in the water level difference over the gate, horizontal (dynamic) forces are transferred via the pendulum bars to the rolling carriages. It is expected that with the assumed active guidance, most of the horizontal forces can be absorbed. The fact that the gate is hanging completely is advantageous for its return to its central position. However, it could be that with a sudden reduction of the water level difference over the gate, the gate will return to its centre position too quickly and thus exert undesirable (dynamic) forces on the carriages. A possible solution is to clamp the gate by also having the push-off guidance device on the opposite side (i.e. the side to which the gate does not lean) actively push against the gate.

Passive or active guidance
Due to the assumed active guidance this design still contains moving parts under water, which was not the initial aim of this design study. Although the maintenance required for an active guidance system is probably significantly less than for a roller carriage, it would be beneficial if these underwater parts could be removed as well. To make this happen, a (partly) passive guidance system could be applied. The friction forces during opening and closing would then be considerably higher, requiring a stronger driving mechanism. It should however be verified if the gate is then still able to enter the recess during closing, as the gate may be pushed to far outwards by horizontal loads. In case of such a passive guidance system the guiding elements wear more quickly and therefore require replacement more often. It is therefore difficult to predict whether a passive or an active guidance requires more inspection and maintenance. As the initial focus was on the balance of the gate in horizontal longitudinal direction and because an active system was expected to at least meet the requirements, the active guidance was chosen as a start. It could however be the case that the passive system is more beneficial in practice.

RAMS aspects
The cantilever rolling gate concept is expected to improve the RAMS (Reliability, Availability, Maintainability & Safety) aspects due to the carriages and rails being located above water. The improvement of the RAMS aspects compared to the conventional rolling gate is purely hypothetical and only qualitatively taken into account and not yet quantified in this study. The exact benefit is therefore unknown.

The *reliability* of the cantilever rolling gate itself will probably not change considerably because the wheel-rail connection and driving system does not change in its essence. There may be a small improvement because the wheels and rails are no longer in salt water and less dirt and debris is present on the rail. On the other hand, the reliability of the locking function will likely improve because any failure of the wheels or rails will lead to a shorter blockage or no blockage at all. This is due to the fact that the carriages and rails are easier to replace because they are located out above water and out of the waterway. [1] As the reliability of the lock function increases, the overall *availability* of the lock function will also increase.

This new concept significantly improves *maintainability* because the roller carriages and rails are located above water and therefore much easier to access. This makes the repair or replacement of one of the components much easier and not dependent on divers or any special construction. Because maintenance work no longer takes place under water, *safety* will also probably increase.

Only wheel/rail connection and balance set as calculation requirements
In the current calculations, the maximum strength and fatigue loads of the wheel-rail connection have been set as the limiting factor for determining the required cantilever length. This has been done because the failure analysis of conventional rolling gates (chapter 3) showed that these components are the ones that most frequently lead to problems. For now, it has been assumed that the other components such as the steel structure of the rolling carriages, the connection between carriages and gate and the foundation of the rails can handle these forces. This limits the conclusion somewhat, as it is not yet known if these parts have sufficient strength capacity. All of these other parts have to be checked and designed in follow-up research. If these parts cannot handle the loads, it could be that the cantilever length has to be increased and/or that these parts have to be strengthened.

[1] It is important to note that this is only true if the lock has double gates and the locking function can be taken over by the second gate in case of repair or maintenance

Theoretical vs. actual contact surface
The wheel load calculations, see Section 6.4 and Appendix E, are based on the current wheels and rails of the Western lock of Terneuzen. Due to the flat running surface of the wheel and rail a theoretical line contact is formed, which is favourable for the stress distribution. The risk is that due to construction tolerances and deformations of the axles of the carriage, the actual contact surface may not be a pure line contact. Therefore it is possible that high stress peaks and some plastic deformation may occur on the sides of the rail or wheels. This is something which is not taken into account in the design yet.

A possible solution is to have wheels which also have a crown radius and thus are double curved. This double curve gives a so called point or ellipse contact surface which generally leads to unfavourable higher stresses. However, a double-curved wheel can be more reliable and redundant as it is less sensitive to irregularities.

8.3. Other ideas

This section discusses other ideas or possibilities for the further design of the cantilever rolling gate.

Filling the CHS trusses with concrete
In the current cantilever truss design the steel Circular Hollow Sections (CHS) are assumed to be hollow. It is important that the trusses are closed off completely airtight so that no inner corrosion can take place. Another solution is to fill the tubes with concrete. In addition to ensuring corrosion protection, this additional concrete also increases local and global buckling strength. In the application of the cantilever rolling gate, it also has the advantage that the counterweight can be slightly smaller.

A quick calculation shows that the total truss structure can accommodate a concrete volume of 6.3 m^3. With a specific concrete weight of 2300 kg/m^3, this equates to an extra weight of 14.5 t. If this concrete were to be used, the required extra buoyancy volume in the gate part could be increased to 119 m^3 (instead of 116 m^3), and the counterweight could be reduced from 1083 t to 1061 t.

Combinations of solutions/variants
Within the case study, one specific solution type has been worked out each time to highlight the differences. It is also possible to think of combinations of these solutions. If, for example, the sub-variant with the upper rail were to be used, it would be possible to also provide it with a counterweight to lighten the load on the back carriage. However, this would not alter the minimum required cantilever length as the front carriage was decisive in this regard. Therefore this type of combination would only lower the loads on the back carriage and not change the dimensions of the cantilever structure.

Also, only some specific solutions for the layout of the rolling carriage(s) have been considered. For example, the research presented only two options regarding the number of wheels (4 or 8 wheels). It may well be possible that a 6 wheel front carriage with for instance an increased wheel width or diameter could also provide enough capacity. As a conceptual study this has not been addressed, but it can be an option to look further into in a latter design stage.

For a carriage with 4 wheels, the widening of the wheel/rail interface and the increase of the wheel diameter were considered separately. A combination in which the wheel/rail width and diameter are both increased is also possible. However, to obtain a width greater than 150 mm and less than 220 mm, a custom-made rail would be required, as there are no standard intermediate sizes in between these widths. A quick calculation shows that it is possible to have a wheel diameter of 1500 mm and a wheel/rail width of 180 mm to reach a cantilever length of 16.6 m.

Varying buoyancy and load monitoring system
Adding additional buoyancy volume is limited by the fact that the gate must be in equilibrium under all circumstances, even in extreme situations. The governing loading situation which defines this additional buoyancy volume is in case of High Water (HW), opening of the gate, no silt or accretion and an favourable dead weight and unfavourable buoyancy volume. The design is such that the gate is stable under all circumstances, without adjusting the buoyancy volume.

It may be possible to increase the amount of buoyancy volume if it is combined with a load monitoring system that monitors the exerted loads on the carriages. Depending on the measured loads a pump system can change the buoyancy volume in real time. In case of the rare governing situation, extra water is pumped inside the buoyancy chamber to ensure a downward force on the front carriage. Such a system can indirectly decrease the required length of the cantilever part.

9

Conclusions & Recommendations

9.1. Conclusions

The objective of this research was to design and evaluate a new type of rolling gate for the Western lock in Terneuzen, for which all sensitive and heavily loaded mechanical parts are both easily accessible and located above water. Having all mechanical parts above the waterline not only makes them easier to inspect and maintain, but it also makes them less prone to fouling or obstruction by debris. In this way, the risk of premature gate failure due to failure of wheels/rails is expected to be lower, increasing the overall availability over the lifetime of the lock. The main research question that this thesis tries to answer is:

> *What is the most optimal conceptual design for a horizontal translation gate in the Western lock in Terneuzen, for which all heavily loaded mechanical supporting elements are both easily accessible and located above water?*

The main research question is answered by the final conceptual case study design presented in Chapter 7. From all the researched options, the Cantilever rolling gate appears to be most feasible (see below). Within the set boundary conditions and based on the performed calculations, the optimal Cantilever rolling gate design at the case study location consists of:

- An added cantilever part with a length of 16.6 meters.
- A cantilever truss structure constructed of Circular Hollow Sections (69 t).
- A counterweight directly below the back carriage (1083 t).
- An 8-wheel front carriage (9 m long).
- A 4-wheel back carriage (6 m long).
- An increased buoyancy chamber volume in the gate part by 116 m^3 (total is 1140.7 m^3).

Table 9.1 shows a comparison of dimensions between the designed Cantilever rolling gate and the current conventional rolling gate at the case study location.

Table 9.1: A comparison of the cantilever rolling gate and the current conventional rolling gate at the case study location of the Western lock in Terneuzen

	Cantilever rolling gate	**Current rolling gate**
Total gate length	61.2 m	44.6 m
Total weight gate structure (incl. counterweight)	2098 tonnes	946 tonnes
Total buoyancy chamber volume in gate part	1141 m^3	1025 m^3
Total lock width	120.8 m	104.2 m
Lower carriages (under water)	0	2
Upper carriages (above water)	2	1
Number of wheels front carriage	8	4
Number of wheels back carriage	4	4

With the added cantilever structure both carriages can be located above water, but the front carriage requires eight instead of four wheels. The connection between carriages and gate is completely different as the cantilever rolling gate hangs on pendulum rods instead of being simply supported on the carriages.

The added cantilever structure of 16.6 m extends the original gate part of 44.6 m by 37% to 61.2 m. The additional structure and its counterweight increase the total gate weight from 946 t to 2098 t. The designed cantilever rolling gate fits at the location of the case study, but the lock chamber and rails should also be lengthened by 16.6 m to fit the extended gate. The main downside of the concept is that it requires more material and space than the conventional rolling gate.

Wheel/rail failure analysis
An analysis of wheel/rail failure cases of existing rolling gates, see Section 3.3, shows that:

- The most delicate parts of a rolling gate are its wheel-rail connections located under water.
- Rails and wheels often fail well before their intended design life.
- Failure of these parts leads to long down-time of the locks and expensive repair works.
- In some cases rolling out of wheels/rails happened due to reoccurring horizontal shear forces unaccounted for in the design.
- The in-variance in extra weight due to fouling and accumulation of silt can add significant loads and should be taken into account in the design.

Variant study
Based on criteria deducted from points of difference between a conventional and a new gate type, the Cantilever rolling gate is favoured over the five other variants because:

- It consists of one single structure.
- The forces are transmitted through the gate itself, without the need for an extra external structure.
- It requires relatively few additional mechanical parts.
- The opening and closing time remains the same as for the conventional rolling gates.

Initiating balance of the cantilever gate
Various methods are possible to ensure balance in the cantilever rolling gate. The least impactful method is to increase the buoyancy chamber volume in the gate to reduce the downward force and overturning moment. However, the buoyancy volume can only be increased to a limited extent, otherwise the gate will lift in one of the extreme loading cases.

Due to this limitation of the maximum buoyancy volume, an additional balancing method is required: a counterweight or an anchored top rail. Based on the current analysis, the counterweight sub-variant is more advantageous as this solution provides the balance of forces in the gate structure itself, eliminating the need for a heavy additional foundation structure. It is a simpler design and it requires less highly loaded sensitive materials like rails. Also, as opposed to the anchored top rail sub-variant, the wheels do not require any tight tolerance restrictions and the carriages are not trapped between two rails and therefore can be freely replaced.

Minimised required cantilever length
An optimally sized cantilever length reduces material use and the required space at the lock site. When maintaining the current wheel diameter and rail width, an 8-wheel front-carriage leads to a optimal cantilever length of 16.6 m. The fatigue design limit of the wheel-rail contact surface of the front-carriage is the determining factor for this length. The 8-wheel front-carriage is the best option and chosen because it uses a wheel-rail configuration that is already in use today and simultaneously allows for a relatively short cantilever length. In addition, the loads are better distributed and therefore high stress concentrations are less likely to occur. The spread of loads is also advantageous for the carriage construction and the foundation of the rails.

Other design configurations including; an increased wheel diameter from 1200 mm to 1700 mm and; an increased rail width from 150 mm to 220 mm result in similar cantilever lengths of respectively 16.3 m and 16.8 m. The base case, a cantilever gate with both carriages having four wheels and the original wheel-rail dimensions, results in a minimum cantilever length of 26.4 m. With the current gate length of 44.6 m, this would lead to an increase in gate length of almost 60%!

Cantilever truss structure
The cantilever extension is designed as a truss structure, as it does not have to seal off and retain water and has an effective use of materials in combination with a relatively strong load-bearing capacity. The trusses are made of Circular Hollow Sections (CHS) due to their low drag coefficient, a good protection against corrosion and a high and effective torsional stiffness. Concluding the truss design, the biggest chord requires an outer diameter of 273 mm with a wall thickness of 30 mm and the smallest brace requires an outer diameter of 244.5 mm with a wall thickness of 12.5 mm. The total weight of the designed cantilever truss structure is 69 t, which is relatively light compared to the weight of the gate part (946 t) and the required counterweight (1083 t).

Optimal conceptual design
The Cantilever rolling gate is the most optimal conceptual design for a horizontal translation gate which has all the mechanical supporting elements easily accessible and above water. It technically can be applied at the Western lock in Terneuzen with the above-mentioned dimensions, specifications and adjustments.

9.2. Recommendations

This research only evaluated conceptual solutions and made a first technical design. Further research is required to make a considered decision on the complete feasibility of the Cantilever rolling gate. As a follow up to this research it is recommended to:

Determine the actual change in non-availability
The availability over the lifetime of a lock nowadays is an important design requirement due to the high costs of vessels being idle. The idea is that a gate without moving parts under water increases the availability, because all sensitive parts are more easily accessible to inspect and maintain. Calculating the actual availability would be valuable information to determine the gain in availability between the conventional gate and the cantilever gate. This would also make it easier to weigh up whether the additional costs of the cantilever construction and extended gate chamber outweigh the increased availability.

Make a total cost comparison
In order to fully evaluate the feasibility of the Cantilever rolling gate, it is required to make an economic assessment of the cantilever gate. It is suggested to do a Life Cycle Cost (LCC) analysis to calculate the costs over the entire life span of the gate. Especially the required extra material and construction costs for the cantilever truss extension and the increased lock chamber dimensions have to be analysed. It is advised to compare the cantilever rolling gate with a conventional gate with respect to the maintenance costs, construction costs and the saved costs for shipping due to the (expected) higher availability of the proposed design.

Evaluate the horizontal force transmission and guidance
In a future design step, it is important to look into the transmission of the horizontal transverse forces and the horizontal guidance of the gate. The currently assumed active guidance system should be elaborated further to see if it is sufficient to guide the cantilever gate during opening and closing and in closed position. It should be checked if the (dynamic) horizontal force component acting on the rolling carriages can be minimised by using the correct guidance system. Amongst the choices for such a guidance system both active and passive variants should be considered to see if the number of moving parts under water can be minimised. In addition, it should be analysed whether the protruding cantilever section could be clamped horizontally transversely in order to achieve better force transfer during opening and closing.

Elaborate on construction and maintenance
It is critical to incorporate the assembly and construction of the cantilever rolling gate in the next design phase. In the current design the cantilever part is assumed to be welded or bolted on to the gate part inside the gate chamber, only to be deconstructed at the end of the lifetime of the gate. It should be checked which of these types of connection methods is most feasible and if assembly on site is possible. Additionally, the maintenance of the cantilever gate and its components should be further detailed. In particular, the exchange of the rolling carriages is not yet sufficiently developed.

Check gate reliability
In a follow-up design, it is important to demonstrate that the new gate system is also sufficiently reliable to meet the dike ring failure norm frequency (1/4000 per year for Terneuzen). Therefore the reliability of closing must be verified.

Check internal gate forces
In conventional gates, the supports are located on both sides and the gate is loaded vertically as if it were a traditional beam (biggest moment-force in the middle of the gate). With the cantilever rolling gate, the two supports are located on the side of the gate at the cantilever part. The gate therefore extends with respect to the support and the greatest moment force in the construction is now right under the cantilever's front support. A check of this different behaviour of internal forces is required to see if the gate can handle these forces, or if the gate construction has to be adapted accordingly.

Further detail the truss structure
Finally, the truss structure design can be optimized and designed in more detail. In particular the fatigue of the tube connection nodes and the welded joints should be reviewed. It is critical to check whether the rotational capacity of the nodes is sufficient, and whether or not second order moments in the nodes must be taken into account.

Bibliography

[1] Y. Attema. *Metingen scheepsgolven buitenhaven Terneuzen*. Dutch. Tech. rep. 1796.MW/U15420/A/YAT. Svasek Hydraulics, Feb. 2015.

[2] DHV B.V. *Subvariantennota (PoC) Zeetoegang IJmond*. Dutch. Variantennota WPPoC-20110513-JSL-01. DHV B.V., Sept. 2011.

[3] DHV B.V. and A. Groffen. *Verbetering waterkering voorhavens Terneuzen - Roldeuren van Westsluis. Constructieve Herberekening*. Tech. rep. OR-SE20092953. DHV B.V., Dec. 2009, p. 13.

[4] Iv-Infra b.v. and C.P. Broekhuizen. *Inspectierapport Risico Inventarisatie Natte Kunstwerken Complexcode 54E-001 Westsluis*. Dutch. Tech. rep. INPA100687-R-460. Iv-infra b.v., Sept. 2011, p. 131.

[5] Iv-Infra b.v. and A. van Sabben. *Analyserapport Waterbouw Westsluis Terneuzen (RINK 2011)*. Dutch. Tech. rep. INPA100687-R-450. Iv-infra b.v., Oct. 2011, p. 131.

[6] Iv-Infra b.v. and W. van der Stelt. *Analyserapport Werktuigbouw Westsluis Terneuzen (RINK 2011)*. Dutch. Tech. rep. INPA100687-R-430. Iv-infra b.v., Oct. 2011, p. 26.

[7] Iv-Infra b.v. and A.J.S. de Wit. *Analyserapport Staalbouw Westsluis Terneuzen (RINK 2011)*. Dutch. Tech. rep. INPA100687-R-420. Iv-infra b.v., Sept. 2011, p. 34.

[8] Christoph Barth. "Kaiserschleuse Bremerhaven wird für Schiffe gesperrt". In: *Nord 24* (June 2019). URL: https://www.nord24.de/bremerhaven/Kaiserschleuse-Bremerhaven-wird-fuer-Schiffe-gesperrt-28735.html (visited on 05/14/2021).

[9] Prof.dr.ir. J.A. Battjes. *CT2100: Vloeistofmechanica*. nl. Delft University of Technology, Apr. 2002.

[10] A. van Beek. *Tribologie: Levensduur en prestatie*. Dutch. Ponsen & Looijen, 2001. ISBN: 90-370-0190-4.

[11] Anton van Beek. *Advanced engineering design. Lifetime performance and reliability*. English. TU Delft, 2012. ISBN: 978-90-810406-1-7.

[12] T.H. Blommaert. *Dienstorder nr. 7, Schutbeperkingen bij Stormvloed*. Oct. 2009.

[13] S.A. Boelwerf. *[B03] Gewichtsberekening roldeuren Westsluis Terneuzen*. 1966.

[14] S.A. Boelwerf. *[B04] Samenvatting der berekeningen sluisdeuren Terneuzen*. Dutch. Jan. 1967.

[15] Ingenieursbureau Boorsma. *Trade off_type deuren*. Dutch. Dec. 2013.

[16] Rijkswaterstaat directie bruggen. *Belastingen roldeur Krammersluis*. nl. Nov. 1981.

[17] Ryszard A. Daniel. *Contact behaviour of lock gates and other hydraulic structures*. Lambert Academic Publishing, 2011. ISBN: 978-3-8443-9154-1.

[18] Rijkswaterstaat - werktuigkundige- en elektrotechnische dienst. *Technische tekening RWSZL-2008-01998 - Onderrolwagen Railbaan Noordzijde roldeur A Westsluis Terneuzen*. Dutch. 2008.

[19] Rijkswaterstaat - werktuigkundige- en elektrotechnische dienst. *Technische tekening RWSZL-2008-03364 Boven-/ onderrolwagen 04. Samenstelling loopwiel onderrolwagen Roldeur A Westsluis Terneuzen*. Oct. 2003.

[20] Rijkswaterstaat - werktuigkundige- en elektrotechnische dienst. *Technische tekening ZLWD-2003-50015 - Details onderdelen loopwiel onderrolwagen 07 Roldeur B Westsluis Terneuzen*. Dec. 2003.

[21] Rijkswaterstaat - werktuigkundige- en elektrotechnische dienst. *Technische tekening ZLWD-2003-50021 Deurconstructie overzicht roldeur A Westsluis Terneuzen*. Mar. 2003.

[22] J.W. Doeksen. "Gate Design For Large, High Head Locks". English. MA thesis. Delft: TU Delft, Feb. 2012.

[23] P. Duuring and C. Rothilde. "De sluisdeuren der Belgische zeesluizen / Les portes d'ecluses maritimes Belges". In: *Tijdschrift der openbare werken België* No.3 (1988).

[24] H. Hertz. "Ueber die Berührung fester elastische Körper." German. In: *Journal für die reine und angewandte Mathematik* 92 (1881), pp. 156–171.

[25] Maurits Houben and Leon Uijttewaal. *Faaldefinities natte beweegbare objecten*. Dutch. Dit kader Faaldefinities natte beweegbare objecten maakt deel uit van de brug- en sluisstandaard. June 2014.

[26] Dick ten Hove et al. *Verkenning maritieme toegankgelijkheid Kanaal Gent-Terneuzen. Leemtes veiligheidsonderzoeken*. Dutch. Tech. rep. 9V5506.A0. Marin, Aviv & Royal Haskoning, July 2010.

[27] J. P. Josephus Jitta. *Sluizen en andere waterbouwkundige kunstwerken in en langs kanalen*. en. Publisher: Erven F. Bohn NV, Haarlem. Haarlem: De Erven F. Bohn N.V., 1947. URL: https:

//repository.tudelft.nl/islandora/object/uuid%3A64760f30-96e5-4fa5-b20b-6352745706b1 (visited on 05/14/2021).
[28] Hansa International Maritime Journal. “Bremerhavener Kaiserschleuse bis September dicht”. In: *Hansa International Maritime Journal* (June 2019). URL: https://hansa-online.de/2019/06/featured/129325/bremerhavener-kaiserschleuse-bis-september-dicht/.
[29] Johnson K.L. *Contact Mechanics*. Cambridge University Press, 1987. ISBN: 978-0-521-34796-9.
[30] Kreiszeitung.de. “Reparatur der Kaiserschleuse kostet 14 Millionen Euro”. German. In: *Kreiszeitung.de* (Oct. 2015). URL: https://www.kreiszeitung.de/lokales/bremen/reparatur-kaiserschleuse-bremerhaven-kostet-millionen-euro-5840847.html (visited on 05/14/2021).
[31] Flanders Hydraulics Research (Waterbouwkundig Laboratorium). *Kanaal Gent-Terneuzen. Tijpoort Westsluis*. Tech. rep. MOD 803-1. Vlaamse Overheid, Departement Mobiliteit en Openbare Werken, Afdeling Waterbouwkundig Laboratorium, Mar. 2007.
[32] Pieter van Lierop. “No standard lock gates for the new sea lock in IJmuiden, the largest lock in the world”. EN. In: *PIANC-World Congress Panama City, Panama 2018* (2018).
[33] Sjaak Michielsen. *E-mail: Update informatie roldeuren Westluis Terneuzen*. Sept. 2019.
[34] Sjaak Michielsen. *E-mail: Vragen omtrent uitwalsen loopwielen Westsluis*. Dutch. June 2016.
[35] Frank Miener. “Auf dem Grund der Kaiserschleuse”. German. In: *Weser Kurier* (Mar. 2015). URL: https://www.weser-kurier.de/bremen/politik/auf-dem-grund-der-kaiserschleuse-doc7e3hvdja25c1gbiq34x7?reloc_action=artikel&reloc_label=/bremen/bremen-wirtschaft_artikel,-Auf-dem-Grund-der-Kaiserschleuse-_arid,1087682.html (visited on 05/14/2021).
[36] W.F. Molenaar and M.Z. Voorendt. *CIE3330 Hydraulic Structures: General lecture notes*. English. Lecture notes. Delft University of Technology, 2020.
[37] W.F. Molenaar and M.Z. Voorendt. *CIE3330 Hydraulic structures: locks*. English. Lecture notes. Delft: Delft University of Technology, 2020.
[38] NEN and IEC. *NEN-EN-IEC 60300-3-3: Dependability managament Part 3-3: Application guide - Life Cycle costing*. Norm NEN-EN-IEC 60300-3-3. Nederlands Elektrotechnisch Comité (NEC) and Nederlands Normalisatie Instituut, 2004.
[39] *nieuwe sluis zeebrugge*. nl. URL: https://www.nieuwesluiszeebrugge.vlaanderen.be/homepagina (visited on 12/02/2021).
[40] Koninklijk Nederlands Normalisatie-instituut. *NEN 6786-1 (nl) Voorschriften voor het ontwerp van beweegbare delen van kunstwerken - deel 1: Beweegbare bruggen (VOBB)*. Dutch. July 2017.
[41] Koninklijk Nederlands Normalisatie-instituut. *NEN-EN 13001-1 (en) Crane safety - General design - Part 1: General principles and requirements*. English. Jan. 2015.
[42] Koninklijk Nederlands Normalisatie-instituut. *NEN-EN 13001-2 (en) Cranes -General design - Part 2: Load actions*. Dutch. Jan. 2005.
[43] Koninklijk Nederlands Normalisatie-instituut. *NEN-EN 13001-3-3 (en) Cranes - General design - Part 3-3: Limit states and proof of competence of wheel/rail contacts*. English. Oct. 2014.
[44] Koninklijk Nederlands Normalisatie-instituut. *NEN-EN 1990+A1+A1/C2 (nl) - Eurocode: Grondslagen voor het constructief ontwerp*. Nov. 2019.
[45] Koninklijk Nederlands Normalisatie-instituut. *NEN-EN 1990+A1+A1/C2/NB (nl) - Nationale bijlage bij NEN-EN 1990+A1:2006+A1:2006/C2:2019 Eurocode: Grondslagen van het constructief ontwerp*. nl. Nov. 2019.
[46] Koninklijk Nederlands Normalisatie-instituut. *NEN-EN 1993-1-1+C2+A1 Eurocode 3: Ontwerp en berekening van staalconstructies - Deel 1-1: Algemene regels en regels voor gebouwen*. nl. Dec. 2016.
[47] NEN - Koninklijk Nederlands Normalisatie-instituut. *NEN-EN 10210-2 (en) - Hot finished steel structural hollow sections - Part 2: Tolerances, dimensions and sectional properties*. EN. May 2019.
[48] Deutsches Institut für Normung. *DIN 19705-1 Stahlwasserbauten - Teil 1: berechnungsgrundlagen*. German. Nov. 2014.
[49] TNO Bouw en Ondergrond, H. Borsje, and A.J. Wubs. *Onderzoek naar het functioneren van de oostelijke roldeur van de Noordersluis te IJmuiden - fase 1*. nl. Tech. rep. TNO-034-DTM-2009-04693. TNO, June 2010.
[50] Tom Ory. “”Van rijden naar glijden” - Haalbaarheidsstudie naar het toepassen van Hydrogeleiding in de Kallosluis”. Dutch. MA thesis. Delft: TU Delft, Aug. 2003.
[51] PIANC. *Final report of the international commission for the study of locks*. English. Tech. rep. Permanent International Association of Navigation Congresses (PIANC), 1986.
[52] P.H. Rigo. *Self propelled floating lock gate - PIANC InCom-WG29*. English. Dec. 2008.

[53] Rijkswaterstaat. *Grotere diepgang Westsluis en kanaal Terneuzen*. Dutch. Tech. rep. Nota S 86.151. Dordrecht: Rijkswaterstaat Dienst Verkeerskunde. Hoofdafdeling Scheepvaart, Apr. 1987.
[54] Rijkswaterstaat. *IJmuiden: bouw nieuwe, grote zeesluis*. nl-NL. webpagina. Last Modified: 2021-02-16T11:22:58. URL: https://www.rijkswaterstaat.nl/water/projectenoverzicht/ijmuiden-bouw-nieuwe-grote-zeesluis (visited on 05/14/2021).
[55] Rijkswaterstaat. *Kenmerkende waarden getijdegebied 2011.0*. Dutch. Tech. rep. Rijkswaterstaat, July 2013.
[56] Rijkswaterstaat. *Referentiewaarden waterstanden waternormalen Terneuzen*. Dutch. 2016.
[57] Rijkswaterstaat. *Richtlijn vaarwegen 2011*. Tech. rep. Rijkswaterstaat, Dec. 2011.
[58] Rijkswaterstaat. *Richtlijnen Ontwerp Kunstwerken (ROK 1.4)*. nl. Rijkswaterstaat Technisch Document (RTD). Apr. 2017.
[59] Bouwdienst Rijkswaterstaat. *Bijlage 1: Draaiboek wisselen deuren en onderrolwagens hansweert (behoort bij bestek ZL-5275)*. Tech. rep. OZ-HAN-D-96.033[C]. Oct. 2001.
[60] Rijkswaterstaat et al. *Leidraad RAMS. Sturen op prestaties en systemen.* Dutch. Tech. rep. Rijkswaterstaat, Mar. 2010.
[61] *Rolling Resistance*. URL: https://www.engineeringtoolbox.com/rolling-friction-resistance-d_1303.html (visited on 05/19/2021).
[62] D. Ros. *Eindrapport onderzoek wielbelast. Ontwerp- en rekenrichtlijn voor de wielgeleiding van roldeuren.* Tech. rep. NIO-R-95048. Bouwdienst Rijkswaterstaat, hoofdafdeling natte infrastructuur, Oct. 1995, p. 16.
[63] Vlaams Nederlandse Scheldecommissie et al. *Uitgangspunten nota Systeemontwerp - WTB (Nieuwe Sluis Terneuzen)*. nl. Tech. rep. VNZT-R-200-0. Vlaams Nederlandse Scheldecommissie, June 2015.
[64] H.M. Slot. *Slijtageonderzoek en materiaaladvies loopwielen onderrolwagens Westsluis Terneuzen*. Dutch. Tech. rep. MT-RAP-06-23483. TNO Industrie en Techniek, Mar. 2006, p. 52.
[65] *Special Crane Rail MRS221 - ArcelorMittal*. URL: https://rails.arcelormittal.com/types-rails/crane-rails/special-crane-rails/rail-mrs221 (visited on 07/21/2021).
[66] International Organization for Standardization. *Cranes - Tolerances for wheels and travel and traversing tracks - Part 1: General*. English. Jan. 2012.
[67] Rijkswaterstaat directie sluizen en stuwen. *Technische tekening TN126 - Nieuwe zeesluis Terneuzen - Notatekening*. Nov. 1963.
[68] Christoph Tarras. “Construction of the new Kaiserschleuse lock in Bremerhaven”. EN. In: 2010 (2010).
[69] Ministerie van Verkeer en Waterstaat. *Hydraulische Randvoorwaarden primaire waterkeringen - voor de derde toetsronde 2006-2011 (HR 2006)*. nl. Aug. 2007.
[70] ir. S.P.V. Vlaenderen. *Eindverslag Onderzoek Wielbelast*. Dutch. Tech. rep. NIO-R-94034. Bouwdienst Rijkswaterstaat, Aug. 1994, p. 48.
[71] dr. ing. M.Z. Voorendt and ir. W.F. Molenaar. *Manual Hydraulic Structures*. en. Feb. 2020.
[72] A. Vrijburcht and A. Glerum. *Design of locks: part 1*. Rijkswaterstaat, 2000. ISBN: 90-369-3305-6. URL: https://repository.tudelft.nl/islandora/object/uuid%3Aafda7af7-ab32-4131-bf05-faa715fca55a.
[73] Jaap Wardenier et al. *Hollow sections in structural applications*. Bouwen met staal Rotterdam„ The Netherlands, 2002.
[74] Rijkshavenmeester Westerschelde and H.J.M. Adan. *Nr. 03-2009: Breedte voor Zeeschepen op het Kanaal van Gent naar Terneuzen*. Apr. 2009.
[75] PIANC WG106. *Innovations in navigation lock design*. English. Tech. rep. 106. PIANC, 2009.
[76] PIANC WG173. *Movable bridges and rolling gates design, maintenance and operation lessons learnt*. English. Tech. rep. WG Report nr. 173. PIANC, 2017.
[77] PIANC WG31. *Life cycle management of port structures. General Principles.* Tech. rep. 31. International Navigation Association, 1998.
[78] P. Wigny and J.M.A.H. Luns. *Verdrag tussen het Koninkrijk België en het Koninkrijk der Nederlanden betreffende de verbetering van het kanaal van Terneuzen naar Gent en de regeling van enige daarmede verband houdende aangelegenheden*. Dutch and French. 1960.
[79] Rijkswaterstaat Zeeland, Michel Fouraschen, and Arnold de With. *Bediening op afstand sluizen Rijkswaterstaat Zeeland*. Tech. rep. July 2006.
[80] Dienstkring Zeeuwsch-Vlaanderen, Bouwdienst Rijkswaterstaat, and Ingenieursbureau Iv-Infra b.v. *Beheer- en onderhoudsplan t.b.v. het sluizencomplex i/h kanaal van Gent naar Terneuzen*. Dutch. Tech. rep. Jan. 2002.

Appendices

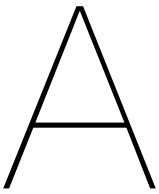

List of rolling gates in large maritime navigation locks

Table A.1: List of rolling gates in large maritime navigation locks

Name and location		Year	Gate type	Chamber			Gate		
				W [m]	L [m]	H [m]	L [m]	W [m]	ton
Old Visartlock Zeebrugge	BE	1907		19.7	210				
Royerlock Antwerp	BE	1908		22	182.5				
Industrial lock bremerhaven	DE	1910	Wheelbarrow	47.3	248	17	37	7	720
Large sealock Emden	DE	1913	Wagon	40	260	20	42.1	7.8	860
Old large Brunsbuttel Lock (2x)	DE	1914		42	310				
Large lock Kiel-Holtenau (2x)	DE	1914	Wagon	42	310			7.9	1250
Large Fishery lock bremerhaven	DE	1925	Wagon	35	181	18.5	37.18	10.08	1027
Small Fishery lock bremerhaven	DE	1925	Wheelbarrow	12	106.5	15.7	12.7	3.3	100
Van Cauwelaart lock Antwerp	BE	1928	Wheelbarrow	35	270	18.25	36.87	7.1	1170
Northern lock IJmuiden	NL	1929	Wagon	50	400	20	52.5	7.8	1400
Northern lock Bremerhaven	DE	1931	Wheelbarrow	45	372	21.2	56.5	8.5	2400
Louis Joubert Lock (saint-nazaire)	FR	1934		50	350				
Julianalock	NL	1938		12	125				
Watier lock Dunkerque	FR	1947		40	280				
Boudewijnlock Antwerp	BE	1955	Wheelbarrow	45	360	18.51	47	8.85	800
Large sealock Wilhelmshaven (2x)	DE	1964	Wagon	57	390	20	60	10	1700
Perm Russia	RU	1965		30	240	10.25			
Zandvietlock Antwerp	BE	1967	Wheelbarrow	57	500	22.48	58.60	10.90	1570
Western lock Terneuzen	NL	1968	Wagon	40	290	19.2	44.2	7	946
Charles de gaulle lock Dunkerque	FR	1970	Wheelbarrow	50	365			10	1700
Ecluse francois 1er, Le Havre	FR	1971	Wheelbarrow	67	401	24	70	10	3300
Andenne-Seilles	BE	1979	Wheelbarrow	25	200				
Kallolock Antwerp	BE	1979	Wheelbarrow	50	360	23.65	51.6	10.9	1470
Bremen Oslebshausen sealock	DE	1982	Wheelbarrow	35	249	17	37		700
Roompotlock	NL	1982		16	100	11.55			
Krammerlocks (2x)	NL	1983	Wagon	24	285	11	27	4	375
Vandammelock Zeebrugge	BE	1983	Wheelbarrow	57	500	24.5	58.6	10.9	2065
Grand mallades	BE	1983		25	200				
Old Kaiserlock Bremerhaven	DE	1987		27	215				
Hansweert (2x)	NL	1987	Wagon	24	280	14.6	27.86	4.69	300
Berendrechtlock Antwerp	BE	1989	Wheelbarrow	68	500	22.67	69.69	10.90	1650
Oranjelock Amsterdam	NL	1995	Hydrofeet	24	200				
Wintam lock Hingene	BE	1997		25	250				
Dieppe 'Admiral Roland' lock	FR	1999	Wagon	28		14.45	28.6	4.2	325
Sevilla lock	ES	2011	Wheelbarrow	42	434	20		6	800
New Kaiser lock Bremerhaven	DE	2011	Lift-and-slide	55	305	21.2	57.4	11.6	2270
Malamocco lock Venice	IT	2014	Hydrofeet	50	380	17	54	6.5	
Kieldrechtlock Antwerp	BE	2016	Wheelbarrow	68	500	27	70	9.92	2000
New Panama Locks	PA	2016	Wheelbarrow	55	458	33.04	57.6	10	4000
Meppelerdieplock	NL	2017	Wagon		125	7	37	3	
New Beatrix lock	NL	2019		25	270				
New lock Ijmuiden	NL	2022	Wheelbarrow	70	500	23	72	10.5	2400
New Lock Terneuzen	NL	2023		55	427				
New Brunsbuttel Lock	DE	2024		42	330				

Sources: [51], [76], [62], [23], [22], [75], [27], [59], [39], [79], [68] & [54]
Some of the sources showed contradictory figures, so not all the numbers in this table may be exactly correct. In most cases the most recent or detailed document has been used as the primary source. Be aware that this table probably is not a complete overview of all the navigation locks with rolling gates in the world, as the writer may have missed some.

B

Idea generation of variants

This appendix shows the results of the generation of ideas for possible new gate variants which have all of their heavily loaded mechanical parts above the waterline. The idea generation consisted of making morphological charts and building k'nex 3D models to concretise the designs.

B.1. Initial morphological charts

Figure B.2 shows the 1st morphological chart that was created to come up with ideas for a gate which has no mechanical parts under water. It shows differences in connection of the wheels and initiation of the balance. Figure B.3 shows the 2nd more extended morphological chart which also incorporated the horizontal guidance. In a later stadium it was decided that the horizontal guidance were to be assumed identical to the current situation to simplify the design process.

B.2. K'nex 3D models

Figure B.1 shows the bascule beam rolling gate made out of K'nex. By building this variant from k'nex it was learned that the placement of the beams with the counterweights on each side of the gate is complex. Also it was noticed that the connection between both rails (the one on the foundation and one on the moving beam) was not perfect and would probably lead to problems if constructed as a real gate.

Figure B.1: A k'nex model of the bascule beam rolling gate

Figure B.4 shows the closing steps of the rolling beam rolling gate variant made from K'nex. In Figure B.4a the beam and gate are both in open position. First the rolling beam closes (Figure B.4b) and then the gate follows (Figure B.4c). Through this model it became clear that the rails on the gate chamber and on the rolling beam cannot be aligned (or they have to be moved sideways mechanically) and that therefore the front and rear carriages do not roll on the same rails. Also, the front carriage and gate have to be locked in place as the rolling beam moves to prevent the gate from moving too early.

Figure B.5 shows a K'nex model of the cantilever rolling gate in open and closed position.

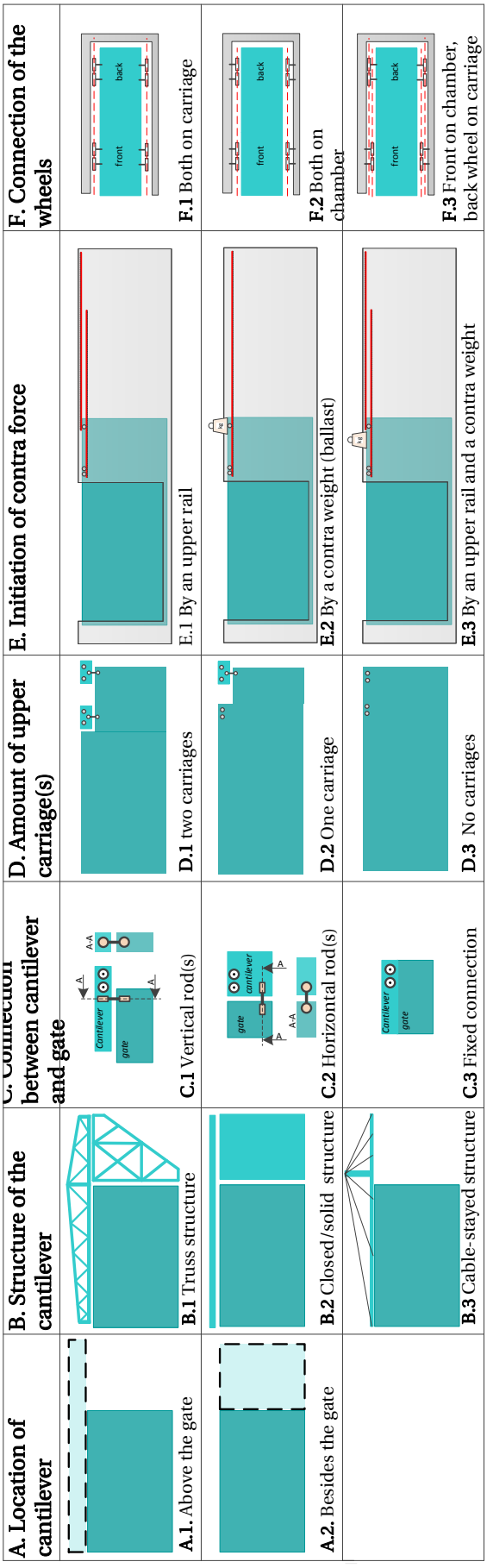

Figure B.2: Initial morphological chart at the start of the variant design phase

Morphological chart

1. Initiating cantilever arm	2. Gate division (way of translating gate structure)	3. Vertical load transfer	4. Horizontal guidance at recess	5. Horizontal guidance type at chamber	6. Horizontal guidance location at gate chamber	7. Initiation of contra force	8. Front (channel side) wheels	9. Back (chamber side) wheels	10. Cantilever arm length	11. gate chamber location	12. Driving mechanism (?)
Above the gate; cable-stayed	solid system (flexibility by spring/hydraulic jack wheel connection)	Rails on recess, wheels on gate/carriage	no guidance (centering by gate structure)	no guidance (centering by gate structure)	no guiding wheels	Contraweight (variable)	2 wheels	2 wheels	short (0,33*gate width)	1 side	cable connection to cable winch
Above the gate; beam	1 large carriage, flexible connection in horizontal plane	Rails on gate, wheels on recess	fully sliding: UHMPWE timber/steel connection (no centering device)	fully sliding: UHMPWE timber/steel connection (no centering device)	both wheels on chamber	clamped by rail	4 wheels	4 wheels	medium (0,5*gate width)	2 sided	tractor pulled
Above the gate; truss structure	1 large carriage, flexible connection in vertical plane	Rails on gate, wheel on recess channel side, rail on recess and wheel on gate chamber side	Partly sliding: bottom UHMWPE to timber/steel connection and top guiding wheels on gate	Partly sliding: bottom UHMWPE to timber/steel connection and top guiding wheels	one wheel on chamber, one on gate	Contraweight (fixed) and clamped by rail	8 wheels	8 wheels	long (0,66*gate width)		penn track
At the level of the gate; fixed	2 small carriages, flexible connection in vertical plane		Partly sliding: bottom UHMWPE to timber/steel connection and top guiding wheels on recess	guiding wheels at top and bottom	both wheels on the gate						
At the level of the gate; flexible	1 small carriage, flexible connection in vertical plane (flexibility by spring/hydraulic jack wheel connection)		guiding wheels at top and bottom; on gate		Only 1 wheel on gate						
			guiding wheels at top and bottom; on recess		Only 1 wheel on chamber						

Figure B.3: 2nd more extended morphological chart (in text)

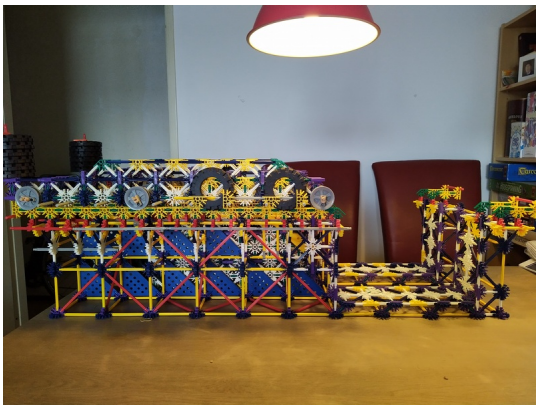

(a) Step 1: Gate and rolling beam in open position

(b) Step 2: Rolling beam in closed position

(c) Step 3: Gate and rolling beam in closed position

Figure B.4: A k'nex model of the rolling beam rolling gate and the three steps of closing of the gate

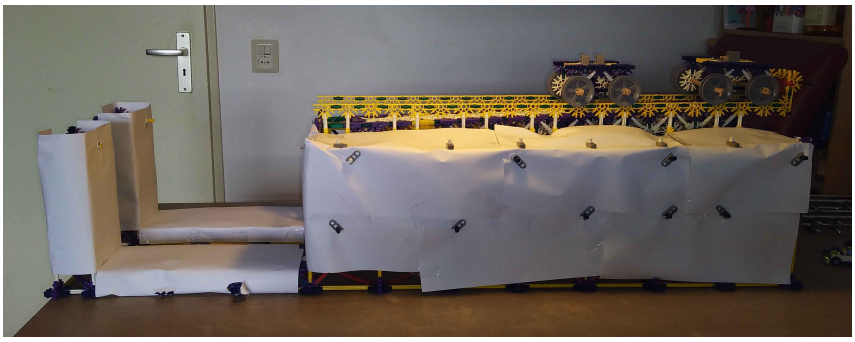

(a) Cantilever gate in open position

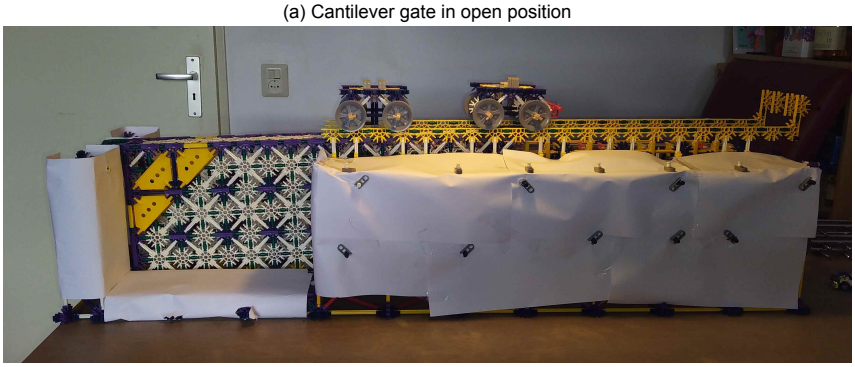

(b) Cantilever gate in closed position

Figure B.5: A k'nex model of the cantilever rolling gate in open and closed position

C

Resistance forces during opening and closing

In this calculation the cantilever length is assumed to be 24 m, both carriage are assumed to have 4 wheels and an assumed contra weight of 500 tonnes is present.

The opening/closing schedule of the current Westsluis as shown in section 5.1.2 table 5.2 is used as input to calculate all the resistance forces related to the opening and closing of the cantilever gate. The summation of these resistance forces under average and maximum condition determine the required pulling force of the driving mechanism for different situations and the maximum exerted moment force on the gate during opening/closing.

The opening and closing of the gate can be split up into:

- An acceleration phase (from 0 m/s till constant move speed of 0.277 m/s)
- Constant movement speed (0.277 m/s)
- Deceleration to crawl speed (from 0.277 m/s to 0.055 m/s)
- Constant crawl speed (0.055 m/s)
- Deceleration to zero (from 0.055 m/s to 0 m/s)

Figure C.1 shows the gate speed plotted over time over the full opening or closing sequence of the gate.

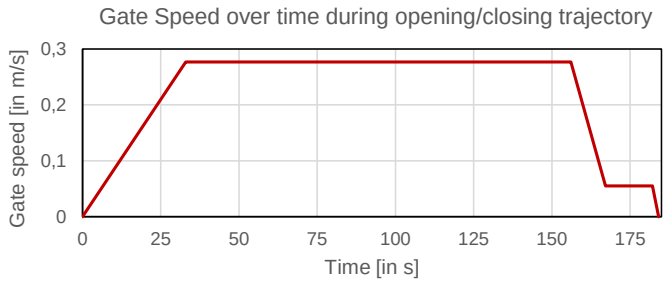

Figure C.1: Gate speed over time during opening/closing trajectory

These operating data can be used to calculate the key times and locations and the accelerations during the different phases, see table C.1.

The guiding system is assumed to be identical to the current gate. Thus the gate is actively guided by push-off devices on both the top and the bottom of the gate structure. The push-off devices consist of a wheel which is pushed against a rail. Therefore the rolling friction is taken as 0.005 according to the “dirty tram rails” from www.engineeringtoolbox.com[61].

Table C.1: Key data (distance, time points & accelerations) regarding opening/closing of the cantilever gate

Parameter	Abbreviation	Value	Unit
Distance moved after acceleration	s_acc	4.57	m
Distance moved from normal speed to crawl speed	s_dec	1.83	m
Distance moved from crawl speed to zero	s_zero	0.06	m
Distance moved during normal speed	s_normal	34.1	m
Time during crawlspeed	t_crawl	15	s
Time during normal speed	t_normal	123.1	s
Total movement time	t_total	184.1	s
Acceleration	a_acc	0.008	m/s^2
Decelerationt o crawl speed	a_deccrawl	-0.020	m/s^2
deceleration to zero	a_deczero	-0.028	m/s^2

C.1. Gate displacement and extracted gate length

The displacement of the gate for each of the different acceleration periods is given by:

$$s_{\text{acc}} = \frac{1}{2} \cdot a \cdot t^2 = \frac{1}{2} \cdot \frac{(v_{\text{move}} - v_0)}{t_{\text{acc}}} \cdot t^2 = \frac{1}{2} \cdot \frac{(0.277 - 0)}{33} \cdot t^2$$

$$s_{\text{normal}} = v_{\text{constant}} \cdot t = 0.277 \cdot t$$

$$s_{dec,crawl} = \frac{1}{2} \cdot \frac{(v_{\text{crawl}} - v_{\text{move}})}{t_{dec,crawl}} \cdot t^2 = \frac{1}{2} \cdot \frac{(0.055 - 0.277)}{11} \cdot t^2$$

$$s_{\text{crawl}} = v_{\text{crawl}} \cdot t = 0.055 \cdot t$$

$$s_{dec,zero} = \frac{1}{2} \cdot \frac{(v_0 - v_{\text{crawl}})}{t_{dec,zero}} \cdot t^2 = \frac{1}{2} \cdot \frac{(0 - 0.055)}{2} \cdot t^2$$

The total travel distance over the full opening/closing sequence (from t=0 till t=184.1) is then given by:

$$s(t) = s_{\text{acc}} \qquad for\ t = 0 \rightarrow\ t = 33$$

$$s(t-33) = s_{\text{acc}}(33) + s_{\text{normal}}(t-33) \qquad for\ t = 33 \rightarrow\ t = 156.1$$

$$s(t-156.1) = s_{\text{acc}}(33) + s_{\text{normal}}(123.1) + s_{dec,crawl}(t-156.1) \qquad for\ t = 156.1 \rightarrow\ t = 167.1$$

$$s(t-167.1) = s_{\text{acc}}(33) + s_{\text{normal}}(123.1) + s_{dec,crawl}(11) + s_{\text{crawl}}(t-167.1) \qquad for\ t = 167.1 \rightarrow\ t = 182.1$$

$$s(t-182.1) = s_{\text{acc}}(33) + s_{\text{normal}}(123.1) + s_{dec,crawl}(11) + s_{\text{crawl}}(15) + s_{dec,zero}(t-182.1) \qquad for\ t = 182.1 \rightarrow\ t = 184.1$$

As opening and closing are split up into different acceleration and deceleration phases, not a single continuous formula can be used to express the behaviour of the gate over time. Therefore it is decided to perform all calculations in excel tables with time intervals of 1 second. Some of the calculations are therefore described in excel formula's.

Extracted gate length

The travel distance of the gate is 41.375 meter while the lock chamber is 40 meters wide. The gate has to travel further in order to seal off. It is assumed that this sealing of distance is equally divided over both sides, thus (41.375-40)/2= 0.6875 m. The gap can then be expressed as:

$$x_{gap,(t)} = s(t) - 0.6875$$

For the first 12.8 seconds the gate is already moving, but no gap occurs as it still has to travel the sealing distance. It should therefore be taken into account that the gap has a minimum value of 0 and a maximum value of 40.

The extracted gate length ($l_{g,ext}$) is the 'inverse' of the gap. In case of opening the length of the extracted gate is given by:

$$l_{g,ext,o} = MIN(40; MAX(0; 40 - s(t) - 0.6875)$$

And for closing:

$$l_{g,ext,c} = MIN(0; MAX\,(40; s(t) - 0.6875))$$

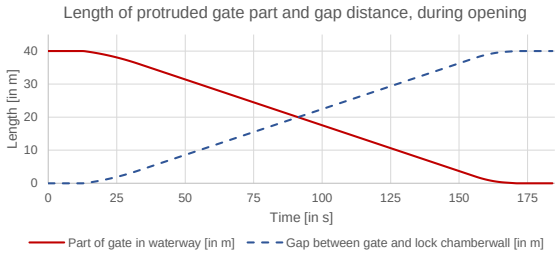

Figure C.2: Protruded gate length and the gap between gate and lock chamber-wall during opening of the gate

Figure C.2 simultaneously shows the extracted gate length and the gap during opening of the gate. In case of closing of the gate these values logically flip around.

C.2. Forces during movement

As also stated in section 6.1.5, the resisting forces during opening and/or closing consist of:

- Mass inertia of the gate
- Mass inertia of the driving mechanism
- Hydrodynamic resistance due to the suction effect
- Hydrodynamic resistance due to waterflow allong the gate
- Rolling resistance of the wheels
- Friction force due to a residual water-head
- Friction force due to a water density difference
- Friction force due to a translation wave
- Friction force due to wind waves
- Friction force due to an extreme ship wave

The magnitude of all of the resistance forces during opening is elaborated below.

C.2.1. Mass inertia of the gate mass

The force due to mass inertia is the simple formula of $F = m \cdot a$. Thus dependant on the mass of the gate structure (W) and the acceleration of the gate (a_g) in the accelerating or deceleration phase of opening or closing:

$$F_i = W \cdot a_g$$

The total weight which is accelerated consists of the weight of the gate and cantilever, the weight of both roller carriages, the trapped water inside the filled buoyancy chambers, the maximum silt and accretion weight and the (possible) contra-weight.

In this calculation the cantilever length is assumed at 24 m with a dead weight of 56.1 tonnes (See xxx). The gate weight is 946 tonnes and the maximum silt weight is 110.9 tonnes (see 3.3). The trapped water inside the filled buoancy chambers is 202 tonnes. With two 4 wheel carriages, the weight of the carriages is 24 tonnes. To calculate the maximum mass inertia force, a contra weight of 500 tonnes is assumed.

Figure C.3 shows the force due to mass inertia during the opening/closing trajectory at the highest lockage water level.

C.2.2. Mass inertia of the driving mechanism

According to [6], the maximum force in the cables of the driving mechanism is 2 kN during the initial acceleration of 0.00839 m/s^2. The ”mass” of the driving system can than be estimated by dividing this maximum force by the maximum acceleration:

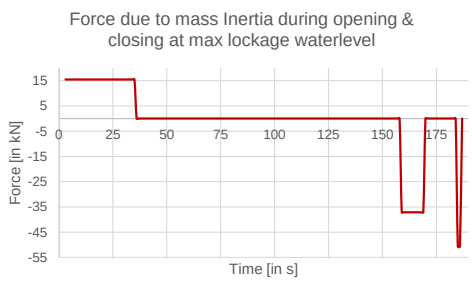

Figure C.3: Force due to mass inertia of the gate mass during opening/closing at highest lockage waterlevel

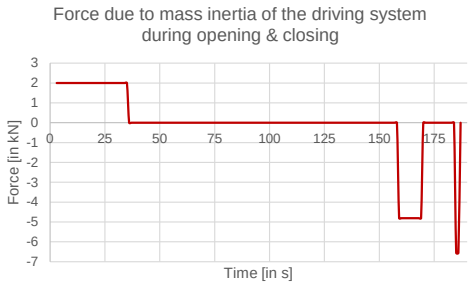

Figure C.4: Force due to mass inertia of the driving system during opening/closing

$$m_{i,driving} = F/a = 2000/0.00839 = 238267\ kg$$

This ”mass” can then be used to calculate the force during opening/closing of the gate. This is shown in figure C.4.

C.2.3. Hydrodynamic resistance due to the suction effect

The hydrodynamic resistance force due the suction effect is created by the movement of the gate and the related water level difference over the length of the gate. The maximum suction force ($F_{suc,max}$) is calculated by:

$$F_{suc,max} = 0.5 \cdot \rho_w \cdot g \cdot B_g \left[\left(h_{\text{wg}} + h_{\text{diff}} \right)^2 - h_{\text{wg}}^2 \right]$$

In which:

ρ_w Is the water density
g Is the gravitational constant
B_g Is the suction width, which is the same as the gate width
h_{wg} Is the height of the water relative to the bottom of the gate
h_{diff} Is the water level difference due the suction effect, which is the water level difference between the front and th

In this case the water level difference due to the suction effect is assumed to be 10 centimetre at maximum travel speed of the gate. The suction effect during acceleration and deceleration is assumed to be linear proportionate. Thus the suction force over the full trajectory of the gate is:

$$F_{\text{suc}}(t) = \frac{v(t)}{v_{\text{move}}} \cdot F_{suc,max}$$

It gradually increases/decreases in a linear line during the acceleration and deceleration phases, as can be seen in figure C.5.

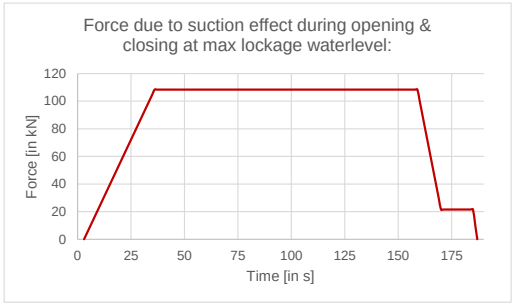

Figure C.5: Hydrodynamic resistance force due to the suction effect

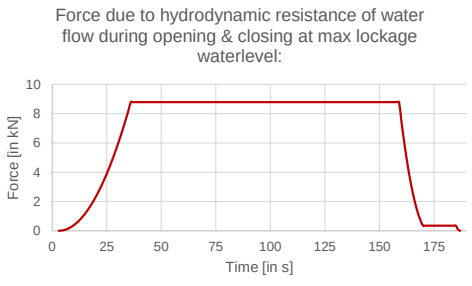

Figure C.6: Hydrodynamic resistance force due to water flow along the gate

C.2.4. Hydrodynamic resistance due to the water flow along the gate

The hydrodynamic drag resistance due to water flow along the gate plating is created by the movement of the gate relative to the water and the resistance of this water as it is in touch with the outer gate plating. It is therefore mainly dependent on the plating in contact with the water and the speed of the gate. The gate plating area is:

$$A_{\text{plate}} = h_{\text{wg}} \cdot L_g \cdot 2$$

Where h_{wg} is the height of the water relative to the bottom of the gate and L_g is the length of the gate. The friction force (F_{plate}) can then be calculated by:

$$F_{\text{plate}} = 0.5 \cdot \rho_w \cdot c_{\text{plate}} \cdot A_{\text{plate}} \cdot v^2$$

In which:

ρ_w Is the water density
c_{plate} Is the friction coefficient of the steel plating
v Is the speed of the gate

In this case the friction coefficient of water sliding against the steel plating is assumed to be 0.15.

The force is dependent on the square of the velocity of the gate. Therefore it is at its max during the constant travel speed of the gate and increases/decreases inverse parabolically during the acceleration and deceleration phase. In case of the highest lockage water level, the hydrodynamic resistance force during opening and closing is shown in figureC.6.

C.2.5. Rolling resistance of the wheels

The rolling resistance force is dependent on the acting vertical loads on both carriages. It can be calculated by summation of the vertical forces acting on both carriages (F_tot) and multiplying them with a rolling friction coefficient (c_f):

$$F_{rr} = F_{tot} \cdot c_f$$

For this calculation the rolling friction is taken as 0.005.

Summation of the vertical forces on both carriages for minimum and maximum lockage water level are shown in tables C.2 and C.3.

Table C.2: Calculation of total force on both carriage at highest lockage water level

Force on front carriage from gate at highest lockage water level	6868	kN
Force on back carriage from gate at highest lockage water level	1839	kN
Force of dead weight of both carriages	235	kN
Total force on both carriages during max. lockage water level	**8942**	kN

Table C.3: Calculation of total force on both carriage at lowest lockage water level

Force on front carriage from gate at lowest lockage water level	7724	kN
Force on back carriage from gate at lowest lockage water level	2411	kN
Force of dead weight of carriages	235	kN
Total force on both carriages during min. lockage water level	**10370**	kN

Thus the rolling resistance during max. lockage water level is:

$$F_{\text{rr},hw} = 8942 \cdot 0.005 = 44.7 \text{ kN}$$

And during min. lockage water level:

$$F_{rr,lw} = 10370 \cdot 0.005 = 51.9 \text{ kN}$$

The rolling resistance is constant during the whole opening and closing trajectory.

This force acts at the height of the connection of the wheel and the rails.

C.2.6. Friction forces due to perpendicular loads

The friction forces occur due to perpendicular loads pushing the gate against the sill/push-off devices. These perpendicular loads can have different causes during different stages of the opening/closing process. Examples are:

- Residual waterhead
- Water density difference
- Translation waves
- Wind waves
- Ship waves

The friction resistance force due to each of these perpendicular loads is calculated by multiplying the friction factor ($\mu_f = 0.005$) of the guidance of the gate with a resultant of one of the perpendicular loads (F_{perp}):

$$F_{f.\text{per}} = \mu_f \cdot F_{\text{perp}}$$

As the friction resistance force is linearly dependent on the friction factor, the friction force due to each of the perpendicular loads can be described separately. Except for the water density difference, all of the perpendicular forces are expressed as a stationary water level difference or hydrostatic load, as shown in figure C.7.

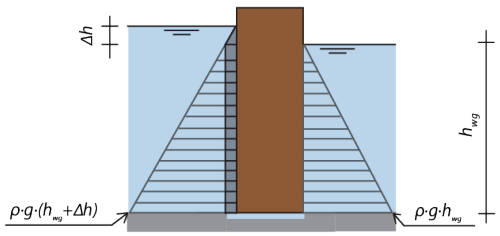

Figure C.7: Perpendicular hydrostatic load during opening/closing due to a water difference over the gate

In some situations (for instance the wind waves), this is a conservative oversimplification. The general formula for the perpendicular load due to a water level difference over the gate ($F_{perp,\Delta h}$) is given by:

$$F_{perp,\Delta h} = l_{g,ext} \cdot \rho_{w,sea} \cdot g \cdot (0.5 \cdot \Delta h^2 + h_{\text{wg}} \cdot \Delta h)$$

In which:

$l_{g,ext}$ is the length of the gate extracted (thus the part of the gate located in the lock chamber)
Δh is the Water level difference due to the perpendicular load
h_{wg} is the height of the water relative to the bottom of the gate

The effective height at which this force applies ($h_{F,perp,\Delta h}$) with respect to the bottom of the gate, is calculated by:

$$h_{F,perp,\Delta h} = \frac{\left(h_{\text{wg}} + \frac{\Delta h}{3}\right) \cdot 0.5 \cdot \Delta h^2 + \frac{h_{\text{wg}}}{2} \cdot h_{\text{wg}} \cdot \Delta h}{0.5 \cdot \Delta h^2 + h_{\text{wg}} \cdot \Delta h}$$

The height relative to N.A.P. can be calculated by subtracting the NAP height of the bottom of the gate (which is -12.82 m NAP).

C.2.7. Friction force due to a residual water-head

The residual waterhead is a result of the optimization between levelling the water between the two reaches and the ship lock passage time. The water inside the lock chamber is for the most part levelled via the culvert system by the water pressure difference between the two reaches. However, as the water level difference levels out, the water pressure also decreases and thus the water flow speed also decreases. Therefore, levelling out of the last few cm's would take relatively long compared to the total lockage time. For most locks, it is therefore decided to already start opening of the gate before the water is completely levelled out in order to save time.

In this case a residual head of 20 cm is assumed. The pressure due to this water level difference is the highest at the start of opening, when the gate is still fully closed. This residual head gradually decreases as the gate opens.

In order to calculate perpendicular load due to the residual head during opening, the progress of the levelling of both water reaches has to be determined. In case of highest lockage water level the water flows inside the lock chamber (from +3.5 m NAP to +3.3 m NAP at the start) and in case of lowest lockage water level the water flows form the lock chamber to the Western Skeldt (from -3.2 m NAP to -3.4 m NAP).

The flow of water from one side to the other is dependent on the water level difference and the net discharge area. During opening, this discharge area becomes larger (as the gate retracts) and the water level difference decreases due to the flow of water in or out of the lock chamber. As a first calculation method, the Bernoulli/Torricelli theorem is used [9]:

$$Q = \mu A \cdot \sqrt{2g\Delta h}$$

In which:

Q is the discharge in m^3/s
μA is the discharge area
g is the gravitational constant
Δh is the water level difference between the two water reaches (waterhead)

Technically, the Bernoulli theorem does not hold, as the flow is not stationary (due to the decreasing water level difference the water flow speed also decreases). However, due to the relatively small opening compared to the size of both water reaches, the local acceleration is insignificant with respect to the advective acceleration and the situation can be regarded as quasi-stationary.

The discharge area is dependent on the water level in the lock chamber and on the opening length, which both change over time. As the water level in the lock chamber increases, the water level difference becomes smaller (thus also changes over time). The general Torricelli formula form above is rewritten for this case:

$$Q(t) = x_{\text{gap}}(t) \cdot h_{\text{lower}}(t) \cdot \sqrt{2g(h_{\text{higher}} - h_{\text{lower}}(t))}$$

In which $x_{\text{gap}}(t)$ is the gap between gate and chamber wall over time, $h_{\text{lower}}(t)$ is the water height at the lower side in the lock chamber at a certain time and h_{higher} is the water height of the Western Skeldt.

The water height inside the basin at a certain moment in time (lock chamber) is calculated by:

$$h_{\text{lower}}(t) = h_{\text{lower}}(0) + (\int_o^t Q(t)dt)/A_{\text{chamber}}$$

As both these formula's are dependent on each other and the gap created by the opening of the gate is not a single linear formula, the calculation of the water height, discharge and gap are all conducted in an incremental way in excel with intervals of 1 second.

Figure C.8 shows the water level change inside the lock chamber at the start of opening at highest lockage water level. The figure clearly shows the increase in water inside the lock chamber. Figure C.9 shows the water level difference during this process. From these graphs it can be concluded that the water level inside the lock chamber is levelled out after circa 50 seconds. In reality this will probably be shorter as the water can also still flow through the culverts.

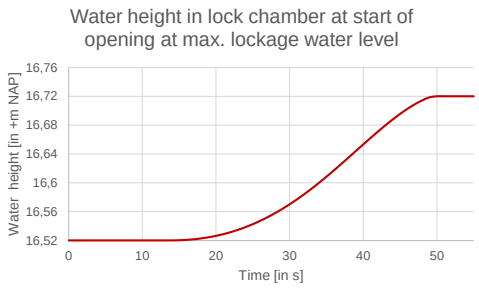

Figure C.8: Water level in the lock chamber (in +m NAP) at the start of opening at maximum lockage water level

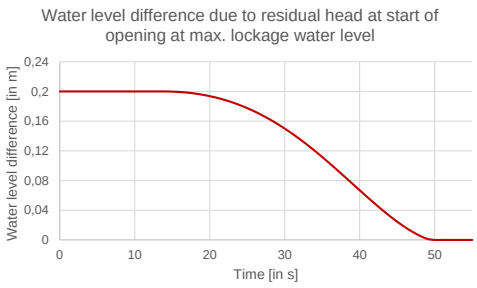

Figure C.9: Water level difference due to residual head at start of opening at maximum lockage water level

The water level difference (Δh) can be used as input for the calculation of the horizontal perpendicular force of the residual head:

$$F_{\text{res}}(t) = l_{g,ext} \cdot \rho_{w,sea} \cdot g \cdot (0.5 \cdot \Delta h(t)^2 + h_{\text{lower}}(t) \cdot \Delta h(t))$$

The friction force due to the residual head ($F_{\text{f.res}}$) is then calculated by:

$$F_{\text{f.res}} = \mu_f \cdot F_{\text{Res}}$$

In case of active guidance ($\mu_f = 0.005$), the friction force over the opening sequence of the gate is shown in figure C.10.

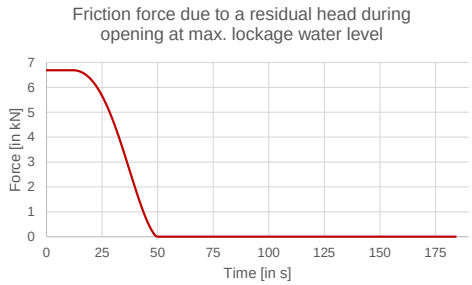

Figure C.10: Friction force due to a residual water level difference during opening at max. lockage water level

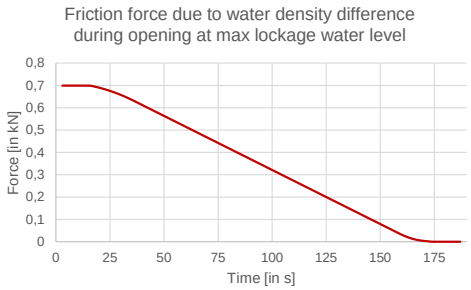

Figure C.11: Friction force due to a water density difference during opening at max. lockage water level

C.2.8. Friction force due to a water density difference

The water density may differ due to the level of salinity. The difference in salinity (and density) can cause a pressure difference over the gate during opening. In case of closing of the gate the water reaches are fully mixed and thus no pressure difference is present. The salt water gradually mixes with the fresh water of the channel during opening of the gate. As this process is relatively slow the pressure difference is assumed to be present over the full opening process of the gate.

The seaside is assumed to be salt water with a water density of 1025 kg/m3 ($\rho_{w,sea}$) and the channel is assumed to be fresh water with a water density of 1000 kg/m3 ($\rho_{w,channel}$). The force due to the water density difference is calculated by:

$$F_{\text{dens}} = l_{g,ext} \cdot (0.5 \cdot \rho_{w,sea} \cdot h_{\max}^2 - 0.5 \cdot \rho_{w,channel} \cdot h_{\max}^2)$$

In which $h_{\max}$is the maximum water level during locking. The friction force due to the water density difference ($F_{\text{f.dens}}$) is then calculated by:

$$F_{\text{f.dens}} = \mu_f \cdot F_{\text{dens}}$$

In case of active guidance ($\mu_f = 0.005$), the friction force due to a water density difference during the opening sequence of the gate is shown in figure C.11.

C.2.9. Friction force due to a translation wave

A translation wave can be caused by sudden water change. For instance the opening of the gate under a water level difference causes a sudden water level change, which causes a translation wave traveling through the lock. The normal filling or emptying of the lock chamber also causes translation waves, but these occur during the full closure of the gate and not during opening or closing. For the case of the Westsluis at Terneuzen the neighbouring locks like the Middelsluis can cause translation waves which reach the Westsluis.

A translation wave (H_{trans}) of 0.1 m is assumed. This wave can occur randomly in time during opening or closing of the gate. It arrives perpendicular on the part of the gate which is extracted. In case of a translation wave, the load will gradually increase as the wave arrives and decrease as the water behind the gate levels out. However, as this wave can occur randomly in time the calculation of the maximum load during the peak of the wave is taken as normative. Therefore the perpendicular load due to a translation wave is calculated by:

$$F_{\text{trans}} = l_{g,ext} \cdot \rho_{w,sea} \cdot g \cdot (0.5 \cdot H_{\text{trans}}^2 + h_{\text{wg}} \cdot H_{\text{trans}})$$

In which:

$l_{g,ext}$ is the length of the gate extracted (thus the part located in the lock chamber)
H_{trans} is the design translation wave height
h_{wg} is the height of the water relative to the bottom of the gate

The friction force due to a translation wave($F_{\text{f.trans}}$) is then calculated by:

$$F_{\text{f.trans}} = \mu_f \cdot F_{\text{trans}}$$

The friction force in case of active guidance ($\mu_f = 0.005$) and during opening of the gate is shown in figure C.12.

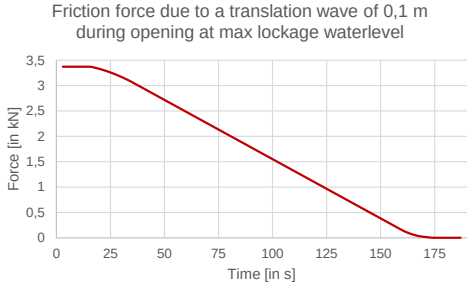

Figure C.12: Friction force due to a translation wave of 0.1 m during opening at max. lockage water level

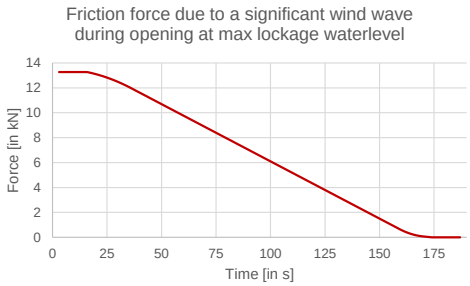

Figure C.13: Friction force due to a significant wind wave during opening at max. lockage water level

C.2.10. Friction force due to wind waves

The normative wind wave during lockage for the Western Skeldt has a significant waveheight (H_s) of 0.39 metre and a waveperiod (T_p) of 4.21 seconds. These parameters do not differ for the 2 loading situations (lowest and highest lockage water level), as the difference in water level has a negligible influence on the wave parameters. The significant waveheight is defined as the average of 1/3 of the highest waves. For now this significant waveheight is also taken as the design waveheight (H_d).

In accordance with the linear wave theory and assuming total reflection against a wall [71], the wave height in front of the wall is double the incoming wave height. For this first calculation the incoming wind wave is considered a stationary load. A quick estimate for the maximum force over the gate can then be calculated by:

$$F_{\text{windwave}} = l_{g,ext} \cdot \rho_{w,sea} \cdot g \cdot (0.5 \cdot H_d^2 + h_{\text{wg}} \cdot H_d)$$

In which:

$l_{g,ext}$ is the length of the gate extracted (thus the part located in the lock chamber)
H_d is the design incoming wave height
h_{wg} is the height of the water relative to the bottom of the gate

As the gate gets retracted inside its chamber, the total length/area of the gate affected by an incoming wind wave decreases and thus the maximum wave forces linearly becomes smaller during opening. The opposite is true for closing. The friction force due to wind waves($F_{\text{f.windwave}}$) is then calculated by:

$$F_{\text{f.windwave}} = \mu_f \cdot F_{\text{windwave}}$$

The friction force in case of active guidance ($\mu_f = 0.005$) and during opening of the gate is shown in figure C.13.

C.2.11. Friction force due to an extreme ship wave

The significant ship waves which reach the Westsluis are caused by passing vessels on the Western Skeldt navigating towards the port of Antwerp. In a measurement and modelling study performed by Svasek, a maximum wave at the Westsluis of +0.25 m and -0.48 m was calculated for the passage of a large container vessel (The MSC London, 399 m long, 54 m wide, 10.3 m draught and 8.8 m/s speed) [1]. The relatively high wave is probably caused by the specific geometrical layout of the harbor in front of the Westsluis.

$$H_{ship,top} = +0.25\ m$$
$$H_{ship,bot} = -0.48\ m$$

Total reflection of the incoming wave is assumed as a conservative starting point. This creates a water level difference of 0.5 m increase or -0.96 m decrease in front of the gate, compared to the still water level. During the top of the ship wave, water level increases and the force of the shipwave is:

$$F_{shipwave,top} = l_{g,ext} \cdot (0.5 \cdot \rho_{w,sea} \cdot g \cdot \left(2{\cdot}H_{ship,top}\right)^2 + h_{\text{wg}} \cdot \rho_{w,sea} \cdot g \cdot 2{\cdot}H_{ship,top})$$

During the bottom of the ship wave, the water level decreases and the perpendicular horizontal force on the gate has the opposite direction:

$$F_{shipwave,bot} = -l_{g,ext} \cdot \rho_{w,sea} \cdot g \cdot (0.5 \cdot \left(2{\cdot}H_{ship,bot}\right)^2 + (h_{\text{wg}} - 2 \cdot H_{ship,bot}) \cdot 2{\cdot} - H_{ship,bot})$$

In which:

$l_{g,ext}$ is the length of the gate extracted (thus the part located in the lock chamber)
H_{ship} is the incoming ship wave
h_{wg} is the height of the water relative to the bottom of the gate

The ship wave can occur at any moment in time and is therefore for this calculation assumed to be always present. The friction force due to a ship wave ($F_{\text{f.ship}}$) is then calculated by:

$$F_{\text{f.ship}} = \mu_f \cdot F_{\text{shipwave}}$$

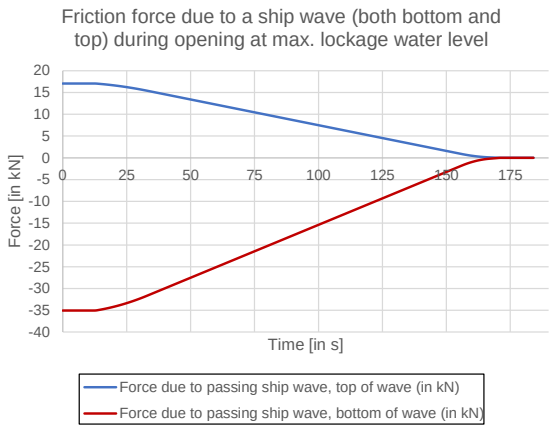

Figure C.14: Friction force due to the top and bottom of a ship wave caused by a vessel passing on the Western Skeldt. During opening at max. lockage water level

The friction force for both the top and bottom of the wave (in case of active guidance ($\mu_f = 0.005$)) and during opening and closing of the gate is shown in figure C.14.

C.3. Loading combinations and results

Some of the loads acting on the gate during opening and closing cannot occur simultaneously or have a really low chance of occur at the same time. For instance, the chance of a translation wave (due to water changes in the Middlelock) in combination with an extreme ship wave is assumed to be really low and can therefore be neglected. All other loads can occur simultaniously. Therefore in this case 2 significant loading combinations are defined:

- LC1: Wind wave in combination with a translation wave
- LC2: Wind wave with an extreme ship (top or bottom) wave

At the highest lockage water level the top wave created by passing vessel is significant, while for the lowest lockage water level the bottom wave is significant, as these wave increase the water difference over the gate structure for the specific situation.

C.3.1. Opening of the gate

Figure C.15 shows all of the calculated resistance forces and the summation in case of loading combination 1 (wind wave with a translation wave) during opening of the gate at the highest lockage water level. Whereas figure C.16 shows all of the force for loading combination 2 (wind wave with extreme top ship wave).

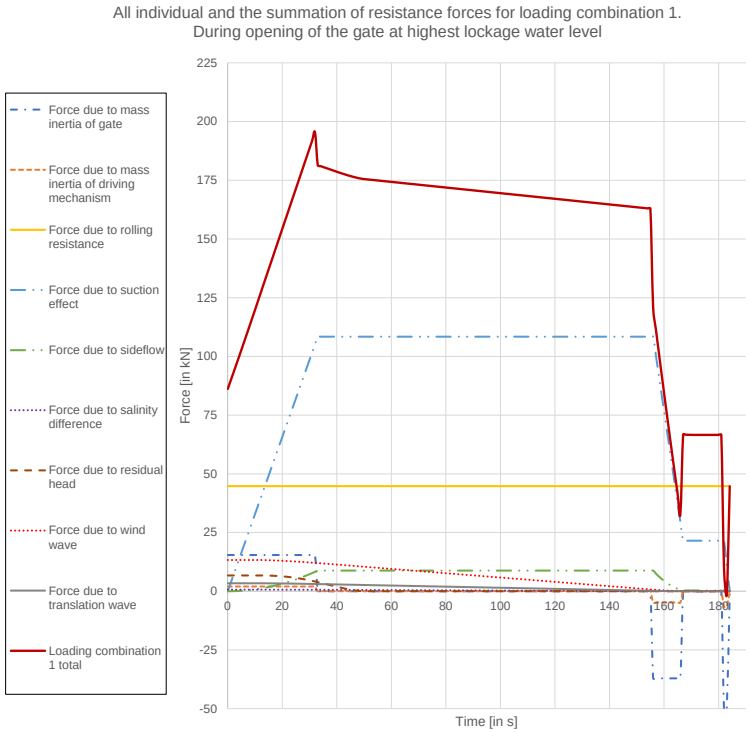

Figure C.15: Individual and summation of resistance forces for loading combination 1: Wind wave and translation wave. During opening of the gate at highest lockage water level.

From both of these figures it can be concluded that the suction effect is the biggest contributor to the resistance force during opening at the highest lockage water level. During opening at the highest lockage water level, the maximum force occurs at the end of the acceleration phase (at t=32) at the start of opening. This is mainly due to the suction effect being at its maximum and the mass inertia force still present (after t=32 this becomes 0). Loading combination 2, where a significant wind wave occurs simultaneously with a wave due to a passing ship is governing for this case. The maximum force is 208 kN.

The graphs and figures in the previous sections all show the forces in case of opening of the gate at the highest lockage water level. All of these calculations have also been performed for the case of opening at the lowest lockage water level. Figure C.17 shows the end result of this calculation in the form of 2 graphs which represent the total summation of all the separate resistance forces for the 2 loading combinations. Figure C.17 shows that loading combination 2 is governing, and has a maximum force of 166 kN (at t=32).

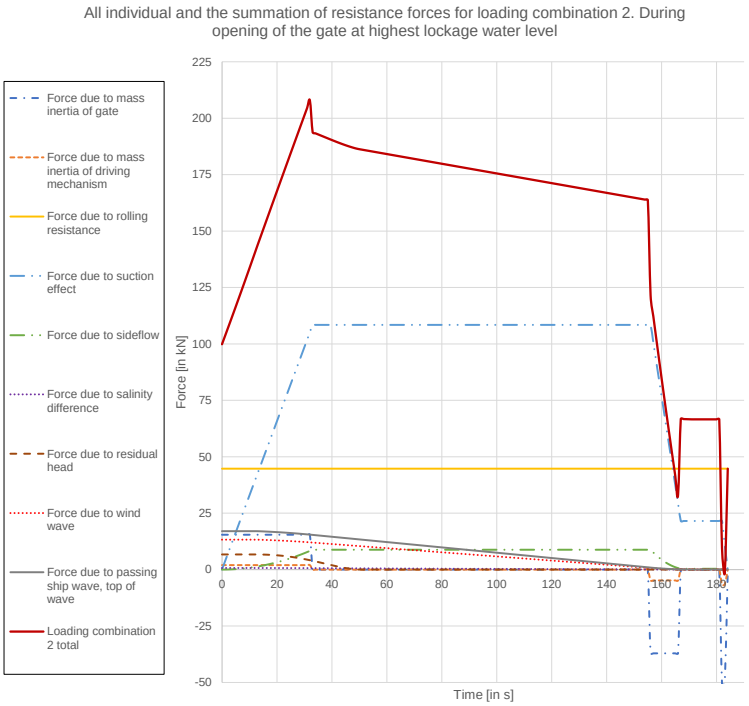

Figure C.16: Individual and summation of resistance forces for loading combination 2: Wind wave and top of passing ship wave. During opening of the gate at highest lockage water level.

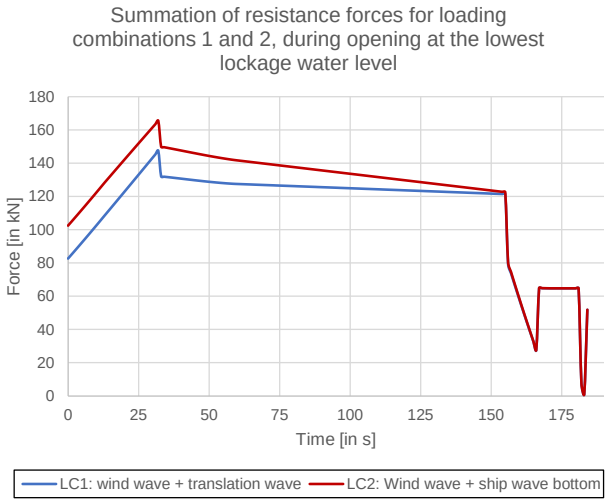

Figure C.17: Total summation of resistance forces for loading combination 1 and 2 in case of opening of the gate at the lowest lockage water level.

C.3.2. Closing of the gate

This subsection elaborates the force during closing of the gate. The calculations are performed in the same manner as previously described, but with a closing gate instead of an opening one and some forces not taken into account. For instance the residual waterhead and the salinity difference are not present during closing of the gate as the water level is completely mixed and leveled out before the gate starts moving. This is also the reason that the highest forces during movement of the gate occur during opening of the gate.

Figure C.18 shows an overview of all the resistance force and the summation of all these resistance forces in case of loading combination 2 (wind wave + extreme ship wave) during closing of the gate at the highest lockage water level. This graph clearly shows the difference compared to the one where the gate is opening. For instance the high peak due to the residual waterhead is gone and the forces due to the horizontal forces increase (instead of decrease) over time due to increased protrusion of the gate as the gate is closing. In this case the maximum force occurs just before the gate starts

decelerating (at t=155), and has a value of 191 kN. During closing at high water loading combination 2 is also governing.

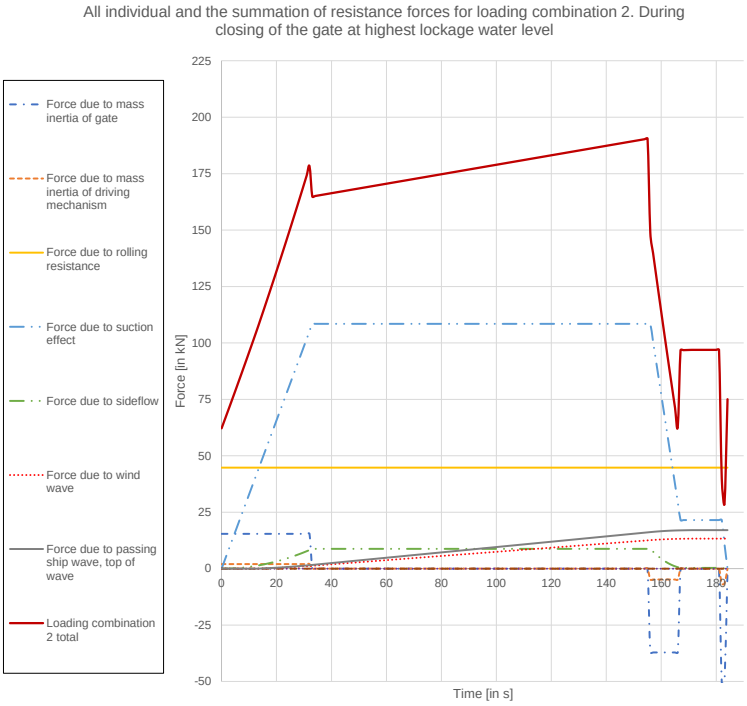

Figure C.18: Individual and summation of resistance forces for loading combination 2: Wind wave and top of passing ship wave. During closing of the gate at highest lockage water level.

Figure C.19 shows the summation of all the resistance forces for the two loading combinations in case of closing of the gate at the lowest lockage water level. In this case loading combination 2 is also governing and has a maximum value of 149 kN (at t=155).

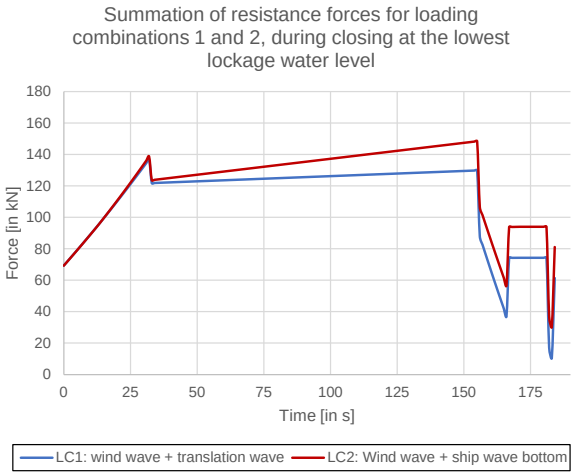

Figure C.19: Total summation of resistance forces for loading combination 1 and 2 in case of closing of the gate at the lowest lockage water level.

C.3.3. conclusions

Table C.4 shows the maximum forces that occur during movement of the gate for the 4 different loading situations.

Table C.4: Overview of the maximum resistance forces during movement of the gate for different situations

	Opening (O)	Closing (C)
Highest lockage water level (HW)	$208\ kN$	$191\ kN$
Lowest lockage water level (LW)	$166\ kN$	$149\ kN$

D

Preliminary cantilever structure design

This appendix shows a preliminary design for the cantilever structure, which is to be attached to the gate to create the cantilever mechanism. The goal is to elaborate the structure itself and to determine an accurate value for the dead weight of the structure. This last goal is especially important, as it influences the load balancing of the total cantilever gate structure.

D.1. Specific assumptions & starting points

The general assumptions and starting points for the design of the gate were elaborated in chapter 5. This section adds some specific assumptions and starting points related to the design of the cantilever structure.

In this calculation, the cantilever structure length is assumed to be 24 meter.

The cantilever structure is assumed to be of a triangle shape, as this is expected to be the most optimal load transfer form towards the two roller carriage supports. The vertical dimension of the cantilever structure is set at 16.8 meter. The width of the structure is the same as the current gate, which is 6.43 meter.

The calculations are done for a static structure, thus the loads due to movement of the gate are not taken into account here.

The cantilever structure is assumed to be constructed of steel, as steel is the most common material applied in these type of structures. The starting point in the design is steel grade S355 (with a yield strength of 355 N/mm^2).

The current gate is a steel structure made of two walls of horizontal and vertical girders with vertical plating, connected to each other by horizontal and diagonal beams. The gate is (besides the closed buoyancy chamber) relatively open in longitudinal direction to allow the flow of water through the gate during opening or closing. The gate part has closed walls in order to seal off in closed position. The cantilever structure does not have to perform this sealing function. It only has to transfer the loads from the gate part towards the supports/carriages. At the same time, it would be beneficial if this structure also has the openness in longitudinal direction to allow the flow of water. Therefore the cantilever structure is designed as an open truss structure.

The trusses are assumed to be made of Circular Hollow Sections (CHS). A CHS has multiple advantages [73]:

- Low drag coefficient as there are no sharp edges. Advantageous for opening/closing of the gate.
- Good protection regarding corrosion due to rounded corners. Especially true for the joints. Increases protection period of coatings.
- High and effective torsional stiffness as the material is uniformly distributed along the polar axis
- The internal void can be used for buoyancy if required.

In this initial design the truss structure is assumed to consist of pin jointed members. This can only be assumed if the joints in the design have sufficient rotation capacity, which is accomplished by limiting the wall slenderness of particular members, especially those in compression. This will be ensured if

the joint parameters are within the range of validity, presented in the book Hollow Sections in Structural Applications [73] and Eurocode 3: EN1993-1-1 [46].

In reality, the centre lines of the trusses often have a certain nodding eccentricity. Also, especially in K joints, an overlap of members may occur. For simplicity reasons, the centre lines of all truss members of a connection are assumed to intersect in one point. Any overlap of members is not taken into account. All welds are assumed to be stronger than the connected brace members to ensure enough deformation capacity.

The cantilever structure is to be connected to the two rolling carriages or “supports” by vertical rods and an intermediate connection system to the truss structure. In reality, the rod connection from the carriages to the truss structure is not located exactly at the joint of the truss structure, but 3 meters inwards. However, to simplify the model, the supports of the cantilever are assumed to be located at the outer joints of the structure.

For now, the detailing and verification of the connections is neglected as it goes into too much detail. The restrictions on dimensions specified by the EN1993-1-1 and the book Hollow Sections in Structural Applications ensure that the rotational capacity of the joints and the members itself should be sufficient.

D.2. Loads and internal forces

Independent of the size and layout of the cantilever structure, the moment force acting from the gate part on the cantilever part can be determined. This moment force consists of the dead weight of the gate structure including maximum silt and shell accretion, minus the smallest possible upwards buoyancy force. The maximum force due to this combination occurs in case of lowest water level as the upward buoyancy force is the smallest then. The cantilever structure is firstly designed for strength, therefore the significant loading combination consist of:

- Dead weight gate part: 946 tonnes ($\gamma_d = 1.25$)
- Max silt weight part: 110.9 tonnes ($\gamma_s = 1.25$
- Most unfavourable buoyancy volume: 655.8 m3, at a water level of -3.5 m N.A.P. ($\gamma_b = 0.9$)

The maximum downward design force of the gate part in the most unfavourable situation is:

$$946 \cdot 9.81 \cdot 1.25 + 110.9 \cdot 9.81 \cdot 1.25 - 655.8 \cdot 9.81 \cdot 1000 \cdot 0.9 = 7170000\ N$$

The analysis of the 3D cantilever truss structure is simplified by taking only one side and modelling it in 2D. This 2D truss is modelled to consist of bars with hinged joints. The load of the gate part is modelled to act on a distance of 22.28 (half the gate length) from the cantilever structure. This is modelled as if it is connected to the 3 side joints by infinitely stiff bars. Due to simplification from 3D structure to 2D structure, the acting load is halved to *3585 kN* per 2D frame.

The significant acting load and the dimensions of the 2D cantilever structure were modelled in the FEM program Matrixframe. This resulted in the internal force distribution shown in figure D.1.

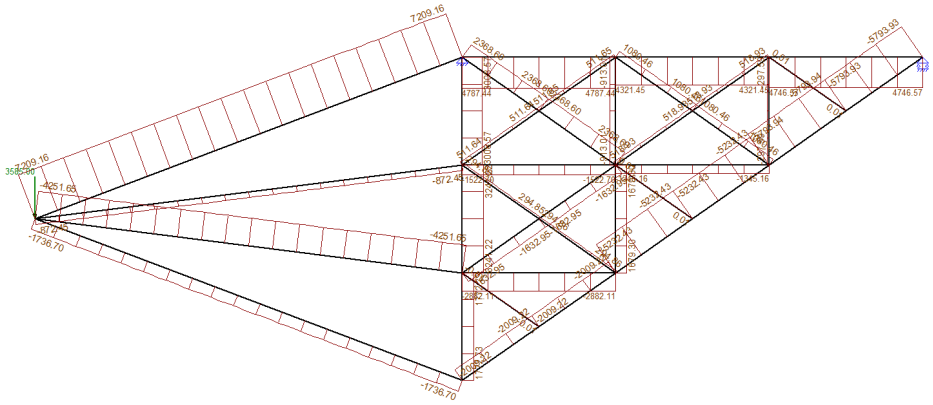

Figure D.1: Internal member forces for the modelled cantilever structure due to the significant static loading situation. Calculated with Matrixframe.

Table D.1: Significant maximum design forces for different member types

Member type	Location	Type of force	Max. design force (in kN)
1	Outer diagonal chord(s)	Compression	-5794
2	Top horizontal chord(s)	Tension	4788
3	Outer vertical chord(s)	Tension	3242
4	Vertical/horizontal brace(s)	Tension	1680
4	Vertical/Horizontal brace(s)	Compression	-2883
5	Diagonal Brace(s)	Tension	2369
5	Diagonal Brace(s)	Compression	-1633

An overview of the significant maximum design forces for specific member types of the structure is shown in table D.1.

D.3. Member design checks

A column/member under compression is susceptible to buckling. The design capacity of the compression member is therefore based on the Euler buckling theory in combination with practical buckling experiments. The true buckle load differs from the theoretical Euler buckling load due to (source: CT2052 Staalconstructies):

- Residual stresses due to heat changes and uneven cooling
- Variation of material properties along the member
- The real stress-strain relation
- Initial deformations
- Size deviations in the cross-section
- Accidental eccentricity of the load

Experiments and investigations on the real buckling behaviour of different type of steel sections have led to the buckling curves incorporated in Eurocode 3. In general, the following unity check should be checked for the buckling stability of members under compression:

$$\frac{N_{\text{Ed}}}{N_{b,Rd}} \leq 1.0$$

In which N_{Ed} is the design load and $N_{b,Rd}$ is the design value of the buckling stability.

The design buckling resistance for cross-sections of type 1, 2 and 3 is defined as:

$$N_{b,Rd} = \frac{\chi \cdot A \cdot f_y}{\gamma_{M1}}$$

In which:

γ_{M1} is the model factor for stability calculations. $\gamma_{M1} = 1.0$
χ is the reduction factor for the specific buckling case, dependant on the appropriate buckling curve and calculated via

$$\chi = \frac{1}{\phi + \sqrt{\phi^2 - \overline{\lambda}^2}} \quad and \ \chi \leq 1.0$$

In which:
$\phi = 0.5\left[1 + \alpha\left(\overline{\lambda} - 0.2\right) + \overline{\lambda}^2\right]$

α is an imperfection factor
$\overline{\lambda}$ is the relative non-dimensional slenderness, given by:

$$\overline{\lambda} = \frac{\lambda}{\lambda_E}$$

Where λ is the slenderness of the member, given by the ratio of the buckling length (l_b) and the radius of gyration (i):

$$\lambda = \frac{l_b}{i}$$

And λ_E is the Euler slenderness:

$$\lambda_E = \pi\sqrt{\frac{E}{f_y}} \; (Euler\ slenderness)$$

The imperfection factor (α) is dependent on the relevant buckling curve:

Table D.2: Imperfection factor related to the appropriate buckling curve

Buckling curve	a0	a	b	c	d
Imperfection factor α	0.13	0.21	0.34	0.49	0.76

The appropriate buckling curve is defined in Eurocode 3. For hot-rolled Hollow sections made of material S355, buckling curve a should be applied. Which has an imperfection factor α of 0.21. For members under compression, the diameter to wall thickness ratio D/T should fall within limits to prevent local buckling. Table 5.2 in Eurocode 3 EN 1993-1-1 specifies the maximum D/T ratios for the different cross-section classes. If the chosen members fall within these limits, it is ensured local buckling will not occur.

D.4. Member dimensions

The structure has been modelled as a truss structure in which all of the lattice members are connected by hinges. To ensure this, the members and their D/T ratios should fall within certain limits called cross-section classes, as stated in Eurocode 3 EN 1993-1-1. For the design of this truss structure cross-section class 1 is aimed for all of the members. This cross-section class ensures enough rotation capacity in the connections by the possibility of formation of a plastic hinge. According to Eurocode 3 EN1993-1-1, for cross-section class 1 in combination with material S355, the diameter to wall thickness ratio D/T should be smaller than 33.

The possible dimensions of Circular Hollow Sections are taken from *NEN-EN 10210-2 Hot finished steel structural hollow sections - Part 2: Tolerances, dimensions and sectional properties* [47].

D.4.1. Outer Diagonal chord

The maximum force in the diagonal chord is -5794 kN, which means that the chord is under compression.

The book Hollow Sections in Structural Applications [73] states that for chords, the effective buckling length can be taken as 0.9 times the system length for in-plane buckling or 0.9 times the length between the supports for out-of-plane buckling. The book also states that the width-to-thickness ratio for a chord in compression is ‘a compromise between joint strength and buckling strength of the member’. This trade-off often leads to relatively stocky sections.

Table D.3 gives multiple options of Circular Hollow Sections that comply to the rules of EN1993-1-1 and have an adequate unity check smaller than 1.

As the joint strength increases with a decreased chord diameter, the most stocky section with an **outside diameter of 273.0 mm and wall thickness of 25 mm** is chosen as it has the thickest wall thickness and thinnest diameter. This is also beneficial for the design of the braces later on as the chord-to-brace thickness ratio should preferably be chosen as high as possible.

D.4.2. Top horizontal chord

The maximum force in the horizontal chord is 4788 kN.

Table D.3: Possible options of CHS members for the outer diagonal chord (compression)

Member length	Buckling length	Outside Diameter	Wall thick-ness	Ratio	Cross-sectional area	Reduction factor	Capacity	Max. chord force	Unity check
l	$l_b = 0.9 \cdot l$	d_0	t_0	d_0/t_0	A_0	χ	$\chi \cdot f_{y0} \cdot A_0$	N_0	-
$[mm]$	$[mm]$	$[mm]$	$[mm]$	-	$[mm^2]$	-	$[kN]$	$[kN]$	-
9765	8789	**273.0**	**25.0**	11	19478	0.91	6326	-5794	*0.92*
9765	8789	323.9	20.0	16	19095	0.94	6397	-5794	*0.91*
9765	8789	355.6	20.0	18	21086	0.95	7147	-5794	*0.81*
9765	8789	406.4	14.2	29	17496	0.97	6018	-5794	*0.96*

Just as for the chord in compression, the diameter- to thickness ratio should be as small as possible for the capacities of the joints. The design capacity of a chord under tension is given by:

$$N_{t,Rd} = A \cdot f_y$$

The design capacity therefore depends on the cross sectional area (A) and the design yield strength (f_y). The following unity check should be validated:

$$\frac{N_{\text{Ed}}}{N_{t,Rd}} \leq 1.0$$

Table D.4 gives multiple options of circular hollow sections that comply to this unity check.

Table D.4: Possible options of CHS members for the top horizontal chord (tension)

Member length	Outside Diameter	Wall thickness	Ratio	Cross-sectional area	Capacity	Max chord force	Unity Check
l	d_0	t_0	d_0/t_0	A_0	$f_{y0} \cdot A_0$	N_0	-
$[mm]$	$[mm]$	$[mm]$	-	$[mm^2]$	$[kN]$	$[kN]$	-
8000	244.5	25	10	17239	6120	4788	0.78
8000	**273**	**25**	11	19478	6915	4788	0.69
8000	323.9	20	16	19095	6779	4788	0.71
8000	355.6	16	22	17070	6060	4788	0.79

For ease of construction and for the design of the braces, the same member is chosen as for the chord under compression: **diameter of 273 mm and a wall thickness of 25 mm**.

D.4.3. Side vertical chord

The maximum force in the vertical chord sections is a tension force of 3242 kN. For the vertical chord under tension the following options are possible which comply to the unity check.

Table D.5: Possible options of CHS members for the side vertical chord (tension)

Member length	Outside Diameter	Wall thickness	Ratio	Cross-sectional area	Capacity	Max chord force	Unity Check
l	d_0	t_0	d_0/t_0	A_0	$f_{y0} \cdot A_0$	N_0	
$[mm]$	$[mm]$	$[mm]$	-	$[mm^2]$	$[kN]$	$[kN]$	-
5600	219.1	20	11	12510	4441	3242	0.73
5600	244.5	20	12	14106	5008	3242	0.65
5600	**273**	**25**	11	19478	6915	3242	0.47

As the maximum force in this vertical chord is smaller than the force in the horizontal chord, this section member could be chosen smaller. However, for the ease of connection to the braces and the validity of the joints, this member is explicitly chosen to be over-dimensioned. For this member also the section with a **diameter of 273 mm and wall thickness of 25 mm** is chosen.

D.4.4. Horizontal and vertical braces

For cost and construction reasons, the aim is to have identical member dimensions for the horizontal and vertical braces. Therefore these two are considered simultaneously.

The maximum compression force in the horizontal braces is -2883 kN. In the vertical braces the maximum compression is -913 kN and the maximum tension force is 1680 kN.

Tables D.6, D.7 and D.8 show the possibilities of member dimensions that comply with the unity checks for the specific loading situations.

Table D.6: Possible options of CHS members for the horizontal braces under compression

Member length	Buckling length	Outside Diameter	Wall thickness	Ratio	Cross-sectional area	Reduction factor	Capacity	Max. chord force	Unity check
l	$l_b = 0.9 \cdot l$	d_0	t_0	d_0/t_0	A_0	χ	$\chi \cdot f_{y0} \cdot A_0$	N_0	-
$[mm]$	$[mm]$	$[mm]$	$[mm]$	-	$[mm^2]$	-	$[kN]$	$[kN]$	-
8000	6000	219.1	16.0	14	10209	0.94	3411	-2883	0.85
8000	6000	**244.5**	**12.5**	20	9111	0.96	3092	-2883	0.93
8000	6000	273.0	12.5	22	10230	0.97	3510	-2883	0.82
8000	6000	323.9	10.0	32	9861	0.98	3433	-2883	0.84

Table D.7: Possible options of CHS members for the vertical braces under compression

Member length	Buckling length	Outside Diameter	Wall thickness	Ratio	Cross-sectional area	Reduction factor	Capacity	Max. chord force	Unity check
l	$l_b = 0.9 \cdot l$	d_0	t_0	d_0/t_0	A_0	χ	$\chi \cdot f_{y0} \cdot A_0$	N_0	-
$[mm]$	$[mm]$	$[mm]$	$[mm]$	-	$[mm^2]$	-	$[kN]$	$[kN]$	-
5600	4200	219.1	16.0	14	10209	0.98	3534	-913	0.26
5600	4200	**244.5**	**12.5**	20	9111	0.98	3183	-913	0.29
5600	4200	273.0	12.5	22	10230	0.99	3598	-913	0.25
5600	4200	323.9	10.0	32	9861	1.00	3500	-913	0.26

Table D.8: Possible options of CHS members for the vertical brace under tension

Member length	Outside Diameter	Wall thickness	Ratio	Cross-sectional area	Capacity	Max chord force	Unity Check
l $[mm]$	d_0 $[mm]$	t_0 $[mm]$	d_0/t_0 -	A_0 $[mm^2]$	$f_{y0} \cdot A_0$ $[kN]$	N_0 $[kN]$	-
5600	219.1	16	14	10209	3624	1680	0.46
5600	**244.5**	**12.5**	20	9111	3234	1680	0.52
5600	273	12.5	22	10230	3632	1680	0.46
5600	323.9	10	32	9861	3501	1680	0.48

As noted before, the joint strength efficiency increases with increasing chord-to-brace thickness t0/ti. The book Hollow Sections in Structural Applications [73] advises an as high as possible ratio, preferably above 2. This means that the thickness of the chord should be more than 2 times thicker than the brace thickness.

As the wall thickness of the chords is 25 mm and assuming a steel grade S355 for both he chord and the brace, the wall thickness of the braces should therefore be 12.5 mm or smaller. For the sake of connecting the braces and chords it would also be best if the outer diameter of the braces is smaller than the diameter of the chords. Thus a diameter of 273 mm or smaller.

Due to the restrictions to the wall thickness and the outside diameter. The tube section with a **diameter of 244.5 mm and a wall thickness of 12.5 mm** is most suitable for the horizontal and vertical braces.

D.4.5. Diagonal braces

In the diagonal braces, the maximum compression force is -1633 kN and the max. tension force is 2369 kN. Both these values are used to determine the most optimal member dimensions. Tables D.9 and D.10 show the possibilities.

Table D.9: Possible options of CHS members for the diagonal braces under compression

Member length	Buckling length	Outside Diameter	Wall thick-ness	Ratio	Cross-sectional area	Reduction factor	Capacity	Max. chord force	Unity check
l	$l_b = 0.9 \cdot l$	d_0	t_0	d_0/t_0	A_0	χ	$\chi \cdot f_{y0} \cdot A_0$	N_0	-
$[mm]$	$[mm]$	$[mm]$	$[mm]$	-	$[mm^2]$	-	$[kN]$	$[kN]$	-
9765	7324	193.7	12.5	15	7116	0.89	2243	-1633	0.73
9765	7324	**244.5**	**10.0**	24	7367	0.93	2442	-1633	0.67
9765	7324	273.0	10.0	27	8262	0.95	2781	-1633	0.59

Table D.10: Possible options of CHS members for the diagonal braces under tension

Member length	Outside Diameter	Wall thickness	Ratio	Cross-sectional area	Capacity	Max chord force	Unity Check
l	d_0	t_0	d_0/t_0	A_0	$f_{y0} \cdot A_0$	N_0	-
$[mm]$	$[mm]$	$[mm]$	-	$[mm^2]$	$[kN]$	$[kN]$	-
9765.24	193.7	12.5	15	7115.7	2526	2369	0.94
9765.24	**244.5**	**10**	24	7367	2615	2369	0.91
9765.24	273	10	27	8262.4	2933	2369	0.81

For the diagonal braces the same restrictions are applicable as for the horizontal and vertical braces. Therefore the wall thickness should not exceed 12.5 mm and the outer diameter preferably should be 273 mm or smaller.

From both tables it becomes apparent that a tube with a **diameter of 244.5 mm and a wall thickness of 10 mm** suffices for the diagonal braces.

D.4.6. Perpendicular braces connecting the modelled 2D frames

In this analysis only the vertical load of the gate part on the cantilever structure is taken into account and used to determine the 2D structure. Horizontal/perpendicular loads are not taken into account and therefore the dimensions of the truss sections in between the 2D truss structures have to be assumed. For now, the connecting horizontal & vertical braces and the diagonal braces are assumed to have the same dimensions as their equivalents in the 2D structure.

Thus the perpendicular horizontal braces in between the 2D frames are made of a CHS with a **diameter of 273 mm and a wall thickness of 12.5 mm**. And the diagonal braces in between the 2D frames are made of a CHS with a **diameter of 273 mm and a wall thickness of 10 mm**.

D.5. Cantilever part mass and buoyancy volume

In this design the member cross-section of all the chords are interchangeable and have the same outer diameter of 273 mm and wall thickness of 25 mm. The horizontal/vertical braces differ in dimensions from the diagonal braces. Therefore, three different tube member dimension types are used in this design. The dimensions and their respective weight per length are shown in table D.11. The specific weight of steel is 7850 kg/m3.

Table D.11: Applied member types and their key numbers

Location	**Tube type**	**Outer diameter**	**Wall thickness**	**Cross sectional area**	**Weight per length**
		$[mm]$	$[mm]$	$[mm^2]$	$[kg/m]$
All chords	1	273	25	19478	152.9
Vertical and horizontal braces	2	244.5	12.5	9111	71.5
Diagonal Braces	3	244.5	10	7367	57.8

With all dimensions of all the truss members known, the total weight of the cantilever structure with a

cantilever length of 24 meter can be determined. A calculation of this weight is shown in table D.12.

Table D.12: Overview of truss members and calculation of the weight of the cantilever structure

Member type	**Member length**	**Nr. of members**	**Total length**	**Tube type**	**Weight per length**	**Total weight**
-	$[m]$	-	$[m]$	-	$[kg/m]$	$[kg]$
Diagonal chords	4.88	12	58.6	1	152.9	8959
Horizontal chords	8.00	6	48.0	1	152.9	7339
Vertical chords	5.60	6	33.6	1	152.9	5137
Horizontal braces in 2D planes	8.00	6	48.0	2	71.5	3433
Vertical braces in 2D planes	5.60	6	33.6	2	71.5	2403
Diagonal braces in 2D planes	4.88	30	146.5	3	57.8	8471
Horizontal braces in between 2D trusses	6.43	16	102.9	2	71.5	7358
Diagonal braces in vertical planes in between 2D trusses	8.53	12	102.3	3	57.8	5917
Diagonal braces in horizontal planes in between 2D trusses	10.26	12	123.2	3	57.8	7123
		TOTAL:	**696.6**		**TOTAL:**	**56140**

Thus the total weight of the triangle shaped cantilever truss structure with a horizontal dimension of 24 m, a vertical dimension of 16.8 m and a width of 6.43 m has a dead weight of 56140 kg, which is 56.14 tonnes. The corresponding Circular Hollow Sections tube dimensions are shown in the tables shown in this appendix.

Table D.13 shows the calculation of the total mass and the mass-distance of each element. The x-distance is calculated from the rightmost side of the cantilever structure. The centre of gravity of the cantilever structure in x-direction is then determined by dividing this mass-distance by the mass of the structure:

$$\frac{880673}{56140} = 15.69m$$

This is relatively close to the centre of gravity of a triangle with a length of 24 meter (which is 16 m).

Table D.14 shows the calculation of the buoyancy volume of the cantilever structure at three significant water levels. For the maximum lockage waterlevel at +3.5 m NAP, the buyoancy volume of the cantilever structure is 26.5 m^3.

Table D.13: Calculation of mass and mass-distance of the cantilever structure in case of a cantilever length of 24 m

Y-Location of element	Quantity	Top height	Bottom height	Length	Weight per length	Element weight	X-location	Mass · Distance
	$Nr.$	$[m\ N.A.P.]$	$[m\ N.A.P.]$	$[m]$	$[kg/m]$	$[kg]$	$[m]$	$[kgm]$
Diagonal chords								
5/6 till top	2	4	1.2	4.9	152.9	1493	22	32849
2/3 till 5/6	2	1.2	-1.6	4.9	152.9	1493	18	26876
1/2 till 2/3	2	-1.6	-4.4	4.9	152.9	1493	14	20904
1/3 till 1/2	2	-4.4	-7.2	4.9	152.9	1493	10	14931
1/6 till 1/3	2	-7.2	-10	4.9	152.9	1493	6	8959
bottom till 1/6	2	-10	-12.8	4.9	152.9	1493	2	2986
Horizontal chords								
Top	6	4	4	8.0	152.9	7339	12	88071
Vertical chords								
2/3 till top	2	4	-1.6	5.6	152.9	1712	24	41100
1/3 till 2/3	2	-1.6	-7.2	5.6	152.9	1712	24	41100
bottom till 1/3	2	-7.2	-12.8	5.6	152.9	1712	24	41100
Horizontal braces in 2D planes								
At 2/3	4	-1.6	-1.6	8.0	71.5	2289	16	36617
At 1/3	2	-7.2	-7.2	8.0	71.5	1144	20	22886
Vertical braces in 2D planes								
From 2/3 till top	4	4	-1.6	5.6	71.5	1602	16	25632
From 1/3 till 2/3	2	-1.6	-7.2	5.6	71.5	801	8	6408
Diagonal braces in 2D planes								
5/6 till top	10	4	1.2	4.9	57.8	2824	14	39532
2/3 till 5/6	8	1.2	-1.6	4.9	57.8	2259	16	36143
1/2 till 2/3	6	-1.6	-4.4	4.9	57.8	1694	18	30496
1/3 till 1/2	4	-4.4	-7.2	4.9	57.8	1129	20	22589
1/6 till 1/3	2	-7.2	-10	4.9	57.8	565	22	12424
Horizontal braces in between 2D trusses								
Top braces	4	4	4	6.4	71.5	1839	12	22073
5/6 braces	3	1.2	1.2	6.4	71.5	1380	12	16555
2/3 braces	3	-1.6	-1.6	6.4	71.5	1380	16	22073
3/6 braces	2	-4.4	-4.4	6.4	71.5	920	16	14716
1/3 braces	2	-7.2	-7.2	6.4	71.5	920	20	18395
1/6 brace	1	-10	-10	6.4	71.5	460	20	9197
Lowest brace	1	-12.8	-12.8	6.4	71.5	460	24	11037
Diagonal braces in vertical planes in between 2D Trusses								
2/3 till top	6	4	-1.6	8.5	57.8	2959	16	47339
1/3 till 2/3	4	-1.6	-7.2	8.5	57.8	1972	20	39449
bottom till 1/3	2	-7.2	-12.8	8.5	57.8	986	24	23669
Diagonal braces in horizontal planes in between 2D Trusses								
Top	6	4	4	10.3	57.8	3561	12	42737
At 2/3	4	-1.6	-1.6	10.3	57.8	2374	16	37988
At 1/3	2	-7.2	-7.2	10.3	57.8	1187	20	23743
					Total:	**56140**	**Total:**	**880573**

Table D.14: Calculation of cantilever structure buoyancy volume for different water levels in case of a cantilever length of 24 m

Element	Volume under water at +3.5 m NAP $[m^3]$	Volume under water at 0.02 m NAP $[m^3]$	Volume under water at -3.4 m NAP $[m^3]$
Diagonal chords			
5/6 till top	0.5	0.0	0.0
2/3 till 5/6	0.6	0.3	0.0
1/2 till 2/3	0.6	0.6	0.2
1/3 till 1/2	0.6	0.6	0.6
1/6 till 1/3	0.6	0.6	0.6
bottom till 1/6	0.6	0.6	0.6
Horizontal chords			
Top	0.0	0.0	0.0
Vertical chords			
2/3 till top	0.6	0.2	0.0
1/3 till 2/3	0.7	0.7	0.4
bottom till 1/3	0.7	0.7	0.7
Horizontal braces in 2D planes			
At 2/3	1.5	1.5	0.0
At 1/3	0.8	0.8	0.8
Vertical braces in 2D planes			
From 2/3 till top	1.0	0.3	0.0
From 1/3 till 2/3	0.5	0.5	0.4
Diagonal braces in 2D planes			
5/6 till top	1.9	0.0	0.0
2/3 till 5/6	1.8	1.1	0.0
1/2 till 2/3	1.4	1.4	0.5
1/3 till 1/2	0.9	0.9	0.9
1/6 till 1/3	0.5	0.5	0.5
Horizontal braces in between 2D trusses			
Top braces	0.0	0.0	0.0
5/6 braces	0.9	0.0	0.0
2/3 braces	0.9	0.9	0.0
3/6 braces	0.6	0.6	0.6
1/3 braces	0.6	0.6	0.6
1/6 brace	0.3	0.3	0.3
Lowest brace	0.3	0.3	0.3
Diagonal braces in vertical planes in between 2D Trusses			
2/3 till top	2.2	0.7	0.0
1/3 till 2/3	1.6	1.6	1.1
bottom till 1/3	0.8	0.8	0.8
Diagonal braces in horizontal planes in between 2D Trusses			
Top	0.0	0.0	0.0
At 2/3	1.9	1.9	0.0
At 1/3	1.0	1.0	1.0
TOTAL	**26.5**	**19.7**	**10.7**

E

Maximum design force on the wheel-rail interface

The aim of this appendix is to define the maximum allowable resistance design force on the wheels and rails of the carriage of the cantilever rolling gate. Four different calculation methods are evaluated and used to calculate this design force between a rail and wheel contact, making a distinction between the strength and fatigue load. The results of each of these calculation methods are evaluated and an appropriate maximum load is defined based on these results. The data of the wheels and rails of the current gate of the Westernlock Terneuzen are used as input for the calculations.

With respect to the calculation of maximum allowable loads on wheel/rail concacts, 4 different calculation methods are presented. The first one is the general Hertz theory from 1882. The other 3 calculations from the three different norms are (probably) all based on this Hertz theory. An overview of the input parameter dependencies for the different calculation methods is shown in table E.1. After introduction of the Hertz theory, the calculations according to the norms NEN 6786 (VOBB), DIN19704:1998 and EN13001 are covered.

Table E.1: Input parameter dependencies for the different calculation methods regarding wheel/rail loads

Parameter	EN13001	NEN 6786	DIN 19704	Hertz
WHEEL				
Wheel diameter	x	x	x	x
Wheel crown radius	x		x	x
Wheel width	x			x
Nr of rolling contacts wheel	x	x	x	
Design tension strength wheel material		x		
Design yield strength wheel material	x		x	
0.2% offset yield strength wheel material				x
Modulus of elasticity wheel material	x		x	x
Poisson's ratio wheel material	x		x	x
Brinell hardnes wheel	x		x	
Depth of top brinell hardness layer	x			
RAIL				
Rail width	x	x		x
Rail corner radius	x	x		x
Rail crown radius	x			x
Nr. of rolling contacts rail	x	x	x	
Design tension strength rail material		x		
Design yield strength rail material	x		x	
0.2% offset yield strength rail material				x
Modulus of elasticity rail material	x		x	x
Poisson's ratio rail material	x		x	x
Brinell hardness rail	x		x	
Depth of top brinell hardness layer	x			
MISC				
Tolerance class	x			
Type of mounting of rail and wheel	x			
Average displacement of related gate motion	x			
Total numer of working cycles during design life	x			
Design nr. of wheel sets used during design life	x			
Skewing angle of the gate	x			
Type of environment	x			

E.1. Input

The wheels and rails of the current Westsluis of Terneuzen are used for the calculations. These wheels and rails have been (re)placed in recent years and are of the highest standard for rolling gates.

The wheels have a diameter of 1200 mm and a width of 150 mm. It has no crown radius and a corner radius of 5 mm. The wheels are of type 42CrMo5-04 made of forging steel and surface hardened (constructed by MG-Valdunes. source: http://www.valdunes.com/index.php/en/products/crane-wheels/mg-valdunes-long-lifetime-steel.html). This material has a yield strength of 550 MPa and Brinell Hardness of 400 MPa up to 35 mm deep [33]. The steel has a modulus of elasticity of 210000 MPa and a Poisson ratio of 0.3.

The rail is a blockrail of type 110 CrV and has a width of 150 mm, no crown and no corner radius. The yield strength of the rail is 1080 MPa and the Brinell hardness is 320 MPa. The steel has a modulus of elasticity of 210000 MPa and a Poisson ratio of 0.3.

An overview of the wheel and rail specifrics in tableform can be found in chapter 5, section 5.3.

A gate lifetime of 50 years is assumed. The average number of gate cycles per year is 9500, which gives a total of 475000 gate cycles for the lifetime of the gate. The assumptions is made that the wheels of the gate are replaced every 25 years, thus twice in the lifetime of the gate. Every cycle the gate displaces 88 meters. (44 m when closing and 44 m during opening). The cantilevergate has two carriages that either can have 4 or 8 wheels per carriage. Both options are elaborated. At the end of the appendix the design resistance forces for both a carriages with 4 or 8 wheels are given.

E.2. Hertz Theory

Most basic contact phenomena are in principal based on the theory proposed by Heinrich Hertz in 1882: 'On the contact of elastic solids' [24]. He performed experiments on optic interference between glass lenses and he was looking into the question if elastic deformation of lenses under action of a force have an influence on the pattern of interference fringes [29]. The theory of Hertz is unfortunately restricted to frictionless surfaces and perfectly elastic solids. The simplification was made that each body can be regarded as an elastic half space loaded over a small elliptical region of its plane surface. This can only be achieved if the dimensions of the contact area are small compared with the dimensions of the bodies and the radii of curvature of both surfaces. The assumptions [29] can be summarized as:

- The surfaces are continuous and non-conforming: $a \ll R'$;
- The strains are small: $a \ll R'$;
- Each solid can be considered as an elastic half-space: $a \ll R'_{x,y}$, $a \ll$ L;
- The surfaces are frictionless.

In which a is the dimension of the contact area, R is the relative radius of curvature, $R'_{x,y}$ is the significant radii of each body and L is the dimension of the bodies both laterally and in depth.

The relative radius of curvature R' (related to the radii of the individual components) is given by:

$$\frac{1}{R'} = \frac{1}{R'_x} + \frac{1}{R'_y};$$

$$\frac{1}{R'_x} = \frac{1}{r_{1,x}} + \frac{1}{r_{2,x}};$$

$$\frac{1}{R'_y} = \frac{1}{r_{1,y}} + \frac{1}{r_{2,y}};$$

Hertz defined theories for a point contact (sphere in contact with a plane/sphere) creating a circle or elliptical contact area. However, in the case for the Westsluis in Terneuzen, the wheels and rails create a line contact (of length l) due to the wheel and rail both not having a crown radius ($r_{1y} = r_{2y} = \infty$). Therefore in this case the formula for the relative radius of curvature reduces to:

$$\frac{1}{R'} = \frac{1}{r_{1x}} + \frac{1}{r_{2x}} = \frac{1}{R_1} + \frac{1}{R_2}$$

In which $r_{1x} = R_1$ and $r_{2x} = R_2$.

As the pressure is equal on both bodies the effective modulus of elasticity E' is defined by:

$$\frac{1}{E'} = \frac{1 - v^2}{2 \cdot E_1} + \frac{1 - v^2}{2 \cdot E_2}$$

Within the contact area the Hertzian pressure is half-elliptic [11] & [10]:

$$p(x) = p_{\max}\left(1 - \frac{x^2}{b^2}\right)^{\frac{1}{2}}, \quad p_{\max} = \frac{4}{\pi}p_m$$

The mean contact pressure of a line contact is given by:

$$p_m = \frac{F}{2bl} = \frac{1}{4}\left(\frac{\pi}{2}\right)^{\frac{1}{2}}\left(\frac{F}{l}\right)^{\frac{1}{2}}\left(\frac{E'}{R'}\right)^{\frac{1}{2}}$$

For a line contact the maximum shear stress ($\tau_{\max} = 0.304\ p_{\max} = 0.387\ p_{\text{m.c}}$) is located at 0.786 *b* beneath the contact surface. Making use of Tresca's shear criterion the critical value of the mean contact pressure ($p_{\text{m.c}}$) is given by:

$$p_{\text{m.c}} = \frac{0.5}{0.387}R_{p0.2}$$

Rewriting the formula for the mean contact pressure and substituting the critical value of the mean contact pressure, the maximum Hertzian contact load is given by:

$$F_c = l \cdot \frac{32}{\pi} \cdot \frac{p_{\text{m.c}}^2}{E'} \cdot R'$$

In case friction or traction is present the formulae of Hertz do not hold as a tangential stress component is added. The previously stated formula's only hold true for a static normal load or in case of free rolling. The stress distributions in case of rolling with traction can be calculated by superimposing normal and tangential stress components.

If no friction or traction is assumed for the contact, and the wheel is defined as the 1st body and the rail as the 2nd body, the maximum Hertzian contact load is:

$$R' = \frac{1}{\frac{1}{R_1} + \frac{1}{R_2}} = \frac{1}{\frac{1}{600} + \frac{1}{\infty}} = 600\ mm$$

$$E' = \frac{1}{\frac{1-v^2}{2 \cdot E_1} + \frac{1-v^2}{2 \cdot E_2}} = \frac{1}{\frac{1-0.3^2}{2 \cdot 210000} + \frac{1-0.3^2}{2 \cdot 210000}} = 230769\ \frac{N}{mm^2}$$

$$p_{\text{m.c}} = \frac{0.5}{0.387} \cdot R_{p0.2} = \frac{0.5}{0.387} \cdot 550 = 710.6\ \frac{N}{mm^2}$$

$$F_c = l \cdot \frac{32}{\pi} \cdot \frac{p_{\text{m.c}}^2}{E'} \cdot R' = (150 - 2 \cdot 5) \cdot \frac{32}{\pi} \cdot \frac{710.6^2}{230769} \cdot 600 = \mathbf{1872\ kN}$$

E.3. NEN 6786 (VOBB)

The Dutch norm NEN 6786-1:2017 [40] has the titel ‘Rules for the design of movable parts of civil structures’. Part 1 is related to the design of movable bridges and has been released in 2017. It states some pretty straightforward rules regarding wheel/rail contacts. The resistance part of the check is only based on the ultimate tensile strength of the weakest part of the contact.

NEN 6786-1 states the contact stress between wheel and rail can be calculated as:

$$\sigma_{ver;O;Ed/V} = \frac{F_{ver;O;Ed/V}}{D \cdot (b - 2 \cdot r)}$$

In which: $\sigma_{ver;O;Ed/V}$ is the value of the surface pressure due to the loading situation ‘transmission overload’ (O) resp. ‘transmission fatigue’ (V);

$F_{ver;O;Ed/V}$ is the value of the vertical force due to the loading situation ‘transmission overload’ (O) resp. ‘transmission fatigue’ (V);
D is the diameter of the wheel; *b* is the width of the rail according to figure E.1; *r* is the radius of the roundings of the rail according to figure E.1.

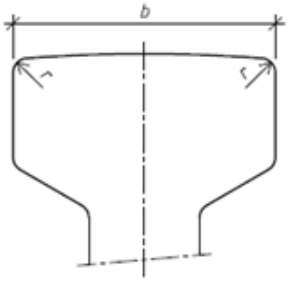

Figure E.1: Rail dimensions [40]

Minimale treksterkte f_u in N/mm²					
Rail	590 ≤ f_u < 690				f_u ≥ 690
Velg van het loopwiel	330 ≤ f_u < 410	410 ≤ f_u < 490	490 ≤ f_u < 590	f_u ≥ 590	f_u ≥ 740
Aantal over-rollingen (× 10^6)					
≤ 2	4,1	5,3	6,6	8,2	10,2
> 2 – 4	3,6	4,6	5,7	7,1	8,9
> 4 - 7,5	3,1	3,9	4,9	6,1	7,6
> 2,5 - 15,0	2,7	3,4	4,3	5,3	6,6
> 15 - 30,0	2,1	3,0	3,7	4,6	5,8
OPMERKING	De opgegeven waarden gelden voor een railprofiel volgens figuur 15.				

Figure E.2: Allowable fatigue contact strength according to NEN6786-1 [40]

The following static strength check should hold:

$$\frac{\sigma_{ver;O;Ed}}{\left(\frac{f_u}{f_{ver;O}}\right)^2} \leq 1$$

In which: f_u is de smallest value of the tension strenght of the material of the wheel or rail; $f_{ver;O}$ is $138\ N^{\frac{1}{2}}/mm$.

And the following fatigue check should hold:

$$\frac{\sigma_{ver,V}}{f_{ver,V}} \leq 1$$

In which:

$f_{ver,V}$ is the allowable contact strength according to figure E.2.

By rewriting the above formula’s, the maximum contact load according to the static calculation method is then given by:

$$F_{ver;O;Ed} \leq \left(\frac{f_u}{f_{ver;O}}\right)^2 \cdot D \cdot (b - 2 \cdot r) \rightarrow F_{max,O;Ed} = \left(\frac{800}{138}\right)^2 \cdot 1200 \cdot (150 - 2 \cdot 0) = \mathbf{6049kN}$$

The maximum strength design contact load is therefore 6049 kN and both the same for a four an eight wheel carriage.

For the maximum contact load with respect to fatigue figure E.2 has to be applied. As the ultimate tensile strength of the wheel and the rail are respectively 800 N/mm2 and 1080 N/mm2, the rightmost

column should be used. In case of a four wheel carriage, the wheel has the most normative rolling contacts; $5.55 \cdot 10^6$. Therefore, the middle row should be applied. Which gives a value for $f_{ver,V,4w}$ of 7.6.

$$F_{ver;O;V,4w} \leq f_{ver,V} \cdot D \cdot (b - 2 \cdot r) \rightarrow F_{max,O;V} = 7.6 \cdot 1200 \cdot (150 - 2 \cdot 0) = \mathbf{1368\ kN}$$

In case of an eight wheel carraige, the rail has the most normative rolling contacts; $7.60 \cdot 10^6$. Which is just above the treshold of the 4th row and thus the value of 6.6 for $f_{ver,V,8w}$ should be applied:

$$F_{ver;O;V,8w} \leq= 6.6 \cdot 1200 \cdot (150 - 2 \cdot 0) = \mathbf{1188\ kN}$$

Thus, according to NEN 6786, the maximum allowable fatigue contact load for a four wheel carriage is **1368 kN** and for an eight wheel carriage is **1188 kN**.

E.4. DIN19704

DIN19704:2014 [48] is a German norm related to Hydraulic Steel Structures which states a proof for static- and fatigue strength for a rail to wheel contact. The calculation method is based on the Hertz theory.

In case of cylindrical rolling ($\frac{R_b}{R} = \infty$) with contact length L, the maximum Hertz contact stress is:

$$\max p_d = \sqrt{\frac{1}{2\pi(1-\nu^2)}} \cdot \sqrt{\frac{F_d \cdot E}{L \cdot R}}$$

In which R is the wheel radius; R_b is the crown radius of the wheel; L is the contact length; E is the modulus of elasticity of the roller or rail material; ν is the Poisson ratio of the roller or rail material and F_d is the design value of the rolling force (determined as a result of the most unfavourable loading combination including partial safety factors and combination coefficients according to DIN19704).

The design value of the maximum Hertzian pressure ($\max p_d$) shall not exceed the value of the design load capacity $p_{R,d}$ ($\max p_d \leq p_{R,d}$). Substituting the design load capacity and rewriting the formula for the maximum Hertz contact stress, the maximum static design load force can be determined:

$$F_{d,max} = 2\pi(1-\nu^2) \cdot \left(p_{R,d}\right)^2 \cdot L \cdot \frac{R}{E}$$

The value of the static design load capacity ($p_{R,d,s}$) depends on the characteristic values of the yield strength ($f_{y,c}$) and on the coefficient $C1$ to be taken from Table 9 from DIN19704-1:2014:

$$p_{R,d,s} = C_1 \cdot f_{y,c}$$

In case of cylindrical rolling, this coefficient $C1$ is 3.59. The modulus of elasticity and Poisson's ratio are both the same for both wheel and rail. The maximum design load force can therefore be calculated by applying the smallest yield strength value of both materials. The maximum static load force can then be calculated by:

$$F_{d,max,stat} = 2\pi(1-0.3^2) \cdot (3.59 \cdot 550)^2 \cdot (150 - 2 \cdot 5) \cdot \frac{600}{210000} = 8916523\ N$$

The maximum static load force therefore is **8917 kN**.

The value of the fatique design load capacity ($p_{R,d,f}$) depends on the fatigue rolling resistance (p_D) and the number of stress cycles (N):

$$p_{R,d,f} = p_D \cdot \sqrt[5]{\frac{10^6}{N}} \qquad for\ N < 10^6$$

$$p_{R,d,f} = p_D \qquad for\ N \geq 10^6$$

The design value of the fatigue rolling resistance depends on the characteristic value of the ultimate tensile strength ($f_{u,c}$), the type of material (steel or stainless steel) and on the coefficient $C1$ to be taken from Table 9 from DIN19704-1:2014. The following applies for components made out of steel:

$$p_D = 0.333 \cdot C_1 \cdot f_{u,c}$$

And for components made out of stainless steel:

$$p_D = 0.296 \cdot C_1 \cdot f_{u,c}$$

In case of cylindrical rolling ($\frac{R_b}{R} = \infty$), $C1$ is 3.59. The maximum fatigue design load has to be calculated separately for both wheel and rail as they have a different number of stress cycles.

In this case, both wheel and rail have more than 10^6 number of stress cycles and are both made of steel. Thus the design value for the fatigue rolling resistance of steel components can directly be used. As the modulus of elasticity and Poisson's ratio are both the same for both wheel and rail, the maximum fatigue design load force can be calculated by applying the smallest ultimate tensile strength value of both materials. The maximum static load force can then be calculated by:

$$F_{d,max,fat} = 2\pi(1 - 0.3^2) \cdot (0.333\ \cdot 3.59 \cdot 800)^2 \cdot (150 - 2 \cdot 5) \cdot \frac{600}{210000} = 2091889\ N$$

Therefore the maximum fatigue design load capacity is 2092 kN.

In this calculation, four or eight wheels on a carriage makes no difference and the capacities for both options are identical.

E.5. EN13001

EN13001 - Crane safety, is a European norm which provides for the mechanical design and theoretical verification of cranes' [41]. Wheel/rail contacts are also applied in the construction of cranes and therefore the norm states some guidelines regarding the 'Limit states and proof of competence of wheel/rail contacts' in part 3.3.

The wheel/rail combination shall be checked for static strength and fatigue strength. For the static strength the material properties of the weaker part must be applied, while for the fatigue strength both parts (wheel and rail) must be checked. Both checks are based on the Hertz pressure on the contact surface and the shear stress below the surface [43].

As in line with the Hertz theory, principally two contact cases generally occur in designs of rails and crane wheels: a line contact and a point contact. Figure E.3 shows the cases in which a line or a point contact should be considered. This depends on the crown radius (r_k) of the rail. As for most cranes the crown radius of the rail is relatively large with respect to the wheel or the rail width. Therefore point contacts will be rapidly transformed into line contacts. Cases in which the crown radius (r_k) is smaller than 5 m fall outside the method given in this standard. In this case the crown radii (r_k) of both wheel and rail are infinite and therefore it is a line contact.

Hardness depth vs. maximum shear
The norm states that the hardness should extend deep enough into the material to cover the depth of maximum shear (preferably twice this depth).

The depth of maximum shear for line contact cases shall be calculated as:

$$z_{\text{ml}} = 0.50 \cdot \sqrt{F_{Sd0,s} \cdot \frac{\pi \cdot D_w \cdot (1 - \nu^2)}{b \cdot E_m}}$$

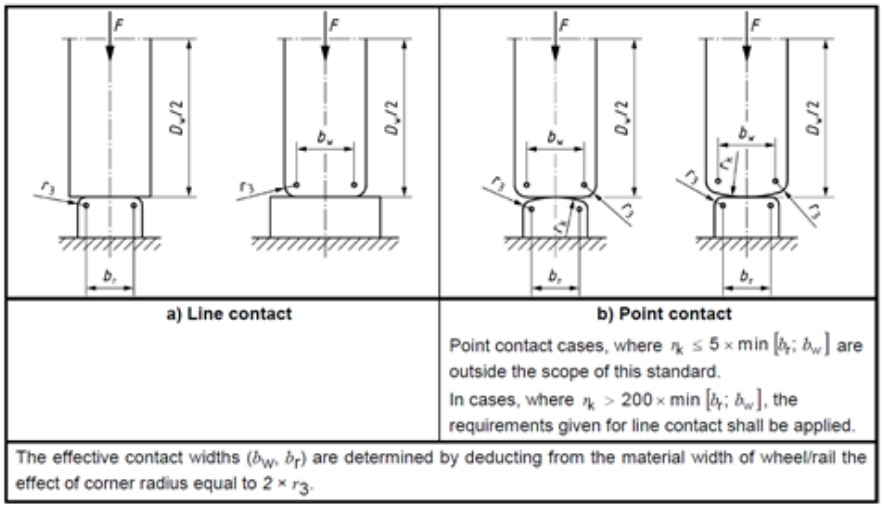

Figure E.3: Line and point contact cases according to EN13001 [43]

$$z_{ml} = 0.68 \cdot \sqrt[3]{\frac{F_{Sd0,s}}{E_m} \cdot \frac{1-v^2}{\left(\frac{2}{D_w} + \frac{1}{r_k}\right)}}$$

In which v is the Poisson ratio, D_w is the wheel diameter, b is the effective load-bearing width taken as $b = min\,[b_r; b_w]$, $F_{Sd0,s}$ is the maximum, non-factored design contact force within the Load Combinations A to C in accordance with EN 13001-2 and E_m is the equivalent modulus of elasticity:

$$E_m = \frac{2 \cdot E_w \cdot E_r}{E_w + E_r}$$

In which E_w is the modulus of elasticity of the wheel material and E_r is the modulus of elasticity of the rail material.

The depth of the hardness is unknown. Therefore this check cannot be done. It is assumed the mentioned hardness at least reaches the maximum shear depth.

E.5.1. Static contact force

For the proof of static strength it shall be proven that (for all relevant load combinations of EN 13001-2 [42]): $F_{Sd,s} \leq F_{Rd,s}$

In which:

$F_{Sd,s}$ is the design contact force
$F_{Rd,s}$ is the limit design contact force

The static limit design contact force ($F_{Rd,s}$) is the force which causes a permanent radial deformation of 0.02 % of the wheel radius and depends on the material properties (Modulus of elasticity, yield stress and hardness of wheel and rail), the geometry (radii) and stiffness and edge effects. It should be calculated separately for both wheel and rail (the smallest value is governing) using one of the two subsequent formula's:

For non-surface hardened materials (e.g. cast, forged, rolled or quenched and tempered);

$$F_{Rd,s} = \frac{(7 \cdot HB)^2}{\gamma_m} \cdot \frac{\pi \cdot D_w \cdot b \cdot \left(1-v^2\right)}{E_m} \cdot f_1 \cdot f_2$$

For surface hardened materials (e.g. flame or induction hardened) provided that the surface hardness is equal or greater than $HB = 0.6 \cdot f_y$ and the hardness extends deep enough to cover the max. shear;

$$F_{Rd,s} = \frac{\left(4.2 \cdot f_y\right)^2}{\gamma_m} \cdot \frac{\pi \cdot D_w \cdot b \cdot \left(1 - v^2\right)}{E_m} \cdot f_1 \cdot f_2$$

In which:

v is the Poisson ratio; D_w is the wheel diameter;
b is the effective load-bearing width taken as $b = min\,[b_r; b_w]$;
HB is the unit-conform hardness based on the natural hardness of the material, at the depth of maximum shear;
γ_m is the general resistance coefficient; $\gamma_m = 1.1$;
f_y is the yield stress of the material below the hardened surface, i.e. the natural yield stress of the material prior to the su
f_1 is the decreasing factor for edge pressure. For point contact it is 1, for line contact it is stated hereafter.
f_2 is the decreasing factor for non-uniform pressure distribution. For point contact it is 1, for line contact it is stated herea

The two formulae above are derived from two bodies in contact of the same width. The factor f_1 gives a correction in case the two bodies are of unequal width, as shown in figure .

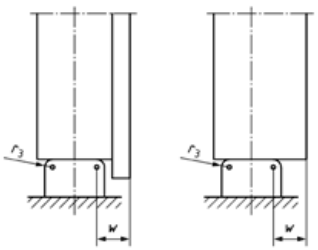

Figure E.4: Width and radius of two bodies of unequal width [43]

Ratio r_3/w	Factor f_1
$r_3/w \le 0{,}1$	0,85
$0{,}1 < r_3/w < 0{,}8$	$\left[0{,}58 + 0{,}15\left(r_3/w\right)\right] / 0{,}7$
$r_3/w \ge 0{,}8$	1,0
where w is the width of the projecting non-contact area and r_3 is the radius of the edge of the non-projecting part (wheel or rail).	

Figure E.5: Decreasing factor(f_1) for edge pressure for a line contact for bodies with an unequal width [43]

In the case of a line contact an ideal uniform pressure distribution across the wheel takes place in case of sufficient elasticity of the rail fixing (or its support) and/or wheels with self-aligning suspension. In other cases, deformation of the crane structure or tolerances in rail alignment result in non-uniform pressure distributions which decreases the limit design contact force. This effect is taken into account by the factor f_2 which is given in figure E.6. It is dependent on the tolerance class according to ISO 12488-1.

	Tolerance class of ISO 12488-1			
	1	2	3	4
Wheels with self-aligning mounting	1,0	1,0	0,95	0,9
Non-aligning wheel mounting, rail mounted on elastic support	0,95	0,9	0,85	0,8
Non-aligning wheel mounting, rail mounted on rigid support	0,9	0,85	0,8	0,7

Figure E.6: Non-uniform pressure distribution factor (f_2) [43]

ISO 12488-1 [66] is an international standard which specifically defines the tolerances for wheels and travel and traversing tracks. The main criterion for the deterimination of the class is the amount of travel during the lifetime of the crane. The class is then defined according to figure E.7 below.

Tolerance class	Limits of travelling and traversing distance km
1	$50\,000 \le L$
2	$10\,000 \le L < 50\,000$
3	$L < 10\,000$, for stationary erected tracks
4	Temporarily erected tracks for building and erection purposes
NOTE L is calculated as the product of the normal travel speed and the specified working time of the relevant travel/traverse mechanism, either by application of customer specified values or through reference to the classification of the mechanism (see ISO 4301-1).	

Figure E.7: Classificaton of tolerance classes according to ISO 12488-1 [66]

Case calculation static limit design contact force

In case of 475000 gate cycles during the lifetime of the gate, the use of 2 wheel sets during this design life and a travel distance of 88 meter, the total travel distance per wheel set is:

$$475000 \cdot \frac{88}{\frac{2}{1000}} = 20900\ km$$

Which defines the tolerance class to be 2.

Both wheel and rail have the same width and therefore the factor f1 for edge pressure is 1.

In this case there is non-aligning wheel mounting and the rail is mounted on a rigid support. The tolerance class is 2 and therefore the factor f2 for non-uniform pressure distribution is 0.85.

Both materials have a modulus of elasticity of $210000\ N/mm^2$ and therefore the equivalent modulus of elasticity is also $210000\ N/mm^2$.

The wheel is surface hardened and it is assumed the hardness extends deep enough to cover the maximum shear. The static limit design contact force for the wheel can therefore be calculated by:

$$F_{Rd,s,wheel} = \frac{(4.2 \cdot 550)^2}{1.1} \cdot \frac{\pi \cdot 1200 \cdot (150 - 2 \cdot 5) \cdot \left(1 - 0.3^2\right)}{210000} \cdot 1 \cdot 0.85 = 9430429\ N$$

The rail is non-surface hardened. Therefore the static limit design contact force for the rail can be calculated by:

$$F_{Rd,s,rail} = \frac{(7 \cdot 300)^2}{1.1} \cdot \frac{\pi \cdot 1200 \cdot (150 - 2 \cdot 5) \cdot \left(1 - 0.3^2\right)}{210000} \cdot 1 \cdot 0.85 = 7793743\ N$$

Thus the static limit design contact force of the rail is governing. Which is **7794 kN**. This value is valid for both a carriage with four and eight wheels, as the amount of wheels has no influence on this calculation.

E.5.2. Fatigue contact force

The proof of fatigue strength covers the hazards related to Rolling Contact Fatigue (RCF). It states that for each wheel and for all pointson the rails the following should hold:

$F_{Sd,f} \leq F_{Rd,f}$

In which $F_{Sd,f}$ is the maximum design contact force for fatigue and $F_{Rd,f}$ is the limit design contact force for fatigue.

The design contact force $F_{Sd,f}$ shall be calculated for regular loads (load combinations A of EN 13001-2) including risk coefficient and with all dynamic factors φi=1 and all partial safety factors $\gamma_p = 1$. Skewing forces acting on guide rollers shall be considered as regular loads.

The resistance design contact force $F_{Rd,f}$ has to be calculated for both wheel and rail via:

$$F_{Rd,f} = \frac{F_u}{\gamma_{cf} \cdot \sqrt[m]{s_c}} \cdot f_f$$

In which:

F_u is the reference contact force;
s_c is the contact force history parameter, calculated separately for wheel and rail;
γ_{cf} is the contact resistance factor for fatigue $\gamma_{cf} (= 1.1)$;
f_f is the factor of further influences and
m is the exponent for wheel/rail contacts $(m = \frac{10}{3} = 3.33)$.

The reference contact force represents the fatigue strength under $6.4 \cdot 10^6$ rolling contacts under constant contact force and a probability of survival of 90 %. It has to be calculated separately for both wheel and rail by the following (the effective load-bearing width is the same in both calculations):

For non-surface hardened materials (e.g. cast, forged, rolled or quenched and tempered);

$$F_u = (3.0 \cdot HB)^2 \cdot \frac{\pi \cdot D_w \cdot b \cdot \left(1 - v^2\right)}{E_m}$$

For surface hardened materials (e.g. flame or induction hardened) provided that the surface hardness is equal or greater than $HB = 0.6 \cdot f_y$ and the hardness extends deep enough to cover the max. shear;

$$F_u = \left(1.8 \cdot f_y\right)^2 \cdot \frac{\pi \cdot D_w \cdot b \cdot \left(1 - v^2\right)}{E_m}$$

The contact force history parameter describes the fatigue effect of the specified use in terms of rolling contacts in a particular wheel/rail pair and is calculated by:

$$s_c = k_c \cdot v_c$$

In which:
k_c is the contact force spectrum factor; v_c is the relative total number of rolling contacts:

$$v_c = \frac{i_{\text{tot}}}{i_D}$$

In which i_{tot} is the total number of rolling contacts during the design life of wheel or rail and i_D is the number of rolling contacts at reference point ($i_D = 6.4 \cdot 10^6$). The contact force spectrum factor is defined as:

$$k_c = 1/i_{\text{tot}} \cdot \sum_{i=1}^{i_{\text{tot}}} \left(\frac{F_{Sd,f,i}}{F_{Sd,f}}\right)^m$$

In which:

i is the index of a rolling contact with $F_{Sd,f,i}$;
i_{tot} is the total number of rolling contacts during the design life of wheel or rail;
$F_{Sd,f,i}$ is the design contact force for fatigue in a contact i;
$F_{Sd,f}$ is the maximum of all forces $F_{Sd,f,i}$ and
m is the exponent for wheel/rail contacts ($m = \frac{10}{3} = 3.33$).

The total number of rolling contacts has to be calculated separately for wheel and rail. For a wheel, one revolution is equivalent to one rolling contact, whereas for a selected point on the rail the passing over by any wheel represents one rolling contact. For a running wheel the total number of rolling contacts is:

$$i_{\text{tot}} = \frac{1}{l_w} \cdot \frac{2 \cdot \overline{x} \cdot C}{\pi \cdot D_w}$$

In which:

$\overline{x}$ is the average displacement of the related crane motion (see EN 13001-1);
C is the total number of working cycles during the design life of the crane (see EN 13001-1);
l_w is the design number of wheel sets used during the design life of the crane (i.e. number of wheel sets replacements +
D_w is the wheel diameter

For a point on the rail with wheels passing over the total number of rolling contacts is:

$$i_{\text{tot}} = 2 \cdot n_W \cdot C$$

The factor of further influences (f_f) takes into account other influences like edge pressures (f_{f1}) , non-uniform pressure distribution (f_{f2}), skewing (f_{f3}) and mechanical abrasion effects (f_{f4}) and is calculated by:

$$f_f = f_{f1} \cdot f_{f2} \cdot f_{f3} \cdot f_{f4}$$

Due to lateral movements of wheels, the edge pressure effect on the wider party (wheel or rail) may be neglected and the factor f_{f1} is set to 1. For the narrower party with the edge radius r3 applies $f_{f1} = f_1$ as stated for the static strength.

For the proof of fatigue strength the non-uniform pressure distribution may be neglected and f_{f2} is set to 1.

$$f_{f3} = 1 \; for \; \alpha \leq 0.005 \; rad$$

$$f_{f3} = \sqrt[3]{\frac{0.005}{\alpha}} \; for \; \alpha > 0.005 \; rad$$

In which $\alpha = \alpha_g + \alpha_w + \alpha_t$ is the skew angle of the crane in radians, calculated in accordance with EN 13001-2 [42].

$$\alpha_g = s_g / w_b$$

In which:

s_g is the slack of the guide as seen in figure E.8;
w_b is the distance between the guide means.

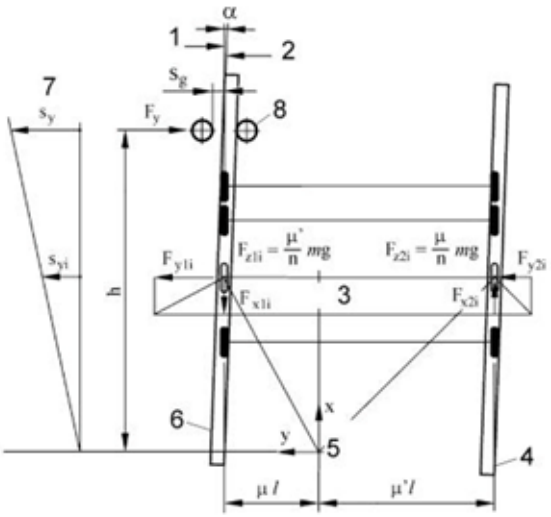

Key

1 direction of motion
2 direction of rail
3 wheel pair i
4 rail 2
5 instantaneous slide pole
6 rail 1
7 slip
8 guide means

Figure E.8: Loads acting on a crane in skewed position [42]

$$\alpha_w = 0.1 \cdot (b_h / w_b)$$

In which b_h is the width of the rail head

The part of the skew angle due to tolerances (α_t) shall be chosen from figure E.9 according to the tolerance class.

	Tolerance class of ISO 12488-1			
	1	2	3	4
Angle α_t [rad]	0,001 5	0,002 5	0,003 5	0,004 5

Figure E.9: Allignment angle of single wheel according to EN13001 [42]

In an unclean environment, the mechanical abrasion effects on the driven wheels shall be taken into account by factor f_{f4}.
$f_{f4} = 0.95$ for driven wheels in an environment with abrasive particles.
$f_{f4} = 1.0$ for non-driven wheels or wheels in an environment without abrasive particles.

Case calculation fatigue limit design contact force
The rail is non-surface hardened and therefore the reference contact force for the rail is:

$$F_{u,rail} = (3.0 \cdot 300)^2 \cdot \frac{\pi \cdot 1200 \cdot (150 - 2 \cdot 5) \cdot \left(1 - 0.3^2\right)}{210000} = 1852535\ N$$

The wheel is surface hardened and it is assumed the hardness extends deep enough to cover the maximum shear. Therefore the reference contact force for the wheel is:

$$F_{u,wheel} = (1.8 \cdot 550)^2 \cdot \frac{\pi \cdot 1200 \cdot (150 - 2 \cdot 5) \cdot \left(1 - 0.3^2\right)}{210000} = 2241567\ N$$

For a wheel the total number of rolling contacts is:

$$i_{tot,wheel} = \frac{1}{2} \cdot \frac{2 \cdot 88 \cdot 475000}{\pi \cdot 1200} = 5543897$$

For a governing point on the rail the total number of rolling contacts for a normative carriage with 4 wheels is:

$$i_{tot,rail,4w} = 2 \cdot 4 \cdot 475000 = 3800000$$

For a carriage with 8 wheels the normative number of rolling contacts for the rail is:

$$i_{tot,rail,8w} = 2 \cdot 8 \cdot 475000 = 7600000$$

The contact force spectrum factor (k_c) is normally calculated by taking all the loads during the lifetime of the gate and taking them into account relatively to the maximum of all those forces. However, in this case the real loads are not yet known. The goal is to determine the maximum allowable load on the wheel/rail set. We assume the most conservative case in which all loads are the maximum load and therefore the contact force spectrum factor will be 1.

The contact force history parameter for the rail in case of a 4 wheel carriage is calculated by:

$$s_{c,rail,4w} = k_{c,rail} \cdot v_{c,rail} = k_{c,rail} \cdot \frac{i_{tot,rail}}{i_D} = 1 \cdot \frac{3800000}{6.4 \cdot 10^6} = 0.59$$

While for an eight wheel carraige the contact force history parameter becomes:

$$s_{c,rail,8w} == 1 \cdot \frac{7600000}{6.4 \cdot 10^6} = 1.19$$

The contact force history parameter for the wheel (for both 4 and 8 wheels) is:

$$s_{c,wheel} = k_{c,wheel} \cdot v_{c,wheel} = k_{c,wheel} \cdot \frac{i_{tot,wheel}}{i_D} = 1 \cdot \frac{5543897}{6.4 \cdot 10^6} = 0.87$$

The factor of further influences consists of 4 factors. As both wheel and rail have the same width, the factor for edge pressure (f_{f1}) is 1. The factor for non-uniform pressure distribution (f_{f2}) may be neglected in case of fatigue loading, and therefore also is 1.
The gate hangs on its 2 carriages via a pendant and horizontal loads are transferred to the horizontal guiding system. Therefore it is assumed no skewing occurs on the wheels and rails and the factor for skewing (f_{f3}) can be set to 1.
The mechanical drive factor (f_{f4}) is also 1, as the wheels are all non-driven.

The factor of further influences therefore is:

$$f_f = f_{f1} \cdot f_{f2} \cdot f_{f3} \cdot f_{f4} = 1 \cdot 1 \cdot 1 \cdot 1 = 1$$

The fatigue limit design contact force for the rail (in case of a 4 wheel carriage) then is:

$$F_{Rd,f,rail} = \frac{F_{u,rail}}{\gamma_{cf} \cdot \sqrt[m]{s_{c,rail}}} \cdot f_f = \frac{1852535}{1.1 \cdot \sqrt[3.33]{0.59}} \cdot 1 = 1969212\ N$$

And the fatigue limit design contact force for the wheel then is:

$$F_{Rd,f,wheel} = \frac{F_{u,wheel}}{\gamma_{cf} \cdot \sqrt[m]{s_{c,wheel}}} \cdot f_f = \frac{2241567}{1.1 \cdot \sqrt[3.33]{0.87}} \cdot 1 = 2127494\ N$$

Thus the fatigue limit design contact force of the rail is governing.

In case of an eight wheel carriage, the fatigue limit contact force of the rail is also governing and is calculated by:

$$F_{Rd,f,rail} = \frac{1852535}{1.1 \cdot \sqrt[3.33]{1.19}} \cdot 1 = 1599497\ N$$

Thus, according to EN13001, the fatigue limit design contact force is 1969 kN for the four wheel carriage and 1599 kN in case of an eight wheel carriage.

E.6. Conclusions

Tables E.2 and E.3 show both the static and fatigue limit design force per calculation method for respectively a four and an eight wheel carriage.

Table E.2: Limit design force per calculation method in case of 4 wheels per carriage

	EN13001	NEN 6786 VOBB	DIN19704	HERTZ THEORY
Static limit design force (in kN)	7794	6049	8917	1872
Fatigue limit design force (in kN)	1969	1368	2092	-

Table E.3: Limit design force per calculation method in case of 8 wheels per carriage

	EN13001	NEN 6786 VOBB	DIN19704	HERTZ THEORY
Static limit design force (in kN)	7794	6049	8917	1872
Fatigue limit design force (in kN)	1599	1188	2092	-

From the tables it can be concluded that the fatigue limit design force is probably governing in all situations. This should however be checked by calculatiing the static and fatigue design loads and checking the unity of each.

The loading capacity of the wheel is in all calculation methods dependent on the material strength (squared), the diameter/radius of the wheel and the length of the wheel-rail contact area. The extent to which other factors are included depends on the sophistication of the calculation method.

The Hertz Theory doesn't have a fatigue limit design force as it only holds true for static normal loading in case of free rolling. The hertz theory is not valid if friction or traction is present, which is definitely present in this case. Therefore the hertz theory will be neglected.

The NEN 6786 method is the most simplistic. For the static strength the ultimate tensile strength of the weakest material is used and divided by a constant value (which is then squared). In the fatigue calculation this value is replaced by a value taken from a table which is dependent on the amount normative rolling contacts and the tensile strength of wheel and rail! This value is then squared and only multiplied with the wheel diameter and the contact length. No other factors or material parameters are included.

The DIN 19704 calculation method is somewhat more sophisticated. It incorporates the Poisson ratio and the elasticity modulus in the formula. The static strength factor is dependent on a constant coefficient multiplied by the yield strength of the weakest material. For the fatigue strength this value is dependent on the number of normative rolling contacts, an extra fatigue factor (0.333) and the ultimate tensile strength of the material.

The EN13001 method is the most elaborate. It also incorporates the Poisson ratio and an equivalent elasticity modulus (dependent on the modulus of elasticity of both materials). The static strength is calculated with the use of the Brinell Hardness or the yield strength, depending on if the material has been surface hardened or not. Both of these values are multiplied by a different constant value. Two decreasing factors take into account possible edge pressures and non-uniform pressure distributions. The fatigue calculation is even more detailed. A reference contact force is calculated in the same way as the static calculation method but with differing constant coefficients. This reference contact force is than divided and multiplied by factors that take into account the force history and further influences. This force history parameter is dependent on the relative number of rolling contacts (compared with a base value) and a contact force spectrum factor. This spectrum factor is calculated by taking an average value of all the forces over the lifetime of the gate, and factoring them with respect to their size. A larger force has a bigger influence on the fatigue life.

From the three normative calculation methods, the EN13001 calculation is the most comprehensive and the NEN 6786 calculation is the most simplistic. Additionally, the NEN 6786 calculation gives the lowest design limit. To be on the safe side the NEN 6786 design limits are taken as input values for the calculations, as they are the strictest.

F

Maple calculations

This appendix shows the maple calculations which have been used to plot the loads on the carriages against a variable cantilever length. These plots are then used to determine the minimum required cantilever length in order to balance the cantilever gate and to meet the safety requirements for the wheel/rail connection.

This maple file only shows the calculations in case of an 8 wheel front carriage. The calculations for a 4 wheel front carriage are not shown here to reduce the amount of pages. The calculations were exactly the same except for the front carriage length and the amount of wheels.

```
> restart;
```

Input variables

Dimensions and heights:

```
> g := 9.81 :#gravitational force in m per s^2
  rho_w := 1000 :#average water density in kg per m^3

  Lg := 44.56 :#casestudy gate length in m
  Bg := 6.43 :#casestudy gate width in m
  Hg := 19.22 :#casestudy gate height in m
  Lcar_front := 9 :# carriage length of front carriage in m
  Lcar_back := 6 :#carriage length of back carriage in m

  Gate_top := 6 :#m NAP
  Gate_bot := -13.22 :#m NAP
  Gate_supports := 4 :#m NAP
  HW := +3.5 :#m NAP
  LW := -3.4 :#m NAP
  MW := 0.02 :#m NAP
```

Weights and volumes:

```
> Wgate := 946 :#casestudy gate weight in tonnes
  Wsilt := 110.9 :#accumulated silt weight in tonnes
  Wcant := 56.14·x/24 :
      #weight of cantilever part. 56.14 tonnes calculated for a cantilever structure of 24 m. Weight for other
      lengths taken proportional
  Wcar_front := Lcar_front·12/6 :
      #weight of a carriage. 12 tonnes at 6 m carriage length, used krammersluizen as an example.
  Wcar_back := Lcar_back·12/6 :

  Vbu_gHW := 735.3 :
      #Buoyancy volume (in m3) of gate at waterlevel of +3.5mNAP (1024.7-405.4+76,9+39,1)
  Vbu_gLW := 696.2 :#Buoyancy volume (in m3) of gate at Low Water (LW)  -3.4 mNAP (1024.7 − 405.4
      + 76, 9)
  Vbu_gMW := Vbu_gLW + (Vbu_gHW − Vbu_gLW)·(MW − LW)/(HW − LW) :

  Vbu_cantHW := 26.54·x/24 :
      #Buoancy volume (in m3) of cantilever structure at +3.5 m NAP. Base volume calculated in case of cant.
      length of 24 m and taken proportional to length.
  Vbu_cantLW := 10.66·x/24 :#buoancy volume (in m3) of cant. structure at -3.4 m NAP
  Vbu_cantMW := 19.72·x/24 :#buoancy volume (in m3) of cant. structure at 0.02 m NAP
```

Forces:

```
> Fgate := Wgate·g :#in kN
  Fsilt := Wsilt·g :#in kN
  Fbu_g_HW := Vbu_gHW·rho_w·g/1000 : #in kN
```

$$Fbu\_g\_LW := \frac{Vbu\_gLW \cdot rho\_w \cdot g}{1000} : \#in\ kN$$

$$Fbu\_g\_MW := \frac{Vbu\_gMW \cdot rho\_w \cdot g}{1000} :$$

$$Fbu\_cant\_HW := \frac{Vbu\_cantHW \cdot rho\_w \cdot g}{1000} :$$

$$Fbu\_cant\_LW := \frac{Vbu\_cantLW \cdot rho\_w \cdot g}{1000} :$$

$$Fbu\_cant\_MW := \frac{Vbu\_cantMW \cdot rho\_w \cdot g}{1000} :$$

$Fcant := Wcant \cdot g$:#in kN

$Fres\_O\_HW := 208$:

#Determined by a separate calculation for the maximum resistance force during opening and closing

$Fres\_O\_LW := 166$:

$$Fres\_O\_MW := \frac{(Fres\_O\_HW + Fres\_O\_LW)}{2} :$$

$Fres\_C\_HW := 191$:

$Fres\_C\_LW := 149$:

$$Fres\_C\_MW := \frac{(Fres\_C\_HW + Fres\_C\_LW)}{2} :$$

Arm lengths:

> $$Arm\_gate := \frac{Lg}{2} + x - \frac{Lcar\_back}{2}$$:#arm length of gate part (from back carriage to the left)

$$Arm\_cant := \frac{2 \cdot x}{3} - \frac{Lcar\_back}{2}$$:#arm length of cantilever part (from back carriage)

$$L\_ab := x - \frac{Lcar\_back}{2} - \frac{Lcar\_front}{2}$$:#distance or arm length between the two supports or carriages.

$$Arm\_resHW := (Gate\_supports - Gate\_bot) - \frac{(HW - Gate\_bot)}{2} :$$

#Arm from supports to resistance forces at HW. Assume res. forces act on half the waterheight over the gate

$$Arm\_resLW := (Gate\_supports - Gate\_bot) - \frac{(LW - Gate\_bot)}{2}$$:#Arm from supports to res. forces at LW

$$Arm\_resMW := (Gate\_supports - Gate\_bot) - \frac{(MW - Gate\_bot)}{2} :$$

#Arm from supports to res. forces at MW

Design choice inputs:

> $Fsafetybackcarriage := 200$:#safety downward force required on each of the carriages

$Nr\_wheels\_front := 8$:#nr. of wheels of the front carriage

$Nr\_wheels\_back := 4$:#nr. of wheels of the back carriage

$Chamberfill := 0.15$:#part or percentage of chambers filled after collision

Design forces for the wheels:

> $Flimit\_str := 6049$:#Strength design capacity per wheel according to NEN6786 VOBB

$Flimit\_fat\_4wheels\_NEN6786 := 1368$:

#Fatigue design capacity per wheel in case of 4 wheels according to NEN6786 VOBB

$Flimit\_fat\_4wheels\_EN13001 := 1969$:

#Fatigue design capacity per wheel in case of 4 wheels according to NEN6786 EN13001

$Flimit\_fat\_8wheels\_NEN6786 := 1188$:

#Fatigue design capacity per wheel in case of 8 wheels according to NEN6786 VOBB

```
Flimit_fat_8wheels_EN13001 := 1599 :
    #Fatigue design capacity per wheel in case of 8 wheels according to NEN6786 EN13001
>
```

Calculation of characteristic forces on front and back carriage during opening/closing and hw/lw.

This section determines the characteristic (thus without taking into account any partial safety factors) reaction forces on the front and back carriage of the cantilever rolling gate for the base case. Thus without applying any additional measures and assuming that both back and front carriages cannot move in vertical direction.

```
>
```

#OPENING

```
> Ffront_HW_O := 1/L_ab ((Fgate − Fbu_g_HW + Fsilt)·Arm_gate + (Fcant − Fbu_cant_HW)·Arm_cant
    − Fres_O_HW·Arm_resHW) :
    #force on front carriage at High Water (HW), by calculating the sum of moments around x=0 or back
    carriage (M=0 in carriage or support)
> Fback_HW_O := -Ffront_HW_O + Fgate + Fsilt + Fcant − Fbu_g_HW :#force on back carriage at HW
> Ffront_LW_O :=
    1/L_ab ((Fgate − Fbu_g_LW + Fsilt)·Arm_gate + (Fcant − Fbu_cant_LW)·Arm_cant
    − Fres_O_LW·Arm_resLW) :
    #force on front carriage at Low Water (LW), by calculating the sum of moments around x=0 or back
    carriage (M = 0 in carriage or support)
> Fback_LW_O := -Ffront_LW_O + Fgate + Fsilt + Fcant − Fbu_g_HW :#force on back carriage at LW
> plot([Ffront_HW_O, Fback_HW_O, Ffront_LW_O, Fback_LW_O], x = 10 ..Lg, axis = [gridlines = [10,
    linestyle = solid]], color = ["Red", "Blue", "DarkRed", "DarkBlue"], linestyle = [solid, solid, longdash,
    longdash], font = ["Arial", 10], labels = ["Cantilever length [m]", "Force [kN]"], labeldirections
    = [horizontal, vertical], labelfont = ["Arial", 10], legend
    = [typeset("Reaction force front carriage during opening (O) at HW (+3.5 m NAP)"), typeset(
    "Reaction force back carriage during opening (O) at HW (+3.5 m NAP)"), typeset(
    "Reaction force front carriage during opening (O) at LW (-3.4 m NAP)"), typeset(
    "Reaction force back carriage during opening (O) at LW (-3.4 m NAP)")], legendstyle = [font
    = ["Arial", 9], location = bottom], title
    = "Characteristic reaction forces on the front and back carriage during opening.", titlefont
    = ["Arial", bold, 10]);
```

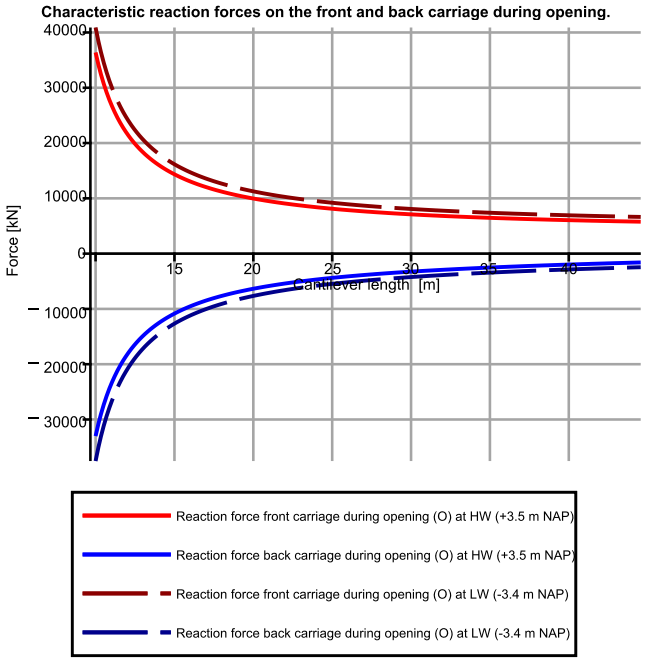

>

 # CLOSING

> $Ffront\_HW\_C := \frac{1}{L\_ab}((Fgate - Fbu\_g\_HW + Fsilt)\cdot Arm\_gate + (Fcant - Fbu\_cant\_HW)\cdot Arm\_cant + Fres\_C\_HW\cdot Arm\_resHW)$:
#force on front carriage at High Water (HW), by calculating the sum of moments around x=0 or back carriage (M=0 in carriage or support)

> $Fback\_HW\_C := -Ffront\_HW\_C + Fgate + Fsilt + Fcant - Fbu\_g\_HW$:#force on back carriage at HW

> $Ffront\_LW\_C := \frac{1}{L\_ab}((Fgate - Fbu\_g\_LW + Fsilt)\cdot Arm\_gate + (Fcant - Fbu\_cant\_LW)\cdot Arm\_cant + Fres\_C\_LW\cdot Arm\_resLW)$:
#force on front carriage at Low Water (LW), by calculating the sum of moments around x=0 or back carriage (M = 0 **in** carriage **or** support)

> $Fback\_LW\_C := -Ffront\_LW\_C + Fgate + Fsilt + Fcant - Fbu\_g\_HW$:#force on back carriage at LW

>

> plot([Ffront_HW_C, Fback_HW_C, Ffront_LW_C, Fback_LW_C], x = 10..Lg, axis = [gridlines = [10, linestyle = solid]], color = ["Red", "Blue", "DarkRed", "DarkBlue"], linestyle = [solid, solid, longdash, longdash], font = ["Arial", 10], labels = ["Cantilever length [m]", "Force [kN]"], labeldirections = [horizontal, vertical], labelfont = ["Arial", 10], legend = [typeset("Reaction force front carriage during closing (C) at HW (+3.5 m NAP)"), typeset("Reaction force back carriage during closing (C) at HW (+3.5 m NAP)"), typeset("Reaction force front carriage during closing (C) at LW (-3.4 m NAP)"), typeset("Reaction force back carriage during closing (C) at LW (-3.4 m NAP)")], legendstyle = [font = ["Arial", 9], location = bottom], title = "Characteristic reaction forces on the front and back carriage during closing.", titlefont = ["Arial", bold, 10]);

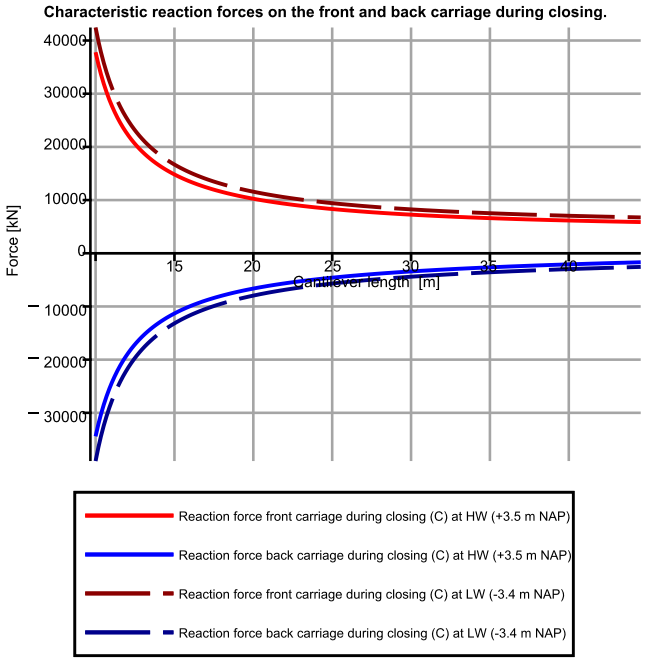

>

>

>

Calculation of max. extra buoancy volume

>

#Determining the max extra buoancy volume. Looking for the limit to which the front carraige does not float up under the most extreme loading situation. Governing loading combination and situation: Deadweight favourable, buoancy unfavourable, start of operations (no silt present), High Water (HW) and max resistance forces during opening!

```
> #Partial safety factors: DW favourable, Buo unfavourable, no silt
  yd_equ := 0.95 :
  ysilt_equ := 0 :
  ybu_equ := 1.05 :
  yres_equ := 1.5 :
```

>

```
> Fbu_extra := 1/(ybu_equ·Arm_gate) ((Fgate·yd_equ − Fbu_g_HW·ybu_equ + Fsilt·ysilt_equ)·Arm_gate
      + (Fcant·yd_equ − Fbu_cant_HW·ybu_equ)·Arm_cant − Fres_O_HW·yres_equ·Arm_resHW
      − Fsafetybackcarriage·L_ab) :
```

```
> Vbu_extra := Fbu_extra·1000/(rho_w·g) :
```

```
> plot([Vbu_extra], x = 10..Lg, y = 0..x = 14, axis = [gridlines = [10, linestyle = solid]], color = ["Coral"],
      linestyle = [solid], font = ["Arial", 10], labels = ["Cantilever length [m]",
      "Max. extra buoyancy volume [m3]"], labeldirections = [horizontal, vertical], labelfont = ["Arial",
      10], title = "Maximum possible additional buoyancy volume.", titlefont = ["Arial", bold, 10]);
```

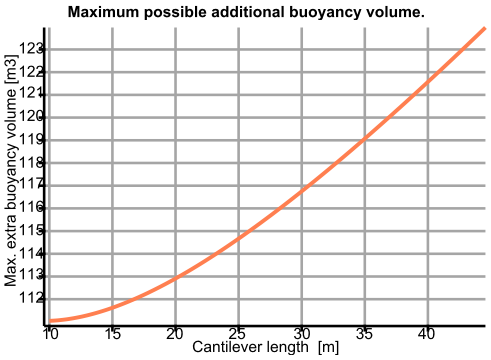

Calculation of required counterweight (in case of counterweight variant)

> ***#Determining the minimum mass of the counterweight. Looking for the limit to which the back carraige does not float up in case of collisiong of the buoancy chambers and 15% of the chambers fills up. . Governing loading combination and situation :*** *Low water* **and** *gate is opening, silt present. Incidental load under which* 15 *% of the chambers fills up. All partial safety factors* 1.

> $Ffront\_LW\_O\_Incidental := \frac{1}{L\_ab}((Fgate + Fsilt - (1 - Chamberfill)\cdot(Fbu\_g\_LW + Fbu\_extra))\cdot Arm\_gate + (Fcant - Fbu\_cant\_LW)\cdot Arm\_cant - Fres\_O\_LW\cdot Arm\_resLW)$:
#force on front carriage at LW, Opening and 15% chambers filled

> $Fcontra := Fsafetybackcarriage + Ffront\_LW\_O\_Incidental - Fgate - Fcant + (1 - Chamberfill)\cdot(Fbu\_g\_LW + Fbu\_extra) + Fbu\_cant\_LW - Fsilt$:

$$Wcontra := \frac{Fcontra}{g} :$$

> *plot*([*Wcontra*], *x* = 14 ..*Lg*, *y* = 0 ..*x* = 14, *axis* = [*gridlines* = [10, *linestyle* = *solid*]], *color* = ["Coral"], *linestyle* = [*solid*], *font* = ["Arial", 10], *labels* = ["Cantilever length [m]", "Min req. contraweight [tonnes]"], *labeldirections* = [*horizontal*, *vertical*], *labelfont* = ["Arial", 10], *title* = "Minimum required counterweight to balance the cantilever gate, in case of 8 wheel front carriage", *titlefont* = ["Arial", *bold*, 10]);

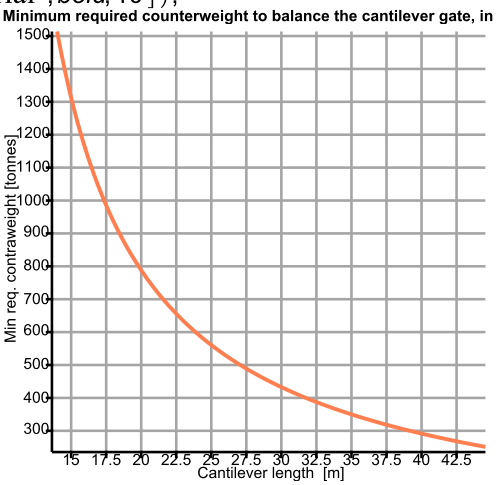

>

Front Carriage (the same for counterweight & upper rail)

> ***#WHEEL STRENGTH check front carriage. Governing loading situation: Front carriage, Low Water (LW) and Closing (C), Silt present, Dead weight unfavourable, buoancy volume favourable.***

>

#Partial safety factors: DW unfavourable, Buo favourable, silt. Silt considered as permanent.

Consequence Class 3 (CC3)

```
yd_str := 1.25 :
ysilt_str := 1.25 :
ybu_str := 0.9 :
yres_str := 1.5 :
```

```
> Ffront_LW_C_str := 1/L_ab ( ( Fgate·yd_str − ( Fbu_g_LW + Fbu_extra ) ·ybu_str + Fsilt·ysilt_str) ·Arm_gate
      + ( Fcant·yd_str − Fbu_cant_LW·ybu_str) ·Arm_cant + Fres_C_LW·yres_str·Arm_resLW) :
  Fcar_front_str := Wcar_front·g·yd_str :
  Fwheelmax_front_str := ( Ffront_LW_C_str + Fcar_front_str) / Nr_wheels_front :
```

```
>
```

```
> plot( [ Fwheelmax_front_str, Flimit_str], x = 10 ..Lg, y = 0 ..x = 12, axis = [ gridlines = [ 11, linestyle = solid] ],
      tickmarks = [ 7, 8], color = [ "Coral"], linestyle = [ solid], color = [ "Blue", "Red" ], font = [ "Arial", 10 ],
      labels = [ "Cantilever length  [m]", "Force [kN]"], labeldirections = [ horizontal, vertical], labelfont
      = [ "Arial", 10 ], legend = [ typeset( "Max design wheel load (ULS Strength check)" ),
      typeset( "Strength design capacity per wheel according to NEN6786" ) ], legendstyle = [ font
      = [ "Arial", 9 ], location = bottom], title
      = "Front carriage max. strength design wheel load, in case of 8 wheel front carriage", titlefont
      = [ "Arial", bold, 10 ] );
```

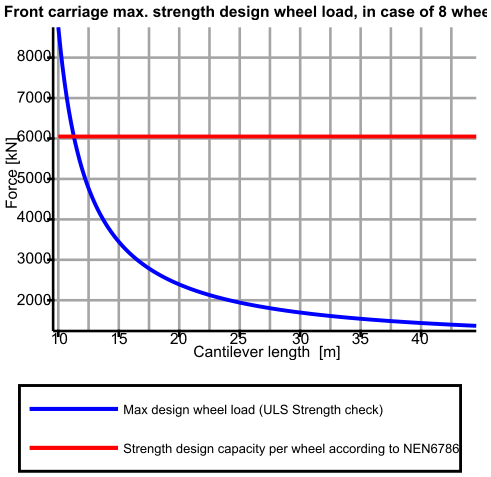


```
> solve( { Fwheelmax_front_str = Flimit_str} );
```

$$\{x = 11.28399837\},\ \{x = 3994.201724\} \tag{1}$$

```
> #WHEEL FATIGUE check front carriage. Governing loading situation: Front carriage, Median Water
      (MW) and Closing (C), Silt present, Fatigue partial safety factors set to 1.
```

```
> Ffront_MW_C_fat := 1/L_ab ( ( Fgate − ( Fbu_g_MW + Fbu_extra ) + Fsilt) ·Arm_gate + ( Fcant
      − Fbu_cant_MW) ·Arm_cant + Fres_C_MW·Arm_resMW) :
  Fcar_front_fat := Wcar_front·g :
  Fwheelmax_front_fat := ( Ffront_MW_C_fat + Fcar_front_fat) / Nr_wheels_front :
```

```
>
```

```
> plot( [ Fwheelmax_front_fat, Flimit_fat_8wheels_NEN6786, Flimit_fat_8wheels_EN13001 ], x = 12 ..Lg, y = 0
      ..x = 12, axis = [ gridlines = [ 10, linestyle = solid] ], tickmarks = [ 7, 8], color = [ "Coral"], linestyle
      = [ solid], color = [ "Blue", "Orange", "Red" ], font = [ "Arial", 10 ], labels
      = [ "Cantilever length  [m]", "Force [kN]"], labeldirections = [ horizontal, vertical], labelfont
      = [ "Arial", 10 ], legend = [ typeset( "Max design wheel load (ULS Fatigue check)" ),
      typeset( "Fatigue design capacity per wheel according to NEN6786"),
      typeset( "Fatigue design capacity per wheel according to EN13001" ) ], legendstyle = [ font
```

= ["Arial", 9], location = bottom], title
= "Front carriage max. fatigue design wheel load, in case of 8 wheel front carriage", titlefont
= ["Arial", bold, 10]);

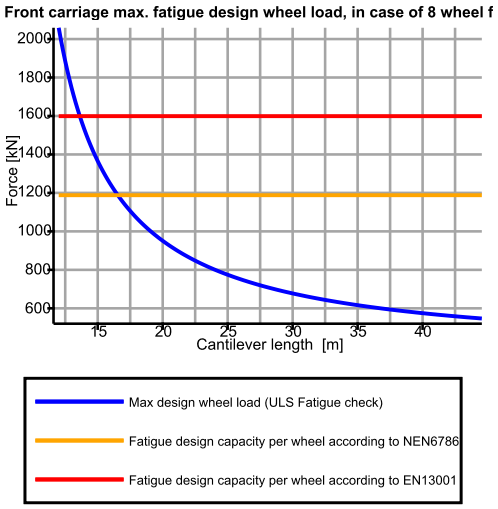

> solve({Fwheelmax_front_fat = Flimit_fat_8wheels_NEN6786});

$$\{x = 16.54799855\},\ \{x = 2090.772861\} \quad (2)$$

> solve({Fwheelmax_front_fat = Flimit_fat_8wheels_EN13001});

$$\{x = 13.62407238\},\ \{x = 3085.427339\} \quad (3)$$

>

Back carriage

Back carriage loads in case of Counterweight

>

> **#WHEEL STRENGTH check back carriage in case of counterweight. Governing loading situation: High Water (HW) and** Opening (O), **Silt not present, Dead weight favourable, buoancy volume unfavourable.**

>

#Partial safety factors: DW unfavourable, Buo favourable, silt. Silt considered as permanent. Consequence Class 3 (CC3)

yd_str := 0.9 :
ysilt_str := 0.9 :
ybu_str := 1.25 :
yres_str := 1.5 :

> $$Ffront\_HW\_O\_str := \frac{1}{L\_ab}((Fgate \cdot yd\_str - (Fbu\_g\_HW + Fbu\_extra)\cdot ybu\_str + Fsilt \cdot ysilt\_str) \cdot Arm\_gate + (Fcant \cdot yd\_str - Fbu\_cant\_HW \cdot ybu\_str)\cdot Arm\_cant - Fres\_O\_HW \cdot yres\_str \cdot Arm\_resHW) :$$

$$Fcar\_back\_str := Wcar\_back \cdot g \cdot yd\_str;$$

$$Fback\_contra\_HW\_O\_str := Fgate \cdot yd\_str - (Fbu\_g\_HW + Fbu\_extra)\cdot ybu\_str + Fsilt \cdot ysilt\_str + Fcant \cdot yd\_str - Fbu\_cant\_HW \cdot ybu\_str - Ffront\_HW\_O\_str + Fcontra \cdot yd\_str :$$

$$Fwheelmax\_contra\_back\_str := \frac{(Fback\_contra\_HW\_O\_str + Fcar\_back\_str)}{Nr\_wheels\_back} :$$

$$Fcar\_back\_str := 105.948 \quad (4)$$

> Flimit_str := 6049;#Strength design capacity per wheel according to NEN6786 VOBB

$$Flimit\_str := 6049 \quad (5)$$

> plot([Fwheelmax_contra_back_str, Flimit_str], x = 12..Lg, y = 0..x = 12, axis = [gridlines = [10, linestyle = solid]], tickmarks = [7, 8], color = ["Coral"], linestyle = [solid], color = ["Blue", "Red"], font

```
= ["Arial", 10], labels = ["Cantilever length  [m]","Force [kN]"], labeldirections = [horizontal,
vertical], labelfont = ["Arial",10], legend
= [typeset("Max design wheel load (ULS Strength check)"),
typeset("Strength design capacity per wheel according to NEN6786")], legendstyle = [font
= ["Arial", 9], location = bottom], title
= "Back carriage max. strength design wheel load, in case of 8 wheel front carriage and a
counterweight", titlefont = ["Arial", bold, 10]);
```

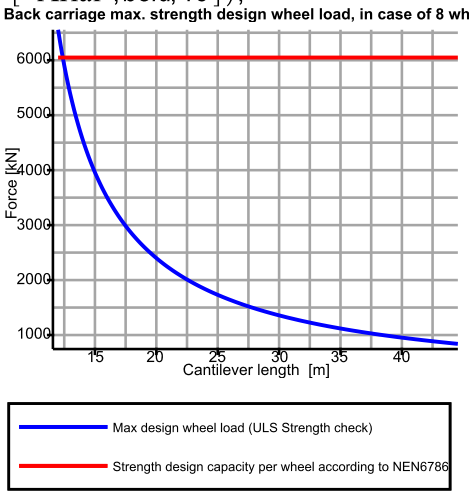


```
> solve({Fwheelmax_contra_back_str = Flimit_str})
```

$$\{x = 12.38021851\},\ \{x = -19.37494137\},\ \{x = -7413.933103\} \tag{6}$$

> #WHEEL FATIGUE check back carriage in case of counterweight. Governing loading situation: Front carriage, Median Water (MW) and Opening- (O), Silt present, Fatigue partial safety factors set to 1.

```
> Ffront_MW_O_fat := 1/L_ab ((Fgate − (Fbu_g_MW + Fbu_extra) + Fsilt)·Arm_gate + (Fcant
    − Fbu_cant_MW)·Arm_cant − Fres_O_MW·Arm_resMW) :
  Fback_contra_MW_O_fat := Fgate − Fbu_g_MW − Fbu_extra + Fsilt + Fcant − Fbu_cant_MW
    − Ffront_MW_O_fat + Fcontra :
  Fcar_back_fat := Wcar_back·g;
  Fwheelmax_contra_back_fat := (Fback_contra_MW_O_fat + Fcar_back_fat)/Nr_wheels_back :
```

$$Fcar\_back\_fat := 117.72 \tag{7}$$

```
>
> plot([Fwheelmax_contra_back_fat, Flimit_fat_4wheels_NEN6786, Flimit_fat_4wheels_EN13001], x = 12
    ..Lg, y = 0..x = 12, axis = [gridlines = [10, linestyle = solid]], tickmarks = [7, 8], color = ["Coral"],
    linestyle = [solid], color = ["Blue", "Orange", "Red"], font = ["Arial", 10], labels
    = ["Cantilever length  [m]","Force [kN]"], labeldirections = [horizontal, vertical], labelfont
    = ["Arial",10], legend = [typeset("Max design wheel load (ULS Fatigue check)"),
    typeset("Fatigue design capacity per wheel according to NEN6786"),
    typeset("Fatigue design capacity per wheel according to EN13001")], legendstyle = [font
    = ["Arial", 9], location = bottom], title
    = "Back carriage max. fatigue design wheel load, in case of 8 wheel front carriage and a
    counterweight", titlefont = ["Arial", bold, 10]);
```

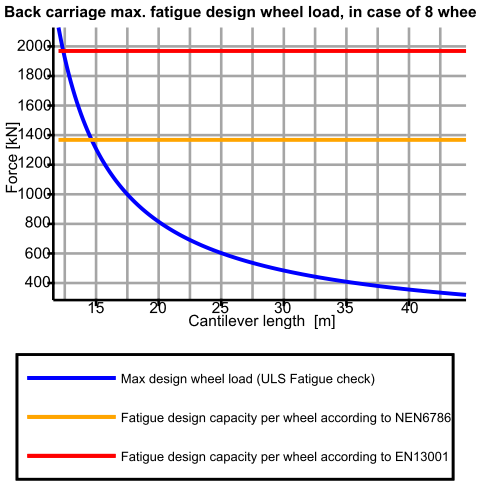


```
> solve( { Fwheelmax_contra_back_fat = Flimit_fat_4wheels_NEN6786} );
```

$$\{x = 14.64753378\},\ \{x = -19.40751791\},\ \{x = -4154.963361\} \quad (8)$$

```
> solve( { Fwheelmax_contra_back_fat = Flimit_fat_4wheels_EN13001} );
```

$$\{x = 12.37739353\},\ \{x = -19.37294516\},\ \{x = -6100.193213\} \quad (9)$$

Back carriage loads in case of upper rail

```
>
> #WHEEL STRENGTH check back carriage in case of upper rail. Governing loading situation:  Low
    Water (LW) and Closing (C), Silt present, Dead weight unfavourable, buoancy volume favourable.
>
    #Partial safety factors: DW unfavourable, Buo favourable, silt. Silt considered as permanent.
    Consequence Class 3 (CC3)
yd_str := 1.25 :
ysilt_str := 1.25 :
ybu_str := 0.9 :
yres_str := 1.5 :

> Ffront_LW_C_str := 1/L_ab ( ( Fgate·yd_str − ( Fbu_g_LW + Fbu_extra ) ·ybu_str + Fsilt·ysilt_str) ·Arm_gate
    + ( Fcant·yd_str − Fbu_cant_LW·ybu_str) ·Arm_cant + Fres_C_LW·yres_str·Arm_resLW) :
Fcar_back_str := Wcar_back·g·yd_str :
Fback_upper_LW_C_str := Fgate·yd_str − ( Fbu_g_LW + Fbu_extra ) ·ybu_str + Fsilt·ysilt_str + Fcant
    ·yd_str − Fbu_cant_MW·ybu_str − Ffront_LW_C_str :

Fwheelmax_upper_back_str := ( Fback_upper_LW_C_str + Fcar_back_str) / Nr_wheels_back :

>
> plot( [ Fwheelmax_upper_back_str,-Flimit_str], x = 12 ..Lg, y = 0 ..x = 12, axis = [ gridlines = [ 10, linestyle
    = solid] ], tickmarks = [ 7, 8], color = [ "Coral"], linestyle = [ solid], color = [ "Blue", "Red" ], font
    = [ "Arial", 10 ], labels = [ "Cantilever length  [m]", "Force [kN]"], labeldirections = [ horizontal,
    vertical], labelfont = [ "Arial", 10 ], legend
    = [ typeset( "Max design wheel load (ULS Strength check)"),
    typeset( "Strength design capacity per wheel according to NEN6786") ], legendstyle = [ font
    = [ "Arial", 9], location = bottom], title
    = "Back carriage max. strength design wheel load, in case of 8 wheel front carriage and an
    upper rail", titlefont = [ "Arial", bold, 10 ] );
```

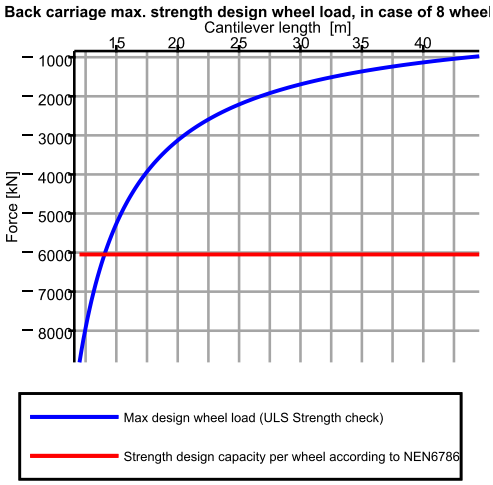


```
> solve( { Fwheelmax_upper_back_str =-Flimit_str} )
```

$$\{x = 14.03611025\},\ \{x = -19.11691923\},\ \{x = -4975.578253\} \tag{10}$$

```
> #WHEEL FATIGUE check back carriage in case of upper rail. Governing loading situation:  Median
      Water-(MW) and Closing-(C), Silt present, Fatigue partial safety factors set to 1.
```

```
> Ffront_MW_C_fat := 1/L_ab ((Fgate - (Fbu_g_MW + Fbu_extra) + Fsilt)·Arm_gate + (Fcant
      - Fbu_cant_MW)·Arm_cant + Fres_C_MW·Arm_resMW) :
  Fback_upper_MW_C_fat := Fgate - Fbu_g_MW - Fbu_extra + Fsilt + Fcant - Fbu_cant_MW
      - Ffront_MW_O_fat :
  Fcar_back_fat := Wcar_back·g;
  Fwheelmax_upper_back_fat := (Fback_upper_MW_C_fat + Fcar_back_fat)/Nr_wheels_back :
```

$$Fcar\_back\_fat := 117.72 \tag{11}$$

```
>
> plot([ Fwheelmax_upper_back_fat,-Flimit_fat_4wheels_NEN6786, -Flimit_fat_4wheels_EN13001 ], x = 12
      ..Lg, y = 0..x = 12, axis = [ gridlines = [ 10, linestyle = solid ] ], tickmarks = [ 7, 8 ], color = [ "Coral" ],
      linestyle = [ solid ], color = [ "Blue", "Orange", "Red" ], font = [ "Arial", 10 ], labels
      = [ "Cantilever length  [m]", "Force [kN]" ], labeldirections = [ horizontal, vertical ], labelfont
      = [ "Arial", 10 ], legend = [ typeset("Max design wheel load (ULS Fatigue check)"),
      typeset("Fatigue design capacity per wheel according to NEN6786"),
      typeset("Fatigue design capacity per wheel according to EN13001") ], legendstyle = [ font
      = [ "Arial", 9 ], location = bottom ], title
      = "Back carriage max. fatigue design wheel load, in case of 8 wheel front carriage and an upper
      rail", titlefont = [ "Arial", bold, 10 ]);
```

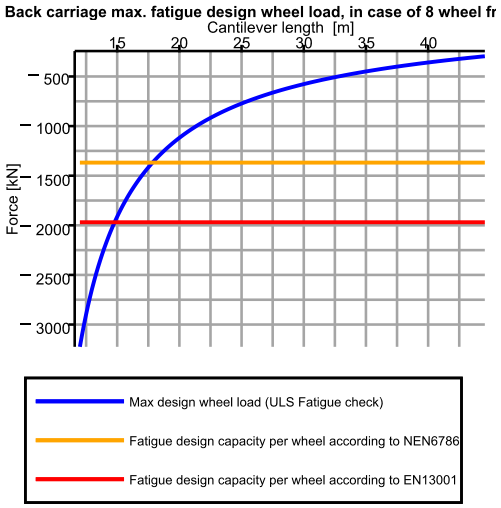


```
> solve( { Fwheelmax_upper_back_fat =-Flimit_fat_4wheels_NEN6786} );
```

$$\{x = 17.84102240\},\ \{x = -18.58361146\},\ \{x = -1167.159224\} \quad \textbf{(12)}$$

```
> solve( { Fwheelmax_upper_back_fat =-Flimit_fat_4wheels_EN13001} );
```

$$\{x = 14.79044586\},\ \{x = -18.74539257\},\ \{x = -1648.406962\} \quad \textbf{(13)}$$

```
>
>
> #CHECKS:
> eval( [ Vbu_extra, Wcontra, Fwheelmax_front_str, Fwheelmax_front_fat ], x = 17.9 );
```

$$[112.3017783,\ 947.4837243,\ 2709.945990,\ 1076.322775] \quad \textbf{(14)}$$

```
> eval( [ Ffront_LW_C_str, Ffront_MW_C_fat, ], x = 17.9 );
```

$$[21458.84292,\ 8434.002201] \quad \textbf{(15)}$$

```
> eval( [ Fgate, Fcant, Fcontra, Fbu_extra, Fbu_g_MW, Fbu_cant_MW, Fsilt ], x = 17.9 );
```

$$[9280.26,\ 410.7553275,\ 9294.815333,\ 1101.680445,\ 7019.839800,\ 144.2838450,\ 1087.929] \quad \textbf{(16)}$$

```
>
>
```

G

Final cantilever structure design

This appendix shows the final cantilever structure design for the case study. The methods, calculations and assumptions are identical to the ones showed in Appendix D and are therefore not explained again. This appendix only shows the results of the calculations and the final conclusion.

G.1. Loads and internal forces

The moment force acting from the gate part on the cantilever part consists of the dead weight of the gate structure including maximum silt and shell accretion, minus the smallest possible upwards buoyancy force:

- Dead weight gate part: 946 tonnes ($\gamma_d = 1.25$)
- Max silt weight part: 110.9 tonnes ($\gamma_s = 1.25$
- Most unfavourable buoyancy volume: 655.8 m3, at a water level of -3.5 m N.A.P. ($\gamma_b = 0.9$)

The maximum downward design force of the gate part in the most unfavourable situation is:

$$946 \cdot 9.81 \cdot 1.25 + 110.9 \cdot 9.81 \cdot 1.25 - 655.8 \cdot 9.81 \cdot 1000 \cdot 0.9 = 7170000\ N$$

Due to simplification from 3D structure to 2D structure, the acting load is halved to *3585 kN* per 2D frame. The significant acting load and the dimensions of the 2D cantilever structure were modelled in the FEM program Matrixframe. This resulted in the internal force distribution shown in Figure G.1.

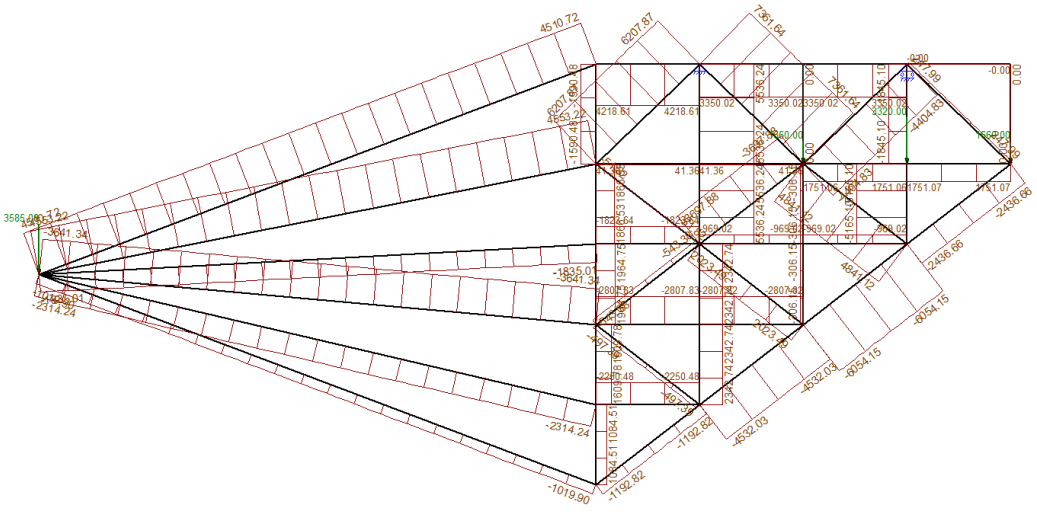

Figure G.1: The calculated internal force distribution in the truss structure.

An overview of the significant maximum design forces for specific member types of the structure is shown in table G.1.

Table G.1: Maximum design forces and member lengths for the different members of the cantilever structure

Location	**Type of force**	**Max. design force** kN	**Member length** mm
Outer diagonal chord	Compression	−6055	5240
Top horizontal chord	Tension	4219	4150
Horizontal brace	Tension Compression	1752 −2808	4150
Vertical brace bottom part	Tension Compression	5537 −5166	3200
Diagonal brace bottom part	Tension Compression	4842 −3698	5240
Vertical brace top part	Tension Compression	5537 −1846	4000
Diagonal brace top part	Tension Compression	7362 −4405	5764

G.2. Member dimensions

The structure has been modelled as a truss structure in which all of the lattice members are connected by hinges. To ensure this, the members and their D/T ratios should fall within certain limits called cross-section classes, as stated in Eurocode 3 EN 1993-1-1. For the design of this truss structure cross-section class 1 is aimed for all of the members. This cross-section class ensures enough rotation capacity in the connections by the possibility of formation of a plastic hinge. According to Eurocode 3 EN1993-1-1, for cross-section class 1 in combination with material S355, the diameter to wall thickness ratio D/T should be smaller than 33. The calculations regarding buckling and member capacity can be found in Appendix D

The possible dimensions of Circular Hollow Sections are taken from *NEN-EN 10210-2 Hot finished steel structural hollow sections - Part 2: Tolerances, dimensions and sectional properties* [47].

G.2.1. Outer Diagonal chord

The maximum force in the diagonal chord is a compression force of -6055 kN. According to the book Hollow Sections in Structural Applications [73] , the effective buckling length can be taken as 0.9 times the system length for in-plane buckling or 0.9 times the length between the supports for out-of-plane buckling for chord members.

Table G.2 gives multiple options of Circular Hollow Sections that comply to the rules of EN1993-1-1 and have an adequate unity check smaller than 1.

Table G.2: Possible options of CHS members for the outer diagonal chord (compression)

Member length	Buckling length	Outside Diameter	Wall thick-ness	Ratio	Cross-sectional area	Reduction factor	Capacity	Max. chord force	Unity check
l	$l_b = 0.9 \cdot l$	d_0	t_0	d_0/t_0	A_0	χ	$\chi \cdot f_{y0} \cdot A_0$	N_0	-
$[mm]$	$[mm]$	$[mm]$	$[mm]$	-	$[mm^2]$	-	$[kN]$	$[kN]$	-
5240	4716	**273.0**	**25.0**	11	19478	0.98	6784	-6055	*0.92*
5240	4716	323.9	20.0	16	19095	0.99	6730	-6055	*0.91*
5240	4716	355.6	20.0	18	21086	1.00	7468	-6055	*0.81*
5240	4716	406.4	14.2	29	17496	1.00	6211	-6055	*0.96*

As the joint strength increases with a decreased chord diameter, the most stocky section with an **outside diameter of 273.0 mm and wall thickness of 25 mm** is chosen as it has the thickest wall thickness and thinnest diameter.

G.2.2. Top horizontal chord

The maximum force in the horizontal chord is a tension force of 4219 kN.

Just as for the chord in compression, the diameter- to thickness ratio should be as small as possible for the capacities of the joints. The design capacity of a chord under tension is given by:

$$N_{t,Rd} = A \cdot f_y$$

The design capacity therefore depends on the cross sectional area (A) and the design yield strength (f_y). The following unity check should be validated:

$$\frac{N_{\text{Ed}}}{N_{t,Rd}} \leq 1.0$$

Table G.3 gives multiple options of circular hollow sections that comply to this unity check.

Table G.3: Possible options of CHS members for the top horizontal chord (tension)

Member length	Outside Diameter	Wall thickness	Ratio	Cross-sectional area	Capacity	Max chord force	Unity Check
l $[mm]$	d_0 $[mm]$	t_0 $[mm]$	d_0/t_0 -	A_0 $[mm^2]$	$f_{y0} \cdot A_0$ $[kN]$	N_0 $[kN]$	- -
4150	244.5	25	10	17239	6120	4219	0.69
4150	**273**	**25**	11	19478	6915	4219	0.61
4150	323.9	16	20	15477	5494	4219	0.77
4150	355.6	14.2	25	15230	5407	4219	0.78

For ease of construction the same member is chosen as for the chord under compression: **diameter of 273 mm and a wall thickness of 25 mm**.

G.2.3. Horizontal braces

For construction and simplicity reasons all of the horizontal braces will be constructed of the same type of member. Both tension and compression forces occur in the horizontal braces and therefore have to be checked both. The maximum compression and tension force in the horizontal braces are respectively -2808 kN and 1752 kN. All of the horizontal braces have a length of 4.15 m.

According to [73], the effective buckling length for a brace has to be taken as 0.75 times the system length for in-plane buckling or 0.75 times the length between the supports for out-of-plane buckling.

Tables G.4 and G.5 show the possibilities of member dimensions that comply with the unity checks for the specific loading situations.

Table G.4: Possible options of CHS members for the horizontal braces under compression

Member length	Buckling length	Outside Diameter	Wall thick-ness	Ratio	Cross-sectional area	Reduction factor	Capacity	Max. chord force	Unity check
l $[mm]$	$l_b = 0.75 \cdot l$ $[mm]$	d_0 $[mm]$	t_0 $[mm]$	d_0/t_0 -	A_0 $[mm^2]$	χ -	$\chi \cdot f_{y0} \cdot A_0$ $[kN]$	N_0 $[kN]$	- -
4150	3113	219.1	16.0	14	10209	0.99	3601	-2808	0.78
4150	3113	**244.5**	**12.5**	20	9111	1.00	3233	-2808	0.87
4150	3113	273.0	12.5	22	10230	1.00	3632	-2808	0.77
4150	3113	323.9	10.0	32	9861	1.00	3501	-2808	0.80

Table G.5: Possible options of CHS members for the vertical brace under tension

Member length	Outside Diameter	Wall thickness	Ratio	Cross-sectional area	Capacity	Max chord force	Unity Check
l $[mm]$	d_0 $[mm]$	t_0 $[mm]$	d_0/t_0 -	A_0 $[mm^2]$	$f_{y0} \cdot A_0$ $[kN]$	N_0 $[kN]$	-
4150	219.1	16	14	10209	3624	1752	0.48
4150	**244.5**	**12.5**	20	9111	3234	1752	0.54
4150	273	12.5	22	10230	3632	1752	0.48
4150	323.9	10	32	9861	3501	1752	0.40

The joint strength efficiency increases with increasing chord-to-brace thickness t0/ti. The book Hollow Sections in Structural Applications [73] advises an as high as possible ratio, preferably above 2. This means that the thickness of the chord should preferably be more than 2 times thicker than the brace thickness.

As the wall thickness of the chords is 25 mm and assuming a steel grade S355 for both he chord and the brace, the wall thickness of the braces should therefore be 12.5 mm or smaller. For the sake of connecting the braces and chords it would also be best if the outer diameter of the braces is smaller than the diameter of the chords. Thus a diameter of 273 mm or smaller.

Due to the restrictions to the wall thickness and the outside diameter. The tube section with a **diameter of 244.5 mm and a wall thickness of 12.5 mm** is most suitable for the horizontal braces.

G.2.4. Vertical braces

The vertical braces can be split up into the members located in the top part with a length of 4 m and the members located in the bottom part with a length of 3.2 m. The goal is to have identical CHS dimensions for all of the vertical brace members as this eases construction.

In this top part the vertical members have a maximum tension force of 5537 kN and a maximum compression force of -1846. The maximum tension force is much larger and therefore governing.

In the bottom part of the structure the vertical members have a maximum tension force of 5537 kN and a maximum compression force of -5166. These values are relatively close and therefore both have to be checked. As the tension force in both the top and bottom part are identical only one has to be checked as the length of the members is not of influence to the tension capacity of the member.

Table G.6 shows the possible options for the members under a tension force and Table G.7 shows options in case of a compression force.

Table G.6: Possible options of CHS members for the vertical braces (tension)

Member length	Outside Diameter	Wall thickness	Ratio	Cross-sectional area	Capacity	Max chord force	Unity Check
l $[mm]$	d_0 $[mm]$	t_0 $[mm]$	d_0/t_0 -	A_0 $[mm^2]$	$f_{y0} \cdot A_0$ $[kN]$	N_0 $[kN]$	-
3200 or 4000	**273**	**20**	14	15986	5643	5537	0.98
3200 or 4000	355.6	16	23	17070	6060	5537	0.91
3200 or 4000	406.4	14.2	29	17496	6211	5537	0.89

Table G.7: Possible options of CHS members for the vertical braces (compression)

Member length	Buckling length	Outside Diameter	Wall thick-ness	Ratio	Cross-sectional area	Reduction factor	Capacity	Max. chord force	Unity check
l	$l_b = 0.75 \cdot l$	d_0	t_0	d_0/t_0	A_0	χ	$\chi \cdot f_{y0} \cdot A_0$	N_0	-
$[mm]$	$[mm]$	$[mm]$	$[mm]$	-	$[mm^2]$	-	$[kN]$	$[kN]$	-
3200	2400	**273**	**20**	14	15986	1.00	5643	-5166	0.92
3200	2400	355.6	16	23	17070	1.00	6060	-5166	0.85
3200	2400	406.4	14.2	29	17496	1.00	6211	-5166	0.83

Unfortunately it is not possible to reach wall thickness for the vertical brace lower than 12.5 in combination with an outside diameter that is identical or smaller than the chords. Therefore the rotation capacity of the joint cannot be guaranteed and the assumed pin jointed members in the analysis may not hold true. However, for now it is decided to choose the CHS profile with a **outside diameter of 273 mm and a wall thickness of 20 mm**. In a later stage it should be checked if the connections have enough rotation capacity or is strong enough to handle the 2^{nd} order moments in case the joint is too stiff.

G.2.5. Diagonal braces

The diagonal braces can also be split up into the members located in the top part (5.76 m) and in the bottom part (5.24 m).

For the bottom part the maximum compression and tension forces in the diagonal members are respectively -3698 kN and 4842 kN. Table G.8 shows some possible CHS profiles in case of compression and Table G.9 in case of tension for the diagonal braces in the bottom part of the cantilever structure.

Table G.8: Possible options of CHS members for the diagonal braces in the bottom part of the cantilever structure (compression)

Member length	Buckling length	Outside Diameter	Wall thickness	Ratio	Cross-sectional area	Reduction factor	Capacity	Max. chord force	Unity check
l	$l_b = 0.75 \cdot l$	d_0	t_0	d_0/t_0	A_0	χ	$\chi \cdot f_{y0} \cdot A_0$	N_0	-
$[mm]$	$[mm]$	$[mm]$	$[mm]$	-	$[mm^2]$	-	$[kN]$	$[kN]$	-
5240	3930	**273**	**20**	14	15986	0.99	5603	-3698	0.66
5240	3930	323.9	16	20	15477	1.00	5494	-3698	0.67
5240	3930	355.6	14.2	25	15230	1.00	5407	-3698	0.68

Table G.9: Possible options of CHS members for the diagonal braces in the bottom part of the cantilever structure (tension)

Member length	Outside Diameter	Wall thickness	Ratio	Cross-sectional area	Capacity	Max chord force	Unity Check
l	d_0	t_0	d_0/t_0	A_0	$f_{y0} \cdot A_0$	N_0	-
$[mm]$	$[mm]$	$[mm]$	-	$[mm^2]$	$[kN]$	$[kN]$	-
5240	**273**	**20**	14	15986	5643	4842	0.86
5240	323.9	16	20	15477	5494	4842	0.88
5240	355.6	14.2	25	15230	5407	4842	0.90

The tension force in the diagonal braces of the bottom part is governing. Ideally, the wall thickness of the diagonal braces should be twice as small as the chords. However, this is not possible in case the outside diameter has to be kept the same or smaller than the chord. Just as for the vertical braces the rotation capacity of the joints cannot be guaranteed. In this case it is also decided to accept a bigger **wall thickness of 20 mm** in combination with an **outer diameter of 273 mm**. It should be checked in a latter stage if this is acceptable for the joint.

The diagonal brace of the top part respectively has a compression force of -4405 kN and a tension force of 7362 kN. In this case the tension force is clearly governing as it is much larger. Table G.10 shows the possible CHS options for this tension force.

Table G.10: Possible options of CHS members for the diagonal braces under tension

Member length	Outside Diameter	Wall thickness	Ratio	Cross-sectional area	Capacity	Max chord force	Unity Check
l	d_0	t_0	d_0/t_0	A_0	$f_{y0} \cdot A_0$	N_0	-
$[mm]$	$[mm]$	$[mm]$	-	$[mm^2]$	$[kN]$	$[kN]$	-
5764	**273**	**30**	9	22902	8130	7362	0.91
5764	355.6	20	18	21086	7486	7362	0.98
5764	406.4	20	21	24278	8619	7362	0.85

The diagonal braces of the top part have to endure the highest loads in the cantilever structure and therefore require a relatively thick wall of the CHS. Therefore, also in this case, the conditions with respect to the chord-brace wall thickness ratios cannot be met. To match the diameters of both chord and brace the outer diameter is taken as **273 mm** and therefore the wall thickness has to be **30 mm**.

G.2.6. Perpendicular braces connecting the modelled 2D frames

In this analysis only the vertical load of the gate part on the cantilever structure is taken into account and used to determine the 2D structure. Horizontal/perpendicular loads are not taken into account and therefore the dimensions of the truss sections in between the 2D truss structures have to be assumed. For now, the connecting horizontal & vertical braces and the diagonal braces are assumed to have the same dimensions as their equivalents in the 2D structure.

Thus the perpendicular horizontal braces in between the 2D frames are made of a CHS with a **diameter of 244.5 mm and a wall thickness of 12.5 mm**. And the diagonal braces in between the 2D frames

are made of a CHS with a **diameter of 273 mm and a wall thickness of 20 mm**.

G.3. Summary

Table G.11 shows an overview of the dimensions and weight per length of the 4 type of CHS used in the cantilever truss structure.

Table G.11: Applied member types and their key numbers

Location	Outer diameter	Wall thickness	Cross sectional area	Weight per length	
		$[mm]$	$[mm]$	$[mm^2]$	$[kg/m]$
Top and diagonal chords	273	25	19478	152.9	
Horizontal braces	244.5	12.5	9111	71.5	
Vertical Braces & Diagonal braces bottom part	273	20	15986	124.8	
Diagonal braces top part	273	30	22902	179.8	

A calculation of the total weight of the cantilever truss structure is shown in table G.12. The total weight of the cantilever truss structure has a dead weight of 69105 kg.

Table G.12: Overview of truss members and calculation of the weight of the cantilever structure

Member type	Member length	Nr. of members	Total length	Weight per length	Total weight
-	$[m]$	-	$[m]$	$[kg/m]$	$[kg]$
Diagonal chords	5.24	8	41.9	152.9	6410
Horizontal chords	4.15	8	33.2	152.9	5076
Horizontal braces in 2D planes	4.15	20	83	71.5	5936
Vertical braces in top part in 2D planes	4.00	10	40.0	124.8	4991
Diagonal braces in top part in 2D planes	5.76	8	46.1	179.8	8290
Vertical braces in bottom part in 2D planes	3.20	20	64.0	124.8	7986
Diagonal braces in bottom part in 2D planes	5.24	12	62.9	124.8	7847
Horizontal braces in between 2D trusses	6.43	20	128.6	71.5	9197
Diagonal braces in horizontal planes in between 2D trusses	7.65	14	107.1	124.8	13370
		TOTAL:	**606.9**	**TOTAL:**	**69105**

Table G.13 shows the calculation of the total mass and the mass-distance of each element. The x-distance is calculated from the rightmost side of the cantilever structure. The centre of gravity of the cantilever structure in x-direction is then determined by dividing this mass-distance by the mass of the structure:

$$\frac{685070}{69105} = 9.91m$$

Table G.14 shows the calculation of the buoyancy volume of the cantilever structure at three significant water levels. For the maximum lockage waterlevel at +3.5 m NAP, the buyoancy volume of the cantilever structure is 25.9 m^3.

Table G.13: Calculation of mass and mass-distance of the cantilever structure in case of a cantilever length of 16.6 m

Y-Location of element	Quantity	Top height	Bottom height	Length	Weight per length	Element weight	X-location	Mass · Distance
	$Nr.$	$[m\ N.A.P.]$	$[m\ N.A.P.]$	$[m]$	$[kg/m]$	$[kg]$	$[m]$	$[kgm]$
Diagonal chords								
3/5 till 4/5	2	0	-3.2	5.2	152.9	1603	2	3325
2/5 till 3/5	2	-3.2	-6.4	5.2	152.9	1603	6	9976
1/5 till 2/5	2	-6.4	-9.6	5.2	152.9	1603	10	16626
bottom till 1/5	2	-9.6	-12.8	5.2	152.9	1603	15	23277
Horizontal chords								
Top	8	4	4	4.2	152.9	5076	8	42133
Horizontal braces in 2D planes								
At 4/5	8	0	0	4.2	71.5	2374	8	19708
At 3/5	6	-3.2	-3.2	4.2	71.5	1781	10	18476
At 2/5	4	-6.4	-6.4	4.2	71.5	1187	12	14781
At 1/5	2	-9.6	-9.6	4.2	71.5	594	15	8622
Vertical braces in 2D planes								
From 4/5 till top	10	4	0	4.0	124.8	4991	8	41429
From 3/5 till 4/5	8	0	-3.2	3.2	124.8	3195	10	33143
From 2/5 till 3/5	6	-3.2	-6.4	3.2	124.8	2396	12	29829
From 1/5 till 2/5	4	-6.4	-9.6	3.2	124.8	1597	15	23200
Bottom till 1/5	2	-9.6	-12.8	3.2	124.8	799	17	13257
Diagonal braces in 2D planes								
From 4/5 till top	8	4	0	5.8	179.8	8290	8	68807
From 3/5 till 4/5	6	0	-3.2	5.2	124.8	3924	10	40708
From 2/5 till 3/5	4	-3.2	-6.4	5.2	124.8	2616	12	32566
From 1/5 till 2/5	2	-6.4	-9.6	5.2	124.8	1308	15	18997
Horizontal braces in between 2D trusses								
Top braces	5	4	4	6.4	71.5	2299	8	19084
4/5 braces	5	0	0	6.4	71.5	2299	8	19084
3/5 braces	4	-3.2	-3.2	6.4	71.5	1839	10	19084
2/5 braces	3	-6.4	-6.4	6.4	71.5	1380	12	17176
1/5 braces	2	-9.6	-9.6	6.4	71.5	920	15	13359
Lowest brace	1	-12.8	-12.8	6.4	71.5	460	17	7634
Diagonal braces in horizontal planes in between 2D Trusses								
Top braces	4	4	4	7.7	124.8	3820	8	31706
4/5 braces	4	0	0	7.7	124.8	3820	8	31706
3/5 braces	3	-3.2	-3.2	7.7	124.8	2865	10	29724
2/5 braces	2	-6.4	-6.4	7.7	124.8	1910	12	23779
1/5 braces	1	-9.6	-9.6	7.7	124.8	955	15	13871
					Total:	**69105**	**Total:**	**685070**

Table G.14: Calculation of cantilever structure buoyancy volume for different water levels in case of a cantilever length of 16.6 m

Element	Volume under water at +3.5 m NAP $[m^3]$	Volume under water at 0.02 m NAP $[m^3]$	Volume under water at -3.4 m NAP $[m^3]$
Diagonal chords			
3/5 till 4/5	0.6	0.6	0.0
2/5 till 3/5	0.6	0.6	0.6
1/5 till 2/5	0.6	0.6	0.6
bottom till 1/5	0.6	0.6	0.6
Horizontal chords			
Top	0.0	0.0	0.0
Horizontal braces in 2D planes			
At 4/5	1.6	1.6	0.0
At 3/5	1.2	1.2	0.0
At 2/5	0.8	0.8	0.8
At 1/5	0.4	0.4	0.4
Vertical braces in 2D planes			
From 4/5 till top	2.0	0.0	0.0
From 3/5 till 4/5	1.5	1.5	0.0
From 2/5 till 3/5	1.1	1.1	1.1
From 1/5 till 2/5	0.7	0.7	0.7
Bottom till 1/5	0.4	0.4	0.4
Diagonal braces in 2D planes			
From 4/5 till top	2.4	0.0	0.0
From 3/5 till 4/5	1.8	1.8	0.0
From 2/5 till 3/5	1.2	1.2	1.2
From 1/5 till 2/5	0.6	0.6	0.6
Horizontal braces in between 2D trusses			
Top braces	0.0	0.0	0.0
4/5 braces	1.5	1.5	0.0
3/5 braces	1.2	1.2	0.0
2/5 braces	0.9	0.9	0.9
1/5 braces	0.6	0.6	0.6
Lowest brace	0.3	0.3	0.3
Diagonal braces in horizontal planes in between 2D Trusses			
Top braces	0.0	0.0	0.0
4/5 braces	1.8	1.8	0.0
3/5 braces	1.3	1.3	0.0
2/5 braces	0.9	0.9	0.9
1/5 braces	0.4	0.4	0.4
TOTAL	**25.9**	**21.5**	**8.7**

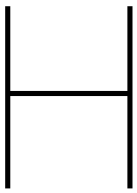

Excel design checks final case study design

This appendix shows the excel calculations which show all the design checks for the final design of the cantilever gate at the case study location. Thus with an 8 wheel front and a 4 wheel back carriage, a cantilever length of 16.6 meter and a 1083 kg counterweight. The calculations are in line with the method explained in Chapter 6 and Appendix F.

Equilibrium, strength and fatigue checks for final design of cantilever rolling gate

INPUT

Parameter	Abbr.	Value	Unit
Cantilever length		16,6	m
Cantilever weight		69,15	tonnes
Contraweight (under back carriage)		1083	tonnes
Extra buoancy volume		116	m3
Front carriage length		9	m
Back carriage length		6	m
Weight of front carriage		18	tonnes
Weight of back carriage		12	tonnes
Amount of wheels front carriage		8	
Amount of wheels back carriage		4	
Percentage of buoancy volume filled in case of collision		0,15	
Buoancy volume cantilever at HW		25,9	m3
Buoancy volume cantilever at LW		8,7	m3
Buoancy volume cantilever at MW		21,5	m3

Constant values

Gravity constant	g	9,81	m/s2
Water density	rho_w	1000	kg/m3
Gate length	Lg	44,56	m
Gate width	Bg	6,43	m
Gate weight	Wg	946	tonnes
Additional silt weight on buoancy chambers	Wsilt	110,9	tonnes
Top height of the gate		6	m NAP
Bottom height of the gate		-13,22	m NAP
Front carriage length		9	m
Back carriage length		6	m
Level of 'supports' of the cantilever		4	m NAP
Highest lockage Waterlevel	HW	3,5	m NAP
Lowest lockage Waterlevel	LW	-3,4	m NAP
Average Water level seaside	MW	0,02	m NAP
Buoancy volume gate at HW		735,3	m3
Buoancy volume gate at LW		696,2	m3
Buoancy volume gate at MW		715,58	m3
Buoancy volume cantilever at HW		25,9	m3
Buoancy volume cantilever at LW		8,7	m3
Buoancy volume cantilever at MW		21,5	m3
Arm to supports of resistance forces at HW	Arm_resHW	8,86	m
Arm to supports of resistance forces at LW	Arm_resLW	12,31	m
Arm to supports of resistance forces at MW	Arm_resMW	10,6	m
Resistance force during opening at HW		208	kN
Resistance force during opening at LW		166	kN
Resistance force during opening at MW		187	kN
Resistance force during closing at HW		191	kN
Resistance force during closing at LW		149	kN
Resistance force during closing at MW		170	kN

Intermediate calculations		
Arm gateforces (from back carriage)	35,9	m
Arm cantilever forces (from back carriage)	8,1	m
Arm between carriages	9,1	m
Arm of contraweigth (from back carriage)	0	m

Max loads for EQU and STR				
	HW, opening	HW, closing	LW, opening	LW, closing
PERMANENT				
Dead weight of gate part (in kN)	9280	9280	9280	9280
Dead weight of cantilever part (in kN)	678	678	678	678
Contraweight at back carriage (in kN)	10624	10624	10624	10624
Upward Buoancy force gate part (in kN. - is upward)	-8351	-8351	-7968	-7968
Upward buoancy force cantilever part (in kN)	-254	-254	-85	-85
Silt and shell accretion (in kN)	1088	1088	1088	1088
VARIABLE				
Combination of resistance forces during opening or closing (moment force in kNm, - is clockwise)	-1843	1692	-2043	1834
INCIDENTAL/SPECIAL				
Leakage of 15% of buoancy chambers	1253	1253	1195	1195

EQUILIBRIUM CHECK

Load combinations and partial safety factors EQU					
Moment in time	**At start of operations**		**After a certain time (at which silt is max)**		**Incident**
	EQU 1	**EQU 2**	**EQU 3**	**EQU 4**	**EQU 5**
Load combination	*DW unfav. Buy fav. no silt*	*DW fav. Buy unfav. No silt*	*DW unfav. Buy fav. Max silt*	*DW fav. Buy unfav. Max silt*	*Leakage of buy. Max silt*
PERMANENT					
Dead weight of gate part	1,05	0,95	1,05	0,95	1
Dead weight of cantilever part	1,05	0,95	1,05	0,95	1
Contraweight at back carriage	1,05	0,95	1,05	0,95	1
Upward Buoancy force gate part	0,95	1,05	0,95	1,05	1
Upward buoancy force cantilever part	0,95	1,05	0,95	1,05	1
Silt and shell accretion	0	0	1,05	0,95	1
VARIABLE					
Comb. of res. forces during opening/closing	1,5	1,5	1,5	1,5	1
INCIDENTAL/SPECIAL					
Leakage of 15% of buoancy chambers	0	0	0	0	1

Forces on supports					
	EQU 1	**EQU 2**	**EQU 3**	**EQU 4**	**EQU 5**
Force on front carriage/support					
HW, opening	7253	218	11757	4293	13065
HW, closing	7835	801	12339	4876	~~13454~~
LW, opening	8798	1930	13302	6005	14478
LW, closing	9437	2569	13942	6644	~~14904~~
min	*7253*	*218*	*11757*	*4293*	*13065*
max	*9437*	*2569*	*13942*	*6644*	*14478*
Force on back carriage/support					
HW, opening	6184	10300	2823	7259	1253
HW, closing	5602	9717	2240	6676	~~864~~
LW, opening	5163	9168	1802	6126	335
LW, closing	4524	8529	1162	5487	~~-92~~
min	4524	8529	1162	5487	335
max	6184	10300	2823	7259	1253

Minimum load front carriage	218	kN
Minimum load back carriage	335	kN

STRENGTH CHECK

Load combinations and their partial safety factors STR					
Moment in time	**At start of operations**		**which silt is max)**		**Incident**
Load combination	**STR 1**	**STR 2**	**STR 3**	**STR 4**	**STR 5**
	DW unfav. Buy fav. no silt	DW fav. Buy unfav. No silt	DW unfav. Buy fav. Max silt	DW fav. Buy unfav. Max silt	Leakage of buy. Max silt
PERMANENT					
Dead weight of gate part	1,25	0,9	1,25	0,9	1
Dead weight of cantilever part	1,25	0,9	1,25	0,9	1
Contraweight at back carriage	1,25	0,9	1,25	0,9	1
Upward Buoancy force gate part	0,9	1,25	0,9	1,25	1
Upward buoancy force cantilever part	0,9	1,25	0,9	1,25	1
Silt and shell accretion	0	0	1,25	0,9	1
VARIABLE					
Combination of resistance forces during opening or closing	1,5	1,5	1,5	1,5	1
INCIDENTAL/SPECIAL					
Leakage of 15% of buoancy chambers	0	0	0	0	1

Forces on supports					
	STR 1	STR 2	STR 3	STR 4	STR 5
Force on front carriage/support					
HW, opening	16349	-8272	21711	-4412	13065
HW, closing	16931	-7689	22293	-3829	~~13454~~
LW, opening	17811	-6228	23173	-2367	14478
LW, closing	18450	-5589	23812	-1728	~~14904~~
min	*16349*	*-8272*	*21711*	*-4412*	*13065*
max	*18450*	*-5589*	*23812*	*-1728*	*14478*
Force on back carriage/support					
HW, opening	1635	16040	-2367	13159	1253
HW, closing	1052	15457	-2950	12576	~~864~~
LW, opening	670	14686	-3332	11805	335
LW, closing	30	14047	-3972	11165	~~-92~~
min	30	14047	-3972	11165	335
max	1635	16040	-2367	13159	1253

Maximum downward design force on front carriage	23812	kN	LW, closing and STR 3 governing
Maximum downward design force on back carriage	16040	kN	HW, opening and STR 2 governing

Calculation of downward force of carriages (STR)		
Characteristic force from front carriage deadweight	177	kN
Characteristic force from back carriage deadweight	118	kN
Strength partial safety factor	1,25	
Design force deadweight front carriage	221	kN
Design force deadweight back carriage	147	kN

Design downward force of front carriage	24033	kN	
Design downward force per wheel on front carriage	3004	kN	8 wheels
Design downward force of back carriage	16187	kN	
Design downward force per wheel on back carriage	4047	kN	4 wheels

Fatigue CHECK

Max Load situations		
	FAT 1	FAT 2
Load combination	MW average load. Opening. Max silt	MW average load. Closing. Max silt
PERMANENT		
Dead weight of gate part (in kN)	9280	9280
Dead weight of cantilever part (in kN)	678	678
Contraweight at back carriage (in kN)	10624	10624
Upward Buoancy force gate part (in kN. - is upward)	-8168	-8168
Upward buoancy force cantilever part (in kN)	-211	-211
Silt and shell accretion (in kN)	1088	1088
VARIABLE		
Combination of resistance forces during opening or closing (moment force in kNm, - is clockwise)	-1965	1787
INCIDENTAL/SPECIAL		
Not applicable	0	0

Load combinations and their partial safety factors	
	FAT 1 & 2
Load combination	Fatigue load combination (all partial safety factors 1), silt present
PERMANENT	
Dead weight of gate part	1
Dead weight of cantilever part	1
Contraweight at back carriage	1
Upward Buoancy force gate part	1
Upward buoancy force cantilever part	1
Silt and shell accretion	1
VARIABLE	
Combination of resistance forces during opening or closing	1
INCIDENTAL/SPECIAL	
Not applicable	0

FORCES ON SUPPORTS		
Force on front carriage/support		
MW, opening	8874	kN
MW, closing	9287	kN

Force on back carriage/support		
MW, opening	4418	kN
MW, closing	4006	kN

Maximum fatigue force from gate front carriage	9287	kN
Maximum fatigue force from gate back carriage	4418	kN

Calculation of downward force of carriages (FAT)		
Characteristic force from front carriage deadweight	177	kN
Characteristic force from back carriage deadweight	118	kN
Strength partial safety factor	1,00	
Design force deadweight front carriage	177	kN
Design force deadweight back carriage	118	kN

Total fatigue force on all wheels front carraige	9463	kN	
Design fatigue force per wheel of front carriage	1183	kN	8 wheels
Total fatigue force on all wheels back carraige	4536	kN	
Design fatigue force per wheel of back carriage	1134	kN	4 wheels

Overview			
	Value	**Unit**	**Requirement**
Equilibrium check			
Minimum load front carriage	218	kN	>200 kN
Minimum load back carriage	335	kN	>200 kN
Strength check wheel loads			
Max downward design load per wheel of front carriage	3004	kN	<6049 kN (NEN6786)
Max downward design load per wheel of back carriage	4047	kN	<6049 kN (NEN6786)
Fatigue check wheel loads			
Design fatigue load per wheel of front carriage	1183	kN	<1188 kN (NEN6786) <1599 (EN13001), 8 wheels carriage, Dw=1200 m bw=150 mm